Characterization of eIF4E-binding proteins that are phosphorylated by TOR and function in cap-dependent translation initiation in Arabidopsis

Ola Srour

UNIVERSITÉ DE STRASBOURG

ÉCOLE DOCTORALE DES SCIENCES DE LA VIE ET DE LA SANTÉ

INSTITUT DE BIOLOGIE MOLECULAIRE DES PLANTES UPR-CNRS 2357

THÈSE

présentée par : **Ola SROUR**

soutenue le : 07 décembre 2016

pour obtenir le grade de : **Docteur de l'Université de Strasbourg**

Mention : Sciences de la Vie et de la Santé

Discipline : Aspects Moléculaires et Cellulaires de la Biologie

Caractérisation de protéines interagissant avec eIF4E, phosphorylées par TOR et modulant l'initiation de la traduction coiffe-dépendante chez *Arabidopsis*

THÈSE dirigée par :

Mme. RYABOVA Lyubov Directrice de recherche, Université de Strasbourg, IBMP-CNRS

RAPPORTEURS EXTERNES

M. MEYER Christian Directeur de recherche, INRA-Centre Versailles-Grignon

M. GALLOIS Jean-Luc Chargé de recherche, INRA-Avignon

EXAMINATEURS INTERNES

M. MARTIN Franck Chargé de recherche, Université de Strasbourg, IBMP-CNRS

INVITE

M. SCHEPETILNIKOV Mikhail Chargé de recherche, Université de Strasbourg, IBMP-CNRS

قال الشّافعي:

"بقَدْرِ الكدِّ تُكتسَبُ المَعَالي ومَنْ طَلَبَ العُلا سَهِرَ اللّيالي "

فمع إشراقةِ فجرِ المحبّةِ, حملْتُ أمتعتي وصرتُ مع كلِّ نسمةٍ من نسمات حياتي. فأبحرْتُ في بحرِ الغربةِ المظلمِ بحثاً عن حُلمٍ راودني مُنْذ صغري وطالما طمحْتُ بتحقيقهِ.

فقضَّ الطّموحُ مضجعي وطردَ من جفنيّ النّوم, وأردْتُ النّجاحَ في حياتي, فجعلْتُ المثابرةَ صديقي الحميم والتّجربة مستشاري الحكيم والحذرَ أخاً أكبرَ والرّجا ءَ عبقريتي الحازمة, وإرادتي قويّةً فلم أطلْ الوقوفَ في محطّاتِ التّعبِ والفشلِ واليأسِ فكان َالصّبرُ مفتاحاً لنجاحي, ووصلْتُ إلى حديقةِ النّجاحِ. ونلْتُ بالسّهرِ وطولِ اللّيالي طريقَ العُلا والمجدِ.

وها هو تاجُ العلمِ أتتوّجُ بهِ اليومَ, فالتّخرجُ هو ضوءُ الصّباحِ الّذي رأيتُه مُع شقشقةِ انتصاراتي وتنصَّتُ إلى تغريدِ انجازاتي وتلمّسْتُ نتائجَه عُلى أرض الواقعِ ولا يمكنني أن أحجُبَ ضوءَهُ.

Acknowledgements

After an intensive period of three years, today is the day. Writing this note of thanks is the final touch on my thesis. I feel that words can't reflect the satisfaction and pleasure I experience now. Countless, are the people that helped and supported me so much through this period, and that deserved all my sincere and deepest thanks.

First and foremost, I would like to express my sincere gratitude to my advisor Dr. Lyuba Ryabova for providing me an opportunity to join her team, for her continuous support, patience and immense knowledge. Besides my advisor, I would like to thank my co-supervisor Dr. Mikhail Schepetilnikov for his insightful comments and encouragement as well as for his hard question which incited me to widen my research. It would have been impossible to conduct this research without their precious support.

My sincere thanks also goes to Drs. Christian Meyer, Jean-Luc Gallois and Franck Martin for accepting to evaluate my thesis and be my thesis committee members.

Thanks to my fellow lab mates for the memorable moments we have spent together. It was truly a remarkable experience. Special thanks to Dr. Nina Lukhovitskaya for her kind endless help and for her stimulating discussions during my thesis. Thank you all for creating this lovely working ambiance.

I would also like to thank Dr. Anne-Marie Duchenne. The door to her office was always open whenever I ran into a trouble or had a question about my research or decisions.

My deepest thanks to my lovely friend and sister, the future doctor, Joelle Magarian. We shared together every single happy and sad moment in the lab, at home, at Lebanon and in many cities in the world. Special thanks for Batoul Srour and Zeinab Wehbe with whom I had unforgettable moments. Surely, I can't forget Nedal Taha for her untiring support in English. Thanks to all my Lebanese friends for being besides me during my stay at Strasbourg and during my thesis.

I would never forget to express my deep gratitude to my second homeland France, which hosted me for nine years. France did not only give me the opportunity to achieve my goals and to be a doctor but France also gave me the French citizenship.

I would like to dedicate my Doctoral dissertation to my family especially my father Hussein and my aunt Raghda. My deepest acknowledgement for the tremendous sacrifices that they made to arrive there and to be doctor. For this and much more, I am forever in their debt.

Ola

Contents

List of abbreviations

Abbreviation	Term
40S	Small ribosomal subunit
4E-BM	eIF4E-binding motif
4E-BP	eIF4E-binding proteins
60S	Large ribosomal subunit
80S	80S ribosome
ADP	Adenosine-5’-diphosphate
ATP	Adenosine-5’-triphosphate
CaMV	Cauliflower mosaic virus
eEF	Eukaryotic elongation factors
eIF	Eukaryotic initiation factors
eRF	Eukaryotic release factors
GDP	Guanosine-5’-diphosphate
GTP	Guanosine-5’-triphosphate
kDa	Kilo Dalton
m^7GTP	7-Methylguanosine 5′-triphosphate
Met-$tRNA_i$	Methionine-initiatior transfer RNA
mRNA	Messenger RNA
ORF	Open reading frame
PABP	PolyA binding proteins
PIC	Preinitiation complex
PTC	Ribosomal peptidyl transferase center
rRNA	Ribosomal RNA
S6K1	Eukaryotic ribosomal protein eS6 kinase-1
sORF	Short upstream open reading frame
TAV	Transactivator/viroplasmin
TC	Ternary complex
TOR	Target of rapamycin
tRNA	Transfer RNA
uORF	Upstream open reading frame
UTR	Untranslated region

Preface

The control of mRNA translation in eukaryotes—a key regulator of gene expression—is involved in a wide range of cell functions, such as cell cycle, differentiation, proliferation, survival and cell death, or even, during embryonic development. Dysregulation of translation is associated with many diseases, like cancers or neurological diseases. In eukaryotes, translation can be controlled at many levels, but initiation constitutes the rate-limiting step in translation and serves as a major target for translational control. The majority of eukaryotic mRNAs possess a 5' cap structure at their end which allows to qualify translation initiation of these mRNA as cap-dependent. The cap structure triggers the assembly of the initiation complex 4F (eIF4F) on the 5' end of mRNA, which facilities the recruitment of the 40S ribosomal subunit. One of the key players in translation is the cap-binding protein eIF4E that plays an essential role in the cap-dependent translation initiation step, in particular, the assembly of eIF4F complex at the cap. It was shown that eIF4E has a high oncogenic potential. For that reason, eIF4E is subject to multiples controls, mainly through its sequestration by eIF4E-binding proteins (4E-BPs) under the control of TOR (Target of rapamycin).

TOR—a critical sensor of nutritional and cellular energy and a major regulator of cell growth—is a large serine/threonine protein kinase. In response to a wide variety of input cellular signals such as growth factors and hormones, nutrients and the cellular energy status, the activity of TOR can be finely modulated by components of the mTORC1 complex or by upstream effectors such as a small GTPase Rheb (Ras homolog enriched in brain). TOR mediates temporal control of cell growth by activating anabolic processes such as ribosome biogenesis, protein synthesis, transcription, and nutrient uptake, and by inhibiting catabolic processes such as autophagy and ubiquitin-dependent proteolysis. TOR controls protein synthesis by phosphorylation of several compounds of the translational machinery, including

its two main targets: 4E-binding proteins (4E-BPs) and 40S ribosomal protein S6 (RPS6) kinases. TOR stimulates the global protein synthesis, and also it preferentially stimulates the translation of selected groups of mRNAs.

4E-BPs are small proteins (in mammals: 4E-BP1, 2 and 3) that interact with eF4E and prevent its participation in the assembly of eIF4F complex at the 5' cap. 4E-BPs share with eIF4G the same canonical eIF4E-binding motif (Y-X-X-X-X-L-ϕ) required for eIF4E binding. 4E-BPs are direct targets of the TOR signaling pathway, their binding to eIF4E is affected by TOR phosphorylation. Non-phosphorylated 4E-BPs outcompete eIF4G for eIF4E binding that leads to repression of cap-dependent translation initiation. Under activation conditions, TOR promotes phosphorylation of several residues on 4E-BP, their release from eIF4E, which can be then engaged in eIF4F complex formation, and activation of translation initiation.

Inappropriate TOR signaling to 4E-BPs and S6Ks is frequently disregulated in cancer and contributes to metabolic diseases such as diabetes and obesity. The TOR signaling pathway is conserved among all eukaryotes, from humans to yeasts and plants. However, the role of TOR in cap-dependent translation initiation is not known and the question of the existence of 4E-BPs in plant remains to be answered.

The main goal of my thesis was to investigate mechanism(s) of cellular translation initiation control by TOR in plants. More generally, in this comparative study we shall address questions about regulation of the plant cap-dependent translation initiation machinery in order to better understand mRNA initiation pathways and their control by TOR signaling in plants. To this end, we have identified and characterized a family of small *Arabidopsis* proteins that contain an eIF4E-binding motif.

To better understand TOR function in regulation of protein synthesis, a brief overview of main steps of protein synthesis and critical translation initiation factors will be presented in

the introductory part of my thesis. I will describe in details the TOR signaling pathway and its direct target: the eIF4E-binding protein family. Various aspects of translation unique to plant will be also discussed.

I. Introduction

1. General overview of translation

Protein synthesis—one of the fundamental mechanisms in living organisms— is a complex and regulated process that allows decoding of the genetic information contained in the messenger RNA (mRNA) to produce proteins.

Translation is performed by the ribosome, which synthesizes proteins by incorporating one by one amino acids into a polypeptide chain based on the information contained in mRNA, using charged transfer RNAs (tRNAs).

mRNA is a nucleotide chain, which starts with a cap structure, a methylated guanosine (m^7G) linked to the first transcript nucleotide via a 5'-5' triphosphate link, and usually terminates with a polyA tail. The mRNA is decoded by triplets nucleotide called codons, starting with an initiation codon (AUG) and ending with one of the three stop codons (UAG, UGA or UAA). The mRNA region which is translated by the ribosome, and located between the initiation codon and the termination codon, is called coding sequence, open reading frame, or ORF. Each codon corresponds to a particular amino acid.

tRNAs are small RNA molecules of 75-95 nucleotides, they act as adapter molecules between mRNA codons and amino acids. Each tRNA contains a complementary anticodon (of three nucleotides) to a particular mRNA codon and carries the corresponding to this codon amino acid. When pairing between mRNA codon and tRNA anticodon is correct, the ribosome incorporates the amino acid carried by aminoacylated tRNA (aa-tRNA) to the growing peptide chain.

The ribosome is a ribonucleoprotein complex, composed of ribosomal RNA (rRNA) and protein. It can be considered as a three-functional entity: (i) genetic function: the ribosome is considered as a decoding device responsible for the arrangement of amino acids in accordance with the nucleotide sequence, (ii) enzymatic function: a peptidyl transferase activity as a result of the transpeptidation reaction, and (iii) function of translocation: in which the

translational machine move along mRNA chain during elongation phase (Spirin 2002). Mammalian ribosomes are composed of two subunits that are designated by their sedimentation coefficients: The smaller 40S and the larger 60S subunits associate to form the functional 80S ribosome. The main functional sites on the ribosome, such as mRNA-binding site of the small subunit, the peptidyl transferase center (PTC) of the large subunit and the tRNA-binding sites are localized in a spacious cavity between the associated subunits. Three tRNA-binding sites—A, P and E—host tRNA according to their aminoacylation state.

- A site: the aminoacyl-tRNA site holds the aa-tRNA carrying the next amino acid to be added.
- P site: the peptidyl-tRNA site holds the tRNA molecule carrying the growing polypeptide chain.
- E site: the exit site, from where tRNA molecule leaves the ribosome.

mRNA translation can be divided into four major phases: initiation, elongation, termination and ribosome recycling, where each phase includes multiple steps that require a set of cellular factors. Initiation includes formation of the 43S preinitiation complex (PIC: pre-initiation complex), 43S PIC loading at the 5'-end of mRNA (48S PIC), mRNA scanning by 43S PIC, recognition of the start codon, and assembly of a functional and active 80S ribosome. Elongation is the synthesis of the polypeptide chain by incorporating one by one amino acids. Translation termination results in release of the synthesized polypeptide after recognition of a stop codon by the ribosome. Once the translation is completed, the ribosome is recycled by dissociation of both 40S and 60S subunits and mRNA.

1.1. Cap-dependent translation initiation

Thus, the translation initiation is a complex process that leads to recruitment of the 40S ribosomal subunit to the mRNA and assembly of the 80S ribosome at the correct initiation AUG codon. At least 11 factors, called eukaryotic initiation factors (eIFs), are required to orchestrate this process (Pestova et al. 2007). Translation initiation can be divided into 3 phases: activation of mRNA by its association with the initiation complex eIF4F, binding of the 43S PIC to the capped structure of mRNA and 43S PIC alignment at initiation codon followed by joining of the 60S ribosomal subunit to form the 80S ribosome (Jackson et al. 2010) **(Figure 1—1)**.

The majority of cellular mRNAs initiate translation by a mechanism qualified as cap-dependent. The cap-dependent translation initiation depends on the presence of cap structure at the 5' end of the mRNA. The cap corresponds to m^7GpppN, where m^7G is a guanosine methylated and N represents any nucleotide. The bond between G and N is via a triphosphate linkage 5'-5'.

1.1.1. Assembly of the preinitiation complex

The first step in translation initiation is the 43S PIC assembly, composed of the small ribosomal subunit (40S), initiator-Met-$tRNA_i$ and the initiation factors eIF1, eIF1A, eIF3 and eIF5. The initiator-Met-$tRNA_i$ binds with high affinity the initiation factor eIF2, when it is bound to GTP, to form a ternary complex (TC) (Kapp and Lorsch 2004). The association of TC with the 40S is promoted by eIF3. Once PIC is formed, it is loaded on the 5' cap of the mRNA by the eIF4F initiation complex. 48S PIC formation is ensured by eIF3 binding to eIF4G, a scaffold subunit of eIF4F (Aitken and Lorsch 2012).

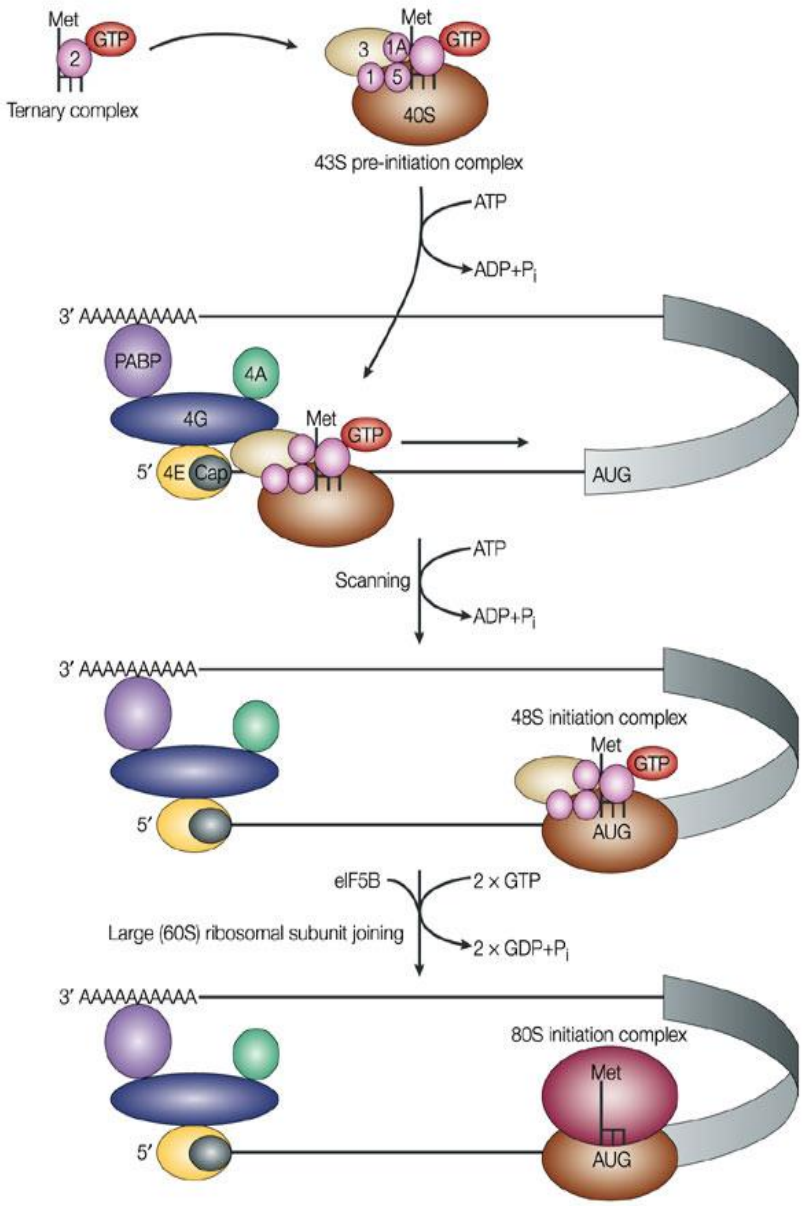

1) Assembly of 43S PIC

2) Formation of the eIF4F complex and 43S PIC loading

3) Scanning and recognition of the initiation codon

Figure 1—1 │Overview of cap-dependent translation initiation in eukaryotes

Cap-dependent translation initiation proceeds in three major steps:

1) Assembly of 43S PIC: eIF1, eIF1A, eIF3 and eIF5 loading on the 40S ribosomal subunit. eIF3 promotes the recruitment of TC—initiator-Met-tRNA$_i$, eIF2-bound GTP.

2) eIF4F formation and 43S PIC loading mRNA cap structure. eIF4F (composed of eIF4E, eIF4G and eIF4A) at the 5' cap of mRNA is presented.

3) Scanning and recognition of initiation codon. 48S PIC scans the mRNA until encounter the AUG initiation codon. 60S joining and start of translation elongation.

Modified from (Gebauer and Hentze 2004), *Nature Reviews Molecular Cell Biology 5: 827-835*

1.1.2. Formation of eIF4F complex and loading of the PIC

The 5'-cap binding complex eIF4F composed of 3 factors—eIF4A, eIF4E and eIF4G, which play an important role in translation initiation (Gingras et al., 1999b). eIF4A, an RNA-dependent RNA helicase, is required to remove secondary structures at the mRNA 5' UTR to ensure the recruitment of 40S and its scanning. eIF4A helicase activity is stimulated by eIF4G and eIF4B (Marintchev 2013). eIF4E is a cap-binding protein that recognizes the 5' cap structure of mRNA (Sonenberg and Shatkin 1978). It is the least abundant factor among eIFs, and its binding to cap is highly regulated. eIF4G, the largest protein within eIF4F complex, acts as a scaffold protein interacting simultaneously with eIF4E, eIF4A, eIF3 and PABP (PolyA binding protein). eIF4F ensures ribosome loading at the mRNA via interactions with eIF4G and eIF3, while mRNA circularization can be achieved via interactions between cap-bound eIF4E and poly(A)-bound PABP (Gingras et al., 1999b). These events ensure 43S PIC recruitment to the 5' cap of mRNA.

1.1.3. Scanning and Recognition of initiation codon

Once loaded at the 5' cap of mRNA, 48S PIC begins scanning the mRNA in the 5' → 3' direction until the anticodon of the initiator-Met-$tRNA_i$ interacts with the first AUG codon within a favorable mRNA initiation context. After the codon-anticodon recognition within the 40S P site, eIF5 stimulates GTP hydrolysis of GTP-bound eIF2, thus leading to the dissociation of the Met-$tRNA_i$ from P site and the release of eIF1, eIF1A, eIF2 and eIF3 factors. Then, eIF5B binds the 40S ribosomal subunit and stimulates the 60S ribosomal subunit joining, resulting in GTP hydrolysis of GTP-bound eIF5B and its release. Assembly of 80S ribosome is achieved by the association of the 2 ribosomal subunits, and translation elongation phase can proceed (Hinnebusch 2011).

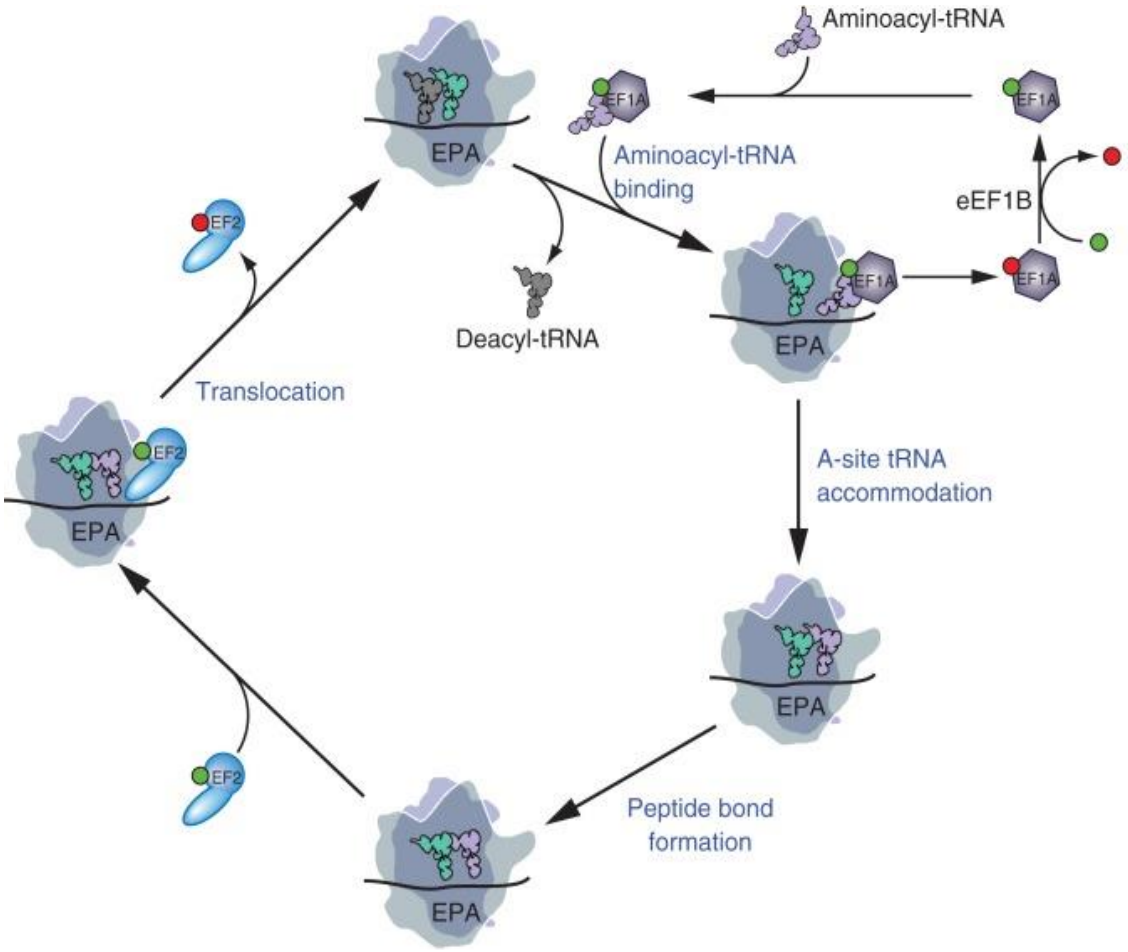

Figure 1—2 │Overview of the translation elongation pathway in eukaryotes

Binding of the eEF1A·GTP·aminoacyl-tRNA ternary complex to 80S— the anticodon loop of the aminoacyl-tRNA interacts with the mRNA in the A-site of 40S. After release of eEF1A·GDP, the aminoacyl-tRNA is accommodated in the A-site. Recycling of the eEF1A·GDP to eEF1A·GTP by the GTP/GDP exchange factor eEF1B. Peptide bond formation and transition of the A- and P-site tRNAs into hybrid states with the acceptors ends of tRNAs moving to the P and E sites, respectively. Binding of eEF2·GTP promotes translocation of tRNAs to P- and E-sites. Release of eEF2·GDP from 80S. After release of the deacylated tRNA from the E-site, the ribosome is ready for the next cycle of elongation.

Modified from (Dever and Green 1999), *Cold Spring Harbor Perspectives in Biology doi: 10.1101/cshperspect.a013706*

1.2. Elongation

The elongation phase of translation, unlike the translation initiation, is conserved during evolution between prokaryotes and eukaryotes (Ramakrishnan 2002; Rodnina and Wintermeyer 2009). This step consists of multiple cycles of the assembly of amino acids one by one by the ribosome. Each cycle proceeds in three steps that are repeated throughout the elongation process: 1) selection of a tRNA anticodon complementary to codon within the mRNA decoding center on 40S, 2) formation of the peptide bond and, finally, 3) translocation of peptidyl-tRNA from A- to P-site. The elongation process requires eukaryotic elongation factors (eEFs) **(Figure 1—2)**.

The first step of elongation—when the initiator-Met-tRNA$_i$ is in the P site. The first step is loading of a new aminoacylated-tRNA in the A site by the eukaryotic elongation factor 1A (eEF1A; its bacterial ortholog is known as EF-Tu) bound to GTP. The accuracy of elongation is controlled during several check-point steps via inspection of a complementary between the mRNA codon and tRNA anticodon (Rodnina et al. 2005). If this is correct, codon anticodon binding triggers a conformational change within eEF1A followed by the hydrolysis of GTP to GDP, and eEF1A release from the ribosome (Pape et al. 1998; Gromadski and Rodnina 2004).

The second step of elongation—the transpeptidation reaction that leads to formation of the peptide bond between the growing polypeptide chain (at the P site) and the amino acid carried by the aa-tRNA (at the A site) within the peptidyl-transferase center of the ribosome (Moore and Steitz 2003), which results in polypeptide chain elongation by one amino acid, and the presence of tRNA at the A site.

The third step is translocation, which requires the intervention of another eukaryotic elongation factor, eEF2 (its bacterial ortholog is known as EF-G). GTP-bound EF-G association with 80S leads to the hydrolysis of GTP that induces the translocation of mRNA and peptidyl-tRNA from A- to P-site of the ribosome. Thus, one codon (3 nucleotides) shift of

mRNA makes the A site free and positions the peptidyl-tRNA in the P-site and the deacylated-tRNA in the E-site (Green and Noller 1997). After the GTP hydrolysis, GDP-bound eEF2 dissociates the ribosome, which is now ready to start a new elongation cycle**.**

1.3. Termination

Translation termination occurs, when the stop codon (UAA, UAG or UGA) within mRNA reaches the A-site of the ribosome (Jackson et al. 2012). These three stop codons code for no amino acid and there is no tRNA for them. Termination depends on several release factors. Class I Release factor 1 (eRF1) binds in the A-site that adds a water molecule instead of amino acid to polypeptide resulting in hydrolysis of the polypeptide chain from the tRNA in the P-site and its release (Nakamura and Ito 2003). Class II Release Factor 3 (eRF3), which is a GTPase, interacts with eRF1 and both factors are ejected from the ribosome after hydrolysis of GTP (Salas-Marco and Bedwell 2004). Finally, ribosome-recycling factor ABC1 triggers splitting 80S on 60S and mRNA-bound 40S (Pisarev et al. 2010). Up to now, translation termination is under intensive investigations by many laboratories.

2. Translation initiation factors (eIFs)

In eukaryotes, at least 11 eIFs orchestrate cap-dependent translation initiation in order to facilitate 40S ribosomal subunit loading on mRNA, correct recognition of the start initiation codon, and 60S subunit assembly to form the 80S ribosome **(Table 2—1).**

2.1. Cap-binding translation initiation factors

Here I will describe factors that activate mRNA—the cap-binding complex eIF4F that is loaded at the 5' cap structure and participates in recruitment of 43S PIC to the mRNA.

2.1.1. eIF4F

eIF4F is a heterotrimeric complex containing three protein factors: (a) eIF4A, 46 kDa protein bearing an RNA-dependent ATPase activity and a helicase activity; (b) eIF4E, a small 24 kDa protein, which binds the 5' cap of mRNA and (c) eIF4G, large multidomain protein of 180 kDa, which acts as a scaffold protein assembling eIF4E, eIF4A, eIF3 and PABP. Cap and poly(A) tail binding proteins, eIF4E and PABP, could circularize an mRNA through simultaneous interaction with the 5′-cap and the poly(A) tail.

a. eIF4A

eIF4A belongs to the family of DEAD-box RNA helicases and has two inter-dependent activities – it acts as RNA-dependent ATPase and bi-directional ATP-dependent RNA helicase. eIF4A lacks any specifity for RNA sequences and acts locally, in ATP-dependent manner, to unwind the secondary and tertiary structures of the 5'UTR region of the mRNA facilitating the binding of the 43S PIC.

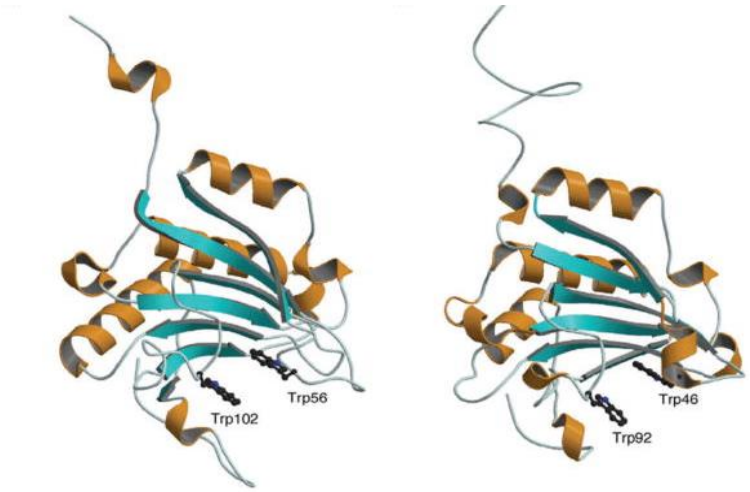

Figure 2—1 │X-ray structure of eIF4E (Left) and predicted 3D structure of eIFiso4E (Right)

The α-helix and β-sheet structures are shown. Two Trp residues participating in cap binding are shown with ball and stick models.
Modified from (Okade et al. 2009), *Journal of Biochemistry 145 (3): 299-307*

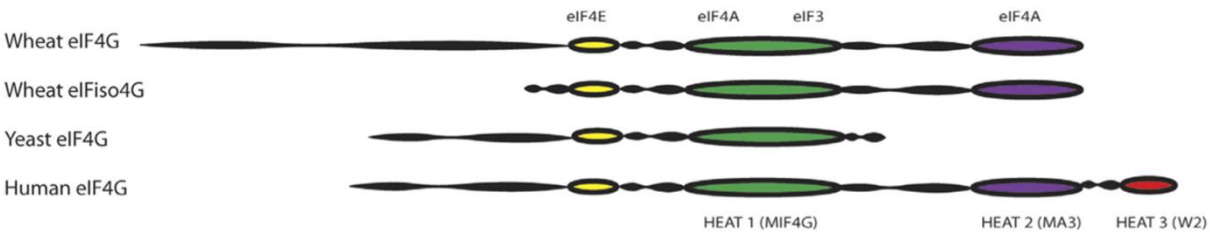

Figure 2—2 │Domain organizations of eIF4G and eIFiso4G

Plant eIF4G and eIFiso4G have similar domain organization, except that eIF4G has N-terminal extension. The eIF4E binding site and HEAT domains are indicated. The HEAT domains interact with eIF4A and eIF3 as indicated. Plant eIF4G and eIFiso4G lack the third HEAT domain present in mammalian eIF4G, and yeast eIF4G only has the HEAT 1 domain.
Modified from (Mayberry et al. 2011), *The Journal of Biological Chemistry 286 (49): 42566-42574*

eIF4A has two separate globular N-terminal and C-terminal α/β domains connected by a flexible linker forming a dumbbell-like structure. Binding of eIF4A to ATP and/or RNA induces conformational modifications between the N- and the C-terminus, indispensable for the helicase activity. The helicase activity modulated by ATP hydrolysis is inefficient and weakly possessive (Rogers et al. 1999). However, eIF4F in combination with eIF4B has an RNA helicase activity which is about 20 times more important than the factor eIF4A associated with eIF4B (Rozen et al. 1990), suggesting that this activity is mainly provided by the eIF4F complex (Pestova* and Hellen 2000).

eIF4A is highly conserved protein in eukaryotes, and was found in plants. Plant eIF4A shares structural and functional properties with yeast and mammalian eIF4A. Wheat germ eIF4A was characterized as a single polypeptide with a molecular weight of approximately 50 kDa, which function is similar to mammalian and yeast eIF4A. However, eIF4A is loosely associated with the cap-binding complex in plants (Lax et al. 1986; Abramson et al. 1988).

b. eIF4E

A cap-binding protein eIF4E is highly conserved throughout eukaryotic species. eIF4E interacts with eukaryotic cytoplasmic mRNA via the 7-methyl G(5')ppp(5')N (N= A, U, G or C) cap. The crystal structure of cap-bound eIF4E reveals its two faces: a concave face on the ventral surface, formed by a strongly bent β sheet of eight anti-parallel β strands, and a convex face on the dorsal face decorated by three α helices. The cap-binding cavity is located on the concave face, and the eIF4E-cap binding involves the interaction between the guanine of the cap and two highly conserved tryptophan residues of eIF4E (Trp56 and Trp102) in mammals **(Figure 2—1)**.

Within the eIF4F complex, eIF4E interacts strongly with eIF4G, at the opposite side of the cap-binding pocket, which in turn initiates translation by recruiting the 43S PIC. It has been

shown that eIF4E-eIF4G interaction is required for eIF4E binding to the mRNA 5'-cap. The interaction between eIF4E and eIF4G depends on a conserved motif of eIF4G, called canonical eIF4E-binding motif (4E-BM). The consensus sequence was identified as Y-X-X-X-X-L-ϕ (where Y denotes Tyr, X denotes any amino acid, L denotes Leu, and ϕ denotes a hydrophobic amino acid) (Marcotrigiano et al. 1999).

In addition, eIF4E binds PABP via eIF4G that promotes mRNA circularization. 5' and 3' UTR joining can up-regulate initiation translation (Gallie 1991; Tarun and Sachs 1995).

c. eIF4G

eIF4G is a multifunctional protein that plays a critical role in translation initiation, where it serves as a scaffold for the assembly of several initiation factors such as eIF4A, eIF4E, eIF3, eIF4B, eIF5 and PABP (Jackson et al. 2010; Hinnebusch and Lorsch 2012). Mammalian eIF4G is a very large multidomain protein of 180 kDa. It contains PABP and eIF4E-binding site at the N-terminal domain and up to three HEAT domains (MIF4G, MA3, W2) at the C-terminal domain (Korneeva et al. 2001; Bellsolell et al. 2006). However, yeast eIF4G retained the MIF4G domain, while plants—the MA3 domain and the MIF4G domain **(Figure 2—2)**. The highly conserved MIF4G domain is responsible for eIF4A binding (Marcotrigiano et al. 2001; Marintchev and Wagner 2004; Yamamoto et al. 2005).

d. eIFiso4F

The particularities of the plant translational machinery include two forms of the cap-binding complex—eIF4F and eIFiso4F—that differ in plants, but eIFiso4F was not found in other eukaryotic species. eIFiso4F contains two corresponding subunits: eIFiso4E and eIFiso4G (Browning et al. 1992; Browning 1996). In plants, eIF4A associates loosely with the cap-binding complex (Lax et al. 1986). eIFiso4F has a similar activity to that of eIF4F *in*

vitro (Browning 1996). eIF4E and eIFiso4E have about 50% similarity in amino acid sequence and molecular weight of about 24 kDa. However, eIF4G and eIFiso4G differ by their molecular weight: 165 kDa and 86 kDa respectively, and share only 30% homology. In comparison to eIF4G, eIFiso4G lost most of the N-terminal part, but their C-terminal domains are similar and both contain the eIF4E-binding site and two HEAT repeat domains (Patrick and Browning 2012).

Arabidopsis thaliana genome possesses four genes that encode cap-binding proteins: eIF4E1, eIF4E2, eIF4E3 and eIFiso4E, and 3 genes that encode: eIF4G, eIFiso4G1, and eIFiso4G2. Knockout of both eIFiso4G genes impairs fertility and seed viability, reduces germination and growth rates as well as chlorophyll levels in *Arabidopsis*. Recent results suggest that both isoforms—eIFiso4G1 and eIFiso4G2—affect translation of mRNAs that encode proteins involved in plant specific functions, such as seed production, fertility, flowering, photosynthesis, and response to environmental factors (Lellis et al. 2010).

The existence of two forms of plant-specific cap-binding complexes suggests their specific role in the translation initiation mechanism and indicates their functional specialization that allows to discriminate between different classes of mRNAs during translation initiation. Both eIF4F and eIFiso4F promote initiation of translation in plants (Gallie and Browning 2001). Their mixed complexes—eIF4G-eIFiso4E or eIFiso4G-eIF4E can function *in vitro* similarly to eIF4F or eIFiso4F, respectively. However, mixed complex activities correlate with eIF4G or eIFiso4G activities in the respective correct complex. Thus, the large subunit is dominant in determining the activity of the mixed complex (Mayberry et al. 2011). Interestingly, eIF4F is about 5-10 folds less abundant than eIFiso4F in wheat germs, maize root tips, and cauliflower florets (Browning et al. 1990; Browning et al. 1992).It has been shown the eIF4F enables more efficient translation than eIFiso4F of mRNAs with either highly structured 5’ UTRs, or multicistronic mRNAs, or uncapped mRNAs. In contrast,

eIFiso4F preferentially up-regulates translation initiation of unstructured mRNA (Gallie and Browning 2001). In addition to its functions in translation initiation of cellular mRNAs, plant eIF4F and eIFiso4F play a role in plant resistance to potyviruses. These viruses are characterized by a positive single-stranded RNA genome with a poly(A) tail at the 3'end and a VPg (viral protein linkend to the genome) linked covalently to the 5'-end of viral mRNAs (Murphy et al. 1991; Revers et al. 1999). VPg functions as a cap analogue that associates with eIF4E (Schaad et al. 2000) or with its isoform eIFiso4E (Wittmann et al. 1997). Mutations in eIF4E or eIFiso4E, as well as eIF4G or eIFiso4G trigger resistance to various viruses, for example *Turnip mosaic virus* (TuMV) (Duprat et al. 2002; Nicaise et al. 2007).

2.1.2. eIF4B

eIF4B is an RNA-binding protein that stimulates the RNA-dependent ATP hydrolysis and ATP-dependent RNA helicase activity of eIF4A, leading to stabilization of eIF4F binding to the 5' cap of mRNA. It also promotes 43S PIC binding to mRNA (Hinnebusch and Lorsch 2012). It's known that eIF4B is one of the least conserved eIFs, and does not appear to play an essential role in translation. Yeast lacking eIF4B gene are perfectly viable, but characterized by a cold sensitive phenotype (Altmann et al. 1993).

Plant eIF4B is not required for eIF4A activity, it can only moderately stimulate the ATP hydrolysis and the helicase activity of eIF4A (Browning et al. 1989). However, wheat eIF4B plays an essential role in initiation of translation, where it acts as a scaffold protein promoting the protein assembly on the mRNA. Wheat eIF4B shares about 29 and 24% amino acid similarity with human and yeast eIF4B, respectively (Cheng and Gallie 2006) **(Figure 2—3)**. The interaction between eIF4B and eIF4G has not been reported in other eukaryotes. Two domains of eIF4B participate in PABP binding, three—RNA binding (Cheng and Gallie 2006), and one—eIF3g binding (Park et al. 2004). PABP-bound eIF4B promotes eIF4F

association with the mRNA by inducing eIF4F binding to the cap structure (Khan and Goss 2005), and PABP binding to the poly(A) tail (Bi and Goss 2000). Thanks to these conserved domains, eIF4B plays a central role in plant translation initiation facilitating interaction between components of the translational machinery.

2.1.3. PABP

5' cap and 3' poly(A) interaction via PABP synergistically stimulates translation of mRNA (Gallie 1991; Tarun and Sachs 1995). PABP contains four N-terminal RNA recognition motifs (RRM1-4) and requires a minimum of 12 adenosine residues for its binding to poly(A) tail (Burd et al. 1991). Each RRM domain consists of two α helices and four anti-parallel β sheets. The C-terminal half of PABP (PABC) is responsible for its homodimerisation, where about 6 PABPs are required for association with the poly(A) tail in mammals. Thus, PABP interacts with eIF4G to bring together the cap and the poly(A) tail for efficient recruitment of 40S and stabilization of mRNA (Tarun and Sachs 1995; Le et al. 1997).

PABP is a highly conserved protein among eukaryotes. *Arabidopsis* genome possess eight PABP-encoding genes with varying tissue specific expression (Le et al. 2000; Belostotsky 2003). Plant PABP interacts with eIF4G/eIFiso4G and eIF4B in wheat germs (**Figure 2—4)**. These interactions promotes PABP binding to the poly(A) tail, which in turn up-regulates eIF4F affinity to the cap structure and stimulates ATPase and helicase activities of eIF4A, eIF4F/eIFiso4F, and eIF4B (Bi and Goss 2000; Cheng and Gallie 2006; Cheng and Gallie 2007). It has been shown that plant PABP promotes translation initiation internaly via binding to the reverse transcriptase of *Turnip mosaic virus* (TuMV) (Dufresne et al. 2008) or the 3'UTR of *Tobacco Etch Virus* (TEV) (Khan et al. 2008; Khan et al. 2009; Yumak et al. 2010; Iwakawa et al. 2012).

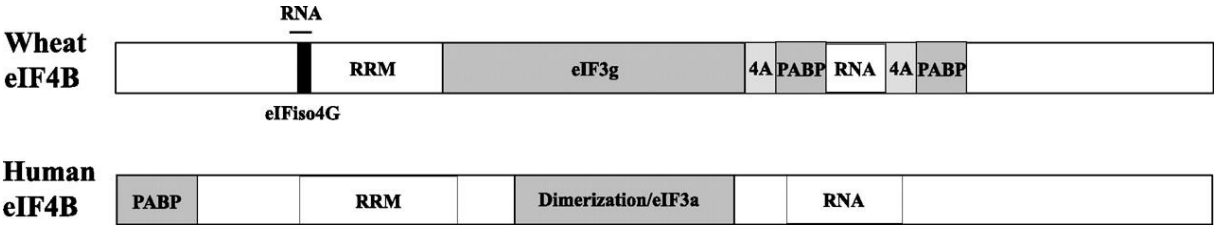

Figure 2—3 │Schematic presentation of wheat and human eIF4B

The RNA and protein binding domains, and their interacting partners are shown.
Modified from (Cheng and Gallie 2006), *The Journal of Biological Chemistry 281: 24351-24364*

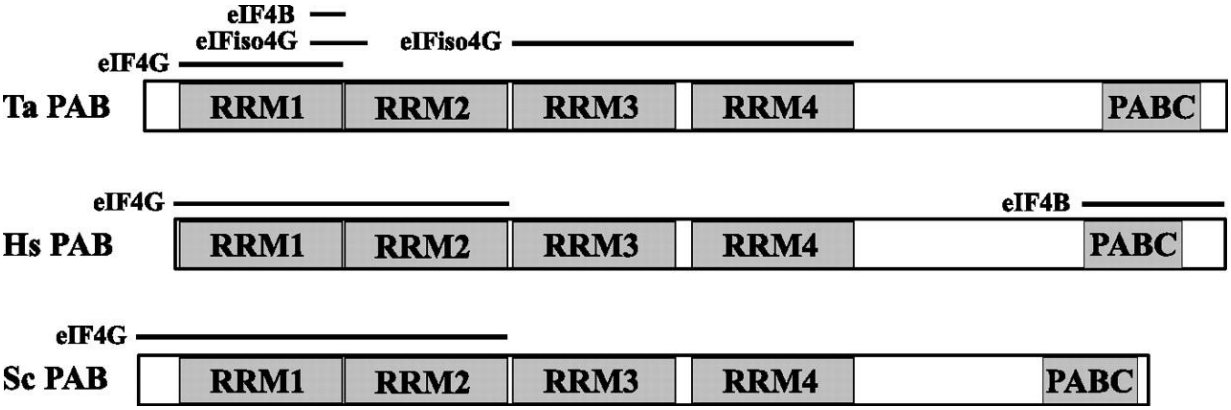

Figure 2—4 │Schematics of eIF4G, eIFiso4G and eIF4B interaction domains of wheat (Ta PAB), human (Hs PAB) and yeast (Sc PAB) PABPs

RRMs and the conserved C-terminal domains are indicated by the shaded boxes.
Modified from (Cheng and Gallie 2007), *The Journal of Biological chemistry 282 (35): 25247-25258*

2.2. The 43S preinitiation complex composition

These factors promote the 43S PIC assembly—eIF2-GTP carries Met-tRNA$_i$ to 40S; eIF1, eIF1A, eIF5 and eIF3 promote TC binding to 40S, eIF3 promotes 43S PIC binding to the mRNA **(Figure 2—5).**

2.2.1. eIF1/eIF1A

eIF1 and eIF1A are highly conserved polypeptides of small size (about 12-17 kDa) in eukaryotes (Hershey and Merrick 2000). Both bind 40S cooperatively with a high affinity (Maag and Lorsch 2003). eIF1A stimulates eIF1 association with 40S (Majumdar et al. 2003). eIF1 is loaded near the P-site, whereas, eIF1A—near the acceptor (A) site of the 40S subunit (Lomakin et al. 2003). eIF1A acts in synergy with eIF3 to promote binding of eIF2-GTP-Met-tRNA$_i$ (TC) to 40S (Olsen et al. 2003; Singh et al. 2004). Furthermore, both eIF1 and eIF1A are required for the 43S PIC scanning along the mRNA (Pestova et al. 1998), and the selection of the correct start codon. Mutations in the yeast SUI1 (homologous to eIF1) cause aberrant translation initiation at codons other than AUG (Yoon and Donahue 1992).

Additionally, eIF1 with eIF2, eIF3 and eIF5 forms a multifactor complex (MFC) that is loaded on 40S, while plant eIF1A binds 40S independently from MFC (Asano et al. 2000; Dennis et al. 2009; Hinnebusch 2014). It has been shown that eIF1 and eIF1A play a role in stress acclimation, since their overexpression leads to salt tolerance in plants (Sun and Hong 2013).

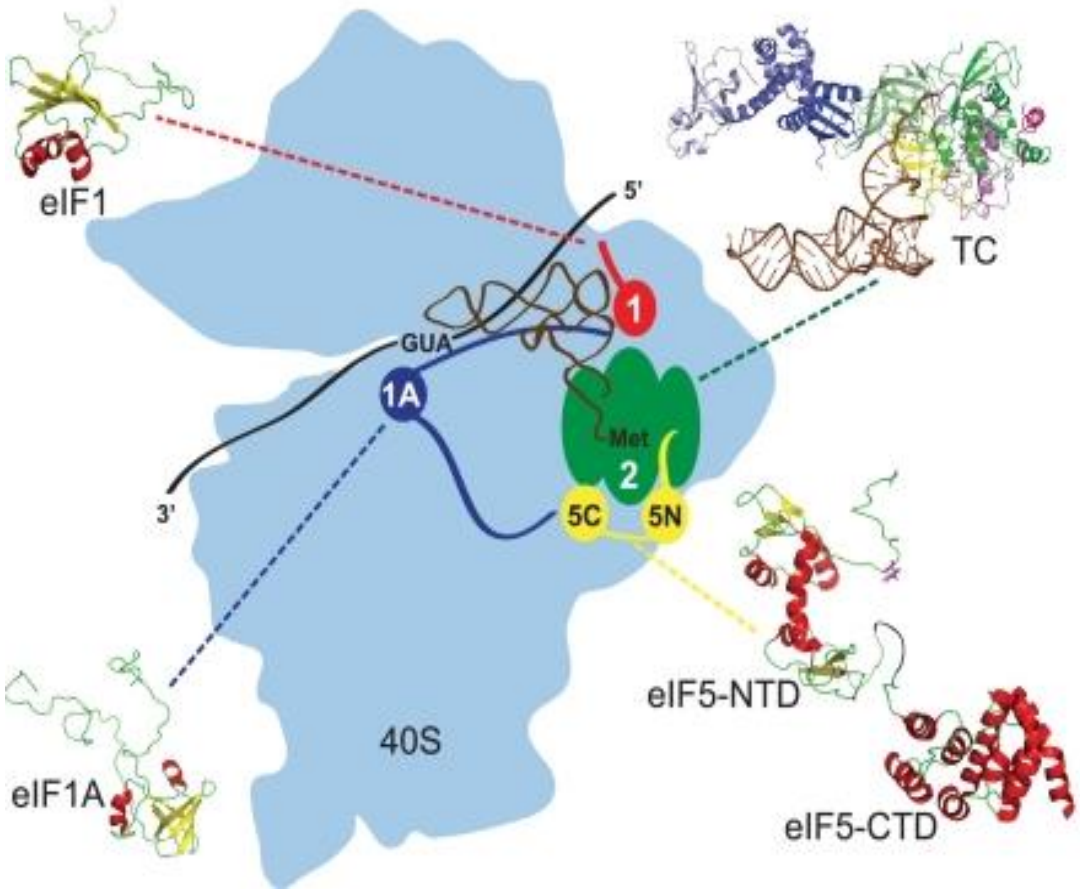

Figure 2—5 │Architecture of the 43S preinitiation complex

Schematic representation of 43S PIC (*light blue*) and PIC factors. Structures of human eIF1, eIF1A, eIF5 (human NTD and yeast CTD), and an archaeal TC are shown. TC composite structure consists of archaeal aIF2 and yeast $tRNA_i$. The structures of eIF1, eIF1A, and eIF5 are displayed with α-helices in *red* and β-strands *in yellow.*

Modified from (Lorsch and Dever 2010), *The Journal of Biological Chemistry 285 (28): 21203-21207*

2.2.2. eIF2/eIF2B

eIF2 is a heterotrimeric complex composed of three essentials subunits—eIF2α, eIF2β, and eIF2γ. eIF2α and eIF2β interact with eIF2γ to form the core of the complex. eIF2 is the most studied translation initiation factor. It is responsible for an active ternary complex formation and its delivery to 40S. TC plays a crucial role in the selection of the AUG start codon. A correct interaction between Met-tRNA$_i$ and AUG codon triggers eIF5-dependent GTP hydrolysis that activates the GTPase activity of the GTP-GDP recycling factor eIF2B (Huang et al. 1997). eIF2B is a guanine nucleotide exchange factor (GEF), which is responsible for the exchange of GDP by GTP for GDP-bound eIF2. eIF2B is composed of 5 subunits, α, β, γ, δ and ε. eIF2Bγ and eIF2Bε are responsible for the eIF2B catalytic activity, while the other three subunits have a regulatory function. The eIF2B catalytic and regulatory complexes interact with eIF2 independently—the first binds eIF2β (Gomez et al. 2002), while the second—eIF2α stimulating the release of GDP-bound eIF2γ (Krishnamoorthy et al. 2001).

Plant eIF2 is structurally and functionally similar to eIF2 from yeast and mammals, except that the third polylysine region within the N-terminal domain of plant eIF2β is missing, indicating that eIF2β is involved in plant specific interactions with Met-tRNA$_i$ (Metz and Browning 1997).

2.2.3. eIF3

The initiation factor 3 (eIF3) is a large protein of 750 kDa molecular weight composed of 13 different subunits in mammals and plants, eIF3a to eIF3m. In yeast, only six orthologues of mammalian eIF3 (a, b, c, i, g, j) are found, where five essential for translation subunits (a, b, c, g, i) form the catalytic "heart" (Hinnebusch 2016). However, eIF3j that promotes eIF3 binding with other eIFs and 40S is not essential (Fraser et al. 2004). eIF3 participates in 43S PIC and 48S PIC formation, the scanning of 43S PIC, and recognition of

the AUG initiation codon. It interacts with many other eIFs and orchestrates their organization on the surface of the 40S subunit.

In plants (wheat and *Arabidopsis*), all eIF3 subunits have been identified and showed strong similarity both in number and sequence to mammalian eIF3 subunits (Checkley et al. 1981; Heufler et al. 1988; Burks et al. 2001). The subunits m and I were described first in plant and then identified in mammalian eIF3 (Burks et al. 2001).

Several studies in *Arabidopsis* suggest that the eIF3 non-core subunit h (eIF3h) plays a role in translation of mRNA that harbors short upstream ORFs (uORFs) within their leader regions (Kim et al. 2004), and virus activated reinitiation after long ORF translation that operates on the *Cauliflower Mosaic Virus* (CaMV) 35S polycistronic mRNA. Here, reinitiation is supported by the viral protein TAV (transactivator/transplasmin). TAV promotes retention of eIF3 via its eIF3g subunit on translating ribosomes during the long translation event (Park et al. 2001; Park et al. 2004). TAV cofactor, reinitiation supporting protein (RISP), interacts also with eIF3 via subunits eIF3a and eIF3c (Thiébeauld et al. 2009).

2.2.4. eIF5/eIF5B

The eIF5 group of proteins contains eIF5, eIF5B and eIF5A, where all are conserved in eukaryotes. eIF5 and eIF5B play a role in the selection of the AUG initiation codon and promotes the codon-anticodon interaction, while eIF5A plays a role in elongation (Dever et al. 2014).

GTPase eIF5 promotes the hydrolysis of GTP-bound eIF2 immediately after the stop codon recognition (Jennings and Pavitt 2010; Nanda et al. 2013; Hinnebusch 2014). eIF5 consists of two functional C- and N-terminal domains. The N-terminal domain contains an "arginine finger" (Arg-15) required for GTPase activity. eIF5 interacts with eIF1 and N-terminal parts of eIF2β and eIF3c via the HEAT repeat domain at its C-terminus (Asano et al.

2000; Yamamoto et al. 2005). The C-terminal domain of eIF5 binds simultaneously eIF4G and the N-terminus of eIF3c, thus facilitating the interaction between the mRNA and the 43S complex (Singh et al. 2005). The C-terminal region of eIF5 is also involved in scanning of the 43S PIC and recognition of the start codon.

GTPase eIF5B contains four domains (I, II, III and IV). The domain I binds GTP and its hydrolysis induces eIF5B conformational changes that promotes the joining of 60S to the 48S complex (Pestova 2000). eIF5B also triggers eIF2-GDP, eIF1, eIF1A and eIF3 dissociation from 80S (Pisareva et al. 2006). When the ribosome is formed, the eIF5-bound GTP is hydrolyzed leading to its release from the ribosome (Pestova 2000).

2.2.5. eIF3j

eIF3j seems to participate in the assembly of the translation initiation machinery. Highly conserved eIF3j is a non-stoichiometric component of eIF3 in all organisms from yeast to mammals. eIF3j has a weak association with the eIF3 complex (Fraser et al. 2004), suggesting that eIF3j moves in and out the eIF3 complex. Indeed, it has been shown that eIF3 lacking the subunit j dissociates 40S in vitro, while eIF3j-bound eIF3 association with 40S is significantly improved (Fraser et al. 2004).

The cryo-EM 3D structure of the yeast 40S-eIF1-eIF1A-eIF3-eIF3j initiation complex (Aylett et al. 2015) suggests that eIF3j is located below the beak of the 40S subunit close to the eIF1A binding site. Accordingly, a direct contact between eIF3j and eIF1A has been described.

Table 2—1 │*Arabidopsis* initiation factors

Modified from (Browning and Bailey-Serres 2015), *The Arabidopsis Book 13: e0176*

Factor	Approximate molecular weight based on TAIR9 data (kDa)	Function	Arabidopsis Gene
eIF1	12.6	43S PIC formation and scanning; start site selection; eIF5-dependent GTP hydrolysis	At4g27130, At5g54760, At5g54940, At11g54290
eIF1(A)	17.6	43S PIC formation and scanning; start site selection	At5g35680, At2g04520
eIF2		TC formation; Met-tRNA$_i$ binding to 40S; eIF5-dependent GTP hydrolysis	
A	42	GCN2 kinase target in plants	At2g40290, At5g05470
B	38		At5g20920, At5g01940, At3g07920
ɣ	50		At1g04170, At4g18330
eIF2A		Unknown in plants; in mammals IRES mediated initiation	At1g73180
eIF2B		Recycles eIF2•GDP to eIF2•GTP; similar function in plants is unknown	
A	42-65		At1g53880, At1g72340, At1g53900
B	43.8		At3g07300
ɣ	49		At5g19485
Δ	37-73		At5g38640, At1g48970, At2g44070

ε	80		At3g02270, At2g34970, At4g18300
eIF3	13 subunits	43S and 48S PIC formation,scanning; start site selection; prevents pre-mature 60S ribosome association	
A	114		At4g11420
B	85		At5g27640, At5g25780
C	103		At3g56150, At3g22860
D	67		At4g20980, At5g44320
E	52		At3g57290
F	32		At2g39990
G	36		At3g11400, At5g06000
H	38	Required for reinitiation after uORF translation	At1g10840
I	36		At2g46280, At2g46290
J	25		At1g66070, At5g37475
K	26		At4g33250
L	60.2		At5g25754, At5g25757
M	50		At3g02200, At5g15610
eIF4A	47	ATP-dependent unwinding of mRNA mRNA binding to 40S subunit	At3g13920, At1g54270
eIF4B	58	ATP-dependent unwinding of mRNA mRNA binding to 40S	At3g26400, At1g13020

eIF4F		composed of eIF4G and eIF4E; ATP-dependent unwinding of mRNA; mRNA binding to the 40S subunit	
eIF4G	188	Interaction with eIF4A, eIF4B, eIF5, eIF4E	At3g60240
eIF4E	26	Binds to eIF4G and m^7GTP cap on mRNA	At4g18040, At1g29590, At1g29550
eIFiso4F		Composed of eIFiso4G and eIFiso4E; Plant specific isoform of eIF4F; ATP-dependent unwinding of mRNA; mRNA binding to 40S	
eIFiso4G	84	Interaction with eIF4A, eIF4B, eIF5, eIF4E	At5g57870, At2g24050
eIFiso4E	22.5	Binds to eIFiso4G and m^7GTP cap on mRNA	At5g35620
eIF5	48.6	60S Joining; GTPase	At1g77840, At1g36730
eIF5B	121-142	Positions Met-$tRNA_i$ at AUG with eIF1A	At1g76810, At1g21160
eIF5C	47	eIF5 “mimic protein” also called 5MP1 or BZW2; regulates eIF2 function by being both a mimic and competitor for eIF5; role unclear un plants	At5g36230, At1g65220
eIF6	26	Prevents association of 60S and 40S subunits	At3g55620, At2g39820
PABP	60-74	Binds poly A on mRNA; interacts with eIF4G	At2g23350, At4g34110, At1g22760, At1g71770, At3g16380, At1g49760, At2g36660, At1g34140, At5g65250

3. Control of translation initiation by target of rapamycin (TOR) in eukaryotes

The mechanistic Target of Rapamycin (TOR) is a serine/threonine protein kinase that belongs to the phosphoinositide 3-kinase (PI3K)-related kinase family (PIKK). It was discovered in 1991 in yeast *Saccharomyces cerevisiae* as a target of rapamycin, an antifungal, anticancer and immunosuppressive compound produced by the bacterium *Streptomyces hygroscopicus* isolated from Easter Island. In 1994, TOR was subsequently identified in mammals, as a 290 kDa protein (Sabatini et al. 1994; Brown et al. 1994). TOR is a highly conserved protein found in all eukaryotes.

The domain organization of TOR is close to other kinases of PIKK family. The N-terminal part contains HEAT (Huntingtin, Elongation Factor 3 has subunit of protein phosphatase 2A, TOR1) repeat motifs, which are involved in protein-protein interactions. The HEAT N-terminal domain is followed by a FAT domain (FRAP, ATM, TRRAP), a FRB domain, which is the target of rapamycin-FKBP12 complex, a ser/thr kinase catalytic domain, and finally a FATC domain (FAT Carboxy-terminus) (Zoncu et al. 2011) **(Figure 3—1—A)**. TOR exists in two functionally and structurally complexes, called TORC1 and TORC2 that differ in their functions, their protein composition and their activation mechanisms (Laplante and Sabatini 2012a).

3.1. mTORC1 and mTORC2 complexes

mTORC1 complex contains mTOR, the scaffold protein Raptor (Regulatory-Associated Protein of mTOR), mLST8 (mammalian Lethal with Sec13 protein 8), PRAS40 (Proline-Rich AKT Substrate 40 kDa) and Deptor (DEP-domain-containing mTOR-interacting protein). On the other hand, mTORC2 complex contains Rictor (Rapamycin-insensitive companion of

mTOR), mSIN1 (mammalian Stress activated protein kinase (SAPK) Interacting Protein 1), Protor (Protein observed with Rictor) in addition to mTOR, mLST8 and DEPTOR that are present in both complexes (Zoncu et al. 2011) **(Figure 3—1—B)**.

Raptor is a large 150 kDa protein containing several HEAT repeats and WD-40 that are involved in protein-protein interactions. Raptor directly binds the N-terminal part of mTOR and facilitates the recruitment of the substrates of mTORC1 complex such that S6K (70 kDa ribosomal S6 kinase 1 and 2) and the 4E-BP (eIF4E-binding proteins 1 and 2) (Hara et al. 2002) through a TOS motif (TOR-signaling) present in many substrates of mTORC1 (Schalm and Blenis 2002; Schalm et al. 2003). Raptor is also required for proper mTORC1 localization in lysosomes, where mTOR is activated (Sancak et al. 2008).

mLST8 is a small 36 kDa protein, which binds the kinase domain of mTOR via seven WD-40 motif repeats. Its function within the mTORC1 complex is unclear, but it has been shown that mLST8 is required for activation of mTORC1 by amino acids. mLST8 is also involved in the stabilization of the kinase domain of mTOR in active confirmation (Kim et al. 2003; Wullschleger et al. 2006).

Deptor is a 48 kDa protein, present in both mTORC1 and mTORC2 complexes; however, it is not an essential component. Deptor interacts with mTOR and partially inhibits mTORC1 and mTORC2 activities (Peterson et al. 2009).

PRAS40 is a 28 kDa protein, present only in mTORC1 complex. It interacts with Raptor and negatively regulates mTORC1 (Haar et al. 2007; Sancak et al. 2007). PRAS40 is a substrate of Akt (also known as PKB) (Kovacina et al. 2003) that phosphorylates PRAS40 leading to its dissociation from mTORC1 and mTORC1 activation.

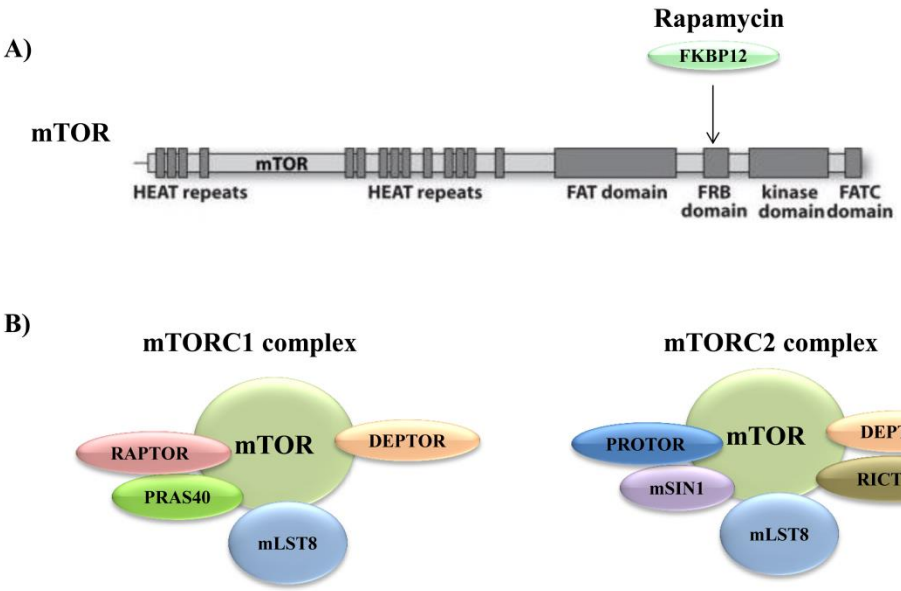

mTORC1 complex		mTORC2 complex	
Composition	**Function**	**Composition**	**Function**
mTOR	serine/threonine kinase	**mTOR**	serine/threonine kinase
RAPTOR	Scafold protein determing mTORC1 specific substartes and controlling its assembly and localization	**RICTOR**	Scafold protein determining mTORC2 specific substrates, and controlling its assembly
mLST8	Unknown function, its loss does not affect mTORC1 activity towards known substrates	**mLST8**	Unknown function but essentiel for mTORC2 activity
DEPTOR	mTORC1 inhibitor	**DEPTOR**	mTORC2 inhibitor
PRAS40	mTORC1 inhibitor	**mSIN1**	Scafold protein controlling mTORC2 assembly and its interaction with SGK
		PROTOR	Related to SGK activation

Figure 3—1 | mTORC1 and mTORC2 complexes

(A) Schematic representation of mTOR organization. mTOR contains Heat repeats on its N-terminus, followed by FAT domain, FRB domain for FKBP12-rapamycin binding, serine/threonine kinase domain, and FATC domain.

(B) mTORC1 and mTORC2 composition and the known functions of each compound.

Modified from (Laplante and Sabatini 2012b), *cell 149:274-293*

3.2. Functional role and activation of mTOR complexes

mTORC1 was initially described as sensitive to rapamycin; while mTORC2 is not, that could explain why the mTORC2 functions are less known. However, it was shown that mTORC2 is mainly implicated in cell survival and cytoskeleton reorganization by modulating the activity of several AGC (protein kinases A, G and C) family members like Akt, SGKA, PKCα and etc (Oh and Jacinto 2011). Due to its sensitivity to rapamycin, mTORC1 is very well described. It was found to control several anabolic mechanisms essential for cell growth and proliferation, such as protein lipid and nucleotide synthesis (Dibble and Manning 2013; Howell et al. 2013). The mTORC1 contributes to the positive regulation of protein synthesis.

A multitude of input cellular signals, such as growth factors, nutrients, and the cellular AMP/ATP ratio **(Figure 3—2)**, regulate the activity of mTORC1 in order to activate biosynthesis of proteins, lipids and nucleotides, and, on other hand, inhibit autophagy (Shimobayashi and Hall 2014).

Growth factors, such as insulin and IGF (Insulin-like Growth Factor 1), stimulate mTORC1 activity through the PI3K/Akt signaling pathway. Activation of the receptor by growth factor with tyrosine kinase activity leads to activation of several phosphorylation cascades in order to phosphorylate Akt kinase. Activated Akt stimulates mTORC1 activity in two ways; first, by reducing the interaction of the repressor PRAS40 with mTORC1 (Haar et al. 2007; Sancak et al. 2007) and, second, by phosphorylation and inactivation of the tuberous sclerosis complex 2 (TSC2) subunit of the TSC1/ TSC2 complex (Manning et al. 2002; Inoki et al. 2002). The TSC1/ TSC2 complex, a negative regulator of mTORC1, has GAP activity that specifically inactivates Rheb GTPase (Ras homolog enriched in brain), which in turn inhibits the kinase activity of TOR (Inoki et al. 2003).

In addition to growth factors, nutrients, amino acids such as leucine, arginine, and glutamine, are essential for the activation of mTORC1 (Hara et al. 1998; Nicklin et al. 2009).

The nutrient signaling towards mTORC1 involves a wide range of proteins orchestrating the activation of small GTPases called, Rag (Ras-related GTP-binding protein). 4 Rag proteins (Rag A, B, C and D) act as heterodimer and, when bound to Raptor, promote mTORC1 localization at the surface of lysosomes, where mTOR can be activated directly by GTP-bound Rheb (Sancak et al. 2008; Kim et al. 2008).

The cellular energy status, precisely ATP/AMP ratio affects mTORC1 activity through the AMP-activated protein kinase (AMPK). A deficit in energy (high AMP/ATP ratio) leads to activation of AMPK kinase, which inhibits mTORC1 via phosphorylation and activation of TSC2 (Inoki et al. 2003), or phosphorylation and inactivation of Raptor (Gwinn et al. 2008).

3.3. TORC1 signaling to the translational machinery in mammals

Protein synthesis, a key step in gene expression in eukaryotes, is essential for cell growth and proliferation and should be precisely regulated at different levels. mTORC1 is at the heart of this process playing a critical role in control of protein synthesis, with a particular emphasis on translation initiation phase, via direct or indirect phosphorylation of components of the cell translational machinery (Ma and Blenis 2009; Roux and Topisirovic 2012). It has been shown that mTORC1 selectively regulates the translation of mRNAs that contain a 5' terminal oligopyrimidine (TOP) motif (Hsieh et al. 2012; Thoreen et al. 2012). The two best characterized substrates of mTORC1 are known as eIF4E-binding proteins (4E-BPs) and the ribosomal S6 kinases (S6Ks).

The control of initiation translation by mTORC1 via 4E-BPs in mammals will be discussed in details in a separate chapter.

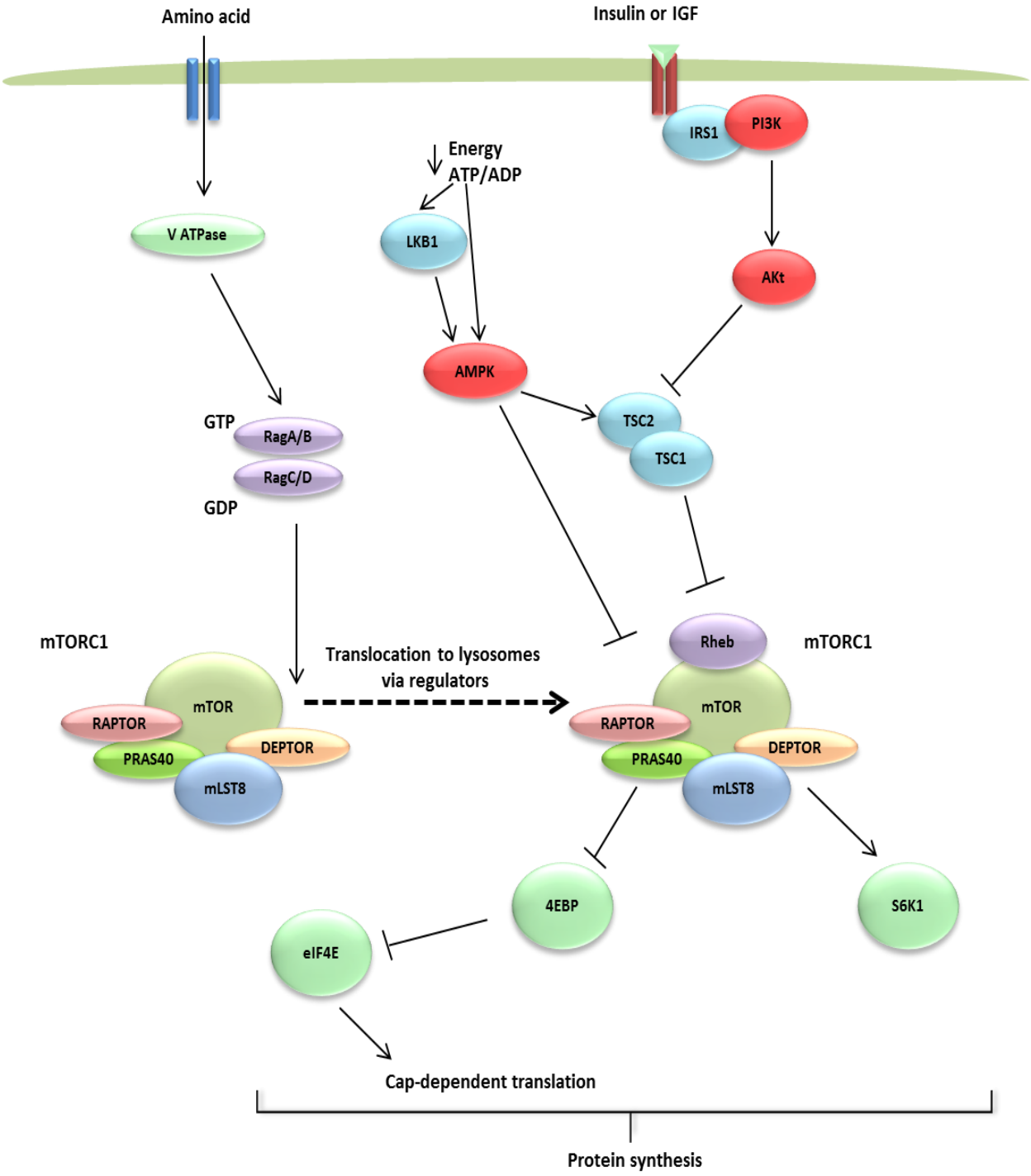

Figure 3—2 │A schematic presentation of mTORC1 and mTORC2 pathways

In response to growth factors, hormones, amino acids and high cellular energy status, PI3K/AKt and Ras/MABK signaling pathways up-regulate mTORC1. mTORC1 can control protein synthesis via S6K1 and 4E-BPs.

Modified from (Laplante and Sabatini 2012a), *Cold Spring Harbor Perspectives in Biology 10.1101*

3.3.1. Control of global and specific mRNA translation by TOR

mTORC1 regulates global mRNA translation particularly at the initiation level by affecting the assembly of the cap-binding complex eIF4F on 5' cap of mRNA. Although eIF4E is significant for the translation of the majority of mRNAs, changes in eIF4E expression or activation affected the translation of select groups of mRNAs. These mRNAs called "eIF4E-sensitive" mRNAs, contain long and structured 5'UTRs (Koromilas et al. 1992), encode for proteins involved in cell survival and proliferation such as cyclins, Myc, VEGF (Vascular Endothelial Growth Factor) or Bcl-XL (Graff and Zimmer 2003). The "eIF4E-sensitive mRNAs" are strongly dependent on the activity of eIF4E, which can be modulated by eIF4E-binding proteins (4E-BPs). 4E-BPs are the direct TOR downstream targets, suggesting that mTORC1 preferentially controls translation of "eIF4E-sensitive" mRNAs. Another group of mRNAs has been described to be selectively dependent on TOR. Indeed, translation of mRNAs that contain a 5' terminal oligopyrimidine (TOP) motif at their 5' end (Hsieh et al. 2012; Thoreen et al. 2012) became resistant to the mTOR inhibition, if 4E-BPs are inactivated. These data place 4E-BPs as principal and unique effectors of mTORC1 in mRNA translation control.

3.3.2. Control of mRNA translation by TOR via S6Ks

mTORC1 controls mRNA translation through the S6 kinases. In mammals, two S6 kinases have been identified (S6K1 and S6K2) (Ma and Blenis 2009); those kinases belong to the AGC kinase family. S6Ks are directly phosphorylated by mTORC1 and PDK1. mTORC1 phosphorylates the hydrophobic motif residue threonine 389 in human p70 S6K1, whereas PDK1 phosphorylates the activation loop at threonine 229 (Magnuson et al. 2011). S6K1 has several substrates involved in the global translation process, such as ribosomal protein S6 of the small 40S ribosomal subunit (RPS6) (Kozma et al. 1990; Banerjee et al. 1990), eIF4B

(Raught et al. 2004; Shahbazian et al. 2006), PDCD4 protein (Programmed Cell Death 4) (Dorrello et al. 2006), SKAR (S6K1 Aly/REF-like substrate) (Ma et al. 2008) and eEF2K kinase (Wang et al. 2001).

In translation control, S6K1 phosphorylates eIF4B (at serine 422) and induces its recruitment to the initiation complex in order to stimulate the helicase activity of eIF4A (Raught et al. 2004; Shahbazian et al. 2006). On the other side, S6K1 phosphorylates the repressor PDCD4 (at serine 67), leading to its dissociation from eIF4A, which then joins the initiation complex (Dorrello et al. 2006). S6K1 phosphorylates and inhibits the kinase eFF2 that is responsible for phosphorylation and inhibition of the elongation factor eEF2 (Wang et al. 2001). Phosphorylation and activation of SKAR (at serine 383 and 385)—another substrate of S6K1—stimulates the first cycle of mRNA translation (Ma et al. 2008). Another substrate of S6K1 is the ribosomal protein S6, which is phosphorylated at 5 residues: serine 235, 236, 240, 244 and 247 (Bandi et al. 1993).

4. Cap-dependent translation control via phosphorylation of 4E-BPs in mammals

mRNA expression is mainly controlled at the translation initiation level—a rate limiting step of translation (Hershey 1991). Particularly, the interaction between the cap-binding protein eIF4E and the large scaffold protein eIF4G is a subject of control via TOR. eIF4E is the least abundant factor among all eIFs, and misregulation of its expression is linked to various diseases and cancers (Furic et al. 2010). eIF4E interaction with eIF4G is regulated by a family of translational initiation repressors 4E-BPs in mammals and Drosophila (Gingras et al. 1999a; Hershey and Merrick 2000; Raught et al. 2000; Gingras et al. 2001). 4E-BPs are key mTOR targets in cap-dependent translation initiation.

4.1. Characterization of 4E-BP1/2/3

4E-BPs represent a family of three isoforms in human genome (also known as PHAS, for phosphorylated heat- and acid-stable), that act as repressors of translation initiation (Pause et al. 1994; Lin et al. 1994; Lawrence Jr and Abraham 1997; Poulin et al. 1998). They are small-molecular weight peptides—4E-BP1 (12.6 kDa), 4E-BP2 (12.9 kDa) and 4E-BP3 (10.3 kDa)—of 118, 120 and 100 amino acid residues, respectively. 4E-BP1 and 4E-BP2 were discovered first and thus better characterized. 4E-BP3 was discovered four years later. 4E-BP1 shares 60% and 57% overall amino acid identity with 4E-BP2 and 4E-BP3, respectively (Pause et al. 1994; Poulin et al. 1998).

Figure 4—1 | Schematic representation of three isoforms of human 4E-BPs

In this schema, phosphorylation sites are indicated *in red*; the conserved motifs required for TOR phosphorylation—the canonical eIF4E binding motif (YXXXXLϕ) is shown *in pink*; TOS motif (FEMDI)—*in bleu*; RAIP motif—*in green*.

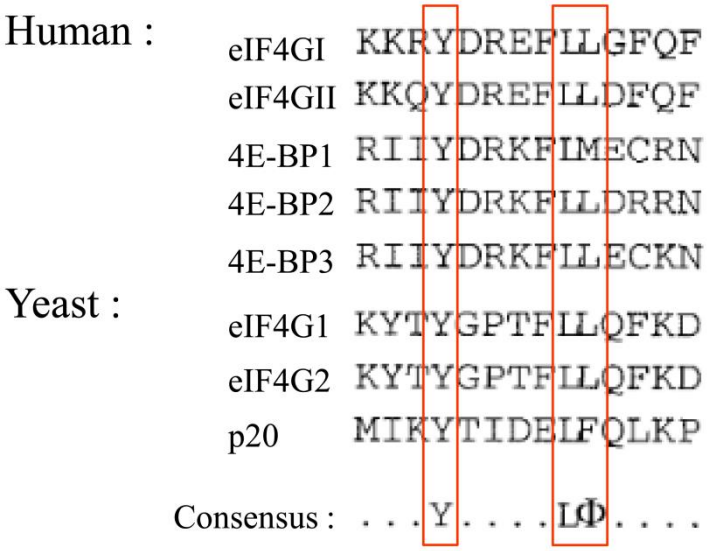

Figure 4—2 | Alignment of eIF4E-binding motifs present in eIF4G and 4E-BP proteins

The eIF4E-binding sites of eIF4G and 4E-BPs from human (4E-BP1, 4E-BP2 and 4E-BP3) and *S. cerevisiae* (p20) are shown. Φ refers to a hydrophobic residue.

Modified from (Gallie 2002), *Plant Molecular biology 50: 949-970*

The transcripts of 4E-BPs are located ubiquitously, but are enriched at high levels in some tissues (Poulin et al. 1998). 4E-BP1 mRNA is expressed in the skeletal muscle, pancreas and adipose tissue; 4E-BP2 mRNA is mainly present in the liver and kidney, but also in the central nervous system; 4E-BP3 mRNA is abundant in skeletal muscle, pancreas, heart and kidney.

4E-BPs are involved in many processes, such as cell growth, cell proliferation, synaptic plasticity, resistance to viral infections, fat metabolism or response to food shortages (Richter and Sonenberg 2005; Sonenberg and Hinnebusch 2007a; Sonenberg and Hinnebusch 2009). In cells, 4E-BPs are important regulators of the global protein synthesis. They inhibit exclusively the cap-dependent translation initiation both *in vitro* and *in vivo* (Pause et al. 1994), but have no effect on cap-independent translation. 4E-BPs don't block eIF4E binding to capped mRNA, but affects eIF4E binding to eIF4G. The inhibition seems to be competitive, since 4E-BPs and eIF4G share a similar eIF4E-binding site, through which they bind to the dorsal, convex surface of eIF4E located directly behind the cap binding site (Pause et al. 1994; Lin et al. 1994; Mader et al. 1995; Marcotrigiano et al. 1999).

4E-BPs are well-known substrates of the TOR signaling pathway, and phosphorylated directly by the Ser/Thr protein kinase TOR (Gingras et al. 2001; Hay and Sonenberg 2004). 4E-BP binding to eIF4E is reversible and depends on the phosphorylation status of 4E-BPs (Pause et al. 1994; Lin et al. 1994; Fadden et al. 1997). Non-phosphorylated or hypo-phosphorylated 4E-BPs interact with eIF4E by outcompeting eIF4G, and prevent the assembly of eIF4F at the cap, leading to repression of cap-dependent translation initiation. In contrast, when 4E-BPs are hyper-phosphorylated, they loss the affinity for eIF4E, and allow it to interact with eIF4G and form a functional eIF4F.

Organism	Protein	Sequence
Human	S6K1	FDIDL
	S6K2	FDLDL
	4E-BP1	FEMDI
	4E-BP2	FEMDI
	4E-BP3	FEMDI
	HIF1α	FVMVL
	PRAS40	FVMDE
	PKCδ	*FVMEF*
	PKCε	*FVMEY*
	STAT3	*FPMEL*
		FDMDL
Drosophila	S6K	FDLEL
	4E-BP	FQLDL
Xenopus	S6K	FDIDL
C. elegans	S6K	FEFEL
Artemnia f.	S6K	FEIEL
Aplysia	S6K	FDLEL

Table 4—1 | Known potential TOS motifs in selected proteins

TOS motifs are shown, where putative TOS motifs are indicated in *Italic*.

Modified from (Lee et al. 2008),*The FEBS Journal 275: 2185–2199*

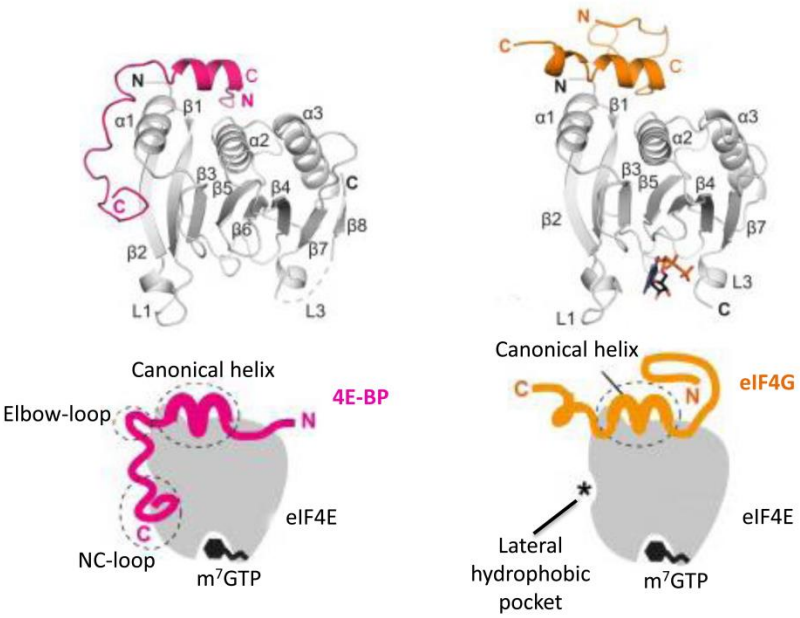

Figure 4—3 | Structures of h4E-BP and eIF4G segment bound to eIF4E

Overview and schematic representation of the structure of eIF4E bound to 4E-BP1, or the eIF4G fragment. Cap analog m^7GTP is shown. 4E-BP1 canonical 4E-binding and non-canonical C-terminal motifs are presented. eIF4G share the same canonical eIF4-binding motif with 4E-BP1.

Modified from (Peter et al. 2015), *Molecular Cell 57, 1074-1087*

Human 4E-BPs contain three conserved domains, where each domain has a specific role. The N-terminal motif of 4E-BP1 and 4E-BP2 is missed in 4E-BP3. The N-terminal motif is followed by the eIF4E-binding site and the TOS motif at the C-terminus **(Figure 4—1)**.

Canonical-eIF4E-binding site, according to its name, is required for interaction with eIF4E. The interaction between eIF4E and eIF4G also occurs through this motif, located in the N-terminus of eIF4G. The motif is highly conserved and contains a consensus sequence, Y-X-X-X-X-L-ϕ (where Y denotes Tyr, X denotes any amino acid, L denotes Leu, and ϕ denotes a hydrophobic amino acid) (Mader et al. 1995; Gingras et al. 1999a). Thus, 4E-BPs and eIF4G share the consensus eIF4E-binidng site. Thank to this motif they compete for binding to eIF4E **(Figure 4—2)**. Mutations in Tyr or Leu residues or the hydrophobic residue (ϕ) abolish 4E-BPs and eIFG interactions with eIF4E (Mader et al. 1995).

TOS motif is a TOR signaling motif located at the C-terminus of 4E-BPs, which contains five amino acids (FEMDI). This motif is essential for substrate binding to Raptor, which interacts with both TOR and 4E-BPs in order to present TOR substrates for TOR phosphorylation (Ma and Blenis 2009). The TOS motif is essential for substrate binding to Raptor and substrate phosphorylation by TOR. Any point mutation in FEMDI motif decreases substrate binding to Raptor, and thus its phosphorylation by TOR (Schalm et al. 2003; Eguchi et al. 2006; Lee et al. 2008). The TOS motif is present in all mTORC1 substrates, such as 4E-BPs and S6K1 **(Table 4—1).**

In addition to the eIF4E-binding site and the TOS motif, a regulatory motif RAIP has been found within 4E-BP1 and 4E-BP2 at the N-terminus, but 4E-BP3 does not contain RAIP. RAIP consist of four amino acid residues (Arg-Ala-Ile-Pro) (Wang et al. 2005), and regulates 4E-BP phosphorylation by TOR. RAIP mutations still promote its binding to Raptor, suggesting that it can have an accessory role in 4E-BP association with Raptor

(Eguchi et al. 2006). This suggestion can be also supported by the fact that RAIP is present only in 4E-BP1 and 4E-BP2, but not in 4E-BP3**.**

4E-BPs are described as an intrinsically disordered proteins, in other words they do not have any degree of secondary structure (Fletcher et al. 1998; Fletcher and Wagner 1998). Within the 4E-BP-eIF4E complex, the peptide with eIF4E-binding motif adopts an energetically favorable L-shaped α-helical conformation similar to that formed by eIF4E-bound eIF4G (Marcotrigiano et al. 1999). Several studies suggested the existence of stabilizing interactions between eIF4E and 4E-BP outside the eIF4E-binding site. A second conserved motif within the C-terminal part of 4E-BP (non-canonical 4E-binding motif, NC-loop) contains PGVTS/T sequence (residues 79-83) and it is involved in 4E-BP binding to eIF4E (Gosselin et al. 2011; Paku et al. 2012). The third non-canonical eIF4E-binding site within 4E-BPs consist an elbow loop immediately after the canonical eIF4E-binding site (Peter et al. 2015) **(Figure 4—3)**. The presence of non-canonical motifs (Elbow loop and NC-loop) increases the affinity of 4E-BPs for eIF4E by three orders of magnitude and both are required for 4E-BPs to outcompete eIF4G for eIF4E binding and repress translation (Paku et al. 2012; Lukhele et al. 2013; Igreja et al. 2014).

4.2. TOR phosphorylation regulates 4E-BP binding to eIF4E

The activity of 4E-BPs can be regulated by its phosphorylation. 4E-BPs phosphorylation on multiple sites affects its association with eIF4E, thus making eIF4E free to interact with eIF4G and initiate translation (Gingras et al. 1999a). 4E-BPs are directly phosphorylated by the FRAP/mTOR pathway downstream of the PI3K-Akt signaling pathway in response to the availability of amino acids, cellular energy status, stressful situations, various hormones, growth factors, etc (Richter and Sonenberg 2005; Ma and Blenis 2009).

(A)

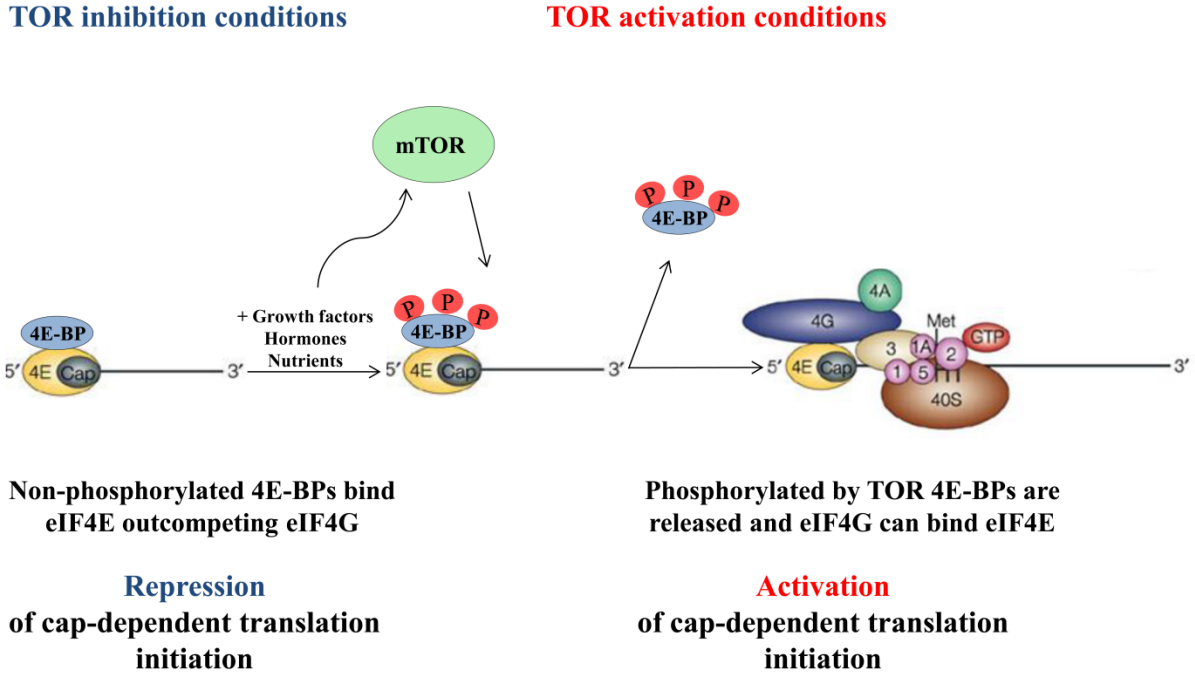

(B)

Phosphorylation hierarchy	Binding to eIF4E	Not binding to eIF4E
Un(P)->Thr 37/Thr 46->Thr 70->Ser 65	Un(P)	Thr 37/Thr 46/Thr 70/Ser 65
	Thr 37/Thr 46	
Un(P)->Thr 70-> Thr 37/Thr 46->Ser 65	Un(P)	Thr 37/Thr 46/Thr 70
	Thr 70	Thr 37/Thr 46/Thr 70/Ser 65

Figure 4—4 ⎪Model of TOR translational control by 4E-BPs

(A) In TOR inactivation conditions, non-phosphorylated 4E-BPs outcompete eIF4G for eIF4E binding that lead to repression of cap-dependent translation initiation. In response to growth factors, hormones or nutrient sufficiency, TOR is activated and phosphorylates 4E-BPs. Phosphorylated 4E-BPs loss their eIF4E binding ability. eIF4E interaction with eIF4G lead to activation of cap-dependent translation initiation.

Modified from (Gebauer and Hentze 2004), *Nature Reviews Molecular Cell Biology 5: 827-835*

(B) **The two models proposed for phosphorylation hierarchy pathway of h4E-BP1**

Modified from (Ayuso et al. 2010), *The Journal of Biological Chemistry 285: 34355-34363*

The use of rapamycin, an inhibitor of mTOR kinase, prevents phosphorylation of 4E-BPs and thus blocks the cell cycle in G1 phase via inhibition of cap-dependent translation initiation (Beretta et al. 1996) **(Figure 4—4).**

In mammalian adipocytes, insulin stimulates phosphorylation of 4E-BP1 and 4E-BP2, leading to their dissociation from eIF4E. These phosphorylation events are sensitive to rapamycin (Lin and Lawrence 1996). However, the mechanism of 4E-BP3 regulation is different than that for 4E-BP1 and 4E-BP2 and independent on the TOR pathway. For example, rapamycin does not affect the association of 4E-BP3 with eIF4E in cultivate human cell (Kleijn et al. 2002).

Among human 4E-BPs, h4E-BP1 is the best characterized isoform with seven phosphorylation sites: Thr 37, Thr 46, Ser 65, Thr 70, Ser 83, Ser 101 and Ser 112 (Fadden et al. 1997; Heesom et al. 1998) **(Figure 4—4—B).** Ser 65 is the first phosphorylation site discovered in h4E-BP1, followed by the discovery of the four other sites, Thr 37, Thr 46, Thr 70 and Ser 83 (Haystead et al. 1994; Fadden et al. 1997). Phosphorylation of Thr 37, Thr 46, Ser 65, and Thr 70 is rapamycin-sensitive, in contrast to phosphorylation of Ser 83 (Mothe-Satney et al. 2000).

Phosphorylation of 4E-BP occurs in multiple steps and in hierarchical order (Gingras et al. 1999a; Gingras et al. 2001). Thr 37 and Thr 46 are first sites that are phosphorylated by mTOR. Phosphorylation of these two sites is insensitive to rapamycin or to serum deprivation, and does not dissociate 4E-BP from eIF4E. However, their phosphorylation is required for phosphorylation of Thr 70, which in turn is necessary for Ser 65 phosphorylation. There is an order in the addition of phosphate group on these residues. First, phosphorylation of Thr 37 and Thr 46 occur as the first event and followed by phosphorylation of Thr 70 and finally phosphorylation of Ser 65 **(Figure 4—4—B)**. Phosphorylation of Thr 70 and Ser 65 is sensitive to rapamycin and serum deprivation, but it is insufficient to dissociate the 4E-BP-

eIF4E complex (Gingras et al. 2001). Only phosphorylation of Thr 37, Thr 46, Thr 70 and Ser 65 is sufficient to liberate eIF4E from 4E-BP1 and activate translation initiation (Gingras et al. 2001; Niedzwiecka et al. 2002; Wang et al. 2005). However, another hierarchical mode was proposed (Ayuso et al. 2010)—Thr 70 is phosphorylated first followed by phosphorylation of Thr 37 and Thr 45, and, finally, phosphorylation of Ser 65 **(Figure 4—4—B).** Two additional phosphorylation sites—Ser 101 and Ser 112—are insensitive to rapamycin and does not affect 4E-BP1 binding to eIF4E (Proud 2006). These sites have been identified only in h4E-BP1, but not in 4E-BP2 and 4E-BP3 (Heesom et al. 1998; Wang et al. 2003). The role of individual phosphorylation sites and mechanisms of 4E-BP regulation are still unclear and require carefully characterization.

4.3. Biological significance of 4E-BPs in cell and diseases

4.3.1. Role in cancer

The essential role of eIF4E in controlling translation initiation, and thus gene expression, makes this actor as a protein with high oncogenic property (Sonenberg 2008). This places 4E-BPs as eIF4E repressors in a number of important tumor suppressors (Martineau et al. 2013). These two players, eIF4E and 4E-BPs, are subjects to regulate protein expression level. Disruption of each of these regulations causes a dysfunction that can lead to the transformation of a normal cell into a cancerous cell.

Overexpression of eIF4E was detected in several cancer types such as, bronchioalveolar, bladder, head, neck, liver, colon, breast cancers (De Benedetti and Graff 2004). eIF4E, when overexpressed, generates tumors in different cellular tissues (Ruggero et al. 2004) that correlates with increased translation of mRNA groups involved in cellular processes such as proliferation, angiogenesis, or survival (Konicek et al. 2008; Silvera et al. 2010). These mRNAs encoding proteins such as cyclin D1, ODC, CDK2, cMYC, Mcl-1,

Bcl-2, VEGF, FGF2 or MMP9 (Clemens 2004; Mamane et al. 2004; Hsieh and Ruggero 2010) are not expressed in normal cell conditions. Thus, 4E-BPs are considered to be as tumor suppressors (Martineau et al. 2013). Overexpression of 4E-BP1 and 4E-BP2 can reverse tumor phenotype associated with overexpression of eIF4E (Rousseau et al. 1996). The phosphorylation state of 4E-BPs plays an important role in the process of cell transformation and cancer development. The analysis of 4E-BPs allows identifying patients at high risk, since 4E-BP1 phosphorylation is an indicator of disease progression in breast or prostate cancer (Rojo et al. 2007; Armengol et al. 2007). Therefore, 4E-BPs are major therapeutic targets in cancer treatment.

4.3.2. Role in brain

4E-BP2 is enriched isoform in brain, where it plays an essential role in synaptic plasticity, learning and memory. Knockout of 4E-BP2 in mice results in alteration in hippocampal long-term potentiation (LTP) and in hippocampus-dependent memory (Banko et al. 2005; Banko et al. 2006; Banko et al. 2007). These alterations are due to the high level of eIF4F complex formation found in KO mice brain. These results highlight the importance of 4E-BP2 in brain and how it controls eIF4F complex formation and how translational control triggers LTP and memory. Alterations in light/dark exploration and rotating rod test in KO mice support the critical role of 4E-BP2 in complex motor skill performance (Banko et al. 2007).

Recent studies demonstrate an asparagine-deamidation of 4E-BP2 which is unique for 4E-BP2 and brain-specific that plays an essential role in synaptic activity (Bidinosti et al. 2010). 4E-BP2 contains an asparagine rich-sequence of six closely spaced asparagines near to its C-terminus, N 99 and N 102 are the two mapped deamidation sites. Deamidation of 4E-BP2 enhances its binding to Raptor which in turn spatially sequesters 4E-BP2 away from

eIF4E. Conversion of asparagine to aspartate in brain 4E-BP2 may compensate the attenuation of PI3K-AKt-mTOR signaling pathway during postnatal development.

4.3.3. Role in apoptosis

Rapamycin, which specifically inhibits the function of mTOR, is helpful in the treatment of several cancer types by inducing apoptosis through 4E-BPs (Proud 2004; Wang et al. 2005). A positive correlation was observed between 4E-BP levels and rapamycin-induced apoptosis in rhabdomyosarcoma cell lines (Houghton and Huang 2004) and colon carcinoma cell lines (Dilling et al. 2002). The ectopic expression of 4E-BPs was reported in proapoptotic expression (Proud 2004). In Ras-transformed fibroblasts, 4E-BP1 induces apoptosis (Polunovsky et al. 2000). Activation of caspase triggers 4E-BP1 cleavage within RAIP motif, that enhance 4E-BP1 phosphorylation by TOR (Tee and Proud 2002). Resulted hypophosphorylated 4E-BP1 sequesters eIF4E and shut down translation of some mRNAs in order to promote translation of IRES-mRNA that encodes protein-induced apoptosis.

4.3.4. Role in immunity

4E-BP constitutes a new effector in activation of the innate immune response in response to viral infection. Cytokines, such as type-I interferons (IFN-α and IFN-β), form the first line of antiviral defense. New way to induce innate immune response has been shown in mice though 4E-BPs (Colina et al. 2008). 4E-BPs negatively regulate the production of type-I IFN by translational repression of the interferon regulatory factor 7 (IRF-7) mRNA. Knockout of both 4E-BP1 and 4E-BP2 in mice, results in increased production of type-IFN making mice resistant to infection by vesicular stomatitis virus (Colina et al. 2008).

4.3.5. Role in metabolism

4E-BPs act as a regulator of metabolism—their misregulation can lead to several pathologies, such as diabetes and obesity (Sonenberg and Hinnebusch 2007b). Knockout of 4E-BP1 and 4E-BP2 in mice results in increase of sensitivity to diet-induced obesity due to the increase of adipogenesis and alterations in fat metabolism, and increased insulin resistance (Le Bacquer et al. 2007). In Drosophila, overexpression of 4E-BP increases the accumulation of fat (Teleman et al. 2005). Thus, 4E-BPs play the role of metabolic brake in response to stress conditions, but not during normal development.

4.4. 4E-BP-like orthologs from non-human organisms

4.4.1. 4E-BP-like orthologs from Leishmania

Leishmania parasites are ancient eukaryotes containing a large polycistronic chromosomal units, which are trans-spliced and polyadenylated into mature monocistronic mRNAs (LeBowitz et al. 1993; Matthews et al. 1994). All mRNAs carry a unique cap structure denoted as cap-4, which is highly modified within the first four nucleotides (m^7Gpppm_3 $^{6,6,2'}$ $Apm^{2'}$ $Apm^{2'}$ Cpm_2 $^{3,2'}U$) as compared with the standard m^7GTP cap found in higher eukaryotic species (Bangs et al. 1992). Four eIF4E orthologues have been characterized in *Leishmania* genome and named as LeishI4E1, LeishI4E2, LeishI4E3 and LeishI4E4. LeishI4E are highly diverged from eIF4E family of higher eukaryotes (Yoffe et al. 2009). Six proteins containing the MIF4G domain were found in *Leishmania* genome, but having a low degree of homology to mammalian eIF4GI. Only LeishIF4G3 was identified as the scaffold protein of the LeishIF4F cap-binding complex (Yoffe et al. 2009). Interaction between LeishIF4E4 and LeishIF4G3 was mediated by the LeishIF4E-containing domain (YPGFSLD) that partly resembles the canonical eIF4E-binding site.

In *Trypanosomatidae* family, as well as in *Ceanorhabditis elegans*, no 4E-BP homologue was identified based on sequence conservation. However, a novel eIF4E-interacting protein (Leish4E-IP) was identified in *Leishmania* (Zinoviev et al. 2011). Leish4E-IP associates with LeishI4E1 (eIF4E ortholog in *Leishmania*) in pull down experiments. This protein was highly conserved between different *Leishmania* species, but showed no homology with other proteins outside the *Trypanosomatidae* family. This protein was described as 4E-interacting protein but does not resemble the consensus 4E-BP from higher eukaryotes. However, LeishIF4E-IP displays some characteristic of 4E-BPs, it contains a consensus eIF4E-binding site required for eIF4E binding, but found at the N-terminus of LeishIF4E-IP. LeishIF4E-IP was considered as unstructured protein, except of the eIF4E-binding site that adopts a helical structure.

In *Leishmania*, it was reported that the prolonged exposure to elevated temperatures during differentiation reduces the affinity of LeishIF4E-IP to LeishIF4E1, and LeishIF4E-IP becomes phosphorylated suggesting that LeishIF4E-IP shares similar properties and functions similar to 4E-BP from higher eukaryotes.

4.4.2. 4E-BP-like orthologs from Drosophila melanogaster

Drosophila contains seven eIF4E isoforms that are differentially expressed during development (Hernández et al. 2005). The large number of eIF4E genes in Drosophila raised the possibility of their regulation by so-far-unknown 4E-BP.

4E-BP family is conserved in flies. One ortholog of mammalian 4E-BP has been identified in Drosophila, and named as d4E-BP. Like mammalian 4E-BPs, d4E-BP was described as a target of the TOR signaling pathway. In d4E-BP, Thr 37, Thr 46, Ser 65, and Thr 70 are identical to 4E-BP1, but Ser 83 is a Thr residue, Ser 101 is Gln, and Ser 112 is absent (Miron et al. 2001; Miron et al. 2003).

CUP, an insect-specific protein, belongs to the 4E-BP family in Drosophila and targets specifically localized transcripts. Cup is involved in translation repression of at least three localized and developmentally essential mRNAs (*nanos*, *oskar*, and *gurken)* (Verrotti and Wharton 2000; Wilhelm et al. 2003; Clouse et al. 2008). No structural conformation has been reported for CUP. A canonical eIF4E-binding site has been found in the N-terminal region of CUP followed by an eIF4E-transporter-like (4E-T-like) region. The eIF4E-binidng site found in CUP is similar to the consensus eIF4E-binding site found in 4E-BPs and eIF4G. The site is sufficient for CUP binding to eIF4E. A second non-canonical eIF4E-binding site that is sufficient to outcompete eIF4G for eIF4E binding, has been mapped in CUP (Nelson et al. 2004; Kinkelin et al. 2012). Mutations within the site reduced CUP binding to eIF4E and triggered destabilization of the associated mRNA (Kinkelin et al. 2012). Two Serine residues (Ser 347 and Ser 350) have been identified as phosphorylation sites in CUP (Zhai et al. 2008), but whether their phosphorylation is implicated in translational repression remains to be clarified.

Mextli (Mxt) is a novel 4E-BP discovered in Drosophila (Hernández et al. 2013). A canonical eIF4E-binding site was found at the Mxt C-terminus. Surprisingly, an MIF4G domain similar to that within eIF4G was found at the Mxt amino-terminal region followed by RNA-binding KH domain. Mxt interacts with RNA, eIF3 and eIF4Es and thus, renders Mxt as a novel type of scaffolding protein alternative to eIF4G. In contrast to other 4E-BPs, Mxt coordinates the assembly of translation initiation complexes and promotes translation like eIF4G.

5. Plant translation initiation

5.1. Aspects of translation initiation unique to plants

The majority of translation events are conserved across eukaryotes; however some modifications are unique to plants. Higher plants, such as *Arabidopsis*, possess two quite distinct cap-binding complexes for 5' cap recognition. In addition to the classical conserved eIF4F complex composed of eIF4E and eIF4G, they also have a plant-specific eIFiso4F complex composed of eIFiso4E and eIFiso4G. These two complexes have similar functions; both can initiate cap-dependent translation *in vitro* and each complex alone is sufficient for translation (Browning 1996). However, they differ quantitatively in their expression levels; eIF4F is about 5-10 times less abundant than eIFiso4F in wheat germ extract (Browning et al. 1990). They have the ability to discriminate between mRNAs groups. eIF4F mainly promotes translation of mRNAs containing complex secondary structures (Gallie and Browning 2001). The two cap-binding proteins, eIF4E and eIFiso4E, share about 50% identity in amino acid sequence and have similar molecular mass around 24 kDa. However, the two scaffold proteins eIF4G and eIFiso4G differ in their molecular mass (180 and 86 kDa, respectively), suggesting that they have different roles in translation regulation mechanism (Browning 1996).

Both eIF4F and eIFiso4F are targets for viral infection in plants, especially for photyviruses that contain a VPg (genome-linked viral protein) covalently linked to the 5'-end of viral transcript. It was suggested that the VPg acts as a cap analogue that also binds to a particular cap-binding complex (eIF4F or eIFiso4F). Mutations of different components of initiation complexes confer resistance to the virus (Duprat et al. 2002; Nicaise et al. 2007). The presence of two initiation complexes in plants may place the virus under selection pressure to prefer one isoform to the other, and to remain the other isoform available for cellular mRNA translation.

The most important difference in translational apparatus between plants and other eukaryotes is that plant orthologs of 4E-BPs are not yet discovered. However, eIF4E can interact with *Arabidopsis* lipoxygenase type 2 as documented by the yeast two hybrid systems and *in vitro* biochemical assays (Freire et al. 2000). Lipoxygenase 2 contains a sequence (between amino acids 175 and 232) involved in eIF4E binding, and is related to the canonical eIF4E-binding site. The interaction between lipoxygenase 2 and AteIFiso4E was decreased by wheat eIFiso4G. However, whether this interaction occurs in planta and its physiological relevance remain unclear.

5.2. TOR signaling pathway in plants

Unlike animals, plants due to their immobility are affected by environmental conditions. They are strongly dependent on nutrient and water availability in soil, exposure to light, temperature, stress, etc ... The challenging goal for plants is to create specific mechanisms to control cell growth, development and enhance its survival in unfavorable external conditions. The major pathway described in yeast and mammals is known as the TOR signaling pathway. In response to growth factors, hormones, nutrients and cellular energy status TOR controls ribosomal biogenesis, transcription and translation that collectively contribute to cell growth (Dennis et al. 1999; Laplante and Sabatini 2012b). The evolutionary conserved TOR up-regulates cell growth in part by positively regulating protein synthesis in plant. Plant TOR is structurally and functionally conserved among all eukaryotes. *Arabidopsis* TOR shares high similarity in amino acid composition with human TOR (Ahn et al. 2011; Xiong and Sheen 2012; Xiong et al. 2013) **(Figure 5—1)**.

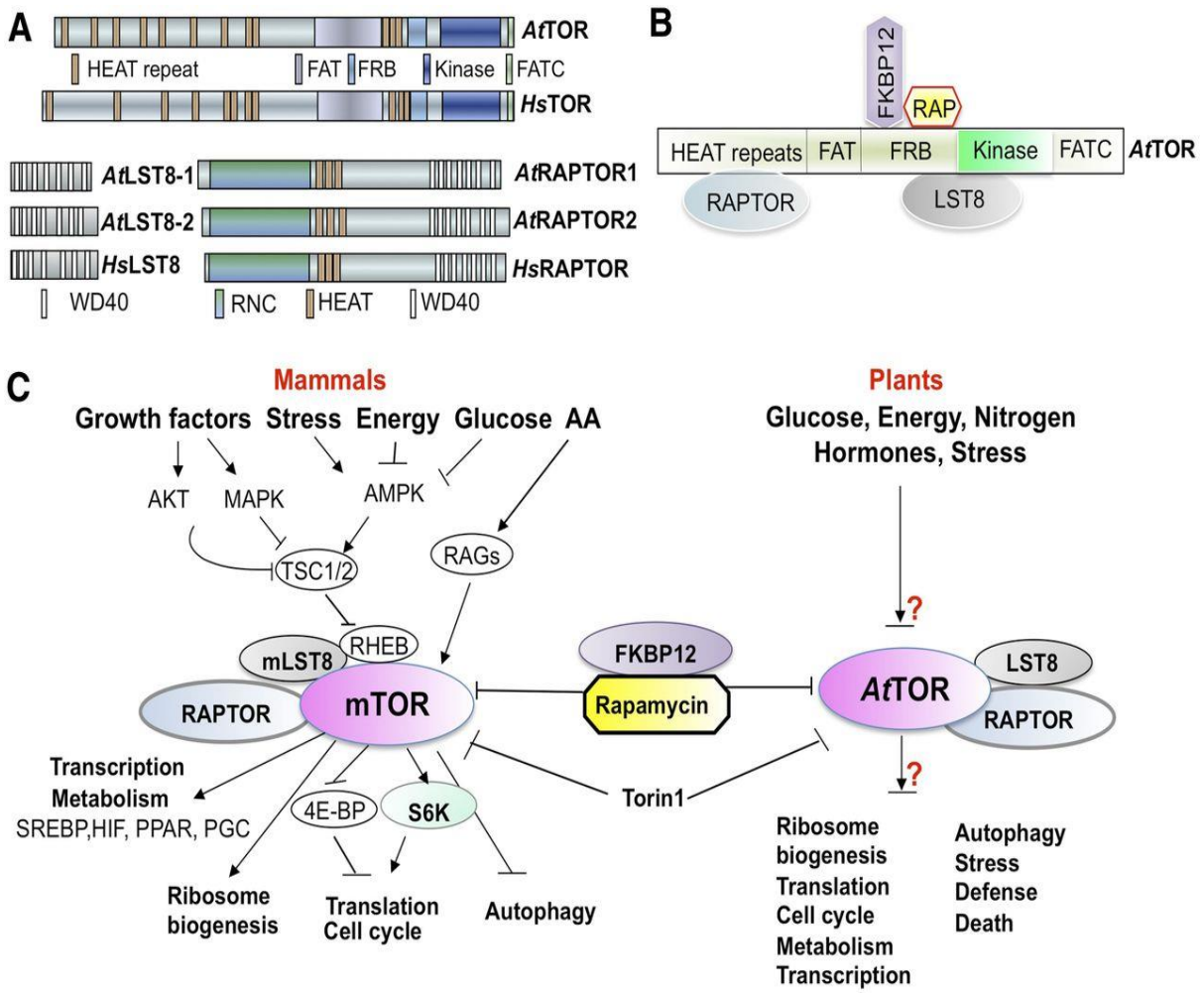

Figure 5—1 │ TOR signaling in Arabidopsis and mammals

(A) Conservation of domain organization in human (Hs) and Arabidopsis (At) TOR signaling components.

(B) Interaction map of Arabidopsis TOR domains and RAPTOR, LST8, FKBP12, and rapamycin (RAP).

(C) Plant and mammalian TOR signaling networks

(AA, Amino acid; FAT, FRAP, ATM, and TRRAP domain; FATC, Carboxy-terminal FAT domain; HEAT repeats, Huntingtin, Elongation factor 3, subunit of protein phosphatase 2A and TOR1; HIF, hypoxia-inducible factor; PGC, peroxisome proliferator-activated receptor-γ coactivator; PPAR, peroxisome proliferator-activated receptor; RNC, Raptor N-terminal Conserved/putative Caspase domain; SREBP, sterol regulatory element-binding protein; TSC1/TSC2, tuberous sclerosis1/tuberous sclerosis2; WD40, WD40 repeat domain).

Modified from (Xiong and Sheen 2014), *Plant Physiology 164: 499-512*

The TOR gene is expressed in all *Arabidopsis* tissues, with the highest level of its expression in young growing tissues (root tips or emerging leaves). The precise characterization of the TOR complex remains uncomplete in plants. Several mTORC1 components and downstream effectors have been identified in *Arabidopsis* based on sequence similarity analysis. *Arabidopsis* genome encodes a single TOR gene like in mammals (Menand et al. 2002; Anderson et al. 2005; Deprost et al. 2005; Deprost et al. 2007; Liu and Bassham 2010), while there are two RAPTOR genes (RAPTOR1/RAPTOR2), and two LST8 genes (LST8-1/LST8-2) in *Arabidopsis*, of which only one (LST8-1) is significantly expressed **(Figure 5—1—A)**. RAPTOR1 is able to interact with the HEAT repeats of TOR (Mahfouz et al. 2006) and LST8-1 direct interacts with FRB and Kinase domains of TOR (Moreau et al. 2012), indicating the existence of the functional TOR pathway in plants **(Figure 5—1—B)**. Until today, there is no evidence of the existence of the TORC2 complex in plants, because the lack of RICTOR and SIN1 in photosynthetic organisms (Dobrenel et al. 2011). However, plants may have TORC2 equivalent with components that differ from those found in the yeast and mammalian TORC2 complex.

In yeast and mammals, rapamycin forms a complex with FKBP12 that inhibits TOR via binding of the rapamycin-FKB12 complex to the FRB domain of TOR. In contrast, *Arabidopsis* TOR is insensitive to rapamycin due to inability of the plant FKBP12 to interact with rapamycin (Menand et al. 2002; Sormani et al. 2007). Interestingly, *Arabidopsis* TOR becomes sensitive to rapamycin, when human or yeast FKBP12 is overexpressed in *Arabidopsis* (Mahfouz et al. 2006; Sormani et al. 2007; Ren et al. 2012). Interestingly, high concentration of rapamycin (10 μM) can inhibit TOR in *Arabidopsis* mesophyll protoplasts or seedling (Xiong and Sheen 2012). It has been shown that *Arabidopsis* TOR is sensitive to TOR inhibitor Torin-1 that outcompetes ATP for TOR kinase domain binding (Schepetilnikov et al. 2013).

Disruption of Arabidopsis *TOR* leads to the premature arrest of endosperm and embryo development (Menand et al. 2002). To overcome the embryo lethality of *null Arabidopsis tor mutants*, ethanol- and estradiol-inducible RNA interference (RNAi) lines have been generated to elucidate TOR functions in *Arabidopsis*. TOR controls growth, development, flowering, senescence, life span by regulating transcription, translation and autophagy (Deprost et al. 2007; Ahn et al. 2011; Ren et al. 2011; Xiong and Sheen 2012; Moreau et al. 2012; Ren et al. 2012; Xiong et al. 2013). Silencing of AtTOR causes leaf senescence, organ growth arrests and reduces rRNA synthesis and polysomes accumulation (Deprost et al. 2007) that leads to constitutive activation of autophagy (Liu and Bassham 2010). Partial inhibition of TOR by rapamycin in *Arabidopsis* lines expressing yeast FKBP12 decreases levels of polysomes (Sormani et al. 2007). Silencing of AtTOR by ethanol-induced *tor*-RNAi also leads to arrest of plant growth and up-regulation of senescence (Dobrenel et al. 2011). Interestingly, it has been shown that TOR signaling is involved in modification of cell walls for root hair development (Leiber et al. 2010). Unlike yeast and mouse, mutations in LST8-1 are not lethal, whereas RAPTOR1 mutations are conditionally lethal in *Arabidopsis*, however both mutations result in some developmental defects (Anderson et al. 2005; Deprost et al. 2007; Moreau et al. 2012).

Arabidopsis genome encodes a set of TOR substrates—two S6 kinases (S6K1/S6K2), 40S ribosome protein 6 (RPS6A/B) (Mahfouz et al. 2006), 2A-phosphatase-associated protein 46 kDa (TAP46) (Ahn et al. 2011), and ErbB3- epidermal growth factor receptor binding protein (EBP1) (Horváth et al. 2006).

Because of embryo lethality of tor mutants in *Arabidopsis*, rapamycin-insensitivity and the lack of biochemical and molecular tools to manipulate endogenous TOR activity, the plant TOR signaling network and its regulatory mechanisms are mostly unknown. However, many homologous proteins described as upstream regulators of TOR in mammals have been found

in plant genome, in particular in *Arabidopsis*. *Arabidopsis* genome encodes TCTP (Translationally Controlled Tumor Protein), RAG (Ras related GTP-binding), PI3K (PhosphoInositide 3-Kinase), AMPK (AMP-activated Protein Kinase), LKB1 and PDK1 (PhosphoInositide-Dependent Kinase 1). In contrast, no homologs has been found for TSC (Tuberous Sclerosis Complex), Akt kinase or Rheb protein (Moreau et al. 2010).

However, it has been shown that the upstream effectors of the TOR pathway in plants include energy balance and glucose status (Xiong and Sheen 2012; Robaglia et al. 2012). TOR signaling is activated by photosynthesis-derived glucose depending on glycolysis-mitochondria-mediated energy and metabolic relays (Xiong et al. 2013). A link between plant TOR and SnRK1 (homologous to mammalian AMPK) signaling pathways has been suggested (Robaglia et al. 2012). Like in mammals, TOR and SnRK1 act in an antagonistic way in response to favorable nutritional and energy conditions to regulate growth-related processes.

Another input signal for the TOR pathway is the phytohormone auxin. In response to auxin, TOR is activated and triggers phosphorylation of its downstream target S6K1 (conserved in eukaryotes) (Schepetilnikov et al. 2013), and two other targets discovered in plants: the subunit h of eIF3 (eIF3h) and reinitiation-supporting protein RISP, involved in reinitiation after short and long ORF translation, respectively (Thiébeauld et al. 2009; Schepetilnikov et al. 2011; Schepetilnikov et al. 2013) **(Figure 5—1—C; Figure 5—2)**.

The TOR/ S6K1 signaling pathway that triggers phosphorylation of a set of components of the translational machinery has been well studied in yeast and mammals and seems to be conserved in plants **(Figure 5—2)**. *Arabidopsis* encodes two putative S6 kinase homologs (S6K1 and S6K2) with high sequence similarity (87%) (Zhang et al. 1994; Mizoguchi et al. 1995; Turck et al. 1998). Like mammals, *Arabidopsis* contains two functional isoforms of S6K with different localization and roles. S6K1 is cytoplasmic and seems to be an ortholog of mammalian p70 S6K. However, S6K2 is preferentially localized in the nucleus and it may be

the functional equivalent of mammalian p85 S6K. S6K1 phosphorylates the ribosomal S6 protein (RPS6) within the cytoplasmic ribosome, while S6K2—the chromatin-bound nuclear form of RPS6 (Mahfouz et al. 2006). It has been shown that RAPTOR1 binds TOR HEAT repeats as well as S6K1 *in vivo* that triggers S6K1 phosphorylation at Thr499 by TOR and Thr229 by PDK1 (Mahfouz et al. 2006; Schepetilnikov et al. 2011). Plant S6K does not carry a canonical TOS motif described in mammals and yeast (Turck et al. 1998; Turck et al. 2004), or plants may have its functional equivalent with a different signature. S6K1 can phosphorylate RPS6 in Torin-1 sensitive manner (Schepetilnikov et al. 2011; Xiong and Sheen 2012).

There are reports suggesting a role of TOR-S6K1 signaling in translation reinitiation in plants (Schepetilnikov et al. 2013). The TOR-S6K1 signaling up-regulated in response to auxin promotes eIF3h phosphorylation and loading of active TOR and eIF3 into polysomes that correlates with increased translation reinitiation of mRNAs that harbor uORFs (Schepetilnikov et al. 2013). After termination of translation, these reinitiation-competent ribosomal complexes can resume scanning and reinitiate thanks to eIF3 assisting recruitment of the ternary complex *de novo*. Furthermore, it has been reported that the TOR-S6K1 pathway is required for translation of viral polycistronic 35S pregenomic mRNA from the Cauliflower mosaic virus (CaMV) via reinitiation. The translational transactivator/ viroplasmin protein (TAV) directly interacts with TOR triggering TOR and S6K1 phosphorylation followed by phosphorylation of RISP to promote translation of the viral polycistronic RNA (Schepetilnikov et al. 2011).

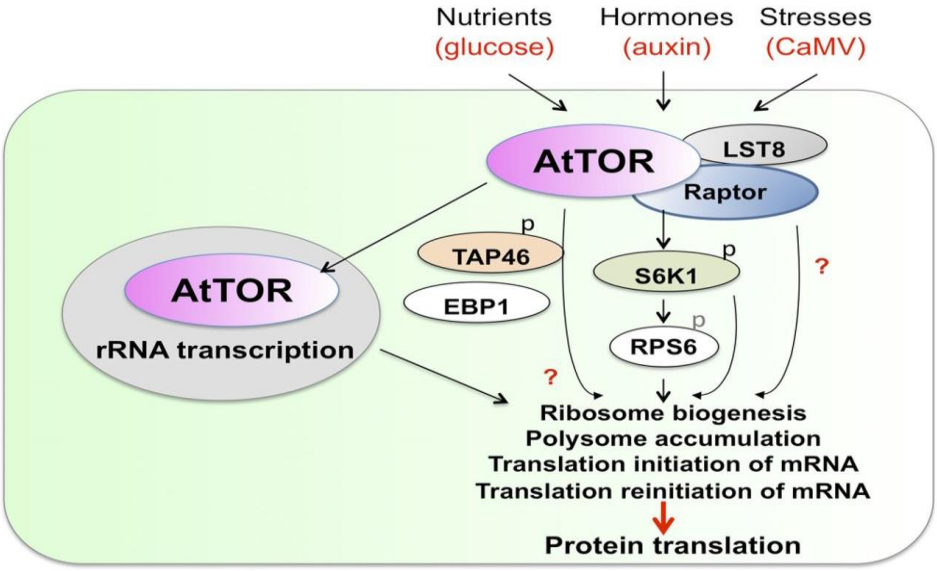

Figure 5—2 │ Model of the role of plant TOR signaling in promoting protein translation

The upstream signals and downstream effectors of plant TOR signaling in controlling protein translation processes are shown. TOR controls protein synthesis at multiple levels, including rRNA transcription, ribosomal biogenesis, polysome accumulation, and various protein translational processes (AtTOR, Arabidopsis TOR; CaMV, *Cauliflower mosaic viru*s).
Modified from(Xiong and Sheen 2014), *Plant Physiology 164: 499-512*

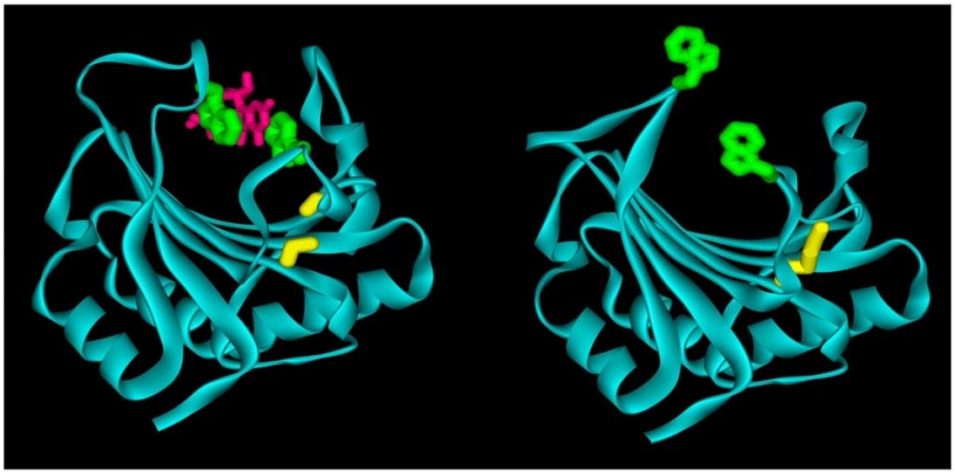

Figure 5—3 │Ribbon diagram comparing the structure of the wild type (right) and C113S mutant (left) of wheat eIF4E

The Trp within the cap-binding pocket is shown *in green*, the m^7GDP is shown *in magenta* and the disulfide bond (right) and positions of the reduced Cys (left) are shown *in yellow.*
Modified from (Monzingo et al. 2007), *Plant Physiology 143(4): 1504-1518*

5.3. No plant 4E-BPs/ Hypothesis–Redox conditions control eIF4E association with cap

The TOR-S6K1 signaling pathway is conserved in plants and plays an essential role in protein synthesis. In response to nutrients (glucose), hormones (auxin) and also under stress (upon CaMV infection), TOR controls protein synthesis at multiple levels, including ribosome biogenesis, rRNA transcription, polysome accumulation and translation reinitiation in *Arabidopsis* **(Figure 5—2)**. Since no ortholog of 4E-BPs have been identified in plants, TOR-independent mechanism of translation initiation regulation has been proposed in plants (Monzingo et al. 2007). The model states that the oxidation status of eIF4E (and/or eIFiso4E) can modulate its cap binding ability in a redox-sensing manner. Indeed, plant eIF4E and eIFiso4E exhibit high affinity to eIF4G and eIFiso4G, respectively, and form tight complexes do not easily dissociate (Mayberry et al. 2011). The crystal structure of wheat eIF4E is similar to eIF4E structure from other species (yeast and mammals)—eight beta-strands, three alpha-helices and three extended loops. Surprisingly, an intramolecular disulfide bridge was observed between two cysteines (Cys-113 and Cys-151) that are unique to plants (Monzingo et al. 2007) (Figure 5—3). Mutations of both Cys to Ser that abolish formation of this unique disulfide bond affect modestly eIF4E binding to m^7GTP. In addition, a subtle changes in the reactivity of lysine residues of eIF4E occurs upon eIF4G binding or disulfide bonds reduction, and can affect the eIF4E binding to the m^7GTP cap analogue (O'Brien et al. 2013). These results support that plant eIF4E (and/or eIFiso4E) may act as a redox sensor in translational initiation control.

My PhD project was focused on mechanisms of cap-dependent translation initiation in *Arabidopsis* and their control by the TOR signaling pathway. I identified a family of small unstructured proteins in *Arabidopsis* and I characterized these proteins as putative TOR downstream targets that can interact with eIF4E/ eIFiso4E in TOR-responsive manner. Their characterization and their effect on cap-dependent translation initiation are presented here.

II. Results

1. Article-1:

TOR-downstream target proteins modulate translation initiation in *Arabidopsis*

Ola Srour, Joelle Makarian, Nina Lukhovitskaya, Mikhail Schepetilnikov* and Lyubov A. Ryabova*

[1]Institut de Biologie Moléculaire des Plantes du CNRS, Université de Strasbourg, 67084 Strasbourg Cedex, France

*To whom correspondence should be addressed:
lyuba.ryabova@ibmp-cnrs.unistra.fr
mikhail.shchepetilnikov@ibmp-cnrs.unistra.fr

Tel: +33 (0)3 88 41 72 61
Fax: +33 (0)3 88 61 44 42

Abstract

In mammals, cap-dependent translation initiation is under the control of TOR (target-of-rapamycin) protein kinase, which suppresses the function of the eIF4E-binding proteins (4E-BPs) that bind to eIF4E and inhibit eIF4F complex formation. Whether TOR regulates translation initiation in plants remains an open question. Here, we identified and characterized two *Arabidopsis* proteins termed TOR regulatory proteins (ToRPs 1 and 2). *In Arabidopsis*, ToRP2, like eIF4G, contains a canonical eIF4E-binding site (4E-BM), while ToRP1, similar to eIFiso4G, exhibits a modified 4E-BM where Tyr is replaced by Phe. In the yeast two-hybrid system, ToRP1 interacted with eIF4E, and, surprisingly, the N-terminal HEAT repeat domain of TOR; the strength of this interaction was modulated by mutations within ToRPs' three conserved motifs. In response to auxin, which activates TOR, ToRPs are phosphorylated; two-dimensional gel electrophoresis and Western blotting detected three and five phosphorylation states of ToRP1 and ToRP2, respectively. These sites are dephosphorylated upon treatment with the TOR inhibitor AZD-8055. Two TOR-specific phosphorylation sites—Ser49 and Ser89—within ToRP1 were identified; their phosphorylation knockout exhibited increased binding to eIF4E, while mimetic mutations abolished binding. *In planta* results suggest that Ser89 phosphorylation is followed by phosphorylation of Ser49. In contrast to plants overexpressing ToRPs, ToRPs knockout plants exhibit increased translation capacity for the CYCB1;1 5'-UTR-containing reporter in plant protoplasts. Taken together, our data suggest that ToRPs are regulatory proteins that participate in the control of cap-dependent translation initiation in plants.

Introduction

In eukaryotes, protein synthesis is controlled mainly at the initiation phase, but the molecular mechanisms of translation regulation are not fully elucidated, particularly in plants. Translation initiation begins with cooperative assembly of eukaryotic initiation factor 3 (eIF3), eIF1, eIF1A, and the eIF2-GTP-Met-tRNA$_i^{Met}$ ternary complex (TC) on the 40S ribosomal subunit, resulting in formation of the 43S preinitiation complex (43S PIC) (Jackson et al. 2010; Browning and Bailey-Serres 2015). The 43S complex than loads onto the capped 5'-end of the mRNA, which is activated by binding of the eIF4F complex composed of cap-binding subunit eIF4E, a scaffold protein eIF4G, and DEAD box RNA-dependent RNA helicase 4A (eIF4A) (Hinnebusch 2014). eIF4F recruits mRNA to the 43S complex via interactions between eIF4G, eIF4B and the 40S-associated eIF3, while TC delivers initiator Met-tRNA$_i^{Met}$ (Pestova et al. 2007). The resulting 43S PIC scans the mRNA until the first AUG codon in a suitable initiation context is encountered, the 60S ribosomal subunit joins, and elongation begins (Kozak 1999). Thus, activation of mRNA translation depends on rapid assembly of the eIF4F complex at the cap structure of the mRNA.

Mammalian/ mechanistic target of rapamycin complex 1 (mTORC1) (Kim et al. 2002), which is the key component of a nutrient- and hormone-dependent signalling pathway, positively controls cell growth in part by stimulating protein synthesis machinery function. mTORC1 facilitates translation via direct or indirect phosphorylation of the components of the host translation machinery (Ma and Blenis 2009; Roux and Topisirovic 2012). Two main substrate classes of mTORC1 have been identified as eIF4E-binding proteins (4E-BPs) and the ribosomal protein S6 kinases (S6Ks) (Gingras et al. 1999a).

4E-BPs represses translation initiation by binding to eIF4E, thus preventing eIF4F complex formation. In mammals and Drosophila, mTORC1 controls translation at the initiation step mainly by affecting assembly of eIF4F on the mRNA 5'-cap via

phosphorylation and inactivation of 4E-BPs (Gingras et al. 1999a; Hershey and Merrick 2000; Raught et al. 2000). 4E-BPs exert their inhibiting effect on translation initiation by competing with eIF4G for binding to the same conserved hydrophobic residue motif of eIF4E, thereby blocking translation initiation. Accordingly, both eIF4G and 4E-BPs share a canonical 4E-binding site of sequence $YX_4L\phi$ (termed 4E-BM, where Y denotes Tyr, X denotes any amino acid, L denotes Leu, and ϕ denotes a hydrophobic residue) (Mader et al. 1995; Marcotrigiano et al. 1999). Binding of 4E-BP to eIF4E is inhibited by phosphorylation of 4E-BPs at multiple sites by TOR, and cap-dependent translation is restored (Gingras et al. 1999a; Gingras et al. 2001). Conversely, (hyper)phosphorylation of 4E-BPs reduces their affinity for eIF4E and releases them from eIF4E. This allows eIF4E to bind eIF4G, with subsequent formation of the eIF4F complex, which leads to translation activation. By repressing translation initiation, 4E-BPs inhibit cell proliferation and act as tumor suppressers (Martineau et al. 2013).

4E-BPs exist as three isoforms—4E-BP1 (PHAS, for phosphorylated heat- and acid-stable), 4E-BP2 and 4E-BP3 containing 118, 120 and 100 aminoacid residues (Pause et al. 1994; Lin et al. 1994; Lawrence Jr and Abraham 1997; Poulin et al. 1998). 4E-BP1 and 4E-BP2 contain several phosphorylation sites that are responsive to TOR, and their phosphorylation proceeds in a hierarchical order (Gingras et al. 1999a; Gingras et al. 2001). While phosphorylation of 4E-BP1 and 4E-BP2 is rapamycin sensitive, phosphorylation of 4E-BP3 is not (Lin and Lawrence 1996; Kleijn et al. 2002). Three 4E-BP motifs, comprising non-canonical and canonical 4E-BMs, are required for 4E-BPs to compete with eIF4G for eIF4E binding, while the C-terminal TOS motif is a binding site for RAPTOR (Peter et al. 2015). Phosphorylation of 4E-BPs by TOR regulates eIF4E availability and thus cap-dependent translation. Thereby, mTORC1 regulates translation efficiency of 5'-terminal oligopyrimidine (TOP)-motif-containing mRNAs (Thoreen et al. 2012).

In flowering plants, the eIF4F complex exists as eIF4E, which pairs with eIF4G, and the plant-specific isoform eIFiso4E, which pairs with eIFiso4G to form eIFiso4F (Mayberry et al. 2011; Patrick and Browning 2012). In *Arabidopsis,* eIF4E is encoded by several genes (eIF4E1, eIF4E2, and eIF4E3), whereas eIFiso4E is encoded by only one gene. *At*eIFiso4G is encoded by two genes, and their double mutant displays defects in growth and reproduction (Lellis et al. 2010). Like mammals, plants posses a single *TOR* gene, down-regulation of which correlates with decreased plant size and resistance to stress (Menand et al. 2002; Deprost et al. 2007; Ren et al. 2012). *Arabidopsis* RAPTOR and LST8 were characterized as components of the TORC1 complex (Mahfouz et al. 2006; Dobrenel et al. 2011; Moreau et al. 2012), while no TORC2 components have yet been identified in plants. The best-characterized substrate of TORC1 in plant translation is S6K1, via which TOR can control growth and proliferation (Schepetilnikov et al. 2011; Xiong and Sheen 2012). *Arabidopsis* plants silenced for TOR expression display reduced polysome abundance (Deprost et al. 2007), suggesting a role for TOR in plant translational control. Indeed, we have characterized a novel regulatory TOR function in translation reinitiation of mRNAs that harbor upstream open reading frames within their leader regions (uORF-mRNAs) (Schepetilnikov et al. 2013). However, the question of whether TOR can control cap-dependent translation initiation remains to be answered.

Here, we identified small unstructured proteins in *Arabidopsis* that are targets of the TOR signaling pathway and can interact with eIF4E. Their characterization and their effect on cap-dependent translation initiation are presented here.

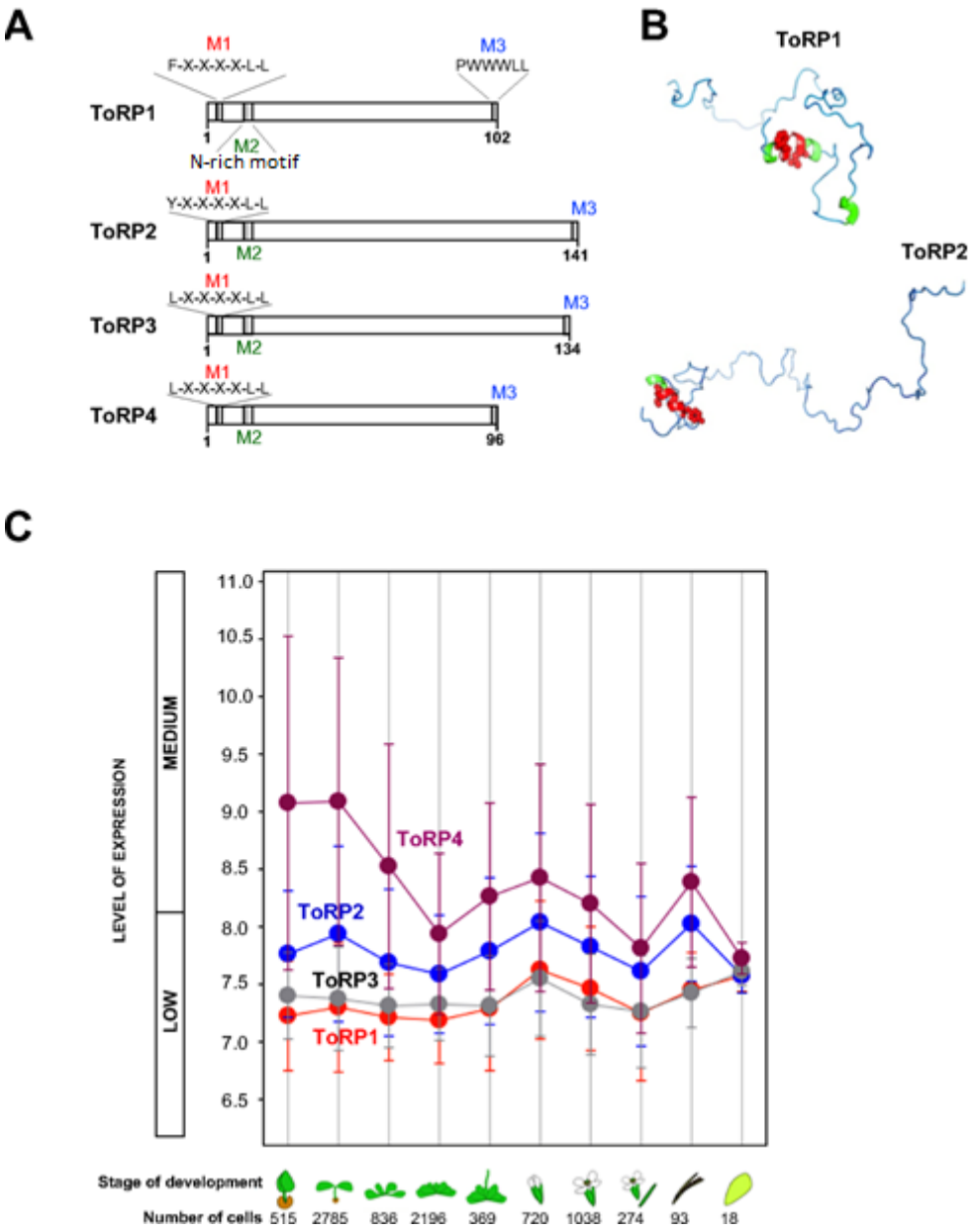

Figure 1—1 | Identification of small proteins that harbor an eIF4E-binding motif in *Arabidopsis*

(A) Schematic representation of *Arabidopsis* TOR Regulatory Proteins (ToRPs) 1–4; three conserved motifs are shown: M1-canonical eIF4E-binding motif YX_4LL (termed 4E-BM, where Y denotes Tyr, X denotes any amino acid, and L denotes Leu); M2-the Asparagine-rich motif and M3-the C-terminal conserved motif.

(B) ToRP1 and ToRP2 putative secondary structure generated by RAPTOR program reveals short α-helixes: *red*, and beta-sheets: *green*.

(C) ToRPs 1–4 transcription profiles were taken from the Genevestigator database (https://www.genevestigator.ethz.ch).

Results

Identification of a small family of proteins carrying canonical and non-canonical eIF4E-binding sites

Thorough analysis of *Arabidopsis* databases resulted in identification of four homologous proteins of 102, 141, 134 and 96 amino acids recently named as TOR Regulatory Proteins (ToRP1, ToRP2, ToRP3- and ToRP4-like proteins, respectively (Fig. 1A). These proteins contain three conserved domains, M1–M3. ToRP2 M1 represents the canonical 4E-binding site of sequence $YX_4L\phi$ (termed 4E-BM, where Y denotes Tyr, X denotes any amino acid, L denotes Leu, and ϕ denotes a hydrophobic residue) found in all mammalian 4E-BPs (Mader et al. 1995; Marcotrigiano et al. 1999). Interestingly, ToRP1 contains a similar motif that begins with F (Phe). However, analysis of 4E-BMs in eIF4G and eIFiso4G revealed both the canonical 4E-BM and the motif where Tyr is replaced by Phe, indicating that, in *Arabidopsis*, eIF4E or iso4E interact with eIF4G or eIFiso4G via YX_4LL and FX_4LL, respectively (Fig. 1A). Moreover, Tyr is replaced by Leu within the 4E-BM-corresponding motif of ToRP3- and ToRP4-like proteins. The M2 motif is enriched by asparagine (Asn; Fig. 2B), which is similar to the case of the mammalian 4E-BP2 protein sequence (Bidinosti et al. 2010). The so-called M3 motif is Trp-rich and found at the C-terminus of ToRPs.

A 3D model of *Arabidopsis* ToRP1 and ToRP2, generated by RaptorX (Källberg et al. 2012), predicts, with high probability, intrinsically disordered proteins that do not have any secondary structure (Fig. 1B), like 4E-BP1 (Fletcher et al. 1998; Fletcher and Wagner 1998). Despite its low abundance in *Arabidopsis thaliana* according to the Genevestigator database (Fig. 1C), we selected ToRP1 to further examine its association with eIF4E or eIFiso4E.

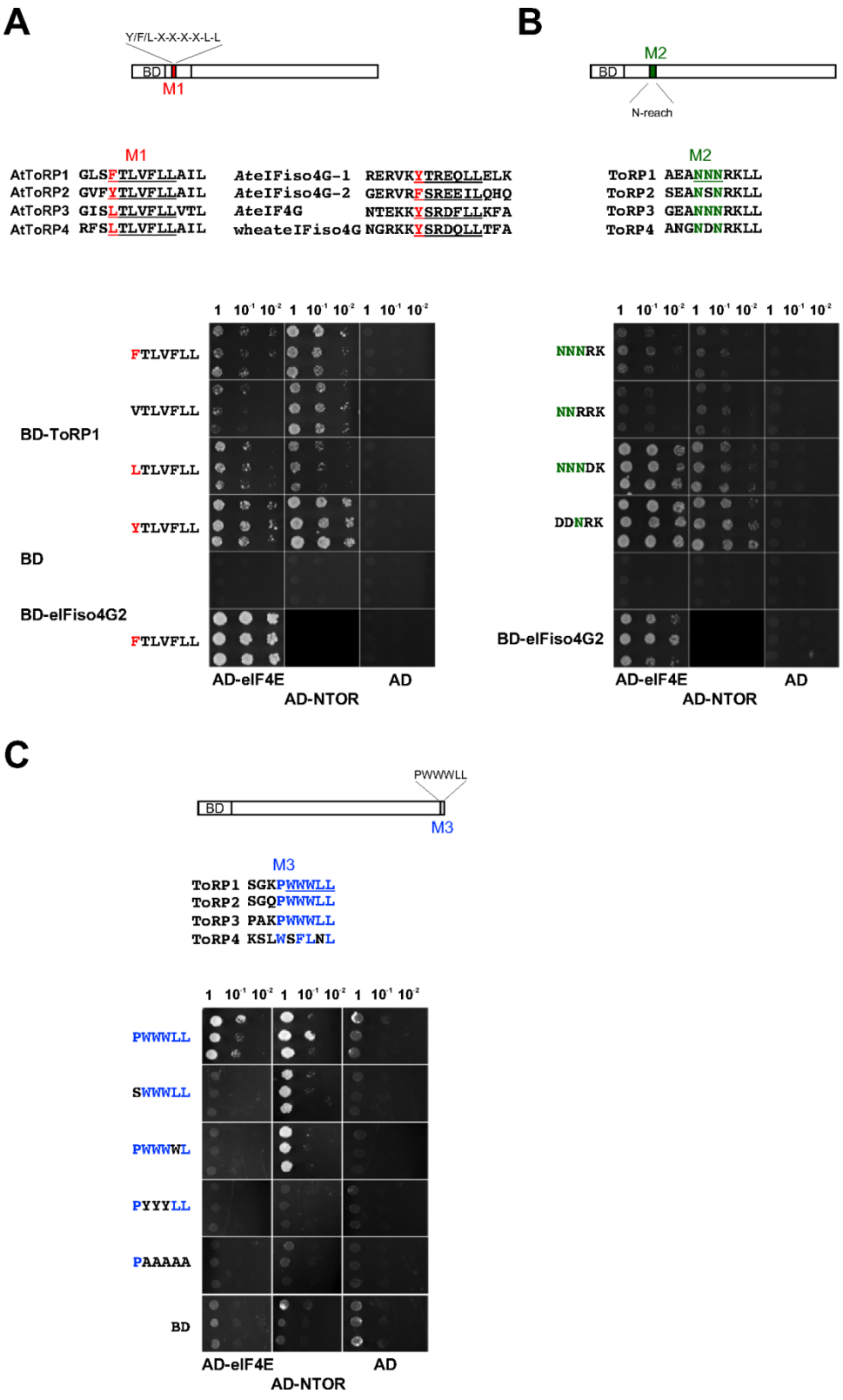
A
Y/F/L-X-X-X-X-L-L
BD
M1
M1
AtoRP1 GLSFTLVFLLAIL
AtoRP2 GVFYTLVFLLAIL
AtoRP3 GISLTLVFLLVTL
AtoRP4 RFSLTLVFLLAIL
AteIFiso4G-1 RERVKYTREQLLELK
AteIFiso4G-2 GERVRFSREEILQHQ
AteIF4G NTEKKYSRDFLLKFA
wheateIFiso4G NGRKKYSRDQLLTFA
B
M2
BD
N-reach
M2
ToRP1 AEANNNRKLL
ToRP2 SEANSNRKLL
ToRP3 GEANNNRKLL
ToRP4 ANGNDNRKLL
1 10-1 10-2 1 10-1 10-2 1 10-1 10-2
FTLVFLL
VTLVFLL
BD-ToRP1
LTLVFLL
YTLVFLL
BD
BD-eIFiso4G2
FTLVFLL
AD-eIF4E
AD
AD-NTOR
1 10-1 10-2 1 10-1 10-2 1 10-1 10-2
NNNRK
NNRRK
NNNDK
DDNRK
BD-eIFiso4G2
AD-eIF4E
AD
AD-NTOR
C
PWWWLL
BD
M3
M3
ToRP1 SGKPWWWLL
ToRP2 SGQPWWWLL
ToRP3 PAKPWWWLL
ToRP4 KSLWSFLNL
1 10-1 10-2 1 10-1 10-2 1 10-1 10-2
PWWWLL
SWWWLL
PWWWWL
PYYYLL
PAAAAA
BD
AD-eIF4E
AD
AD-NTOR

Figure 1—2 | *Arabidopsis* ToRP1 binds eIF4E and the N-terminal HEAT repeat domain of TOR, where M1-3 motifs attenuate this binding in the yeast two-hybrid system

(A-C) *Yeast two-hybrid interactions* between eIF4E and eIF4G and ToRP1 or its mutant derivatives. *Upper panel* Schematic presentation of ToRP1 fusion with the Gal4 binding domain (BD; the motif under investigation is indicated). *Central panels* (A) Alignment of the canonical eIF4E binding motifs from *Arabidopsis* ToRPs 1–4 and eIF4G/eIFiso4G from *Arabidopsis* and wheat. Sequence alignment of the ToRP M2 motifs (B) and the ToRP M3 motifs (C). Sequence alignment prepared according to Blossom 62 amino-acid substitution matrixes.

Bottom panel Yeast two-hybrid interactions between the Gal4 activation domain (AD), AD-NTOR, AD-eIF4E and BD-eIFiso4G2, and WT or mutated ToRP1-fused to BD. Yeast two-hybrid interactions are shown in triplicate for each combination of AD and BD fusion proteins. Equal OD_{600} units and 1/10 and 1/100 dilutions were spotted from left to right and incubated for 2 days. Mutations are highlighted by red (M1), green (M2) and blue (M3).

ToRP1 binds eIF4E in the yeast two-hybrid system

Considering the role of 4E-BM in eIF4E binding, we wished to study ToRP1 binding to eIF4E, and we used the eIFiso4G to eIF4E interaction as a positive control. We first determined that ToRP1 can interact with eIF4E in the yeast two-hybrid system, albeit with somewhat lower intensity than eIFiso4G2 (Fig. 2A). Further, mutation of Phe for Tyr at the first position of ToRP1 4E-BM improved the ToRP1–eIF4E interaction substantially, while substitution of Phe by Val nearly abolished the interaction. Surprisingly, substitution of Phe by Leu, which is present at this position in ToRP3- and ToRP4-like proteins, did not reduce ToRP1 binding to eIF4E, indicating that 4E-BM with Leu in place of Tyr can induce eIF4E binding as well as wild type. Careful investigation of ToRP sequences did not reveal the canonical TOS motif that is normally present at the C-terminus of mammalian 4E-BPs, and that functions in presenting various substrates to TOR for phosphorylation. Therefore, we investigated whether ToRP1 interacts with TOR directly via either the N- or C-terminal half of TOR. Surprisingly, in the yeast two-hybrid system, ToRP1 interacts with the HEAT repeat domain of TOR (NTOR; Fig. 2), but not with the C-terminal half of TOR (data not shown).

Although substitution of Phe for Val abolished binding of ToRP1 to eIF4E, binding to NTOR was not affected, indicating that TOR binding is not dependent on 4E-BM.

The ToRP1 M2 motif is connected to 4E-BM via a 9- to 10-amino-acid linker similar to the motif present in human 4E-BP2 (Peter et al. 2015). Interestingly, mutations of asparagine, or two conserved asparagine residues, for aspartate (N26D or N25D/N26D) within the M2 motif of ToRP1 drastically increased binding to both eIF4E and NTOR (Fig. 2B). Moreover, asparagine deamidation of 4E-BP2 enriched in brain was described as a brain-specific posttranslational modification (Bidinosti et al. 2010). The ToRP1 C-terminus (M3) is rich in aromatic residues, and plays a critical role in ToRP1 binding to eIF4E in the yeast two-hybrid system, since mutations—P97S and L100W—inhibited interactions with eIF4E, and substitution of three Trp residues for Tyr residues, or replacement of five C-terminal amino acids by alanines abolished interaction with both eIF4E and NTOR (Fig. 2C).

Interaction between ToRPs and eIF4E was confirmed by pull-down assays. ToRP1 specifically interacts with both eIF4E- and eIFiso4E-GST fusions in GST pull-down assays (Fig. 3A). Next, we tested whether ToRP1 can interact with eIF4E or eIFiso4E in a cap-bound conformation. Thus, we used m^7-GTP-Sepharose 4B pre-bound with either recombinant eIF4E or eIFiso4E purified from *E. coli*. Firstly, we found that ToRP1 does not associate with cap-sepharose (Fig. 3B *Left panel*). Next, m^7-GTP-Sepharose 4B beads were incubated with excess eIF4E or eIFiso4E (*Upper panel*), followed by incubation of washed bound fractions with or without ToRP1. ToRP1 specifically associates with cap-bound eIF4E (Fig. 3B *Central panel*) and cap-bound eIFiso4E (Fig. 3B *Right panel*). These results suggest that ToRP1 binds eIF4E or eIFiso4E.

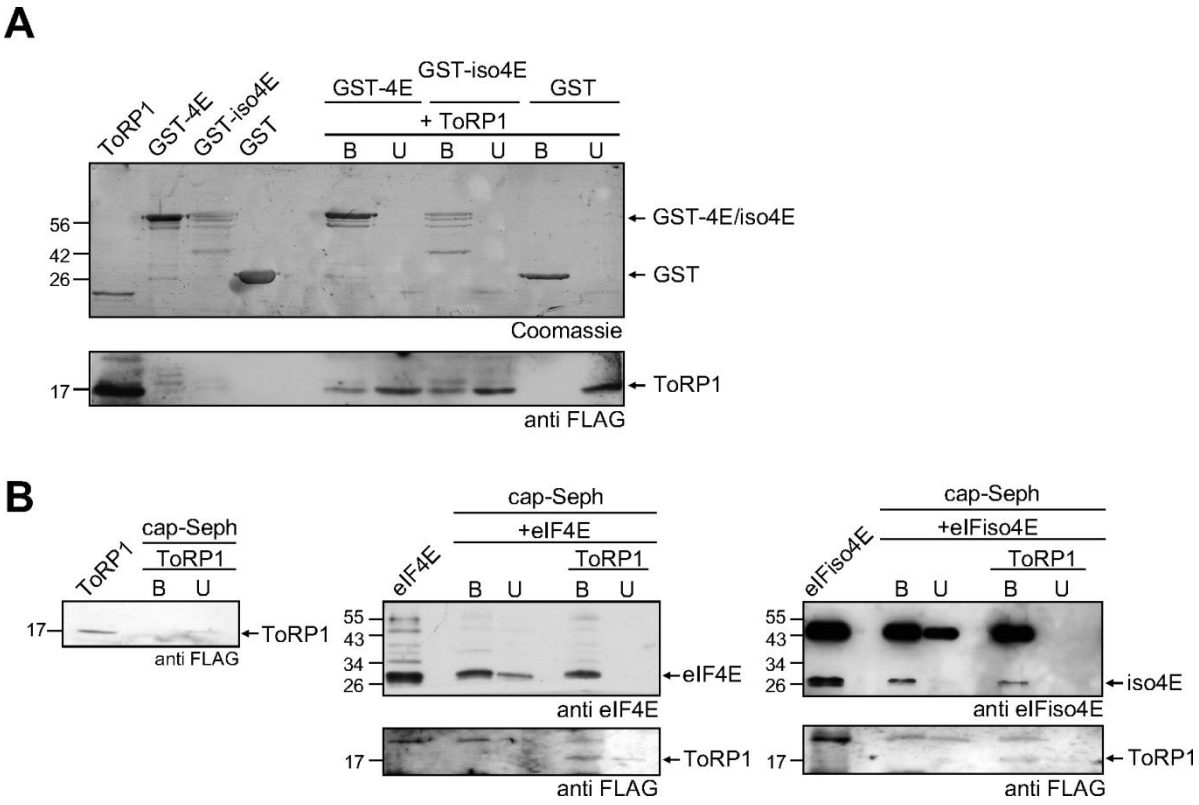

Figure 1—3 | *Arabidopsis* ToRP1 specifically pulls-down eIF4E (and eIFiso4E) when bound or not to cap structure

(A) *GST pull-down assay* eIF4E-, eIFiso4E-tagged GST and GST alone were assayed for interaction with recombinant FLAG-tagged ToRP1. *Upper panel* GST-fusion fractions were stained by Coomassie blue. *Bottom panel* ToRP1 was revealed by Western blot using anti FLAG antibodies. Results shown represent the means obtained in three independent experiments.

(B) *Cap-sepharose pull-down assay* ToRP1 did not associate with cap-sepharose. *Left panel* Recombinant eIF4E-, eIFiso4E were prebound to cap-sepharose. The washed complex between eIF4E or eIFiso4E with cap-sepharose was assayed for interaction with recombinant FLAG-tagged ToRP1. eIF4E and eIFiso4E *Upper panels* and FLAG-tagged ToRP1 *Bottom panels w*ere revealed by western blot with anti eIF4E and eIFiso4E antibodies, and anti FLAG antibodies, respectively.

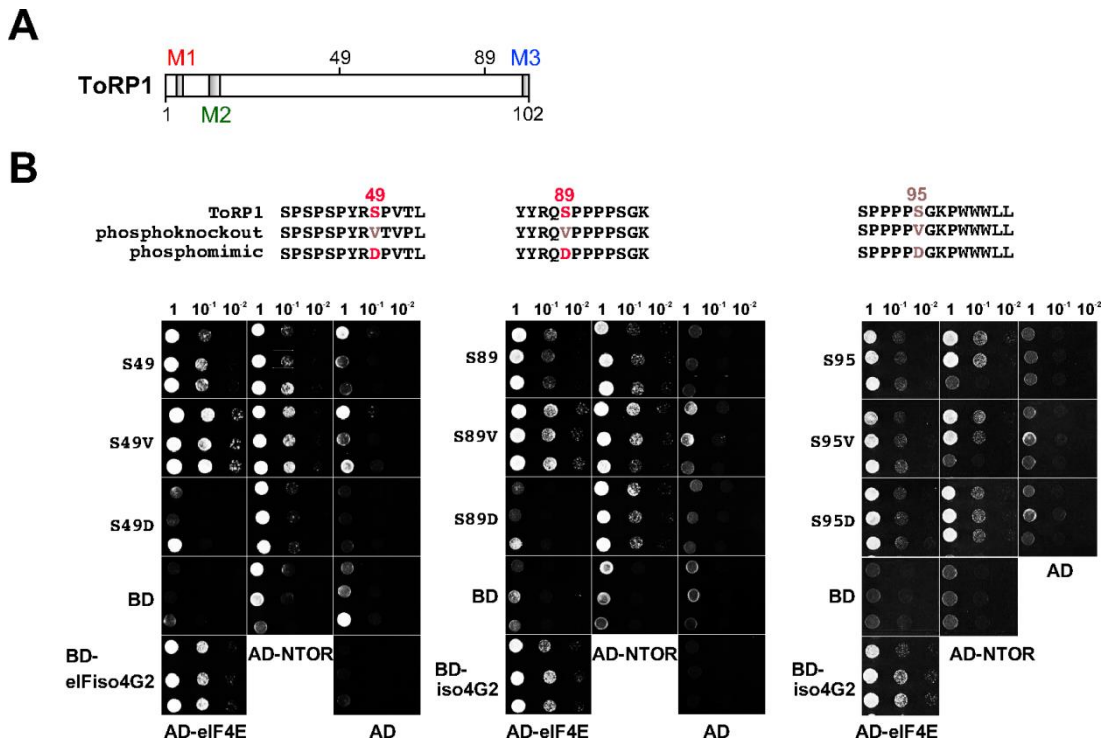

Figure 1—4 | ToRP1 binding to eIF4E is responsive to phosphorylation of Ser49 and Ser89

(A) Schematic representation of ToRP1 (the positions of two putative TOR-specific phosphorylation sites are indicated).

(B) *Yeast two hybrid interactions*. *Upper panels* The WT sequence motif surrounding S49, S89 and S95, and corresponding mimetic and phosphorylation knockout mutations are presented.

Bottom panels Yeast two-hybrid interactions between AD, AD-eIF4E, AD-NTOR and BD, BD-eIFiso4G2, BD-ToRP1 and its mimetic and phosphorylation knockout mutants. Yeast two-hybrid interactions are shown in triplicate for each combination of AD and BD fusion proteins. Equal OD_{600} units and 1/10 and 1/100 dilutions were spotted from left to right and incubated for 2 days.

Replacing Ser49 or Ser89 with Val increases ToRP1–eIF4E binding, while Ser49 or Ser89 to Asp mutation abolishes ToRP1–eIF4E binding

Analysis of phosphorylation sites within the known TOR substrates—Hs4E-BP1 (S65 motif), ULK1 (S758 motif), Grp10 (S150 motif) and PatL1 (S184 motif) (Kang et al. 2013)—revealed similar motifs within ToRP1 at positions of Ser49 and Ser89 and ToRP2 at positions Ser49 and Ser128, respectively (Fig. 4), indicating ToRP phosphorylation by TOR.

We considered the possibility that ToRP1 phosphorylation site Ser49 or Ser89 mimetic or knockout mutations might affect its interactions with eIF4E. S49V or S89V ToRP1 mutants exhibited increased association with eIF4E, while S49D and S89D mutants failed to interact with eIF4E in the yeast two-hybrid system (Fig. 4B, *Left* and *Central panels*, respectively). Strikingly, ToRP1 carrying a S49D mutation exhibited strongly reduced binding to NTOR. In contrast, similar mutations of Ser95, which is unrelated to known TOR phosphorylation sites, affected ToRP1 interaction neither to eIF4E nor to NTOR (Fig. 4B, *Right panel*). Thus, ToRP1 phosphorylation weakens its association with both eIF4E and NTOR, while dephosphorylated ToRP1 revealed stronger interactions with eIF4E. These results encouraged us to investigate ToRP1 and ToRP2 phosphoisoforms *in planta*.

ToRP2 in *Arabidopsis* resolves into five phosphorylation forms by two-dimensional electrophoresis

Previously, we reported that phytohormone auxin treatment of *Arabidopsis* seedlings induced TOR phosphorylation at S2424 and S6K1 at TOR-specific residue T449, while application of TOR inhibitor AZD-8055 led to TOR inactivation (Schepetilnikov et al. 2013). AZD-8055 binds to the TOR kinase domain within the ATP-binding pocket and inactivates TOR (Chresta et al. 2010; Montané and Menand 2013). Considering the role of auxin in TOR activation, we analyzed the impact of TOR activation on phosphorylation status of ToRP1 and ToRP2

proteins *in planta*. To address this question, WT, or ToRP1- or ToRP2-overexpressing seedlings were grown either with 100 nM synthetic auxins (2,4D) or 0.5 µM concentration of AZD-8055 (a two-fold reduced AZD-8055 concentration was used to prevent any overall cytotoxic effect on seedlings during prolonged drug treatment) 7 days after germination (7 dag). To monitor phosphorylation status of ToRP 1 and ToRP 2, we analyzed both auxin- and AZD-8055 treated extracts in parallel experiments by two-dimensional (2D) gel electrophoresis and Western blotting using polyclonal antibodies raised against the M2 motif, which is highly conserved within ToRP1 and ToRP2; the antibody recognizes both ToRP1 and ToRP2.

In the first dimension, pH 7–10 strips with a nonlinear gradient were used to increase the resolution in the pH 7–10 region that corresponded to the theoretical pI=10.4 and 9.9 of ToRP1 and ToRP2, respectively. Three different phosphorylation states were detected for ToRP1 under auxin treatment, and there was no phosphorylation after AZD-8055 application (Fig. 5A). Five different phosphorylation states were detected for ToRP2 in response to auxin, and low intensity bands were detected under conditions of TOR inactivation (Fig. 5B). Isoform 5 was detected in the most acid position (pI=7) and likely corresponded to the hyperphosphorylated form. In the presence of auxin, there was an increase in spots 4 and 5 of ToRP2 (Fig. 5B, *Left panel*), when compared with AZD-8055 conditions (Fig. 5B, *Right panel*). The hypophosphorylated form was designated as spot 1; this spot migrates in SDS PAGE with a slower mobility than the phosphorylated ToRP2. We concluded that both ToRP1 and ToRP2 contain multiple phosphorylation sites, and that their phosphorylation is responsive to TOR.

To confirm ToRP1 and ToRP2 phosphorylation in response to TOR, we generated *ToRP2ox* seedlings that stably express myc-tagged ToRP2 from the 35S-promoter. When anti ToRP1/2 antibodies were used, 2D gel analysis revealed a phosphorylation pattern for ToRP2

(Fig. 5C, *Upper panel*) similar to that in Fig. 5B. Here, auxin induced an increase in ToRP2 spots 4 and 5 (Fig. 5C *2,4D*), as compared with the pattern that corresponds to TOR inactivation, where all isoforms were of a similar size (Fig. 5C *AZD-8055*).

Identification of Ser49 and Ser89 as putative TOR phosphorylation sites prompted us to raise phospho-specific antibodies that react against Ser49-P or Ser89-P within both ToRP1 and ToRP2. Ser49 phosphorylation was detected in ToRP2 isoforms 4 and 5, while anti-Ser89-P antibodies recognized ToRP2 isoforms 3, 4 and 5. These experiments indicate that form 4 corresponded to ToRP2 phosphorylated at Ser49, while form 3 corresponded to phosphorylation at Ser89. Thus, both ToRP1 and ToRP2 contain multiple phosphorylation sites that are phosphorylated in response to auxin in a TOR-responsive manner.

Regulation of translation by ToRP1 or ToRP2 in plant protoplasts

As ToRP1 and ToRP2 are phosphorylated in a TOR-responsive manner, and ToRP1 binding to eIF4E is regulated by its phosphorylation status at S49 and S89 in the yeast two-hybrid system, we set out to determine whether ToRP1 or ToRP2 can contribute to cap-dependent translation initiation *in planta*. We have selected two cellular genes that encode CYCB1;1 (Li et al. 2005) and GIP1 (Batzenschlager et al. 2013). In our reporter vector, GUS ORF was placed downstream of either CYCB1;1 or GIP1 5'-UTRs (Fig. 6A). Several *Arabidopsis* genotypes have been employed—plants overexpressing myc-tagged ToRP1 (*ToRP1ox*) and ToRP2 (*ToRP2ox*), and the *torp1 torp2 Arabidopsis* line, where ToRP1 and ToRP2 genes were knocked-out using the CRISPR/Cas9 system (Fauser et al. 2014)—to prepare mesophyll protoplasts. Protoplasts were transformed with the two reporter plasmids depicted in Fig. 6B: *pmonoGFP*, containing a single *GFP* ORF; and either p*CYCB1;1 5'-UTR-GUS* or p*GIP1 5'-UTR-GUS*, where GUS serves as a marker of translation initiation efficiency, and GFP as a control for transformation/internal ribosome entry site (IRES) (Zeenko and Gallie 2005);

translation initiation efficiency. First, we compared cap-dependent translation efficiency of WT and *ToRP1ox* genotypes (Fig. 6C, *Upper panels*). Transient overexpression of *CYCB1;1 5'-UTR-GUS* or *GIP1 5'-UTR-GUS* reporters led to a marginal decrease in cap-dependent over cap-independent translation in *ToRP1ox* as compared with WT. The negative effect of ToRP2 overexpression in *ToRP2ox* was more pronounced for *CYCB1;1 5'-UTR-GUS* (Fig. 6C, *Central panel*). Here, transient overexpression of *CYCB1;1 5'-UTR-GUS* led to a three-fold decrease in transient expression, while *GIP1 5'-UTR-GUS* mRNA translation was reduced to a lesser extent compared with WT protoplasts. Thus, *ToRP2ox* transgenic plants are less efficient in cap-dependent translation initiation than WT plants. Note that the levels and integrity of GUS-containing mRNAs during 18 h of protoplast incubation were found to be similar for the two genotypes under investigation, although it was reported that *CYCB1;1* mRNA translation initiation is strongly dependent on cap structure, and thus is susceptible to suppression by 4E-BPs (Graff and Zimmer 2003).

To further confirm that translation initiation is sensitive to, at least, ToRP2, we asked whether ToRP1 and ToRP2 knockout would boost translation of our reporters (Fig. 6C, *Bottom panels*). Indeed, we observed a significant increase in cap-dependent over cap-independent translation for both reporters in *torp1 torp2* as compared with WT. In agreement with the above findings, the *CYCB1;1 5'-UTR*–containing reporter was expressed two-fold more efficiently in protoplasts lacking ToRPs than in WT. We therefore concluded that *CYCB1;1* mRNA translation is ToRP2 sensitive. Overall, these experiments indicate that ToRPs 1 and 2 are phosphorylated in a TOR-responsive manner and can negatively regulate cap-dependent translation.

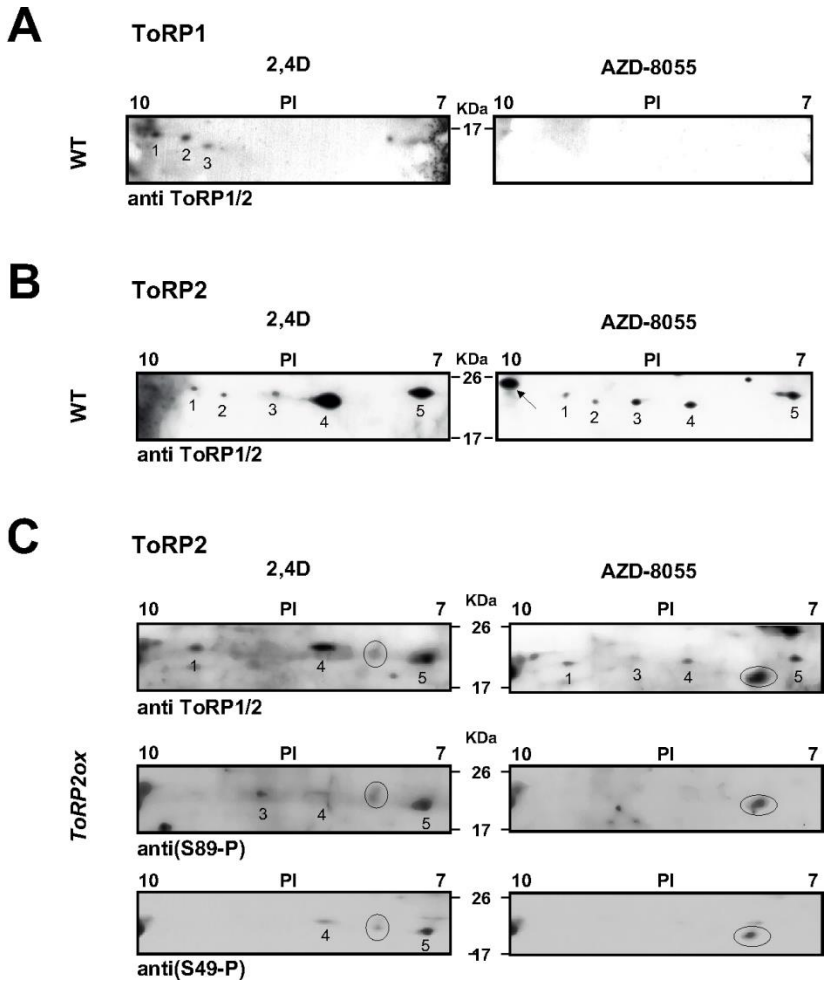

Figure 1—5 | Sensitivity of ToRP1 and ToRP2 phosphorylation to auxin and TOR inhibitor AZD-8055 revealed by two-dimensional gel electrophoresis

Samples of extracts prepared from 7 dag WT (A, B) or ToRP2 overexpressing seedlings (*ToRP2ox*) (C) grown on agar containing either 2,4D or AZD-8055 were subjected to two-dimensional gel electrophoresis and western blotting with anti M2 ABs (A, B and C *Upper panel*), anti S89-P phospho ABs (C *Central panel*) and anti S49-P phospho ABs (C *Bottom panel*). The antibody-reactive spots were designated as 1 to 3 for ToRP1, and 1 to 5 for ToRP2. The figures are representative results from three independent experiments.

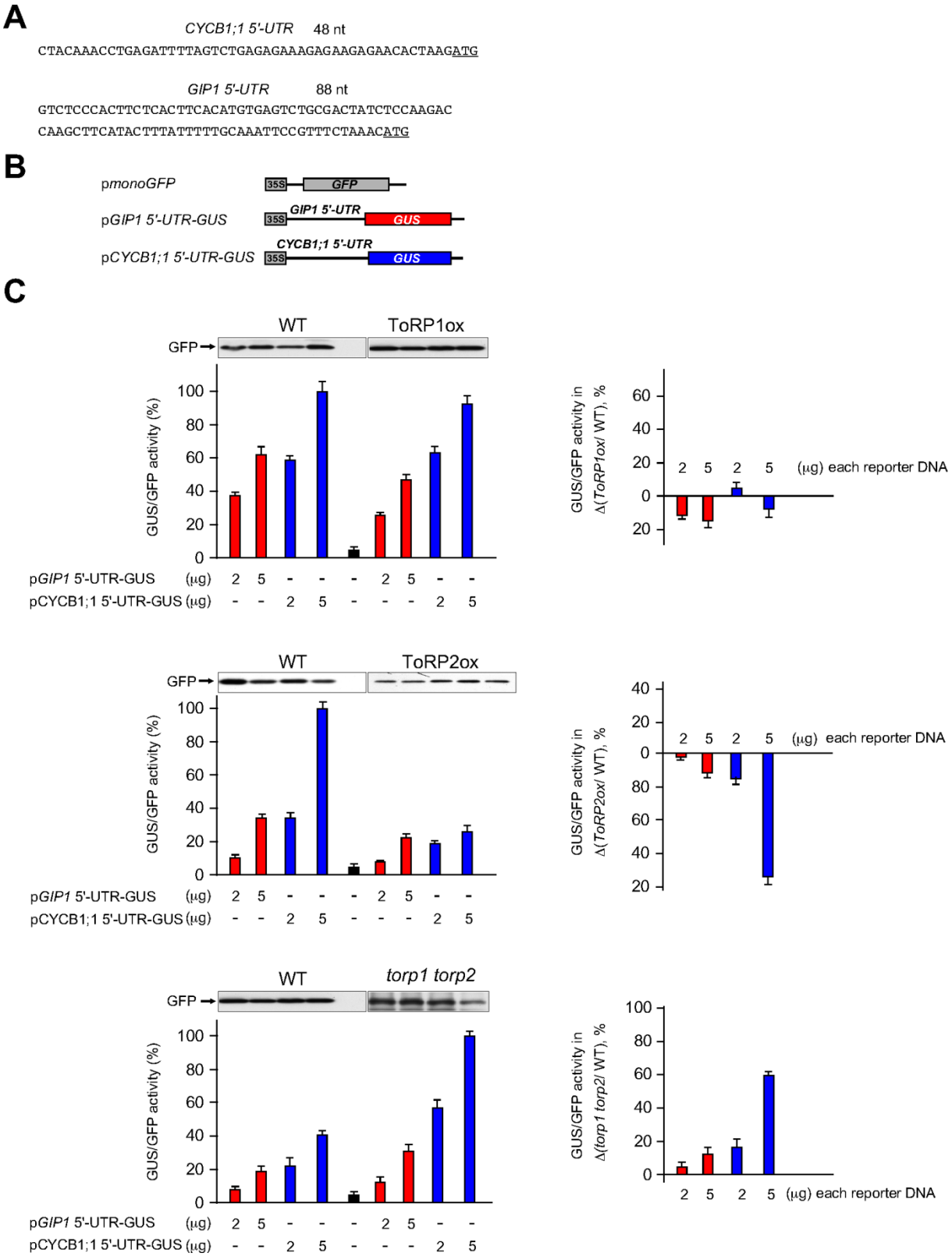
A
CYCB1;1 5'-UTR 48 nt
CTACAAACCTGAGATTTTAGTCTGAGAGAAAGAGAAGAGAACACTAAGATG
GIP1 5'-UTR 88 nt
GTCTCCCACTTCTCACTTCACATGTGAGTCTGCGACTATCTCCAAGAC
CAAGCTTCATACTTTATTTTTGCAAATTCCGTTTCTAAACATG
B
pmonoGFP
35S
GFP
pGIP1 5'-UTR-GUS
GIP1 5'-UTR
GUS
pCYCB1;1 5'-UTR-GUS
CYCB1;1 5'-UTR
C
WT
ToRP1ox
GFP
GUS/GFP activity (%)
pGIP1 5'-UTR-GUS (µg) 2 5 - - - 2 5 - -
pCYCB1;1 5'-UTR-GUS (µg) - - 2 5 - - - 2 5
GUS/GFP activity in Δ(ToRP1ox/ WT), %
(µg) each reporter DNA
WT
ToRP2ox
GFP
GUS/GFP activity (%)
pGIP1 5'-UTR-GUS (µg) 2 5 - - - 2 5 - -
pCYCB1;1 5'-UTR-GUS (µg) - - 2 5 - - - 2 5
GUS/GFP activity in Δ(ToRP2ox/ WT), %
(µg) each reporter DNA
WT
torp1 torp2
GFP
GUS/GFP activity (%)
pGIP1 5'-UTR-GUS (µg) 2 5 - - - 2 5 - -
pCYCB1;1 5'-UTR-GUS (µg) - - 2 5 - - - 2 5
GUS/GFP activity in Δ(torp1 torp2/ WT), %
(µg) each reporter DNA

Figure 1—6 | ToRP effects on cap-dependent translation initiation in plant protoplasts

(A) Sequences of two 5'-UTRs from CYCB1;1 and GIP1 mRNAs used for protoplast experiments are presented.

(B) Structure of the reporter plasmids containing (1) either 5'-UTRs from CYCB1;1 or GIP1 mRNAs placed upstream of GUS ORF, and (2) TuMV IRES upstream of GFP-encoding ORF.

(C) Cap-dependent translation is sensitive to ToRP1 and ToRP2 levels in *ToRP1ox*, *ToRP2ox* and *torp1 torp2*–derived mesophyll protoplasts. Each pair of protoplasts was transfected in duplicate with indicated concentrations of the 5'-UTR reporter constructs and 5 µg of GFP-containing reporter plasmids. 18 hours post-transformation, protoplasts were harvested and GFP, GUS (β-glucuronidase) activities were measured, and the GUS/GFP activity ratio was calculated. The highest value within each protoplast pair (WT and *ToRP1ox*, or WT and *ToRP2ox*, or WT and *torp1 torp2*) was set at 100%. In addition, GFP accumulation was verified by western blot using anti GFP antibodies. Data are presented as the mean ± standard error. Relative ratio between WT and mutant genotype was quantified and are presented in the *Right panel*

GUS-containing mRNA levels and integrity after 18 h of incubation was monitored by sqPCR.

Discussion

Until now, it was unclear whether TOR participated in cap-dependent translation initiation in plants. We have identified a set of proteins—TOR Regulatory Proteins (ToRPs)—ToRPs 1 to 4, and demonstrated (1) ToRP1 binding to eIF4E and the N-terminal HEAT repeat domain of TOR *in vitro* (Figs 2 and 3); (2) ToRP1 and ToRP2 phosphorylation at several phosphorylation sites *in planta* that appeared to be responsive to auxin (Fig. 5); (3) two of these phosphorylation sites have been identified as S49 and S89, the phosphorylation status of which modulates ToRP1 binding to eIF4E in the yeast two-hybrid system (Fig. 4); (4) these proteins can function as translation repressors in plant protoplasts (Fig. 6).

Taken together, our results suggest that, in plants, TOR may regulate cap-dependent translation via ToRPs in a manner similar to human 4E-BPs 1 and 2, albeit displaying plant-specific features. Among the three ToRP conserved motifs, one is the canonical 4E-binding site (4E-BM), the second is an N-rich motif that resembles the motif within Hs4E-BP2 (Bidinosti et al. 2010), and the third, which is located at the C-terminus, differs from the canonical TOS motif found in mammalian 4E-BPs. Strikingly, amino acid substitutions within M3 negatively modulate ToRP1 binding to both eIF4E and NTOR, strongly indicating M3 importance for ToRP1 binding capacity. The TOS motif is missing in ToRPs, suggesting that plant proteins may interact directly with the HEAT domain of TOR to present themselves for TOR phosphorylation.

3D models of ToRPs 1 and 2, generated by RaptorX, predict with high probability structurally disordered proteins (Fig. 1B), as was also shown for 4E-BP proteins (Fletcher and Wagner 1998). In mammals, 4E-BP binds eIF4E cooperatively via three motifs: 4E-BM adopts an L-shaped α-helical conformation similar to that of eIF4G when bound to eIF4E (Marcotrigiano et al. 1999); a second site consisting of an elbow loop PGVTS/T sequence (Peter et al. 2015); and the third non-canonical motif at the C-terminus (Gosselin et al. 2011;

Paku et al. 2012). Indeed, a site similar to the elbow loop could be found within ToRPs 1 and 2; however, its involvement in eIF4E binding remains to be demonstrated.

ToRPs contain several phosphorylation sites that resemble those present in well-known substrates of TOR kinase. Two of them, when unphosphorylated (Ser49 and Ser89 phosphorylation knockout mutants), allow stronger binding of ToRP1 to eIF4E, and their mimetic mutations were sufficient to dissociate ToRP1 from eIF4E. Thus, interaction between ToRP1 and eIF4E is likely governed by inactivation of TOR by AZD-8055 and dephosphorylation of ToRPs (Fig. 5).

Selected groups of mRNA were suggested to be dependent on 4E-BPs and, thus, on TOR: eIF4E-sensitive mRNAs with large and structured 5'-UTRs (Koromilas et al. 1992), encoding for proteins involved in cell survival and proliferation, such as cyclins, Myc, VEGF (Vascular Endothelial Growth Factor) or Bcl-XL (Graff and Zimmer 2003), and mRNAs harboring TOP sequences at the 5'-mRNA end (Thoreen et al. 2012). These data are in good agreement with our results, which demonstrate high sensitivity to high ToRP2 levels of cyclin-encoded mRNA translation. Together, our results suggest a model of how ToRPs may contribute to TOR-mediated control of translation initiation (Fig. 7). Our preliminary model states that, under conditions of TOR inhibition (AZD-8055), TOR is dephosphorylated, followed by ToRP1/2 dephosphorylation and binding to eIF4E (eIFiso4E), leading to translation repression of eIF4E-sensitive mRNAs. In response to auxin, TOR becomes active and phosphorylates ToRPs. ToRPs dissociates from eIF4E (eIFiso4E), which leads to restoration of eIF4F (eIFiso4F) complex formation.

However, further investigations are required to reveal the role of TOR in ToRP phosphorylation and in cap-dependent translation initiation *in planta*. One open question is whether ToRPs can overcome the tight binding affinity between the canonical type 1 cap-binding proteins, eIF4E and eIFiso4E, with their respective eIF4G subunits, which is higher

that for mammalian orthologs and estimated to be at the sub-nanomolar level (Mayberry et al. 2011). An alternative model suggests that eIF4E (eIFiso4E) cap-binding activity might be modulated in response to the redox state of the cell. Indeed, it was demonstrated that the oxidation state of eIF4E and eIFiso4E can be critical for their binding to the cap-structure (Monzingo et al. 2007). Thus, regulation of eIF4E-dependent translation initiation in plants might be regulated by various pathways depending on both TOR and/or cell physiological conditions.

Control of mRNA translation pathways plays a fundamental role in many aspects of gene expression, cell growth and proliferation. A growing number of examples speak in favour of a widespread influence of TOR signalling on different steps of protein synthesis. Here, we have revealed that the TOR signalling pathway contributes to translation initiation in plants, thus opening far-reaching perspectives of protein synthesis control at multiple levels.

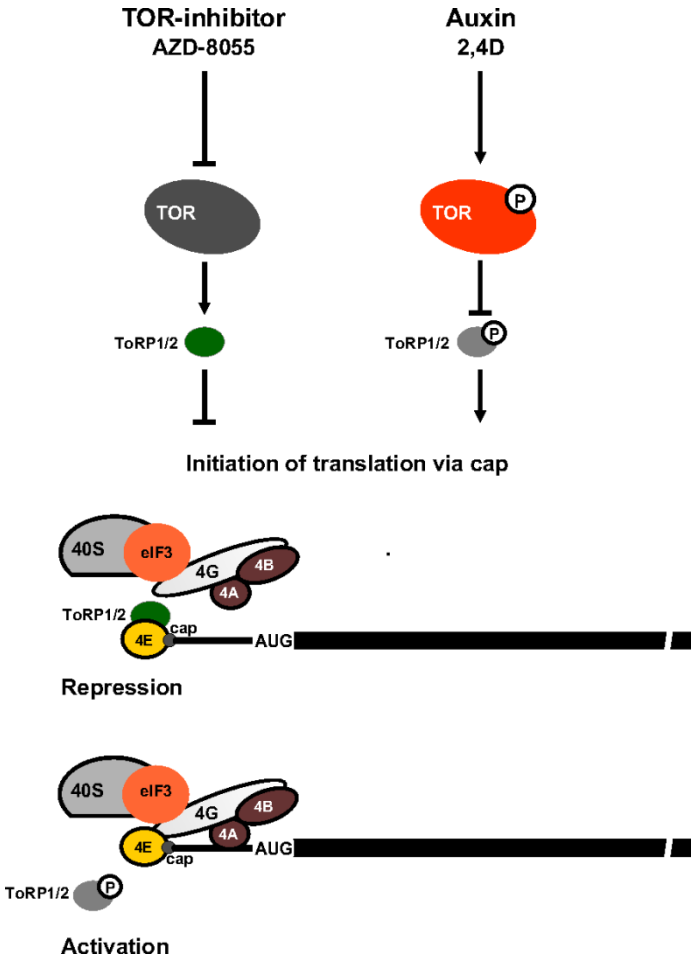

Figure 1—7 | Provisional model of ToRP1 and ToRP2 function in cap-dependent translation initiation

ToRP1 and ToRP2 phosphorylation is sensitive to AZD-8055 and responsive to auxin, and thus active TOR can maintain both proteins in an activated phosphorylation state. We demonstrated that ToRPs, when not phosphorylated, bind eIF4E, preventing eIF4F complex formation. In contrast, active TOR triggers their phosphorylation, followed by eIF4E dissociation that would restore eIF4F (see Discussion).

Materials and methods

Expression constructs and antibodies

Detailed descriptions of plasmid construction, oligos and antibodies can be found in the Materials and Methods.

Seeds were sterilized, followed by washing, drying and plating on appropriate MS-Agar (Murashige and Skoog medium with MSMO-salt mixture; Sigma®) plates. The plates were stored for 24 hours at 4 °C in the dark, for germination synchronization. *Arabidopsis thaliana* plants were grown for 7 days under long-day conditions (16 h light at 21 °C and 8 h darkness at 17 °C). To study phosphorylation of ToRP proteins in response to TOR, *A. thaliana* seedlings were grown with either TOR inhibitor (AZD-8055) or TOR activator (2,4-D) (MS-Agar plates were supplemented with either 0.5 µM AZD or 0.1 µg/mL 2,4-D).

ToRP1 and *ToRP2* genes were synthetically designed and optimized for codon usage in *E. coli* by Dapcel, Inc. The protein coding sequence surrounded by FLAG-ToRP1-6xHis or FLAG-ToRP2-6xHis was cloned downstream of the T7 promoter and gene 10 leader sequences, and transformed into BL21 (DE3) pLysS *E. coli* strains for expression.

Anti eIF4E and eIFiso4E antibodies were kindly provided by Gallois Jean-Luc (INRA-UR 1052 Génétique et Amélioration des Fruits et Légumes (GAFL), Montfavet). Polyclonal Rabbit Anti ToRP1/2 antibodies were raised against the central conserved motif (CRLLRGKQTMTEFEPL) and prepared by Eurogentec®. ToRP phosphoantibodies (Anti-S49-P and Anti-S89-P) were raised against peptide 1 (YSPSPSPYR[pS]PVTLP) and peptide 2 (ERFYYRQ[pS]PPPSGK), which contain the S49 and S89 phosphorylation sites, respectively, and were obtained from ProteoGenix®.

Pull-down experiments

Glutathione-*S*-transferase pull-down assays were carried out as described in Park et al. (2001). Co-immunoprecipitation experiments were performed as described in Thiébeauld et al. (2009) and Supplemental Data.

Cap-binding experiments

A cap-binding assay was used to study the interaction between FLAG-ToRP1-6xHis with eIF4E1 and eIFiso4E3 prebound to Immobilized γ-Aminophenyl-m^7GTP (C_{10}-spacer) (Jena Bioscience). The assay was performed in two steps—eIF4E1 and eIFiso4E were incubated with m^7GTP agarose, and, after washing of unbound eIF4E/iso4E, the complex was further incubated with FLAG-ToRP1-6xHis. A 20 µL aliquot of the first supernatant (Unbound fraction, U) and of resuspended beads (bound fraction, B) was used for analysis in SDS-PAGE, to evaluate the efficiency of cap-binding. Next, eIF4E1- or eIFiso4E-bound to m^7GTP beads were further incubated with recombinant proteins. Binding was carried out in a reaction mixture containing 500 µL of binding buffer for 1 h at 4 °C under constant rotation. The first unbound (U) and bound (B) fractions were separated by 15% SDS-PAGE gel followed by Coomassie™ blue staining or immunoblotting analysis.

Purification of GST-fusion proteins

Recombinant eIF4E1 and eIFiso4E proteins were purified using a GST-trap HP column, followed by elution with specific cleavage of GST by PreScission® protease.

GST pull-down assays

Equivalent molar ratios of purified proteins (FLAG-ToRP1-6xHis) were incubated with GST-fusion proteins (GST-eIF4E1 and GST-eIFiso4E3) or GST alone at 4 °C for 2 h as described in Schepetilnikov et al. (2013). Total bound (B) and unbound fractions (U) were separated by electrophoresis on 15% SDS-PAGE followed by Coomassie™ blue staining or immunoblotting.

Two-dimensional gel electrophoresis

Protein phosphorylation bands were separated according to standard protocol. We used commercially ReadyStrips IPG strips (Bio-Rad) of 7 cm length that allow loading of 10–100 µg of proteins in the pH range 7–10.

Yeast two-hybrid assay

GAL4-based yeast two-hybrid protein interaction assays were performed according to Thiébeauld et al. (2009).

Arabidopsis protoplasts

Arabidopsis protoplasts prepared from either a suspension culture, or from 3- to 4-week-old plantlets (mesophyll protoplasts) were transfected with plasmid DNA by the PEG method as described in Materials and methods. Protoplasts were prepared from *Arabidopsis thaliana* wild-type, ToRP1- or ToRP2-overexpressing lines, or knockout lines as described in Yoo et al. (2007). Protoplasts were co-transfected with two reporter plasmids—monocistronic reporter—pmonoGFP (a transfection marker), and a β-glucuronidase-encoding GUS reporter fused to the 5'-UTR of GIP1 or CyclinB1;1—p*GIP1* 5'UTR-GUS or p*CYCB1;1* 5'UTR-GUS. 2 and 5 µg of each leader-GUS-containing construct, and 5 µg of pmonoGFP were used for co-transfection of the protoplasts indicated.

Acknowledgments

We are grateful to A. Komar (*DAPCEL Inc*) for recombinant ToRP1 and ToRP2 design, and N. Baumberger and L. Herrgott for helpful assistance in protein analysis. We thank C. Meyer for helpful discussions. This work was supported by French Agence Nationale de la Recherché—BLAN-2011_BSV6 010 03 and ANR-14-CE19-0007—funding to L.R. and by a PhD fellowship from the Ministry of Research to O.S.

References

Batzenschlager, M., K. Masoud, N. Janski, G. Houlné, E. Herzog, J.-L. Evrard, N. Baumberger, M. Erhardt, Y. Nominé, B. Kieffer, A.-C. Schmit, and M.-E. Chabouté. 2013. The GIP gamma-tubulin complex-associated proteins are involved in nuclear architecture in Arabidopsis thaliana. *Front. Plant Sci.* 4:480.

Bidinosti, M., I. Ran, M.R. Sanchez-Carbente, Y. Martineau, A.-C. Gingras, C. Gkogkas, B. Raught, C. Bramham, W.S. Sossin, M. Costa-Mattioli, L. DesGroseillers, J.-C. Lacaille, and N. Sonenberg. 2010. Postnatal deamidation of 4E-BP2 in brain enhances its association with raptor and alters kinetics of excitatory synaptic transmission. *Mol. Cell*. 37:797–808. doi:10.1016/j.molcel.2010.02.022.

Browning, K.S., and J. Bailey-Serres. 2015. Mechanism of Cytoplasmic mRNA Translation. *Arabidopsis Book*. 13:e0176. doi:10.1199/tab.0176.

Chresta, C.M., B.R. Davies, I. Hickson, T. Harding, S. Cosulich, S.E. Critchlow, J.P. Vincent, R. Ellston, D. Jones, P. Sini, D. James, Z. Howard, P. Dudley, G. Hughes, L. Smith, S. Maguire, M. Hummersone, K. Malagu, K. Menear, R. Jenkins, M. Jacobsen, G.C.M. Smith, S. Guichard, and M. Pass. 2010. AZD8055 Is a Potent, Selective, and Orally Bioavailable ATP-Competitive Mammalian Target of Rapamycin Kinase Inhibitor with In vitro and Antitumor Activity. *Cancer Res.* 70:288 LP-298.

Deprost, D., L. Yao, R. Sormani, M. Moreau, G. Leterreux, M. Nicolaï, M. Bedu, C. Robaglia, and C. Meyer. 2007. The Arabidopsis TOR kinase links plant growth, yield, stress resistance and mRNA translation. *EMBO Rep.* 8:864 LP-870.

Dobrenel, T., C. Marchive, R. Sormani, M. Moreau, M. Mozzo, M.-H. Montané, B. Menand, C. Robaglia, and C. Meyer. 2011. Regulation of plant growth and metabolism by the TOR kinase. *Biochem. Soc. Trans.* 39:477 LP-481.

Fauser, F., S. Schiml, and H. Puchta. 2014. Both CRISPR/Cas-based nucleases and nickases can be used efficiently for genome engineering in Arabidopsis thaliana. *Plant J.* 79:348–359. doi:10.1111/tpj.12554.

Fletcher, C.M., A.M. McGuire, A.-C. Gingras, H. Li, H. Matsuo, N. Sonenberg, and G. Wagner. 1998. 4E Binding Proteins Inhibit the Translation Factor eIF4E without Folded Structure. *Biochemistry*. 37:9–15. doi:10.1021/bi972494r.

Fletcher, C.M., and G. Wagner. 1998. The interaction of eIF4E with 4E-BP1 is an induced fit to a completely disordered protein. *Protein Sci.* 7:1639–1642.

Gingras, A.-C., S.P. Gygi, B. Raught, R.D. Polakiewicz, R.T. Abraham, M.F. Hoekstra, R.

Aebersold, and N. Sonenberg. 1999. Regulation of 4E-BP1 phosphorylation: a novel two-step mechanism. *Genes Dev.* 13:1422–1437.

Gingras, A.-C., B. Raught, S.P. Gygi, A. Niedzwiecka, M. Miron, S.K. Burley, R.D. Polakiewicz, A. Wyslouch-Cieszynska, R. Aebersold, and N. Sonenberg. 2001. Hierarchical phosphorylation of the translation inhibitor 4E-BP1. *Genes Dev.* 15:2852–2864. doi:10.1101/gad.912401.

Gosselin, P., N. Oulhen, M. Jam, J. Ronzca, P. Cormier, M. Czjzek, and B. Cosson. 2011. The translational repressor 4E-BP called to order by eIF4E: new structural insights by SAXS. *Nucleic Acids Res.* 39:3496–3503. doi:10.1093/nar/gkq1306.

Graff, J.R., and S.G. Zimmer. 2003. Translational control and metastatic progression: Enhanced activity of the mRNA cap-binding protein eIF-4E selectively enhances translation of metastasis-related mRNAs. *Clin. Exp. Metastasis*. 20:265–273. doi:10.1023/A:1022943419011.

Hershey, J.W.B., and W.C. Merrick. 2000. 2 The Pathway and Mechanism of Initiation of Protein Synthesis. *Cold Spring Harb. Monogr. Arch. Vol. 39 Transl. Control Gene Expr.*

Hinnebusch, A.G. 2014. The Scanning Mechanism of Eukaryotic Translation Initiation. *Annu. Rev. Biochem.* 83:779–812. doi:10.1146/annurev-biochem-060713-035802.

Jackson, R.J., C.U.T. Hellen, and T. V Pestova. 2010. The mechanism of eukaryotic translation initiation and principles of its regulation. *Nat Rev Mol Cell Biol*. 11:113–127.

Källberg, M., H. Wang, S. Wang, J. Peng, Z. Wang, H. Lu, and J. Xu. 2012. Template-based protein structure modeling using the RaptorX web server. *Nat. Protoc.* 7:1511–1522. doi:10.1038/nprot.2012.085.

Kang, S.A., M.E. Pacold, C.L. Cervantes, D. Lim, H.J. Lou, K. Ottina, N.S. Gray, B.E. Turk, M.B. Yaffe, and D.M. Sabatini. 2013. mTORC1 Phosphorylation Sites Encode Their Sensitivity to Starvation and Rapamycin. *Science (80-.).* 341.

Kim, D.-H., D.D. Sarbassov, S.M. Ali, J.E. King, R.R. Latek, H. Erdjument-Bromage, P. Tempst, and D.M. Sabatini. 2002. mTOR Interacts with Raptor to Form a Nutrient-Sensitive Complex that Signals to the Cell Growth Machinery. *Cell*. 110:163–175. doi:10.1016/S0092-8674(02)00808-5.

Kleijn, M., G.C. Scheper, M.L. Wilson, A.R. Tee, and C.G. Proud. 2002. Localisation and regulation of the eIF4E-binding protein 4E-BP3. *FEBS Lett.* 532:319–323. doi:10.1016/S0014-5793(02)03694-3.

Koromilas, A.E., A. Lazaris-Karatzas, and N. Sonenberg. 1992. mRNAs containing extensive secondary structure in their 5' non-coding region translate efficiently in cells

overexpressing initiation factor eIF-4E. *EMBO J.* 11:4153–4158.

Kozak, M. 1999. Initiation of translation in prokaryotes and eukaryotes. *Gene*. 234:187–208. doi:http://dx.doi.org/10.1016/S0378-1119(99)00210-3.

Lawrence Jr, J.C., and R.T. Abraham. 1997. PHAS/4E-BPs as regulators of mRNA translation and cell proliferation. *Trends Biochem. Sci.* 22:345–349. doi:10.1016/S0968-0004(97)01101-8.

Lellis, A.D., M.L. Allen, A.W. Aertker, J.K. Tran, D.M. Hillis, C.R. Harbin, C. Caldwell, D.R. Gallie, and K.S. Browning. 2010. Deletion of the eIFiso4G subunit of the Arabidopsis eIFiso4F translation initiation complex impairs health and viability. *Plant Mol. Biol.* 74:249–263. doi:10.1007/s11103-010-9670-z.

Li, C., T. Potuschak, A. Colón-Carmona, R.A. Gutiérrez, and P. Doerner. 2005. Arabidopsis TCP20 links regulation of growth and cell division control pathways. *Proc. Natl. Acad. Sci. U. S. A.* 102:12978–12983. doi:10.1073/pnas.0504039102.

Lin, T.A., X. Kong, T.A. Haystead, A. Pause, G. Belsham, N. Sonenberg, and J.C. Lawrence. 1994. PHAS-I as a link between mitogen-activated protein kinase and translation initiation. *Science (80-.).* 266:653 LP-656.

Lin, T.-A., and J.C. Lawrence. 1996. Control of the Translational Regulators PHAS-I and PHAS-II by Insulin and cAMP in 3T3-L1 Adipocytes. *J. Biol. Chem.* . 271:30199–30204. doi:10.1074/jbc.271.47.30199.

Ma, X.M., and J. Blenis. 2009. Molecular mechanisms of mTOR-mediated translational control. *Nat Rev Mol Cell Biol*. 10:307–318.

Mader, S., H. Lee, A. Pause, and N. Sonenberg. 1995. The translation initiation factor eIF-4E binds to a common motif shared by the translation factor eIF-4 gamma and the translational repressors 4E-binding proteins. *Mol. Cell. Biol.* 15:4990–4997.

Mahfouz, M.M., S. Kim, A.J. Delauney, and D.P.S. Verma. 2006. Arabidopsis TARGET OF RAPAMYCIN Interacts with RAPTOR, Which Regulates the Activity of S6 Kinase in Response to Osmotic Stress Signals. *Plant Cell*. 18:477–490.

Marcotrigiano, J., A.-C. Gingras, N. Sonenberg, and S.K. Burley. 1999. Cap-Dependent Translation Initiation in Eukaryotes Is Regulated by a Molecular Mimic of eIF4G. *Mol. Cell*. 3:707–716. doi:10.1016/S1097-2765(01)80003-4.

Martineau, Y., R. Azar, C. Bousquet, and S. Pyronnet. 2013. Anti-oncogenic potential of the eIF4E-binding proteins. *Oncogene*. 32:671–677.

Mayberry, L.K., M.L. Allen, K.R. Nitka, L. Campbell, P.A. Murphy, and K.S. Browning. 2011. Plant Cap-binding Complexes Eukaryotic Initiation Factors eIF4F and eIFISO4F:

MOLECULAR SPECIFICITY OF SUBUNIT BINDING. *J. Biol. Chem.* 286:42566–42574. doi:10.1074/jbc.M111.280099.

Menand, B., T. Desnos, L. Nussaume, F. Berger, D. Bouchez, C. Meyer, and C. Robaglia. 2002. Expression and disruption of the Arabidopsis TOR(target of rapamycin) gene. *Proc Natl Acad Sci U S A*. 99. doi:10.1073/pnas.092141899.

Montané, M.-H., and B. Menand. 2013. ATP-competitive mTOR kinase inhibitors delay plant growth by triggering early differentiation of meristematic cells but no developmental patterning change. *J. Exp. Bot.* 64:4361–4374. doi:10.1093/jxb/ert242.

Monzingo, A.F., S. Dhaliwal, A. Dutt-Chaudhuri, A. Lyon, J.H. Sadow, D.W. Hoffman, J.D. Robertus, and K.S. Browning. 2007. The Structure of Eukaryotic Translation Initiation Factor-4E from Wheat Reveals a Novel Disulfide Bond. *Plant Physiol.* 143:1504–1518. doi:10.1104/pp.106.093146.

Moreau, M., M. Azzopardi, G. Clément, T. Dobrenel, C. Marchive, C. Renne, M.-L. Martin-Magniette, L. Taconnat, J.-P. Renou, C. Robaglia, and C. Meyer. 2012. Mutations in the Arabidopsis Homolog of LST8/GβL, a Partner of the Target of Rapamycin Kinase, Impair Plant Growth, Flowering, and Metabolic Adaptation to Long Days. *Plant Cell* . 24:463–481. doi:10.1105/tpc.111.091306.

Paku, K.S., Y. Umenaga, T. Usui, A. Fukuyo, A. Mizuno, Y. In, T. Ishida, and K. Tomoo. 2012. A conserved motif within the flexible C-terminus of the translational regulator 4E-BP is required for tight binding to the mRNA cap-binding protein eIF4E. *Biochem. J.* 441:237 LP-245.

Park, H.-S., A. Himmelbach, K.S. Browning, T. Hohn, and L.A. Ryabova. 2001. A Plant Viral Reinitiation; Factor Interacts with the Host Translational Machinery. *Cell*. 106:723–733. doi:10.1016/S0092-8674(01)00487-1.

Patrick, R.M., and K.S. Browning. 2012. The eIF4F and eIFiso4F Complexes of Plants: An Evolutionary Perspective. *Comp. Funct. Genomics*. 2012:287814.

Pause, A., G.J. Belsham, A.-C. Gingras, O. Donze, T.-A. Lin, J.C. Lawrence, and N. Sonenberg. 1994. Insulin-dependent stimulation of protein synthesis by phosphorylation of a regulator of 5'-cap function. *Nature*. 371:762–767.

Pestova, T. V, J.R. Lorsch, and C.U.T. Hellen. 2007. 4 The Mechanism of Translation Initiation in Eukaryotes. *Cold Spring Harb. Monogr. Arch. Vol. 48 Transl. Control Biol. Med.*

Peter, D., C. Igreja, R. Weber, L. Wohlbold, C. Weiler, L. Ebertsch, O. Weichenrieder, and E. Izaurralde. 2015. Molecular Architecture of 4E-BP Translational Inhibitors Bound to

eIF4E. *Mol. Cell*. 57:1074–1087. doi:10.1016/j.molcel.2015.01.017.

Poulin, F., A.-C. Gingras, H. Olsen, S. Chevalier, and N. Sonenberg. 1998. 4E-BP3, a New Member of the Eukaryotic Initiation Factor 4E-binding Protein Family. *J. Biol. Chem.* . 273:14002–14007. doi:10.1074/jbc.273.22.14002.

Raught, B., A.-C. Gingras, S.P. Gygi, H. Imataka, S. Morino, A. Gradi, R. Aebersold, and N. Sonenberg. 2000. Serum-stimulated, rapamycin-sensitive phosphorylation sites in the eukaryotic translation initiation factor 4GI. *EMBO J.* 19:434–444.

Ren, M., P. Venglat, S. Qiu, L. Feng, Y. Cao, E. Wang, D. Xiang, J. Wang, D. Alexander, S. Chalivendra, D. Logan, A. Mattoo, G. Selvaraj, and R. Datla. 2012. Target of Rapamycin Signaling Regulates Metabolism, Growth, and Life Span in Arabidopsis. *Plant Cell* . 24:4850–4874. doi:10.1105/tpc.112.107144.

Roux, P.P., and I. Topisirovic. 2012. Regulation of mRNA Translation by Signaling Pathways. *Cold Spring Harb. Perspect. Biol.* . 4. doi:10.1101/cshperspect.a012252.

Schepetilnikov, M., M. Dimitrova, E. Mancera-Martínez, A. Geldreich, M. Keller, and L.A. Ryabova. 2013. TOR and S6K1 promote translation reinitiation of uORF-containing mRNAs via phosphorylation of eIF3h. *EMBO J.* 32:1087 LP-1102.

Schepetilnikov, M., K. Kobayashi, A. Geldreich, C. Caranta, C. Robaglia, M. Keller, and L.A. Ryabova. 2011. Viral factor TAV recruits TOR/S6K1 signalling to activate reinitiation after long ORF translation. *EMBO J.* 30:1343–1356. doi:10.1038/emboj.2011.39.

Thiébeauld, O., M. Schepetilnikov, H.-S. Park, A. Geldreich, K. Kobayashi, M. Keller, T. Hohn, and L.A. Ryabova. 2009. A new plant protein interacts with eIF3 and 60S to enhance virus-activated translation re-initiation. *EMBO J.* 28:3171–3184.

Thoreen, C.C., L. Chantranupong, H.R. Keys, T. Wang, N.S. Gray, and D.M. Sabatini. 2012. A unifying model for mTORC1-mediated regulation of mRNA translation. *Nature*. 485:109–113. doi:10.1038/nature11083.

Xiong, Y., and J. Sheen. 2012. Rapamycin and Glucose-Target of Rapamycin (TOR) Protein Signaling in Plants. *J. Biol. Chem.* . 287:2836–2842. doi:10.1074/jbc.M111.300749.

Yoo, S.-D., Y.-H. Cho, and J. Sheen. 2007. Arabidopsis mesophyll protoplasts: a versatile cell system for transient gene expression analysis. *Nat. Protoc.* 2:1565–1572.

Zeenko, V., and D.R. Gallie. 2005. Cap-independent Translation of Tobacco Etch Virus Is Conferred by an RNA Pseudoknot in the 5′-Leader. *J. Biol. Chem.* . 280:26813–26824. doi:10.1074/jbc.M503576200.

2. Purification of recombinant FLAG-ToRP1/2-6xHis proteins

Mammalian 4E-BPs are considered to be intrinsically unstructured proteins – they lack a stable globular tertiary structure (Fletcher et al. 1998; Fletcher and Wagner 1998). However, 4E-BPs can be stabilized by interaction with eIF4E. When interacting with eIF4E, the peptide containing the eIF4E-binding site adopts an energetically favorable L-shaped α-helical conformation (Marcotrigiano et al. 1999).

The 3D putative structure of *Arabidopsis* ToRP1/2 proteins generated by RaptorX suggests that ToRP1/2 share structural and binding properties with the canonical 4E-BPs from mammals. *Arabidopsis* ToRP1 and ToRP2 contain no well-defined structural domains, except the canonical eIF4E-binding motif located at the N-terminal part of ToRP1/2 that adopts an α-helical conformation similar to that within mammalian 4E-BPs.

Due to several unique structural characteristics – very small size, high proline and low aromatic acid content – purification and *in vitro* studies of recombinant ToRP1 and ToRP2 proteins represent a difficult task.

Thus, for expression and purification of ToRP1 and ToRP2 recombinant proteins, I had to screen a wide range of conditions to optimize expression and/or purification steps: expression with different tags was done in different *E. coli* strains, expression and induction were carried out under different temperatures, and Ni-column loading and elution efficiencies were compared at different pH.

2.1. Expression of Arabidopsis ToRP1/2 fused to different tags in BL21 (DE3) pLysS E. coli

PCR products corresponding to full-length *Arabidopsis* ToRP1/2 were introduced into (i) the expression vector pGEX-6P1 to obtain GST tag fused to the protein N-terminus or (ii) into the expression vector pHMGWA to obtain two different tags: Maltose Binding proteins (MBP) and 6xHis were fused to the N- and C-terminus of ToRP1 (ToRP2), respectively. The advantage of double MBP- and 6xHis tags is to increase protein solubility and to purify these proteins using the Nickel-column. Both vectors were expressed in BL21 (DE3) plysS *E. coli* strain under normal conditions: growth at 37 °C to an OD_{600} 0.5, then 0.5 mM IPTG induction at 37 °C for 1 hour. However, ToRP1/2 production in *E. coli* was bellow detectable levels.

2.2. ToRP1/2 codon optimization for expression in BL21 (DE3) pLysS E. coli

After a failed production of ToRP1/2 in *E. coli*, we decided to optimize codon usage of a plant gene for expression in *E. coli*, which also leads to proper protein folding and thus increased protein stability, solubility and production. Here, two tags were added: FLAG and 6xHis tags on the N- and C-terminus, respectively. FLAG Tag allows monitoring ToRP1/2 expression and purification by immunoblot analysis using anti-FLAG antibody.

The optimized constructs were then cloned into the expression vector pET3a and used to transform BL21 (DE3) pLysS *E. coli* strain. Standard conditions were applied for expression: bacterial growth at 37 °C until OD_{600} reached 0.5, then IPTG induction for 1 hour at 37 °C. To assess FLAG-ToRP1-6xHis and FLAG-ToRP2-6xHis expression levels, equal volumes of non-induce and induce samples were loaded into 15 % SDS-PAGE followed by immunoblot analysis with anti-FLAG antibody. Strikingly, FLAG-ToRP1-6xHis and FLAG-ToRP2-6xHis recombinant protein expression levels were significantly improved. Resulting FLAG-ToRP1-6xHis and FLAG-ToRP2-6xHis migrate in SDS-PAGE as 17 kDa and 22 kDa proteins, respectively, that corresponds to their predicted sizes.

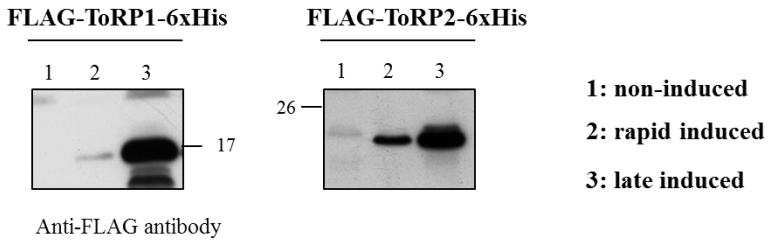

Figure 2—1 | Rapid and late-IPTG induction of FLAG-ToRP1-6xHis and FLAG-ToRP2-6xHis

FLAG-ToRP1-6xHis and FLAG-ToRP2-6xHis were expressed in BL21 (DE3) pLysS *E. coli* strains at 37 °C until 0.5 DO_{600} (for rapid-IPTG induction) or 1.5 DO_{600} (for late-IPTG induction). After addition of 0.5 mM of IPTG, bacterial culture continued to grow for 1 hour at 37 °C. An equal volume of non-induced (1) and induced samples (2 and 3 for rapid- and late-induction conditions, respectively) were loaded on 15% SDS-PAGE, followed by immunoblot analysis with anti-FLAG antibody.

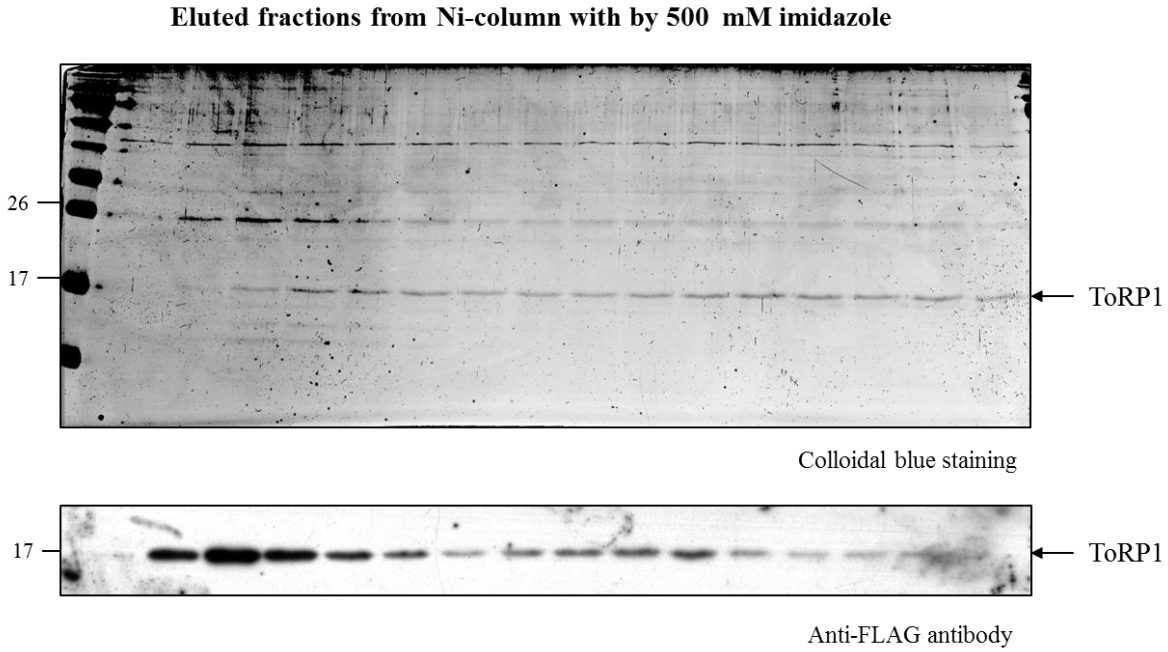

Figure 2—2 | Purification of FLAG-ToRP1-6xHis recombinant protein using Ni-sepharose column

FLAG-ToRP1-6xHis was loaded on Ni-sepharose column, and eluted with 300 mM and 500 mM of imidazole. Several elution fractions (500 mM imidazole) were analyzed by 15% SDS-PAGE followed by either Colloidal blue staining (upper part) or immunoblot analysis using anti-FLAG antibody (bottom panel). Protein markers are shown on left. FLAG-ToRP1-6xHis migration corresponds to 17 kDa protein.

2.3. Expression strategies: rapid vs. late IPTG induction

However, FLAG-ToRP1-6xHis and FLAG-ToRP2-6xHis proteins were largely insoluble and mainly present in the pellet fraction. Next goal was to increase the solubility of such unstructured proteins. To address this question, several combinations of temperature/time conditions for IPTG induction were tested. The bacterial growth at 37°C remained unaffected until DO_{600} 0.5, followed by IPTG induction under different conditions: 37 °C for 30 min; 37 °C for 1 h; 25 °C for 1 h; 25 °C for 2 h; 18 °C for 2 h; 18 °C overnight. However, the solubility of both proteins was not improved in all tested conditions.

After that, I tested two different strategies of IPTG induction: rapid and late induction. Transformed bacteria were grown at 37 °C until DO_{600} reached 0.5 (rapid induction) or 1.5 (late induction). IPTG was added to cultures for 1h at 37 °C. Increased protein levels were detected in samples upon late-induction condition in comparison to rapid-induction conditions. Thus, ToRP1 and ToRP2 protein levels were significantly increased by using late-induction *versus* to rapid-induction conditions **(Figure 2—1).**

2.4. Purification of FLAG-ToRP1/2-6xHis recombinant proteins

2.4.1. Expression of FLAG-ToRP1/2-6xHis in late-IPTG induction conditions

A single colony from BL21 (DE3) pLysS *E. coli* transformed cells was used to inoculate 25 mL of LB medium containing 0.2% (w/v) Glucose and appropriate antibiotics (100 µg/mL Ampicillin and 25 µg/mL Chloramphenicol). The preculture was incubated overnight at 37 °C under shaking conditions, and used to inoculate one liter of the fresh LB medium. Incubation at 37 °C continued until the bacterial culture has reached the stationary phase (OD_{600} about 1.5). 0.5 mM of IPTG was used for late-induction of both FLAG-ToRP1/2-6xHis proteins

during 1 hour at 37 °C. Cells were harvested by centrifugation; bacterial pellets were stored at -20 °C or used immediately for purification.

2.4.2. Purification of FLAG-ToRP1/2-6xHis on Ni-sepharose column

His-tagged ToRP1 and ToRP2 proteins were purified using 1 mL HisTrap HP column (GE Healthcare®) based on binding of the histidine residues present at the C-terminus of ToRP1/2 to immobilized nickel ions. Elution and recovery of captured His-tagged proteins from Ni-column was accomplished by imidazole.

Bacterial pellets resuspended in 80 mL of **Extraction buffer** were sonicated by eight 30 sec-cycles at 40% of amplification power. Supernatant was isolated by lysate centrifugation at 16 000 x g for 25 min at 4 °C and further filtrated through the 0.45 µm filter. Supernatant that contains 6xHis-tagged proteins was loaded on Ni-column (1 mL) already equilibrated with 10 mL of Extraction Buffer. After loading, the column was washed with **Washing buffer** (60 mL). 10 mM imidazole in the Washing buffer help to prevent nonspecific binding of endogenous proteins that have histidine clusters. FLAG-ToRP1-6xHis was eluted by imidazole in two steps (300 mM followed by 500 mM of imidazole). In contrast, FLAG-ToRP2-6xHis proteins were eluted by increasing concentration of imidazole in 3-steps (100 mM, 200 mM and 500 mM). All elution fractions were analyzed by 15% SDS-PAGE **(Figure 2—2 for ToRP1 and Figure 2—3 for ToRP2)**, and ToRP— enriched fractions were aliquoted and stored at -80 °C.

> ***Extraction buffer:*** *50 mM Tris-HCl (pH 9.0), 300 mM NaCl, 5 % glycerol, cOmplete® protease inhibitor cocktail (Roche®)*
>
> ***Washing buffer:*** *Extraction buffer supplemented with 10 mM imidazole*
>
> ***Elution buffer:*** *Extraction buffer supplemented with 100, or 200, or 500 mM imidazole*

In order to mimic the physiological environment conditions favorable to maintain a stable and proper folded conformation of proteins, purification conditions are normally optimized the way that pH of all buffers is close to the pI (isoelectric point) of purified protein. Since pI for ToRP1 and ToRP2 have been reported to be around 10.4 and 9.9, respectively, a small scale purification (50 mL culture) was performed at increasing pH levels: 7.5, 8.0 and 9.0. At pH 9.0, levels and purity of 6xHis-tagged ToRP1 and ToRP2 eluted from the Ni-column increased substantially, suggesting that I reached optimum conditions for protein folding and specificity of protein interaction with Ni-column **(Figure 2—4)**. Also, protein solubility was improved at pH 9 (data not shown).

Note that FLAG-ToRP1/2-6xHis proteins contain only few aromatic acids. The poor composition of aromatic acids makes the Coomassie™ blue staining as well as colloidal blue staining quite inefficient and require to use western blot for visualization of both ToRP proteins.

All conditions tested in my study to express and purify FLAG-ToRP1-6xHis and FLAG-ToRP2-6xHis are listed in the **Table 2—1**.

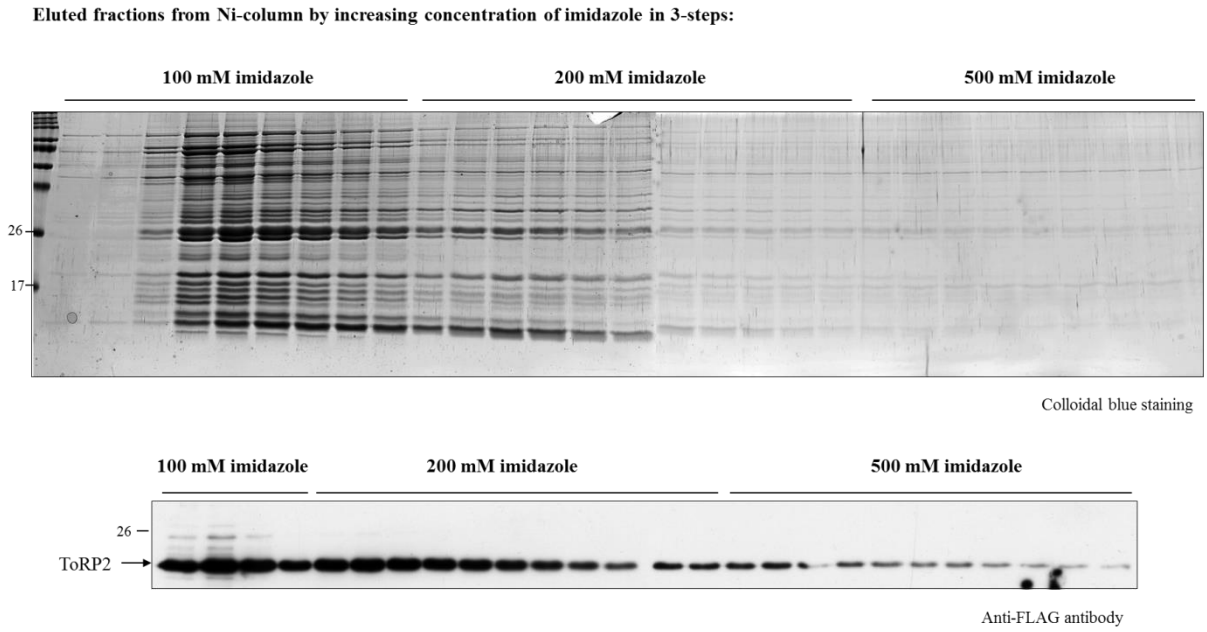

Figure 2—3 | Purification of FLAG-ToRP2-6xHis recombinant protein using Ni-sepharose column

FLAG-ToRP2-6xHis was loaded on Ni-sepharose column, and eluted in three steps by increasing imidazole concentrations (100, 200 and 500 mM imidazole). Several elution fractions were analyzed by 15% SDS-PAGE followed by Colloidal blue staining (upper panel) or immunoblot using anti-FLAG antibody (bottom panel). FLAG-ToRP2-6xHis migration corresponds to about 22 kDa protein marker.

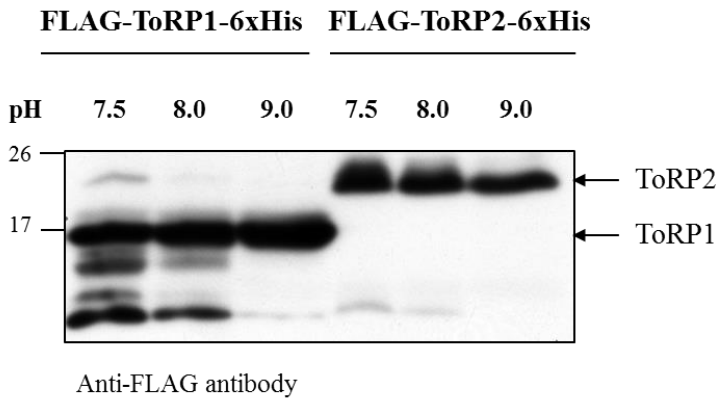

Figure 2—4 | FLAG-ToRP1-6xHis and FLAG-ToRP2-6xHis purification on Ni-sepharose column using buffers at different pH

FLAG-ToRP1-6xHis and FLAG-ToRP2-6xHis were loaded on Ni-sepharose column in buffers at different pH—7.5, 8.0 and 9.0. An equal volume of eluted proteins were analyzed by 15% SDS-PAGE and immunoblot using anti-FLAG antibody.

Expression in *E. coli*				
Methods	**Induction starts**	**GST-ToRP1/2**	**MBP-ToRP1/2-6xHis**	**FLAG-ToRP1/2-6xHis (improved codon usage)**
Rapid induction	0.5 DO_{600}	No	No	Low
Late induction	1.5 DO_{600}	No tested	No tested	High

Protein yield after elution from Ni column	
	FLAG-ToRP1/2-6xHis (improved codon usage)
pH 7.5/8.0	Low
pH 9.0	High

Table 2—1 | ToRP protein yield summary obtained using different conditions of its expression (upper part) and purification (bottom part)

Optimized conditions for FLAG-ToRP1-6xHis and FLAG-ToRP2-6xHis protein production in *E. coli*: Bacterial growth at 37 °C until 1.5 DO_{600}; Late-IPTG induction for 1 h at 37 °C; Protein purification at pH 9.0 using Ni-sepharose column.

3. Knockout of ToRP1 and ToRP2 genes in Arabidopsis

3.1. CRISPR/Cas9 system

To knockout ToRP1 and ToRP2 genes in *Arabidopsis*, we used the CRISPR/Cas9 system for plant genome editing, which is based on RNA-guided genome editing mechanism found in bacteria. CRISPR/Cas9 is a rapidly developing genome editing technology that has been successfully applied in many organisms, including plants. The main effector is CRISPR (Cluster Regularly Interspaced Short Palindromic Repeats)-associated nuclease (Cas9). Cas9 is an RNA-guided DNA endonuclease from *Streptococcus pygogenes* that can be targeted to a specific genomic sequence by an easily engineered 20 bp RNA guide sequence that binds to its DNA target by Watson-Crick base-pairing. Target recognition is dependent on the so-called "protospacer adjacent motif" (PAM), for which the consensus sequence, NGG, is adjacent to the 3' end of the 20 bp target. In natural case, bacterial Cas9 forms a complex with two short RNA molecules called CRISPR RNA (crRNA) and transactivating crRNA (trans-crRNA), which guide the nuclease to cleave non-self DNA on both strands at a specific site (Gasiunas et al. 2012). The biotechnological application of CRISP/Cas9 is rely on the fact that crRNA/trans-crRNA heteroduplex could be replaced by one chimeric RNA (so-called guide RNA (gRNA)) and the gRNA could be programmed to target specific sites (Jinek et al. 2012).

3.2. Cloning protocol

All constructs were kindly provided by Holger Puchta (Botanisches Institut II, Karlsruhe-Germany). The detailed cloning procedure is described in (Fauser et al. 2014). Both pEn-Chimera and pDe-CAS9 vectors used in this study are compatible with Gateway®

technology. The CRISPR spacer is introduced into pEn-Chimera using BbsI resulting in entry-vector that will be then transferred into pDE-CAS9 by a single site Gateway® LR reaction. The vectors and the primers used in this study are listed in **Table 3—1** and **Table 3—2,** respectively.

The 20 nt long protospacer sequence 5' of NGG was picked **(Figure 3—1)**, and a couple of oligonucleotide primers specific to the ends of the protospacer sequence was designed using on-line service (http://www.genomic.arizona.edu/crispr). Two microliters of each oligos (the final concentration 100 µM) were denatured in 46 µL of dH_20 at 95 °C for 5 min, and then incubated for 20 min at room temperature for annealing. Before that, 10 µL of pEn-Chimera were digested in the presence of 1 µL BbSI and 2 µL 10X NEB buffer 2. The digestion mix was made up to a total volume of 20 µL and incubated at 37 °C for up to 1 hour. The digested vector was purified by a simple PCR Clean-up extraction step and then adjusted to a concentration final of 5 ng/µL. Ligation of the annealed oligos and digested pEn-Chimera was performed for 1 h at room temperature in a total volume of 10 µL containing: 2 µL pEn-chimera, 3 µL annealed oligos, 1 µL T4 DNA ligase and 5 µL 2X Quick ligase buffer. 5 µL of the ligation mix was transformed into DH5α cells and then plated on 1% LB-agar plates supplemented with 100 µg/mL of Ampicillin. To check the transformants cells, a colony-PCR step is carried out using forward-oligo and SS129 as primers, under these conditions (Anneal at 56 °C, 30 sec elongation, 30 cycles). Expected band at 370 bp was obtained and verified by sequencing using SS42 primer.

The entry-vector pEn-Chimera obtained will be transferred into pDE-CAS9 by a simple Gateway® LR reaction. The reaction mix containing 2 µL entry-vector (at 100 ng/µL), 3 µL pDE-CAS9 (at 50 ng/µL), 4 µL TE buffer (pH 8.0), 1 µL LR Clonase II, was incubated at room temperature for 2 h followed by Proteinase K treatment. For that, 1 µL of Proteinase K was added to the mix and then incubated at 37 °C for 10 min. The whole LR mixture was then

transferred into DH5α bacteria and selected on LB-agar plates supplemented by 100 µg/mL spectinomycin. A colony-PCR was done using SS42 and SS43 primers under these conditions (Anneal at 60 °C, 1 min elongation, 35 cycles). 1070 pb band was obtained as expected, and sequenced using SS42 primer. The vector obtained was then transformed in Agrobacterium GV3101 cells.

Table 3—1 | Constructs used in this study

Construct	Characteristics	Bacterial resistance	Selection in plants
pEn-Chimera	A Gateway entry vector coding for a customizable sgRNA	Amp	/
pDe-CAS9	A binary Gateway destination vector coding for a codon-optimized Cas9	Spec + ccdB	PPT (Basta)

Table 3—2 | Primers used in this study

Primer	5' sequence
Forward ToRP1/2	ATTG + protospacer
Reverse ToRP1/2	AAAC + reverse-complement protospacer
SS129	CACAGGAAACAGCTATGAC
SS42	TCCCAGGATTAGAATGATTAGG
SS43	CGACTAAGGGTTTCTTATATGC

3.3. Plant transformation

Arabidopsis plants were typically produced using "floral dip" method that consists on Agrobacterium-mediated transformation of *Arabidopsis* (Clough and Bent 1998). Agrobacterium cells transformed with the desired plasmids were used to inoculate 10 mL of

LB medium containing the appropriate antibiotics, and incubated overnight at 28 °C under constant shaking at 250 rpm. Next day, 1 mL of the starter culture was diluted in 100 mL of the same LB medium. Bacterial growth was continued for additional 24 h at 28 °C. Agrobacterium cells were harvested by centrifugation for 10 min at 4 000 x g at room temperature, and then resuspended in 5 mL of **Resuspension buffer**. The mixture was incubated for 1 to 4 hours at room temperature, and then diluted in 100 mL of **Inoculation buffer**. The early developing inflorescences of *Arabidopsis* plants were dipped in the Agrobacterium cell suspensions for 30 sec. Plants were placed in darkness conditions for 24 h and then grown under long-days conditions (16 h of light, 8 h of darkness) between 17 and 21 °C until the siliques appear.

***Resuspension buffer**: 10 mM $MgCl_2$, 150 µM Acetosyringone*

***Inoculation buffer**: 100 mL of dH_2O supplemented with 5% (w/v) sucrose and 30 µL of Silwet L-77*

3.4. Screen for primary transformants based on BASTA-selection

After Agrobacterium-mediated transformation, seeds obtained were sprinkled onto wet soil in pot. When seedlings start grown, 10 µg/mL of BASTA (known as PhosPhinoThricin-PPT) was used to spray seedlings several times (first spray after 2 weeks and second spray after 3 weeks). The primary transformants (T1) were selected as BASTA-resistant seedlings and then transferred onto new soil pot for maturation, and T2 seeds collected. A rapid BASTA-based selection on MS-agar plates was used for identifying transformed seedlings. T2 seeds were sterilized and plated on MS-agar plates supplemented with 10 µg/mL of PPT. After 2 days of stratification, seeds were grown under long day conditions (16h of light at 21 °C and 8h of darkness at 17 °C) for 7-10 days. The number of surviving germinated seedlings is counted. The T2 single-insert lines that displays 3:1 segregation ratio were grown to maturation and T3

seeds were collected. Another round of BASTA-based selection on MS-agar plates was useful to identify the homozygosity or heterozygosity of the T3 transformants. The level of protein expression was assessed by immunoblot analysis using anti-ToRP1/2 antibody. The type as well as the location of mutation created by CRISPR-CAS9 was identified by PCR genotyping assay.

3.5. Selection of potential torp1 torp2 knockout candidate

Two specific protospacers were designed to knockout ToRP1, or both ToRP1 and ToRP2 genes in *Arabidopsis*. The first 20 nt protospacer sequence (position 122-152 nt in 5' of CGG) were designed to the 5'-region of ToRP1 gene in order to specifically knockout only ToRP1. The second 20 nt protospacer (position 30-50 nt in 5' of TGG) were designed to the central conservative region (M2 domain) of both ToRP1 and ToRP2 genes in order to target the both genes in *Arabidopsis* **(Figure 3—1)**.

Immunoblot analysis using anti-ToRP1/2 antibody was performed on T3 plants to select potential *torp1 torp2* knockout candidates. The 300 seeds (T3 generation) were collected from T2 single-insertion plants. No ToRP1 protein expression has been detected in one from randomly analyzed T3 plants (N° line: 139) **(Figure 3—2)**. Indeed, PCR genotyping analysis on the T3 lines showed a deletion of the entire ToRP1 gene and a deletion of the first 300 nt of ToRP2 gene **(Figure 3—3)**. These results suggested that at least one line of T3 plants was selected as a potential *torp1 torp2* knockout candidate.

3.6. Phenotypic defects in torp1 torp2 KO plants

Seeds from *torp1 torp2* (T3 generation of KO line number 139) as well as WT plants were sterilized and plated on MS-agar plates. Seeds were stratified for 48 hours at 4 °C in dark, and then seeds were germinated and vertically grown under long-day conditions (16h of light at

21 °C and 8h of darkness at 17 °C). After 7-10 days, images of root tips were captured **(Figure 3—4).** Phenotypic analyzes have shown that *torp1 torp2* knockout plants are statistically bigger and possess longer roots as compared with WT plants. According to our model, the bigger size of *torp1 torp2* plants can be explained by the fact that knockout of ToRP1 and ToRP2 genes may enhance cap-dependent translation initiation on mRNAs that might promote growth.

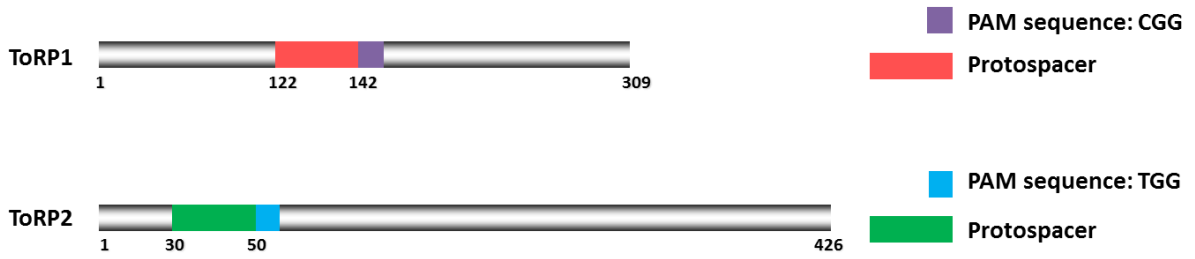

Figure 3—1 | Protospacers used in this study

20 nt protospacer sequence (from 122-152 nt, and 30-50 nt) 5' of NGG PAM were picked in ToRP1 and ToRP2 genes respectively, to knockout ToRP1 and ToRP2 genes in *Arabidopsis*.

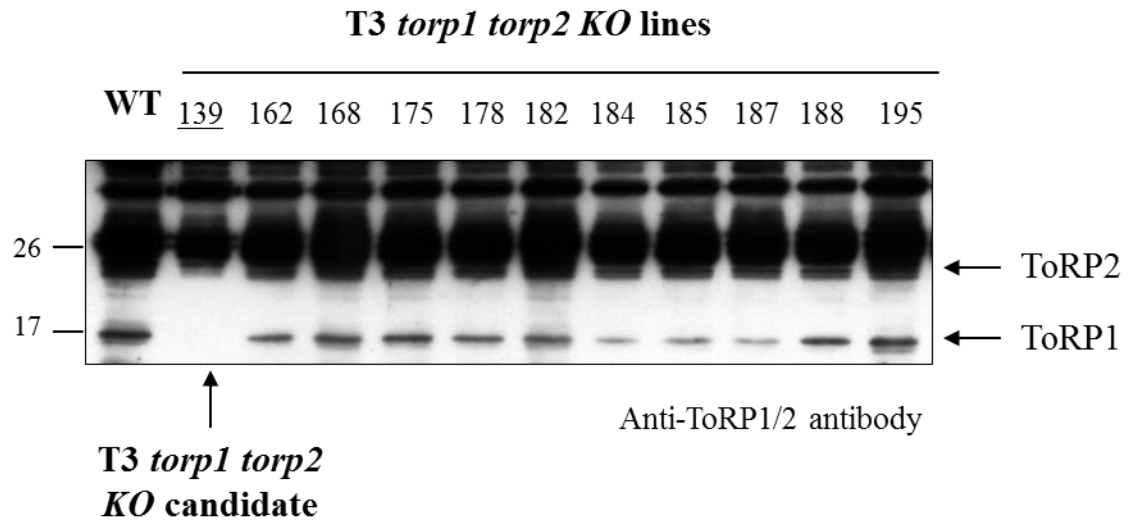

Figure 3—2 | ToRP1 and ToRP2 expression levels in T3 *torp1 torp2* lines

The level of protein expression of ToRP1 and ToRP2 in the T3 *torp1 torp2* knockout lines as well in WT was analyzed by immunoblot analysis using anti-ToRP1/2 antibody. In T3 line n°139, no ToRP1 and ToRP2 expression levels were detected.

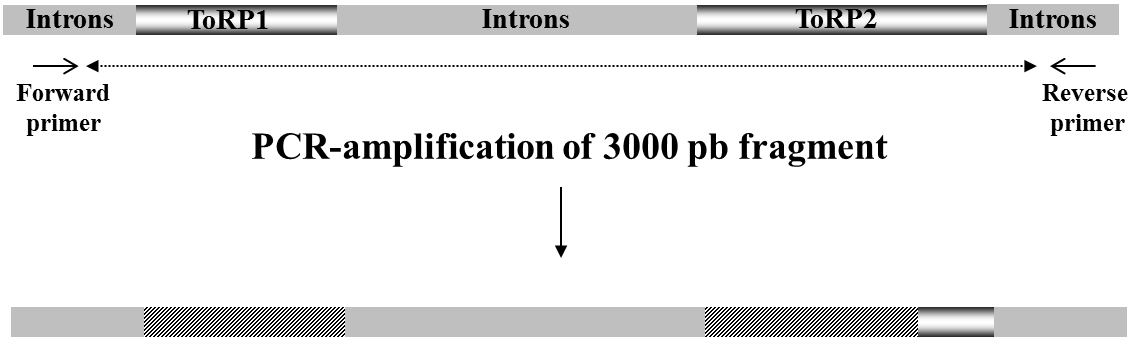

Figure 3—3 | PCR-genotyping analysis

The genome of T3 *torp1 torp2* knockout candidates was analyzed by PCR. Both forward and reverse primers were supposed in a intron region to amplify a fragment of 3000 bp, which includes both ToRP1 and ToRP2 genes. Only a fragment of 100 pb located at the end of ToRP2 gene was detected.

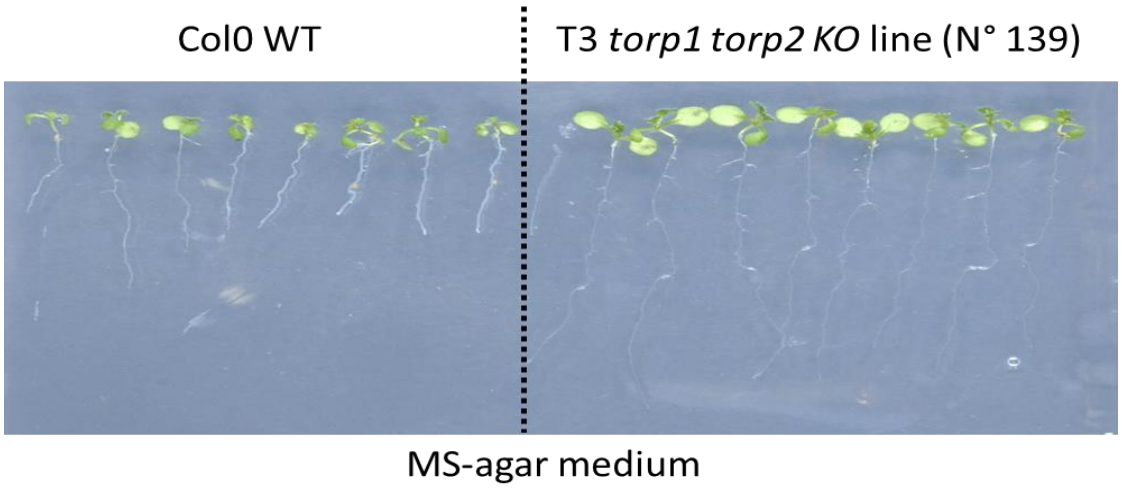

Figure 3—4 | Phenotypical analysis of *torp1 torp2 KO* plants

We analyze the root length of *torp1 torp2 KO* plants. The T3 generation of *torp1 torp2 KO* plants (line n° 139) as well WT plants were grown under long-days conditions (16h of light at 21 °C and 8h of darkness at 17 °C) on vertical MS-agar plates for 7-10 days.

4. Overexpression of myc-tagged ToRP1 and ToRP2 in Arabidopsis

4.1. Constructs

The PCR products amplified from cDNAs of ToRP1 and ToRP2 were introduced to the pGWB18 vector [(35S promoter, N-4xMyc) (--35S promoter-4xMyc-R1- CmR-ccdB-R2--)] by Gateway® technology. The CmR-ccdB cassette – Choloramphenicol resistance (CmR) and suicide (ccdB) genes – were replaced by the gene of interest. pGWB18 contain the 35S promoter upstream of the cloning site and give a myc tag fused to the N-terminus of ToRP1 and ToRP2. pGWB18 as well as all pGWB vectors confer resistance to both kanamycin and hygromycin in plants. Myc-tagged ToRP1 and ToRP2 constructs were designed in the laboratory and transformed into Agrobacterium cells ready for generation of transgenic plants.

4.2. Plant transformation

Transgenic plants were transformed via Agrobacterium-mediated transformation as described previously *(Section 3.3. Plant transformation —Knockout of ToRP1 and ToRP2 genes in Arabidopsis).*

4.3. Screening for the homozygots

Hygromycin B- based selection was used for the identification of *Arabidopsis* transformants. Seeds obtained after floral-dip transformation, were sterilized and then plated on 1% agar containing MS medium supplemented with 35 µg/mL of Hygromycin B. Plates were kept in dark for 48 h at 4 °C for seeds stratification, and then plants were grown under conditions for 7-10 days under long-day conditions (16h of light at 21 °C and 8h of darkness at 17 °C).

Hygromycin B-resistant seedlings were easily identified as they have long hypocotyls (0.8-1.0 cm) whereas non-resistant seedlings have short hypocotyls (0.2-0.4 cm). Total numbers of transformants were counted. T1 independent single-insert lines displaying a 3:1 segregation ratio were used to analyze the expression level of protein by immunoblot analysis using anti-myc antibody. From the independent transformant T1 lines that display 3:1 segregation ratio and high level of protein expression, 12 plants were transferred to soil and grown to maturation and T2 seeds collected. T2 independent single-insert lines that display a 3:1 segregation ratio were grown to get homozygous lines. T3 seeds were collected from T2 single-insert lines with the highest level of expression, and then homozygous single-insert T3 lines are used for analysis. Immunoblot analysis using anti-myc antibody was performed to evaluate the level of protein expression in T3 transgenic plants **(Figure 4—1)**.

4.4. Toxicity of ToRP1 overexpression

Several homozygous single-insert T2 and T3 lines were identified for myc-tagged ToRP2—*ToRP2ox*. However, the segregation ratio observed for myc-tagged ToRP1—*ToRP1ox* in the T3 and T4 transformant lines was different from classical 3:1. We observed additional heterogeneity in the myc-ToRP1 transgenic populations: some of myc-ToRP1 transformant lines were bigger and green and some were smaller and yellow **(Figure 4—2)**. To test if toxicity and plant death are related to the use of hygromycin B at high concentration, T3 transformant myc-ToRP1 lines (*ToRP1ox*) were grown on MS-agar plates under two different conditions: mock treated and supplemented with 30 µg/mL hygromycin B. In the presence or absence of hygromycin B, plants behave in the same way, meaning that their growth problems are not related to hygromycin B. We proposed that the overexpresssion of myc-tagged ToRP1 itself may be toxic for plants.

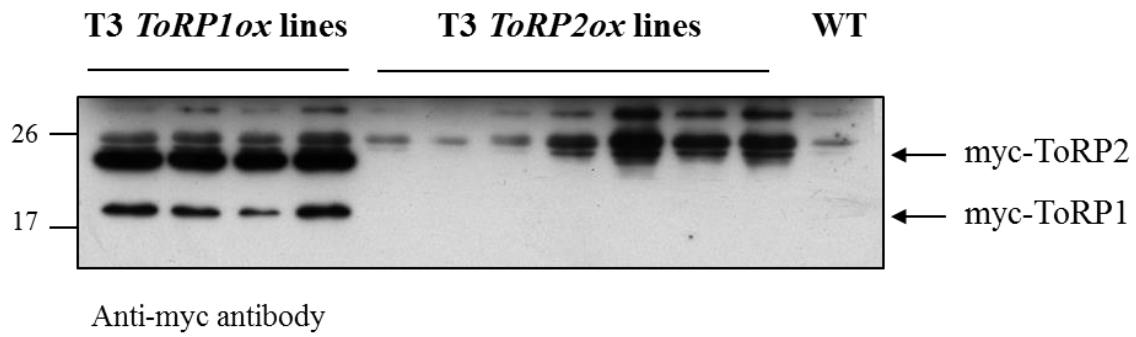

Figure 4—1 | Myc-ToRP1/2 expression levels in *ToRP1ox* and *ToRP2ox*

The level of myc-ToRP1 and myc-ToRP2 protein overexpression in the T3 *ToRP1ox* and *ToRP2ox* lines respectively, was analyzed by immunoblot analysis using anti-myc antibody. WT plants are used as a control.

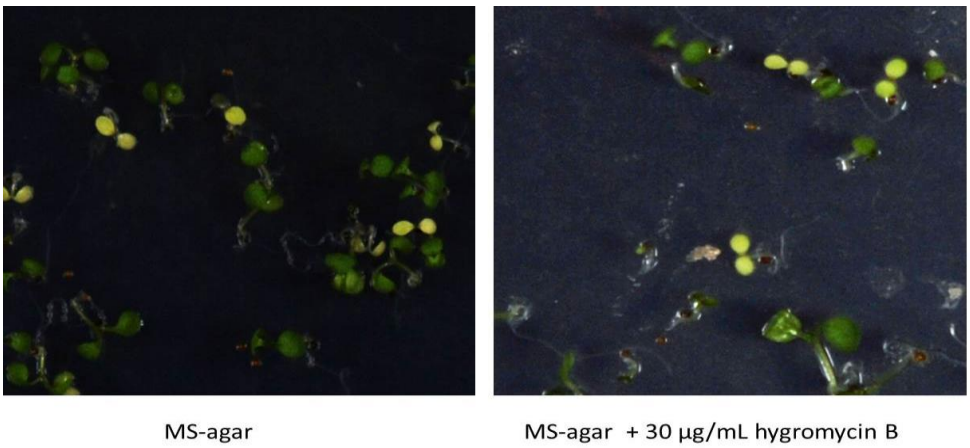

Figure 4—2 | Toxicity of myc-ToRP1 overexpression

T3 myc-ToRP1 overexpression (*ToRP1ox*) plants were grown on MS-agar medium, without or with 30 µg/mL hygromycin B. After 2 days of stratification at 4 °C, plants were grown for 7-10 days under long-day conditions (16h of light at 21 °C and 8h of darkness at 17 °C).

5. Article-2:

RISP can promote reinitiation at uORFs in plants via interaction with both 40S and 60S ribosomal subunits

Eder Mancera-Martínez[1#], Ola Srour[1], Joelle Makarian[1], Odon Thiébeauld[1], Johana Chicher[2], Philippe Hammann[2], Yaser Hashem[3], Mikhail Schepetilnikov[1] and Lyubov A. Ryabova[1]*

[1]Institut de Biologie Moléculaire des Plantes, Centre National de la Recherche Scientifique, UPR 2357, Université de Strasbourg, Strasbourg, France

[2]Platforme Proteómique Strasbourg-Esplanade, Centre National de la Recherche Scientifique, FRC 1589, Université de Strasbourg, Strasbourg, France

[3]CNRS, Institut de Biologie Moléculaire et Cellulaire, Architecture et Réactivité de l'ARN UPR9002, Université de Strasbourg, 67084 Strasbourg, France

#Current address: CNRS, Institut de Biologie Moléculaire et Cellulaire, Architecture et Réactivité de l'ARN UPR9002, Université de Strasbourg, 67084 Strasbourg, France.

*To whom correspondence should be addressed:
lyuba.ryabova@ibmp-cnrs.unistra.fr
Tel: +33 (0)3 67 15 53 31
Fax: +33 (0)3 88 61 44 42

Keywords: translation (re)initiation, phosphorylation via TOR, eIF2, 40S and 60S intersubunit-bridge, initiator tRNA recruitment

Abstract

Target-of-rapamycin (TOR) is required for translation reinitiation events in plants. TOR mediates phosphorylation of the scaffold protein reinitiation supporting protein (RISP), altering its association with eukaryotic initiation factor 3 (eIF3) and the 60S ribosomal subunit (60S) protein L24 (eL24). We show here that, in addition, RISP physically interacts with eIF2 via eIF2β and 40S via the major TOR downstream target eS6. The RISP binding is affected by mutations of a single residue, Ser267, which shown to be phosphorylated through the TOR/S6K1 pathway, that switches the RISP protein between two functionally distinct forms—the phosphorylated version of RISP (RISP-S267D) interacts preferentially with the C-terminal tails of eS6 and eL24, which are in close spatial vicinity on 80S, while the non-phosphorylatable version (RISP-S267A) prefers eIF2 and eIF3. Accordingly, we demonstrate that eIF3a/RISP-S267A/eIF2β and eS6/RISP-S267D/60S ternary complexes form *in vitro*. Transient overexpression of eIF2β in plant protoplasts up-regulates cell reinitiation capacity. An eS6 triple phosphorylation mimic, but not a phosphorylation-knockout mutant, overcomes the translation reinitiation deficiency of plants underexpressing eS6. Thus, RISP and eS6 can link 60S to 40S in response to TOR activation, indicating involvement of 80S ribosomes in reinitiation events.

Introduction

Translation initiation is the rate-limiting step of protein synthesis in eukaryotes and requires rapid assembly of the 43S preinitiation complex (43S PIC) composed of eukaryotic initiation factor 3 (eIF3), eIF1, eIF1A, the eIF2•GTP•Met•tRNAi^{Met} ternary complex (TC) and the 40S ribosomal subunit (40S[1,2]). eIF3 is composed of 13 distinct subunits in mammals and plants—eIF3a-eIF3m[3], and stimulates binding of tRNAi^{Met} to 43S PIC via the eIF2β subunit of a heterotrimer eIF2 that comprises eIF2α, β and γ subunits[4,5]. After translation termination, posttermination complexes are splitted by ribosome recycling factor ABCE1 and eRF1 into 60S and tRNA/mRNA-associated 40S subunits[6]. Frequently after terminating translation 40S can resume scanning and reinitiate at downstream AUGs. Reinitiation competence of ribosome depends on duration of elongation, and occurs mainly after translation of short upstream ORFs (uORFs)[7]. In this case, some eIFs, including eIF3, may remain transiently associated with ribosomes through short elongation and termination, and assist 40S scanning and *de novo* recruitment of tRNAi^{Met} and/or the 60S ribosomal subunit.

uORFs are common in mammals and plants, being present in at least 30%–45% of full-length mRNAs[8,9], where many of these are translated[10]. In eukaryotes, a target of rapamycin (TOR) signaling pathway integrates nutrient and energy sufficiency, hormones and growth factors to provide additional levels of translation initiation control via phosphorylation of several targets within the cell translation machinery[11-14]. In Arabidopsis, translation reinitiation is under control of the TOR signaling pathway[15]. Active TOR promotes translation reinitiation of mRNAs that harbour uORFs within their leader regions via phosphorylation of eIF3h that bolster the reinitiation capacity of post-terminating ribosomes, but the underlying molecular mechanisms remain enigmatic[15-17].

Reinitiation after translation of a long ORF is rare, but does occur in specific circumstances, for example, it is activated in *Cauliflower mosaic virus* (CaMV) by a single viral protein transactivator/viroplasmin (TAV)[18,19]. TAV promotes both activation of TOR and thus its downstream target S6K1 (the kinase of the 40S ribosomal protein S6, eS6), and retention of eIF3 and reinitiation supporting protein (RISP), on ribosomes throughout longer elongation[20,21]. RISP—a novel and specific target of TOR/S6K1—was identified as a TAV cofactor that assists TAV in reinitiation after long ORF translation, if phosphorylated[22]. Active TOR binds polyribosomes concomitantly with polysomal accumulation of TAV, eIF3 and RISP, with RISP being phosphorylated[21]. Strikingly, the phosphorylation status of RISP

regulates its interaction with the cell translation machinery—it associates with eIF3 before phosphorylation and, when phosphorylated, binds TAV and the 60S ribosomal protein L24 (eL24) via its C-terminal tail. Although RISP connections with either eIF3 or 60S are exploited by TAV to promote reinitiation after long ORF translation, whether RISP alone regulates gene expression when associated with the cell translation machinery remains to be determined.

Here, we present evidence that RISP functions in cellular initiation and reinitiation of translation, where its phosphorylation status is crucial for selection of partners within the cell translation machinery. Our results reveal a new role for eS6—the most studied target of TOR signaling, in supporting retention and re-use of 60S during translation reinitiation. This becomes possible since the C-terminal ends of eS6 and eL24 protrude out of 80S and, according to our data, can be connected by RISP in response to TOR activation.

Results

RISP interacts with intact eIF2 via subunit β

Previously, we characterized RISP as able to interact physically with eIF3 subunits a/c via its H2 helix and, when pre-bound to eIF3, with 40S, and to associate *in vitro* with the C-terminal half of the 60S ribosomal protein L24 (eL24) via its H4 helix[22] (**Fig. 1a**). *In planta*, RISP was found in preinitiation complexes containing eS6, eIF3c and eIF2α indicating that RISP together with eIF3 plays a role in initiation of translation[22]. Thus, our first objectives were to confirm whether RISP is found in eIF3-containing preinitiation complexes *in vivo*, and to investigate the possible link between RISP and eIF2 in detail.

As a first step, we elaborated a method of high-resolution mass spectrometry to identify factors that associate globally with RISP. To do this, RISP immunoprecipitated from *Arabidopsis rispa/35S:RISP-GFPox* line transgenic for GFP-tagged RISP using anti-GFP antibodies was subjected to liquid chromatography-tandem mass spectrometry analysis (LC-MS/MS). We identified 8 out of 13 eIF3 subunits, with subunits a and c being highly represented. eIF3 subunits b, h and f were also efficiently immunoprecipitated with RISP (**Supplementary Table 1**; **Supplementary Fig. 1**). We also identified TOR, already known as a direct eIF3-binding protein in mammals[23] and upstream effector of RISP[21]. Thus, several eIF3 subunits and TOR are immunoprecipitated by RISP from *Arabidopsis thaliana*.

Since eIF2 was not identified within GFP-RISP IP complexes, we assayed full-length RISP for direct binding to entire eIF2 purified from wheat germ in a GST-pull down assay (**Fig. 1b**). All three eIF2 subunits were present in the bound fraction after incubation with GST-RISP, strongly indicating GST-RISP binding to eIF2. Next, we tested the capacity of each eIF2 subunit to interact with RISP using the yeast two-hybrid assay (**Fig. 1c**). Only subunit β fused to the Gal4 binding domain (BD) interacted strongly with RISP fused to the Gal4 activation domain (AD-RISP), while α and γ were inactive, suggesting that subunit β is primarily responsible for eIF2 binding to RISP. Consistent with association of eIF2β and RISP in yeast, purified recombinant eIF2β and RISP interacted specifically in the GST pull-down assay (**Fig. 1d**). Thus, RISP associates with eIF2 via subunit β. It is known that eIF3 can promote eIF2 recruitment indirectly via eIF5, which bridges eIF3c with eIF2β in yeast and mammals[24-26], and directly, when eIF2β binds eIF3c in yeast and plants[24, 27-28] and eIF3a in yeast[29]. **Fig. 1e** shows that, as in yeast, GST-tagged eIF3a in addition to eIF3c can contact

eIF2β in *Arabidopsis*.

To delineate regions of RISP involved in eIF2β binding, we performed a dissection based on predicted tertiary structure. A 3D model of *Arabidopsis* RISP, generated by RaptorX[30], predicts, with high probability, four coiled-coil structure domains (**Fig. 1a**). The archaebacterial aIF2β[31] exhibits strong conservation with *Arabidopsis* eIF2β despite the fact that eIF2β has an N-terminal extension of 114 aminoacids. The aIF2β N-terminal α-helix is connected by a flexible linker to a central α-β domain, followed by a C-terminal zinc-binding domain (Schmitt et al. 2010). The 3D structure of aIF2β suggests possible folding of the conserved C-terminal part of the *Arabidopsis* subunit (C-terminus, aa 114–268). Accordingly, the eIF2β sequence was dissected into a C-terminal part, the N-terminus, and a short central α-helix (aa 121-144) that is also present within aIF2β (**Fig. 2b**).

RISP and eIF2β truncation and deletion mutants (different colors in **Fig. 2**) fused to the AD or BD domain were tested to delineate regions important for binding. The N-terminal part of RISP (aa 1–190) binds eIF2β strongly, while the C-terminal part (aa 190–389) did not bind (**Fig. 2c**). Binding was stronger between eIF2β and RISP lacking H1, but an internal deletion of H2 (aa 120–190) abolished RISP binding to eIF2β. Thus, RISP domain H2 seems to be a key contact for eIF2 subunit β. eIF2β-C binds RISP as strongly as full-length eIF2β, while the N-terminus (aa 1–121) does not (**Fig. 2c**). However, elongation of the eIF2β N-terminal fragment by an additional 23 aa (aa 1–144; eIF2β-NΔ124) restored the interaction, suggesting that a segment spanning residues 121–144 is required for RISP binding. On the 3D structure of aIF2β (**Fig. 2b**) the N-terminal alpha helix shown in black corresponds to this putative RISP binding fragment (aa 121–144). Thus, results from the yeast two-hybrid system suggest that the eIF2β α-helix downstream of two blocks of lysine residues is responsible for RISP H2 binding. Interestingly, the H2 helix is implicated in binding of eIF3a/c and eIF2β.

Phosphorylation of RISP at Ser267 decreases its binding to eIF2β

RISP is phosphorylated at Ser267 within the motif RGRLES—a pattern (R/KxR/KxxS/T) found in many Akt or S6K1 substrates—by S6K1 in a TOR-responsive manner[21]. Earlier results revealed that RISP phosphorylation can reduce its binding to eIF3c[21]. To gain a better understanding of how RISP phosphorylation changes its binding characteristics to eIF2β, we tested RISP phosphorylation mutants—the phospho-knockout mutant S267A and mimic S267D—for their binding capacities to eIF2β in a yeast two-hybrid quantitative β-galactosidase assay. As shown in **Fig. 2e**, the phosphorylation-inactive mutant

RISP-S267A has a reproducibly stronger interaction with eIF2β than the phosphorylation mimic RISP-S267D or wild-type RISP that has high phosphorylation status in yeast[21]. The GST pull-down assay presented in **Fig. 2f** suggests that GST-tagged eIF2β binds RISP-S267A somewhat stronger compared with its phosphomimetic mutant (RISP-S267D) or WT (data not shown). Overall, these data suggest that RISP, when non-phosphorylated, interacts preferentially with eIF2β and, as it was shown previously[15], the eIF3 subunit c.

To further confirm a link between RISP and eIF2β *in planta*, we analyzed their effect on translation initiation and reinitiation in plant protoplasts prepared from *Arabidopsis* suspension cultures. To address this question, we monitored translation of a β-glucuronidase (GUS) reporter ORF downstream of either of a short synthetic leader (*short GUS*; marker of the frequency of translation initiation events), or the auxin responsive factor 5 (ARF5) leader carrying six uORFs (*ARF5-GUS*), where GUS ORF translation would require reinitiation (**Fig. 3a**). A marker of transformation efficiency—*monoGFP* with a single GFP ORF downstream of the tobacco etch virus (TEV) 5'-leader—initiates via a cap-independent mechanism[32]. Under the conditions used, ARF5 leader uORFs reduced *GUS* ORF translation by about 70% compared with that of *shortGUS* mRNA (**Fig. 3b**). Here, overexpression of RISP-S267A up-regulates expression of both the short leader- and ARF5-containing GUS reporter by 1.5- and 2-fold, respectively. eIF2β overexpression either alone or in combination with RISP-S267A is somewhat indifferent for *shortGUS* mRNA translation (**Fig. 3c**). In contrast, eIF2β cotransfection gives a 2-fold increase only for *ARF5-GUS* translation (**Fig. 3d**), supporting earlier data that eIF2 is a limiting factor in reinitiation. Interestingly, eIF2β seems to be the most labile of the three subunits (eIF2α /β /γ) within the intact complex (Beilsten-Edmands et al., 2015), indicating that eIF2β overexpression might up-regulate cellular eIF2 levels. Moreover, the simultaneous overexpression of eIF2β and RISP-S267A or at significantly lesser extend RISP, but not RISP-S267D, impaired eIF2β-induced *ARF5-GUS* translation, indicating that RISP-S267A efficiently outcompetes for eIF2β.

Since RISP is involved in multiple interactions with eIF3 subunits a and c, and eIF2β via the same helix H2, we wanted to know whether RISP can be positioned within the 43S PIC according to the known contact points between eIF3, eIF2 and 40S. We used cryo-EM data[33-35] to generate the 43S PIC model to integrate the RISP 3D model generated by RaptorX[30] within the surroundings of eIF3a, eIF3c and eIF2β on 40S. Strikingly, placement of RISP H2 in close proximity to both the eIF3 subunit a (aa 615-640, approximately) and the subunit c (its N-terminal extension is shown in blue) on the intersubunit face might still allow contact with eIF2β (**Fig. 3e, f**).

RISP interacts with the C-terminal α-helix of ribosomal protein S6 (eS6)

RISP, when phosphorylated, can associate with the C-terminal tail of eL24, which protrudes out of 60S towards the C-terminus of eS6[36]. According to the 3D-structure of *S. cerevisiae* and human 80S, eL24 protrudes out of 60S to form a new interaction site on the 40S subunit with eS6 and 18S rRNA[36,37]. Indeed, RISP was detected in fractions of 60S and 80S when wheat germ extract was fractionated on a sucrose gradient[22]. Since, 60S-bound eL24 and 40S-bound eS6 can form an inter-subunit bridge via their C-terminal tails; RISP binding to eL24 may influence formation of such a bridge.

To test this hypothesis, we first looked for a complex between *Arabidopsis* eL24 and eS6 *in vitro*. All attempts to reveal direct interaction between eL24 and eS6 and their deletion mutants failed (data not shown). We then tested if RISP can provide additional contacts between eL24 and eS6 using the yeast two-hybrid system (**Fig. 4**). Although AD-RISP interacts strongly with BD-S6 under our yeast two-hybrid system conditions, none of the RISP fragments assayed interacted with full-length eS6 (**Fig. 4a**), probably indicating the critical importance of RISP tertiary structure for this interaction. Taking advantage of the known 3D conformation of ribosome-bound eS6[36]; **Fig. 4b**), eS6 was dissected into three fragments. Two fragments of eS6—the central fragment, MS6 (aa 83–177) and the C-terminal alpha-helix, CS6 (aa 177–249)—bind RISP as strongly as the full-length protein (**Fig. 4c**). However, the longer C-terminal fragment of eS6, ICS6 (aa 130–249) failed to interact with RISP, indicating that the RISP binding site is somewhat concealed by a 47-aa fragment insertion in our yeast two-hybrid conditions. Since direct interaction between MS6 and the central segment of eL24 within the 80S ribosome has been suggested[37], we concentrated on characterization of the CS6 alpha-helix interaction with RISP by the GST pull-down assay. The RISP and GST-tagged CS6 interaction *in vitro* was specific (**Fig. 4d**)—RISP was present in the bound fraction after incubation with GST-CS6. Thus, our results indicate that RISP can potentially mediate the interaction between 40S and 60S ribosomal subunits by providing contacts with the C-terminal domains of eL24 and eS6, which are both solvent-exposed within 80S.

Given that RISP phosphorylation up-regulates its interaction with eL24[21], we next tested whether RISP phosphorylation would also govern its interaction with the C-terminal α-helix of eS6 in the yeast two-hybrid system. Remarkably, compared with controls, wild type RISP and the phosphorylation mimic mutant of RISP (RISP-S267D) interacted reproducibly more strongly with CS6 than the RISP phosphorylation inactive mutant (**Fig. 4e**). These

results confirm that phosphorylation of RISP promotes its interaction with both the C-terminus of eS6 and, according to our earlier data, eL24.

60S retention by eS6 C-terminal α-helix requires RISP phosphorylated at S267

To further confirm the hypothesis that TOR-responsive RISP phosphorylation governs recruitment of RISP to both eL24 and eS6, while attenuating RISP binding to both eIF3 and eIF2, RISP phosphorylation mimic and phospho-knockout mutants were assayed for reconstitution experiments in the GST pull-down assay with direct targets of RISP—eIF3a, the C-terminal α-helix of eS6 and wheat germ 60S ribosomal subunits.

Although eIF2β was implicated in interaction with eIF3 via a (**Fig. 1e**) and c subunits[28], the same subunits associate with RISP[22], suggesting multiple contacts between eIF3a/ eIF3c, RISP and eIF2β. We used GST-tagged eIF3a pre-bound with either RISP-S267A or RISP-S267D mutants to demonstrate that RISP binding does not interfere with eIF2 accommodation by eIF3a. Thus, GST-eIF3a bound to glutathione beads was incubated with excess RISP, either phosphorylation mimic or knockout (**Fig. 5a**), followed by incubation of bound fractions with or without eIF2β. Although, both RISP knockout and phosphomimic remain bound to GST-eIF3a after extensive washing, the level of GST-eIF3a-bound RISP-S267A was reproducibly 2-fold higher than that for RISP-S267D (fractions 12 and 18, respectively). Accordingly, the eIF2β component was about 2-fold enriched in the eIF3a-bound RISP-S267A as compared with eIF3a/RISP-S267D. Neither eIF2β nor RISP interacted with GST alone (**Fig. 5a**, lanes 6 and 8, respectively). These results suggest that eIF3-bound RISP also has the capacity to accommodate eIF2.

Next, we assayed *in vitro* assembly of a complex between the eS6 C-terminal domain, to mimic eS6 C-terminus folding on 40S, and analyzed whether each of the RISP phosphorylation mutants can pull down the 60S ribosomal subunit. Indeed, a significant fraction of RISP-S267A and RISP-S267D was found in the GST-eCS6 bound fraction (**Fig. 5b**, lanes 8 and 14, respectively). Remarkably, RISP phosphorylation knockout (RISP-S267D) bound to GST-CS6 was able to pull down 60S, as manifested by the presence of at least two 60S ribosomal proteins in the GST-CS6-bound fraction. No 60S interacted with RISP-S267A bound to GST-CS6 (**Fig. 5b**); thus, RISP failed to bridge CS6 and 60S before being phosphorylated, but was fully able to connect the C-terminal α-helix of eS6 and 60S after phosphorylation. These results suggest that the phosphomimetic mutant of RISP promotes formation of a bridge between the C-proximal helices of eS6 and 60S likely via

eL24. As TOR triggers RISP phosphorylation during translation, and, given that eS6 is a TOR major downstream target among ribosomal proteins in eukaryotes[2] and is phosphorylated**,** we next asked whether eS6 phosphorylation plays a role in (re)initiation of translation.

Arabidopsis plants overexpressing eS6 phosphorylation mimic (eS6-S237D/S240D/S241D) are more competent for reinitiation of translation

Phosphoproteomic studies in *Arabidopsis* suggest significant quantitative increase in phosphorylation state of two redundant and interchangeable eS6a and eS6b proteins (*RPS6A* and *RPS6B*[38]; in response to high CO_2 and light, auxin and cytokinin availability[39-42]. First, we decided to test a role of phosphorylation of several closely spaced phosphorylation sites—S231, S237 and S240[40,41,43] in eS6 binding to RISP. Two of these sites are characterized by a pattern found in many plant S6K1 substrates (S231, DRRSES; S237, LAKKRS; **Fig. 6a**). Strikingly, phosphomimetic mutants of eCS6 at S231, or S237, or S240, display statistically more significant interactions with RISP-S267D than their phospho-knockout mutants (**Fig. 6b**).

To directly test the functional consequences of eS6 phosphorylation, we next varied intracellular concentrations of "phosphorylated" eS6 *in planta* to assess effects of eS6 phosphorylation on plant reinitiation capacities. We took advantage of T-DNA insertion *s6a* knockout mutant, where total eS6 level was reduced to S6B levels (**Fig. 6c**), and used it to obtain 35S-promoter-driven stable expression of either the S6B phosphorylation mimic mutant (*s6a/S6B*$^{S/D}$) where three closely spaced serines, S237, S240 and S241, were replaced by either D (*S237D/S240D/S241D*), or phospho-knockout mutant (*s6a/S6B*$^{S/A}$*)* with A (*S237A/S240A/S241A*; all mutant phenotypes are shown in **Fig. S2 a, b**). Western blot analysis of obtained homozygous lines suggests that low S6B levels in *s6a* mutant were nearly restored in our transgenic lines (**Fig. 6c**). However, 35S-promoter-driven expression of S6B did not significantly restore *S6a* mutant developmental defects such as growth retardation and leaf asymmetry (**Supplementary Fig. 2**).

To determine the contribution of eS6 to regulating initiation or reinitiation events, we used mesophyll protoplasts generated from WT seedlings, *s6a* and *s6a/S6B*$^{S/A}$, and *s6a/S6B*$^{S/D}$ transgenic lines, and compared their (re)initiation capacities. Initiation events were monitored with the construct containing the β-glucuronidase (GUS) ORF following a short leader (p*shortGUS*), while the impact of events undergoing reinitiation after short ORF translation were followed with reporter plasmid *ARF5-GUS* (**Fig. 6d**). We also tested whether a special

case of reinitiation after long ORF translation under control of a CaMV translation transactivator/ viroplasmin (TAV) is sensitive to phosphorylation status of eS6. Here, we used the bicistronic reporter plasmid p*biGUS*, containing two consecutive ORFs: CaMV ORF VII and GUS, where GUS serves as a marker of transactivation, and with or without the reporter plasmid expressing TAV[44] (Fig. **6d**).

The levels of transiently expressed GUS from p*short-GUS* did not differ significantly in WT, *s6a*, *s6a/S6B*$^{S/D}$ and *s6a/S6B*$^{S/A}$ protoplasts (**Fig. 6d**, lane 1). In contrast, translation reinitiation on *ARF5-GUS* mRNA was reduced 3-fold in *s6a* as compared with that in WT protoplasts, strongly suggesting a role for eS6 in translation renitiation (**Fig. 6d**, lane 2). The level of reinitiation was partially restored in *s6a/S6B*$^{S/A}$, and fully restored in *s6a/S6B*$^{S/D}$-derived protoplasts. Virus-induced reinitiation after long ORF translation that is strictly dependent on TAV—upstream ORF VII blocks downstream GUS ORF expression and no GUS activity appeared in all tested protoplasts without TAV—was reduced by 2-fold (**Fig. 6d**, cf lanes 3/4 in WT and *s6a*). Strikingly, the transactivation ability of TAV was decreased further in *s6a/S6B*$^{S/A}$-derived, but fully restored in *s6a/S6B*$^{S/D}$-derived protoplasts. Thus, TAV-controlled reinitiation after long ORF translation is eS6-dependent, and requires eS6 phosphorylation. No significant differences in RNA transcript or TAV/GFP levels were seen in any of the protoplasts tested (**Fig. 6d**). These results suggest a role for eS6 in translation reinitiation, and suggest that eS6 phosphorylation is necessary for plants to acclimate to reinitiation events.

Discussion

uORFs within the leaders of mRNAs have been implicated in translational control of plant growth and development, including meristem maintenance[45] and responses to auxin[9,15]. Despite inhibition of main ORF translation by one or multiple uORFs, reinitiation persists by a mechanism that relies on activation of target-of-rapamycin, TOR[15], but the role of TOR has not been completely understood. We previously described a TOR downstream target, the reinitiation supporting protein, RISP, that, when phosphorylated, promotes reinitiation after long ORF translation under the control of the virus-specific translation transactivator TAV[21,22]. Here, we identified RISP as a dynamic partner for assembly of either the eIF3-containing complex with eIF2, or 40S and 60S ribosomal subunits via the eS6–eL24. Aside from eIF3 and the 60S ribosomal protein eL24[22], here we identified two additional RISP-interacting partners—eIF2, which is primarily responsible for initiator tRNA delivery, and, strikingly, the 40S ribosomal protein eS6, which, together with eL24, may form a specific bridge between the 40S and 60S ribosomal subunits[37]. These interactions appear to strengthen previously proposed RISP function in recruitment of TC and open a new attractive role for RISP in 60S joining *de novo* or retention of 60S during post-termination events. *In planta*, reinitiation defects of the eS6 deficient mutant *Arabidopsis* are restored only by overexpression of an eS6 phosphomimetic mutant, although we did not modify all eS6 C-terminal phosphorylation sites. The interaction between RISP and these two clusters of partners is governed by phosphorylation of RISP at S267 within its α-helix 3. Thus, our studies have uncovered a molecular mechanism underlying the role of phosphorylation in the dynamic interactions between RISP and its partners. When non-phosphorylated, RISP physically associates with eIF3 and eIF2, whereas after phosphorylation it can maneuver to 80S via binding to eS6 and eL24 C-terminal α-helices, which are exposed to solvent[36].

However, S267 seems not to be a critical interface for interaction with its multiple partners; we assume that phosphorylation of RISP may trigger conformational rearrangements that weaken the association with eIF3 and eIF2, and strengthen alternative interactions on 80S. Also, phosphorylation can modulate RISP–eS6 protein–protein interactions via modulating their ionic contacts. In mammals, active TOR or inactive S6K1 interact readily with eIF3, but dissociate if their active status is changed[23].

Our experimental design, which combined *in vitro* and protoplast examination of eIF3a and eIF2 binding to a RISP phosphorylation mutant, allowed us to demonstrate ternary

complex formation between eIF2β•RISP•eIF3c and selection of the RISP phospho-knockout mutant as a preferential partner within the complex. Although, *in planta*, eIF2α-complexes contain RISP[22], MS-MS analysis failed to identify eIF2 subunits in GFP-RISP-complexes suggesting possibly transient contacts, but reveal the presence of eIF3 subunits and TOR, indicating the possibility of RISP phosphorylation directly within eIF3-containing complexes, as suggested in mammals[23]. Taking into account the previous results of interaction mapping, we may locate RISP in close proximity to both eIF3a and eIF3c on 40S (**Fig. 3e, f**) in the position that is well adapted for eIF2β capture according to the recently published architecture of the 43S PIC[35]), the 48S-open/closed PIC[34] and the 40S•eIF1•eIF3 complex[33]. The latter structures suggest an extended orientation for eIF3c N-terminus and eIF3a that encircles the 40S towards to the subunit interface.

In contrast, RISP preferentially associates with eS6 and, as shown previously[15], eL24. Within the 3D structure of 80S[36,46], 40S and 60S are connected by two long protein helices extending from the left eL19 (eB12 bridge) and right sides of the 60S subunit interface eL24 (eB13, located near the main factor binding site of 60S). Strikingly, the putative RISP 3D structure is well suited for integration into the elongating 80S (**Fig. 7a**) or the putative open conformation of 80S (**Fig. 7b**), where 60S is connected to 40S via RISP-mediated interactions between eS6/eL24 C-terminal protruding ends. The latter hypothesis is of importance since it gives functional meaning to the eS6- and eL24-protruding ends. Our hypothesis of 60S retention during 80S reinitiation correlates well with *in vitro* data suggesting scanning and reinitiation by terminating 80S in mammals[6], and the crucial importance of ribosomes splitting at the termination step to allow specific recognition of downstream AUG codons in yeast[47]. However, whether RISP binding would interfere or not with the function of ribosome recycling factor, ABCE1[48], remains to be examined.

Our study has revealed a role for eS6 in plant translation reinitiation, where it can function in an ensemble with eL24. In contrast to eS6, eL24 has long been known as a reinitiation-supporting factor that is critical for 60S joining to the 48S PIC[49,50] and translation of uORF-containing mRNAs such as ARF3 and ARF5[9,51].

Based on our findings, we propose a model (**Fig. 7c**) in which RISP can mediate either 43S PIC assembly or translation reinitiation depending on its phosphorylation status. Before being phosphorylated, RISP is recruited to 43S PIC as a complex with eIF3, where RISP helix 2 contacts eIF3 subunits a and/or c (**Fig. 3e, f**). Here, the eIF3/RISP complex participates in ternary complex recruitment via eIF2 (**Fig. 3e, f**). TOR, which is present in RISP/eIF3-containing complexes, triggers phosphorylation of S6K1. One might expect that

phosphorylation of RISP by activated S6K1 would proceed in close proximity to 48S PIC[23]. Although RISP is attached to eIF2-eIF3 before phosphorylation, its phosphorylation could trigger RISP-P relocation to the eS6 C-terminus and/or eL24. An interesting possibility is that the link between RISP and eS6/eL24 could be used for the retention of RISP through elongation (RISP positioning on 80S is proposed in **Fig. 7b**) and, during resuming of scanning. These novel interactions between RISP and the 40S ribosomal protein eS6 could ensure the re-use of 60S via the eS6•RISP•eL24 interaction network (see putative model of 60S holding by scanning 40S via RISP in **Fig. 7c**). Recruitment of TC *de novo* could be achieved either via eIF3 alone or via its complex with RISP, if nonphosphorylated RISP is available. Clearly there are many layers of eS6 function in translation under the control of TOR, and many of these are yet to be explored in eukaryotes and explained at the molecular level. Thus, phosphorylation of eS6, which has attracted much attention since its discovery, seems to be important in plant translation reinitiation. Obviously, further work on the functional consequences of eS6 phosphorylation is needed to better understand the role of phosphorylation in translational control.

Methods

Plant materials and growth conditions. *Arabidopsis thaliana* ecotype Columbia-0 (Col-0) and *s6a*[38] were grown under standard greenhouse conditions with supplemental light on a 16 h/8 h dark cycle. *s6a* was kindly provided by T. Desnos (LBDP, Université Aix-Marseille-II, France). *rispa Arabidopsis* line was described[22]. All the plants were in Col-0 ecotype background. *s6a* line was transformed by the floral dip method with either p*GWB2-eS6B,* or p*GWB2-eS6B-S237A/S240A/S241A,* or p*GWB2-eS6B-S237D/S240D/S241D,* or p*GWB5-eS6B-cMyc*. Then *s6a/S6B, s6a/S6B*$^{S/D}$ and *s6a/S6B*$^{S/A}$ homozygous lines were screened based on hygromycin resistance. The *rispa* line was transformed with p*GWB5-RISP-GFP*, and two *rispa/RISP-GFPox* homozygous lines ectopically expressing RISP-GFP were isolated based on hygromycin resistance.

Protoplast assays. p*shortGUS* (or p*monoGUS*) and p*monoGFP* were described previously[21] and p*ARF5-GUS*[15]. PCR product corresponding to AteIF2β was amplified from eIF2β cDNA (At5g20920) with pairs of specific primers and cloned into p*monoGUS* to replace GUS and obtain the p*eIF2β* construct. The RISP coding sequence was subcloned under the control of the *CaMV* 35S promoter into p*TAV* (p35S-P6)[22] to obtain p*RISP*. p*RISP-S267A* and p*RISP-S267D* were generated by substitution of Ser at the position 267 to Ala (S267A) and Asp (S267D), respectively, within RISP ORF by site-directed PCR mutagenesis. Arabidopsis protoplasts from *Arabidopsis* suspension cell cultures and mesophyll protoplasts from 2-week WT, s6a, *s6a/S6B*$^{S/D}$, or *s6a/S6B*$^{S/A}$ plantlets were transfected with plasmid DNA by the PEG method[52]. 5 µg p*monoGFP* and either 5 µg p*shortGUS* or p*ARF5-GUS*, without or with increasing concentrations of p*RISP* (or phosphorylation mutants of RISP) and/ or p*eIF2β* as indicated were used for cotransformation of *Arabidopsis* suspension culture protoplasts (Fig. 3b-d). 5 µg p*monoGFP* and (1) 5 µg p*shortGUS* or (2) 10 µg p*ARF5-GUS*, or two pairs of plasmids—(3) 10 µg p*biGUS*[44] and 10 µg p*35S* or (3/4) 10 µg p*biGUS* and p*TAV* (p35S-P6)[53] were used to transform mesophyll protoplasts prepared from WT, *s6a, s6a/S6B*$^{S/D}$, or *s6a/S6B*$^{S/A}$ *Arabidopsis* (Fig. 6d). After over-night incubation at 26°C in WI buffer (4 mM MES pH 5.7, 0.5 M Mannitol, 20 mM KCl) transfected protoplasts were harvested by centrifugation and protein extract was prepared in GUS extraction buffer (50 mM NaH_2PO_4 pH 7.0, 10 mM EDTA, 0.1% NP-40). The aliquots were immediately taken for GUS reporter gene assays. GUS activity was measured by a fluorimetric assay using a FLUOstar OPTIMA

fluorimeter (BMG Biotech)[54]. pmonoGFP expression was monitored by western blot using anti-GFP antibodies (Chromotek) and/ or by determining GFP fluorescence. The values given are the means from at least three independent experiments. GUS mRNA levels after protoplasts incubation were determined as indicated in supplementary information.

GST pull-down assay. PCR products corresponding to RISP, eIF3aΔ (aa 1-646), eIF2β and eS6 C-ter (CS6) were inserted into pGEX-6P1 (Pharmacia Biotech) as in-frame fusions with GST. The in vitro Glutathione-S-transferase pull-down assay was performed as described previously[20]. GST pull-down assays were set up as follows: molar equivalents of purified proteins were incubated with the immobilized GST or GST-tagged protein at 4°C for 2 h under constant rotation. Binding of GST or GST-RISP to wheat eIF2, GST or GST-RISP to His-eIF2β, GST or GST-eIF2β to RISP phosphorylation mutants, and GST or GST-eIF3a to His-eIF2β was carried out in a 300 µL reaction containing 50 mM HEPES pH 7.5, 100 mM KCl, 3 mM magnesium acetate, 0.1 mM EDTA, 0.5 % v/v Igepal 360® (Sigma-Aldrich®) and cOmplete® protease inhibitor cocktail (Roche®). Sepharose beads and associated proteins (bound fraction, B) were recovered by centrifugation at 500g for 5 min and thoroughly washed as before (4 washing steps). Fifty µL of the first unbound fraction (U) solution and bound fraction were used for SDS-PAGE analysis. Binding of GST or GST-eIF3a (—GST or GST-CS6—) to RISP phosphorylation mutants—RISP-S267A or RISP-S267D—was carried out in 3-fold increased reaction mixture (900 µl) overnight at 4 °C. After intensive washing, GST-eIF3a-RISP-S267A or GST-eIF3a-RISP-S267D complexes were split into three equal fractions, washed and used for incubation with or without eIF2β, 70 pmol (—purified 60S ribosomal subunits, respectively, 100 pmol—) during 2 h at 4 °C. eIF2β– or 60S-bound complex formation was analyzed (Fig. 5). The bound fractions (B) as well as 50 µL of the unbound fraction (U) were separated by a 12% SDS-PAGE gel and stained by Coomassie™ blue.

Protein purification. Wheat germ eIF2 was kindly provided by K. Browning (University of Texas at Austin, USA). GST-fusion and His-tagged proteins were expressed in Rosetta 2 DE3 pLysS (Novagen®) and purified using Glutathione Sepharose4B beads or HisTrap HP columns (GE Healthcare®), according to supplier protocol.

Yeast two-hybrid assay. PCR products corresponding to eIF2 α, β and γ subunits were amplified from eIF2α (AT5G05470.1), eIF2β (AT5G20920.1) and eIF2γ (AT1G04170.1)

cDNAs with pairs of specific primers and cloned into the pGBKT7 vector (Clontech®) as in-frame fusion with the BD-domain to obtain the pBD-eIF2 subunit variants. eIF2β and eS6 deletion mutants fused to the BD-domain in the pGBKT7 vector were produced by deletion mutagenesis of the pGBK-eIF2β and eS6 (AT5G10360.1) cDNA. RISP (AT5G61200.3) and its deletion mutants fused to AD were produced by PCR from the original pGAD-RISP[22] and cloned between the NdeI and BamHI sites of pGADT7 (Clontech®). PCR product corresponding to RISP-S267D and RISP-S267A were generated by substitution of Ser at position 267 to Asp (S267D) or to Ala (S267A) from pGAD-RISP by site-directed PCR mutagenesis and cloned into pGADT7 vector to obtain the pGAD-RISP-S267D and pGAD-RISP-S267A constructs.

Yeast two-hybrid protein interaction assays were performed according to ref. 21. Constructs containing GAL4 AD-domain and BD-domain fusion variants were co-transformed into AH109 cells. Transformants were selected onto SD-Leu-Trp plates. Surviving yeast colonies were picked as primary positives and transferred on SD-Leu-Trp-Ade selection plates to score protein interaction. β-Galactosidase activity was measured by using the Gal-Screen® assay system (Tropix® by Applied Biosystems®) The values given are the means from more than three independent experiments. Yeast expression levels of all the BD- and AD-fusion variants were monitored by immunoblot analysis with anti-HA (Sigma-Aldrich®) and anti-cMyc (Santa-Cruz Biotechnology®) antibodies of yeast cell lysates using a rapid urea/SDS lysis procedure (data not shown).

Mass spectrometry analysis. Samples were prepared for mass-spectrometry analyses as described[55]. Briefly, samples solubilized in Laemmli buffer were precipitated with 0.1 M ammonium acetate in 100% methanol. After a reduction-alkylation step (Dithiothreitol 5 mM - Iodoacetamide 10 mM), proteins were digested overnight with 1/25 (W/W) of sequencing-grade porcin trypsin (Promega). The peptide mixtures were resolubilized in water containing 0.1% FA (solvent A) before being injected on nanoLC-MS/MS (NanoLC-2DPlus system with nanoFlex ChiP module; Eksigent, ABSciex, Concord, Ontario, Canada, coupled to a TripleTOF 5600 mass spectrometer (ABSciex)). Peptides were eluted from the C-18 analytical column (75 µm ID x 15 cm ChromXP; Eksigent) with a 5%-40% gradient of acetonitrile (solvent B) for 90 minutes. Data were searched against a TAIR database containing the GFP-TOR sequence as well as decoy reverse sequences (TAIR10_pep_20101214). Peptides were identified with Mascot algorithm (version 2.2, Matrix Science, London, UK) through the ProteinScape 3.1 package (Bruker). They were

validated with a minimum score of 30, a p-value<0.05 and proteins were validated respecting a false discovery rate FDR<1%.

Molecular modeling. The 3D structural model of *Arabidopsis* RISP was created using RaptorX[56] based on tropomyosin structure (PDB: 1C1G) and represented graphically by PyMOL (http://www.pymol.org).

Acknowledgments

We are grateful to J-M Daviere and N. Baumberger for helpful assistance in plant genetics and protein analysis, respectively. This work was supported by French Agence Nationale de la Recherche—BLAN-2011_BSV6 010 03, France—for funding L.R., and CONACYT, Service de Coopération Universitaire de l'Ambassade de France au Mexique to E. M-M. This work was supported in part by the ANR grant @RAction program 'ANR CryoEM80S' and the LABEX: ANR-10-LABX-0036_NETRNA and benefits from a funding from the state managed by the French National Research Agency as part of the Investments for the future program (to Y.H.).

References

1. Jackson, R. J., Hellen, C. U. T. & Pestova, T. V. The mechanism of eukaryotic translation initiation and principles of its regulation. *Nature Reviews Molecular Cell Biology* **11,** 113–127 (2010).
2. Browning, K. S. & Bailey-Serres, J. Mechanism of Cytoplasmic mRNA Translation. *The Arabidopsis Book* **13,** e0176–39 (2015).
3. Hinnebusch, A. eIF3: a versatile scaffold for translation initiation complexes. *Trends Biochem. Sci.* **31,** 553–562 (2006).
4. Flynn, A., Oldfield, S. & Proud, C. G. The role of the beta-subunit of initiation factor eIF-2 in initiation complex formation. *Biochim. Biophys. Acta* **1174,** 117–121 (1993).
5. Huang, H. K., Yoon, H., Hannig, E. M. & Donahue, T. F. GTP hydrolysis controls stringent selection of the AUG start codon during translation initiation in Saccharomyces cerevisiae. *Genes Dev* **11,** 2396–2413 (1997).
6. Skabkin, M. A., Skabkina, O. V., Hellen, C. U. T. & Pestova, T. V. Reinitiation and other unconventional posttermination events during eukaryotic translation. *Mol. Cell* **51,** 249–264 (2013).
7. Kozak, M. Constraints on reinitiation of translation in mammals. *Nucleic Acids Res* **29,** 5226–5232 (2001).
8. Calvo, S. E., Pagliarini, D. J. & Mootha, V. K. Upstream open reading frames cause widespread reduction of protein expression and are polymorphic among humans. *Proc. Natl. Acad. Sci. U.S.A.* **106,** 7507–7512 (2009).
9. Zhou, F., Roy, B. & Arnim, von, A. G. Translation reinitiation and development are compromised in similar ways by mutations in translation initiation factor eIF3h and the ribosomal protein RPL24. *BMC Plant Biology* **10,** 193 (2010).
10. Ingolia, N. T., Lareau, L. F. & Weissman, J. S. Ribosome profiling of mouse embryonic stem cells reveals the complexity and dynamics of mammalian proteomes. *Cell* **147,** 789–802 (2011).
11. Gingras, A. C., Raught, B. & Sonenberg, N. Regulation of translation initiation by FRAP/mTOR. *Genes Dev* **15,** 807–826 (2001).
12. Sengupta, S., Peterson, T. R. & Sabatini, D. M. Regulation of the mTOR complex 1 pathway by nutrients, growth factors, and stress. *Mol. Cell* **40,** 310–322 (2010).
13. Ma, X. M. & Blenis, J. Molecular mechanisms of mTOR-mediated translational control. *Nature Reviews Molecular Cell Biology* **10,** 307–318 (2009).
14. Dobrenel, T. *et al.* TOR Signaling and Nutrient Sensing. *Annu Rev Plant Biol* **67,** annurev–arplant–043014–114648 (2016).
15. Schepetilnikov, M. *et al.* TOR and S6K1 promote translation reinitiation of uORF-containing

mRNAs via phosphorylation of eIF3h. *EMBO J.* **32,** 1087–1102 (2013).

16. Kim, T. H., Kim, B. H., Yahalom, A., Chamovitz, D. A. & Arnim, von, A. G. Translational regulation via 5' mRNA leader sequences revealed by mutational analysis of the Arabidopsis translation initiation factor subunit eIF3h. *Plant Cell* **16,** 3341–3356 (2004).
17. Roy, B. *et al.* The h subunit of eIF3 promotes reinitiation competence during translation of mRNAs harboring upstream open reading frames. *RNA* **16,** 748–761 (2010).
18. Futterer, J. & Hohn, T. Role of an upstream open reading frame in the translation of polycistronic mRNAs in plant cells. *Nucleic Acids Res* **20,** 3851–3857 (1992).
19. Ryabova, L. A., Pooggin, M. M. & Hohn, T. Translation reinitiation and leaky scanning in plant viruses. *Virus Res* **119,** 52–62 (2006).
20. Park, H. S., Himmelbach, A., Browning, K. S., Hohn, T. & Ryabova, L. A. A plant viral 'reinitiation' factor interacts with the host translational machinery. *Cell* **106,** 723–733 (2001).
21. Schepetilnikov, M. *et al.* Viral factor TAV recruits TOR/S6K1 signalling to activate reinitiation after long ORF translation. *EMBO J.* **30,** 1343–1356 (2011).
22. Thiebeauld, O. *et al.* A new plant protein interacts with eIF3 and 60S to enhance virus-activated translation re-initiation. *EMBO J.* **28,** 3171–3184 (2009).
23. Holz, M. K., Ballif, B. A., Gygi, S. P. & Blenis, J. mTOR and S6K1 mediate assembly of the translation preinitiation complex through dynamic protein interchange and ordered phosphorylation events. *Cell* **123,** 569–580 (2005).
24. Asano, K., Clayton, J., Shalev, A. & Hinnebusch, A. G. A multifactor complex of eukaryotic initiation factors, eIF1, eIF2, eIF3, eIF5, and initiator tRNA(Met) is an important translation initiation intermediate in vivo. *Genes Dev* **14,** 2534–2546 (2000).
25. Das, S., Maiti, T., Das, K. & Maitra, U. Specific interaction of eukaryotic translation initiation factor 5 (eIF5) with the beta-subunit of eIF2. *J. Biol. Chem.* **272,** 31712–31718 (1997).
26. Fletcher, C. M., Pestova, T. V., Hellen, C. U. & Wagner, G. Structure and interactions of the translation initiation factor eIF1. *EMBO J.* **18,** 2631–2637 (1999).
27. Dennis, M. D. & Browning, K. S. Differential phosphorylation of plant translation initiation factors by *Arabidopsis thaliana* CK2 holoenzymes. *J Biol Chem* **284,** 20602–20614 (2009).
28. Dennis, M. D., Person, M.D. & Browning, K. S. Phosphorylation of plant translation initiation factors by CK2 enhances the *in vitro* interaction of multifactor complex components. *J Biol Chem* **284,** 20615–20628 (2009).
29. Valášek, L., Nielsen, K. H. & Hinnebusch, A. G. Direct eIF2-eIF3 contact in the multifactor complex is important for translation initiation in vivo. *EMBO J.* **21,** 5886–5898 (2002).
30. Källberg, M., Wang, H., Wang, S., Peng, J., Wang, Z., Lu, H. & Xu, J. Template-based protein structure modeling using the RaptorX web server. *Nature Protocols* **7**, 1511-1522 (2012).
31. Schmitt, E., Naveau, M. & Mechulam, Y. Eukaryotic and archaeal translation initiation factor 2: a heterotrimeric tRNA carrier. *FEBS Lett.* **584,** 405–412 (2010).

32. Zeenko, V. & Gallie, D. R. Cap-independent translation of tobacco etch virus is conferred by an RNA pseudoknot in the 5'-leader. *J. Biol. Chem.* **280,** 26813–26824 (2005).
33. Erzberger, J. P. *et al.* Molecular Architecture of the 40S·eIF1·eIF3 Translation Initiation Complex. *Cell* **158,** 1123–1135 (2014).
34. Llácer, J. L. *et al.* Conformational Differences between Open and Closed States of the Eukaryotic Translation Initiation Complex. *Molecular Cell* (2015). doi:10.1016/j.molcel.2015.06.033
35. Georges, des, A. *et al.* Structure of mammalian eIF3 in the context of the 43S preinitiation complex. - PubMed - NCBI. *Nature* (2015).
36. Ben-Shem, A. *et al.* The Structure of the Eukaryotic Ribosome at 3.0 A Resolution. *Science* (2011). doi:10.1126/science.1212642
37. Khatter, H., Myasnikov, A. G., Natchiar, S. K. & Klaholz, B. P. Structure of the human 80S ribosome. *Nature* (2015). doi:10.1038/nature14427
38. Creff, A., Sormani, R. & Desnos, T. The two Arabidopsis RPS6 genes, encoding for cytoplasmic ribosomal proteins S6, are functionally equivalent. *Plant Mol. Biol.* **73,** 533–546 (2010).
39. Turck, F., Zilbermann, F., Kozma, S. C., Thomas, G. & Nagy, F. Phytohormones participate in an S6 kinase signal transduction pathway in Arabidopsis. *Plant Physiol.* **134,** 1527–1535 (2004).
40. Boex-Fontvieille, E. *et al.* Photosynthetic control of Arabidopsis leaf cytoplasmic translation initiation by protein phosphorylation. *PLoS ONE* **8,** e70692 (2013).
41. Turkina, M. V., Klang Årstrand, H. & Vener, A. V. Differential phosphorylation of ribosomal proteins in Arabidopsis thaliana plants during day and night. *PLoS ONE* **6,** e29307 (2011).
42. Carroll, A. J., Heazlewood, J. L., Ito, J. & Millar, A. H. Analysis of the Arabidopsis cytosolic ribosome proteome provides detailed insights into its components and their post-translational modification. *Mol. Cell Proteomics* **7,** 347–369 (2008).
43. Reiland, S. *et al.* Large-scale Arabidopsis phosphoproteome profiling reveals novel chloroplast kinase substrates and phosphorylation networks. *Plant Physiol.* **150,** 889–903 (2009).
44. Bonneville, J. M., Sanfacon, H., Futterer, J. & Hohn, T. Posttranscriptional trans-activation in cauliflower mosaic virus. *Cell* **59,** 1135–1143 (1989).
45. Zhou, F., Roy, B., Dunlap, J. R., Enganti, R. & Arnim, von, A. G. Translational control of Arabidopsis meristem stability and organogenesis by the eukaryotic translation factor eIF3h. *PLoS ONE* **9,** e95396 (2014).
46. Anger, A. M. *et al.* Structures of the human and Drosophila 80S ribosome. *Nature* **497,** 80–85 (2013).
47. Young, D. J., Guydosh, N. R., Zhang, F., Hinnebusch, A. G. & Green, R. Rli1/ABCE1 Recycles Terminating Ribosomes and Controls Translation Reinitiation in 3′UTRs In Vivo. *Cell* **162,** 872–884 (2015).
48. Nürenberg, E. & Tampé, R. Tying up loose ends: ribosome recycling in eukaryotes and archaea. *Trends Biochem. Sci.* **38,** 64–74 (2013).

49. Baronas-Lowell, D. M. & Warner, J. R. Ribosomal protein L30 is dispensable in the yeast Saccharomyces cerevisiae. *Molecular and Cellular Biology* **10,** 5235–5243 (1990).
50. Dresios, J., Derkatch, I. L., Liebman, S. W. & Synetos, D. Yeast ribosomal protein L24 affects the kinetics of protein synthesis and ribosomal protein L39 improves translational accuracy, while mutants lacking both remain viable. *Biochemistry* **39,** 7236–7244 (2000).
51. Nishimura, T., Wada, T., Yamamoto, K. T. & Okada, K. The Arabidopsis STV1 protein, responsible for translation reinitiation, is required for auxin-mediated gynoecium patterning. *Plant Cell* **17,** 2940–2953 (2005).
52. Yoo, S. D., Cho, Y. H. & Sheen, J. Arabidopsis mesophyll protoplasts: a versatile cell system for transient gene expression analysis. *Nat Protoc* **2,** 1565–1572 (2007).
53. Kobayashi, K., Tsuge, S., Nakayashiki, H., Mise, K. & Furusawa, I. Requirement of cauliflower mosaic virus open reading frame VI product for viral gene expression and multiplication in turnip protoplasts. *Microbiol. Immunol.* **42,** 377–386 (1998).
54. Pooggin, M. M., Hohn, T. & Futterer, J. Role of a short open reading frame in ribosome shunt on the cauliflower mosaic virus RNA leader. *J. Biol. Chem.* **275,** 17288–17296 (2000).
55. Chicher, J. *et al.* Purification of mRNA-programmed translation initiation complexes suitable for mass spectrometry analysis. *Proteomics* (2015). doi:10.1002/pmic.201400628
56. Källberg, M., Wang, H., Wang, S., Peng, J., Wang, Z., Lu, H. & Xu, J. Template-based protein structure modeling using the RaptorX web server. *Nature Protocols* **7**, 1511-1522 (2012).

Legend to Figures

Figure 1 RISP binds eIF2 via its subunit β (**a**) Putative RISP 3D-structure generated by Modeller reveals α-helixes: *red* H1, *black* H2, *grey* H3 and *blue* H4. RISP binding sites for eIF3a, eIF3c, eL24 and the S267-P position are indicated. (**b**) Wheat germ-purified eIF2 was identified as a putative RISP interactor by GST pull-down assay. GST N-terminally tagged RISP can specifically pull-down all three eIF2 subunits. The unbound (U) and bound (B) glutathione bead samples were examined by SDS-PAGE and Coomassie staining. (**c**) The eIF2β subunit was selected as a RISP interactor by the yeast two-hybrid system (Y2H). Equal OD_{600} units and 1/10 and 1/100 dilutions were spotted from left to right. Gal4 activation domain (AD)-fused to RISP, but not GST alone, interacts specifically with eIF2β fused to Gal4 binding domain (BD). eIF2α and γ subunits do not display interaction with AD-RISP. (**d**) GST-RISP, but not GST alone, interacts with His-tagged eIF2β in GST pull-down assay. All fusion proteins were expressed and purified from *E. coli*. (**e**) eIF3a was shown as a eIF2β partner in *Arabidopsis* by GST pull-down. GST N-terminally tagged eIF3a pulls-down His-tagged eIF2β. The unbound (U) and bound (B) GST-eIF3a samples were revealed by Coomassie staining. Boundaries of vertically sliced images that juxtapose lanes that were non-adjacent in the gel are delineated by a discontinuous line. All the experiments were reproduced at least two times with similar results.

Figure 2 Phosphorylation state-dependent interactions of RISP with eIF2β. (**a**) Schematic representation of RISP domains shown as boxes: *red* H1; *black* H2; *grey* H3 and *blue* H4. (**b**) Except for a 114 N-terminal amino acid extension, the *Arabidopsis* eIF2β sequence is highly similar to that of archaeal eIF2β (aIF2β). The aIF2β 3D-structure is presented[31]: *blue* C-terminus homologous to *At*eIF2βC (aa 121–268); *black* central helix corresponding to aa 121–144 of *At*eIF2β; *red* N-terminal domain. (**c**) The H2 domain from RISP is sufficient to interact with *At*eIF2β in the Y2H assay. RISP deletion derivatives fused to AD (*left panel*) are depicted as boxes according to the color-code in panel a. Equal OD_{600} units and 1/10 and 1/100 dilutions were spotted from left to right. (**d**) The central domain (aa 121–144) from *At*eIF2β is required for interaction with RISP in the Y2H assay. *At*eIF2β deletion derivatives fused to BD (*left panel*) are depicted as boxes according to the color-code in panel b. (**e**) RISP phosphorylation knockout (AD-RISP-S267A) interacts more strongly with BD-eIF2β than AD-RISP and the AD-tagged RISP phosphomimetic mutant (AD-RISP-S267D) in

quantitative β-galactosidase activity assay. Interactions were scored by measuring β-galactosidase activity in liquid assay. The highest value of β-galactosidase activity with AD-RISP-S267A was set to 100%. (**f**) GST pull-down experiments confirmed that GST-eIF2β (G-2β) interacts preferentially with His-tagged RISP-S267A (RISP-A) as compared with RISP-S267D (RISP-D). GST-eIF2β and RISP mutants were purified from *E. coli*. Unbound (U) and bound (B) samples were examined by SDS-PAGE and Coomassie staining (*left panel*). Comparable quantification of interactions in bound fractions 9 and 11 (*right panel*). Boundaries of vertically sliced images that juxtapose lanes that were non-adjacent in the gel are delineated by a discontinuous line. All the experiments were reproduced at least two times with similar results. (e) Multiple comparisons (Turkey's test) are based on one-way ANOVA test. Data are presented as mean and error bars indicate SD (****P< 0.0001, n=3). (f) Values, expressed in arbitrary densitometric units, are averages of three different measurements from two biological replicates and error bars indicate SD.

Figure 3 Phosphorylation state-dependent interactions of RISP with eIF2β during translation reinitiation in *Arabidopsis* protoplasts. (**a**) Scheme of reporter plasmids used in transient expression experiments in *Arabidopsis* suspension protoplasts: p*monoGFP* (marker for transformation efficiency), p*short-GUS* (harbors 50-nt 5'-UTR, marker for initiation efficiency) and p*ARF5-GUS* (marker for reinitiation efficiency). Short upstream ORFs (uORFs) within ARF5 5'-UTR are depicted as open boxes. (**b**) Transiently expressed phosphorylation knockout mutant of RISP up-regulates initiation and reinitiation events. Protoplasts have been transformed by p*monoGFP* and either p*short GUS* (*in red*) or p*ARF5-GUS* (*in blue*) without or with the effector plasmid that codes for RISP WT or one of its phosphorylation mutants—RISP WT (RISP-S), RISP-S267D (RISP-D) and RISP-S267A (RISP-A) in amounts indicated above the panel. Both GFP fluorescence and β-glucuronidase functional activity were analysed in the same 96-well microtiter plate. Functional levels of GUS expressed from p*short-GUS* normalized to corresponding GFP levels were set at 100%. GUS-containing mRNA levels and integrity analyzed by sqRT–PCR; LC—loading control are presented below the panel. Results shown represent the means obtained in three independent experiments. (**c**) eIF2β does not increase initiation efficiency with or without RISP-A. Protoplasts have been transformed with p*monoGFP*, p*short GUS* (*red bars*) and pRISP-A in increasing amounts of the effector plasmid encoding eIF2β as indicated. Functional levels of GUS expressed from p*short-GUS* normalized to corresponding GFP levels were set at 100%. GUS-containing mRNA levels and integrity were analyzed by sqRT–

PCR; GFP levels were also analysed by immunoblotting; LC—loading control. Results shown represent the means obtained in three independent experiments. (**d**) eIF2β out-competes RISP-A, decreasing its reinitiation capacity. Protoplasts have been transformed with p*monoGFP*, p*ARF5-GUS* (*blue bars*) and eIF2β with increasing amounts of the effector plasmid expressing RISP-S, or -A or -D as indicated. Functional levels of GUS expressed from p*ARF5-GUS* normalized to corresponding GFP levels were set at 100%. (**e**, **f**) Representative example of structural arrangement of eIF3, eIF2 and tRNA in the DHX29-bound 43S complex[35]. We show eIF3a and eIF3c extensions in red and in blue, respectively; their densities are reproduced from refs. 33,34. 40S is depicted in grey and presented as frontal (e) and intersubunit views (**f**). RISP, tRNAiMet, eIF3 and eIF2 subunits are colored as indicated. RISP fits well to a position on 40S in close proximity to the eIF3a C-terminus and the eIF3c N-terminus and the central domain of eIF2β. All the experiments were reproduced at least two times with similar results. (**b-d**) Quantification represents the means (n=3, error bars=SD) obtained in three independent experiments.

Figure 4 Phosphorylation state-dependent interactions of RISP with eS6. (**a**) The full-length RISP is required to interact with eS6 in Y2H assay. RISP deletion derivatives fused to AD (*left panel*) are depicted as boxes according to the RISP color-code. Equal OD_{600} units and 1/10 and 1/100 dilutions were spotted from left to right. (**b**) eS6 3D-structure in a ribosome-bound conformation is presented[36]: *red* N-terminal-ribosome bound domain; *black* central domain proposed to interact with the 60S ribosomal protein eL24; *blue* C-terminal α-helix that protrudes out of 40S. (**c**) The C-terminal and central domains can interact with RISP in Y2H assay. eS6 deletion derivatives fused to BD (*left panel*) are depicted as boxes according to the color-code of eS6 shown in panel b. (**d**) GST pull-down experiments confirmed that the eS6 C-terminal α-helix interacts with His-tagged RISP. GST-CS6 and RISP-His were purified from *E. coli* (*left fractions*). Unbound (U) and bound (B) samples were examined by SDS-PAGE and Coomassie staining. (**e**) BD-CS6 interacts strongly with RISP and its phosphomimetic mutant (RISP-S267D), but not with RISP-S267A in quantitative β-galactosidase activity assay. The highest value of β-galactosidase activity with AD-RISP is set to 100%. All the experiments were reproduced at least two times with similar results. (e) Multiple comparisons (Turkey's test) are based on one-way ANOVA test. Data are presented as mean and error bars indicate SD (****P< 0.0001, n=3).

Figure 5 The ternary complexes between phosphorylation knockout mutant of RISP, eIF3a and eIF2β, and phosphomimetic mutant of RISP, the eCS6 C-terminal α-helix and wheat germ 60S can be reconstructed *in vitro*. **(a)** GST pull-down experiments with RISP phosphorylation mutants pre-bound to glutathione beads-attached GST-eIF3a or GST. After removal of unbound RISP variants (fractions 11 and 17), GST-eIF3a-RISP-S267A (fraction 12) and GST-eIF3a-RISP-S267D complexes (fraction 18) were further incubated without or with His-eIF2β. Unbound (U, fractions 15 and 21) and bound (B, fractions 14 and 20) fractions were assayed by SDS-PAGE and stained with Coomassie blue. GST, GST-eIF3a, His-RISP-S267A, His-RISP-S267D and His-eIF2β were overexpressed in *E. coli* and purified by affinity chromatography (*left panel*). Densitometric quantification of binary (His-RISP mutant/GST-eIF3a) and ternary (eIF2β/binary complex) complexes (*bottom panel*). (**b**) His-RISP phosphorylation mutants were incubated with GST-CS6 or GST-bound to glutathione beads. The glutathione-bound (B) fractions 8 and 14 were washed to remove unbound fractions (U, fractions 9 and 15) and further incubated with 60S ribosomal subunits purified from wheat germ. Unbound (U, fractions 13 and 19) and bound (B, fractions 12 and 18) samples were assayed by SDS-PAGE and stained with Coomassie blue. GST-CS6 was produced in *E. coli*. Stars indicate 60S ribosomal proteins specifically co-precipitated with the GST-CS6/RISP-S267D binary complex. All the experiments were reproduced at least two times with similar results. (a) Values, expressed in arbitrary densitometric units, are averages of three different measurements from two biological replicates and error bars indicate SD.

Figure 6 Phosphorylation of eS6 promotes its binding to RISP and reinitiation capacity of *Arabidopsis* protoplasts. (**a**) Alignment of the C-terminal tail of eS6 plant homologues. Serine phosphorylation sites—Ser231, Ser237, Ser240 and Ser241—are shown in bold. (**b**) eCS6 and its phospho-mimetic mutants (BD-CS6-S231D, BD-CS6-S237D, BD-CS6-S240D) as compared with their phosphoknockout mutants (BD-CS6-S231A, BD-CS6-S237A, BD-CS6-S240A) interact preferentially with RISP phosphorylation mimic in quantitative β-galactosidase activity assay. Interactions were scored by measuring β-galactosidase activity in liquid assay. The value of β-galactosidase activity with BD-CS6-WT and either AD-RISP or AD-RISP-S267D was set to 100%. (**c**) Western blot analysis of total eS6 levels in WT, *s6a*, *s6a/S6B*$^{S/A}$ and *s6a/ S6B*$^{S/D}$ *Arabidopsis* mutant lines were conducted on extracts from 7 dag seedlings. (**d**) Comparable analysis of initiation and reinitiation capacities of WT and *s6a*, *s6a/S6B*$^{S/A}$ and *s6a/S6B*$^{S/D}$ *Arabidopsis* plantlets in transient expression experiments in mesophyll protoplasts, where S6B$^{S/A}$ (S237A/S240A/S241A) and S6B$^{S/D}$

(S237D/S240S/S241D) contain triple S237/S240/S241 mutations. The 5 µg reporters—p*monoGFP* and either p*short-GUS* (*initiation marker*), or p*ARF5-GUS* (*reinitiation after short ORF translation marker*), or p*biGUS* without or with p*TAV* (*reinitiation after long ORF translation marker*)—presented at the top were used for protoplast transformation. GUS/GFP ratios from in WT plants were set as 100% for each reporter plasmid in WT protoplasts. GUS/GFP activity ratios are shown in *red* (p*short-GUS*), *blue* (p*ARF5-GUS*) and *black* (p*biGUS*) bars. TAV and GFP protein levels were analyzed by immunoblot and shown in the bottom panels. GUS-containing mRNA levels were analyzed by semiquantitative RT-PCR. All the experiments were reproduced at least two times with similar results. (b) Multiple comparative tests (Turkey's test) are based on one-way ANOVA test. Data are presented as mean and error bars indicate SD (**p< *0.005*; ***p< *0.0005;* ****P< 0.0001, n=3). (d) Quantification represents the means (n=3, error bars=SD) obtained in three independent experiments.

Figure 7 Proposed scheme of RISP binding to 40S and 60S via eS6 and eL24 and RISP function during elongation and 40S posttermination scanning. (**a**) Model states that before phosphorylation, RISP can function within the 43S PIC, assisting eIF3 in TC recruitment. In response to TOR activation, RISP and eS6 are phosphorylated and, together with eL24, establish a bridge between 40S and 60S ribosomal subunits. See text for details. (**b**) Close up front view of the RISP/ elongating 80S complex highlighting the possible eS6/RISP/eL24 interaction network in the vicinity of the eB13 intersubunit bridge. The cryo-EM structure of the human 80S (see ref. 37; 40S and 60S are depicted in *grey* and *blue*, respectively) and RISP (3D model in *pink*) are presented. RISP was docked in close proximity to eS6 (*black*) and eL24 (*dark blue*) C-terminal domains. (**c**) Close-up front view of the predicted complex between RISP (atomic model) and the 40S-60S posttermination scanning complex. The predicted complex shows the atomic structure of 40S (in *grey*) and 60S (in *blue*) from the yeast 80S ribosome[36]. To build putative 80S open conformation, 60S body was rotated away from 40S by 30°. The 3D RISP model was docked with no clash in close proximity to eS6 (*black*) and eL24 (*dark blue*) C-terminal helixes.

Mancera et al_Fig. 1

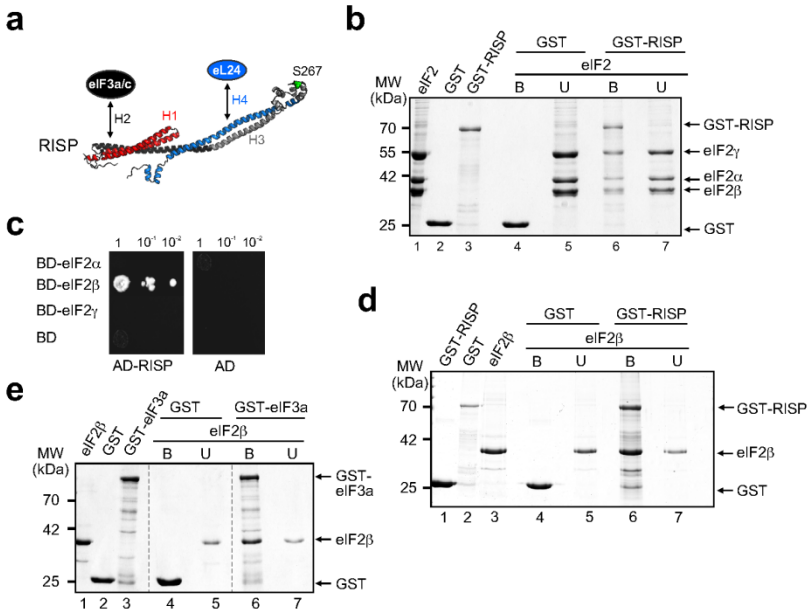

Mancera et al_Fig. 2

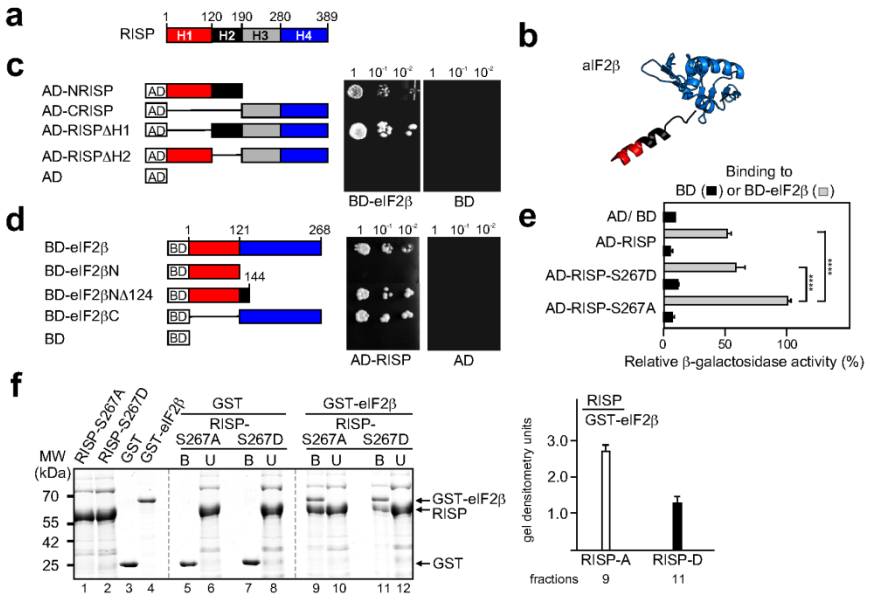

Mancera et al_Fig. 3

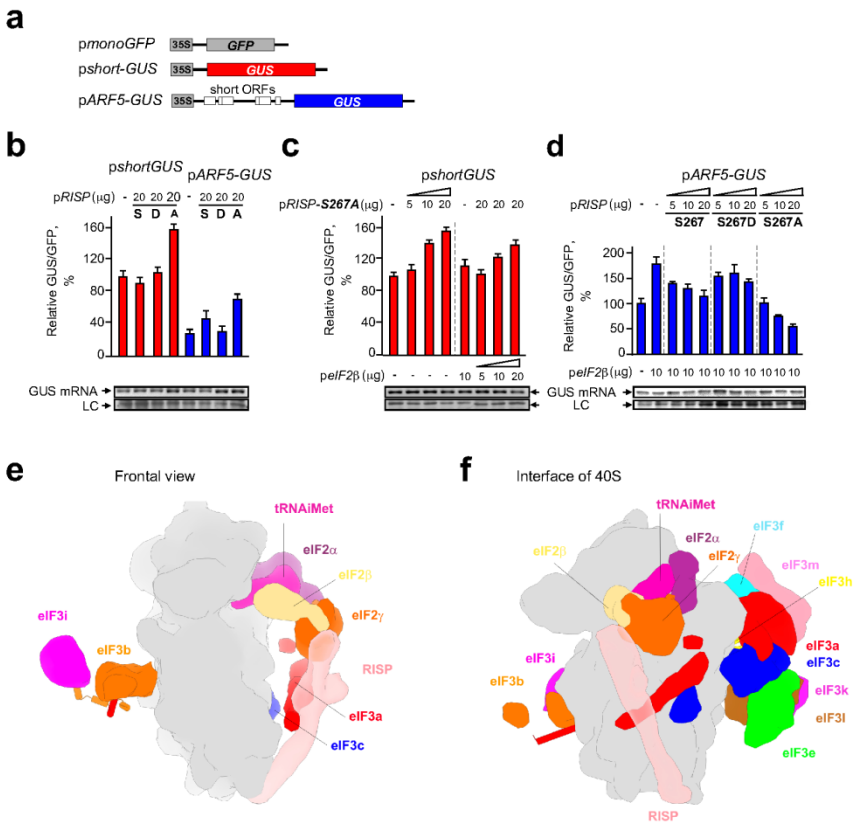

Mancera et al_Fig. 4

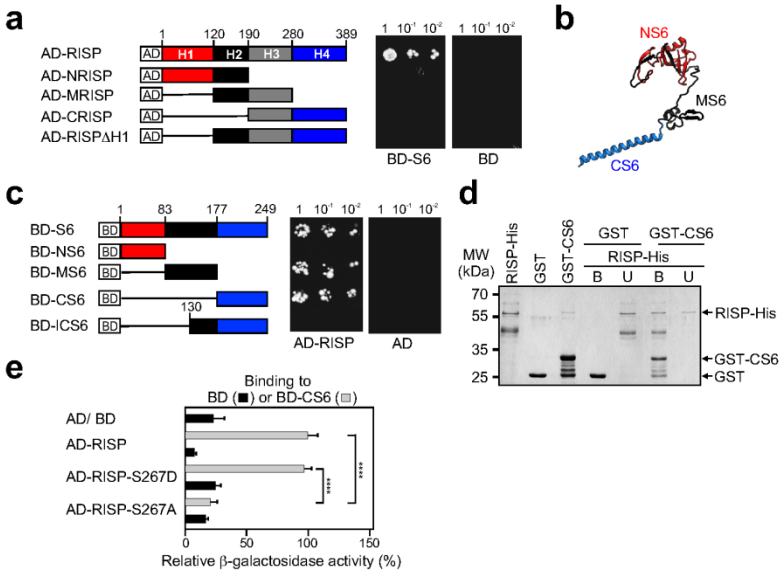

Mancera et al_Fig. 5

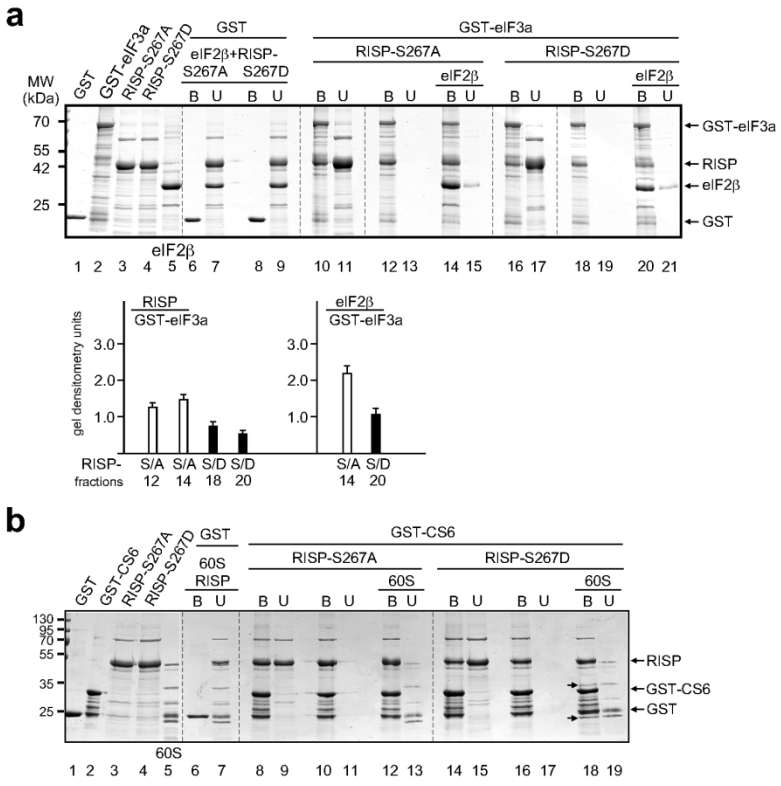

Mancera et al_Fig. 6

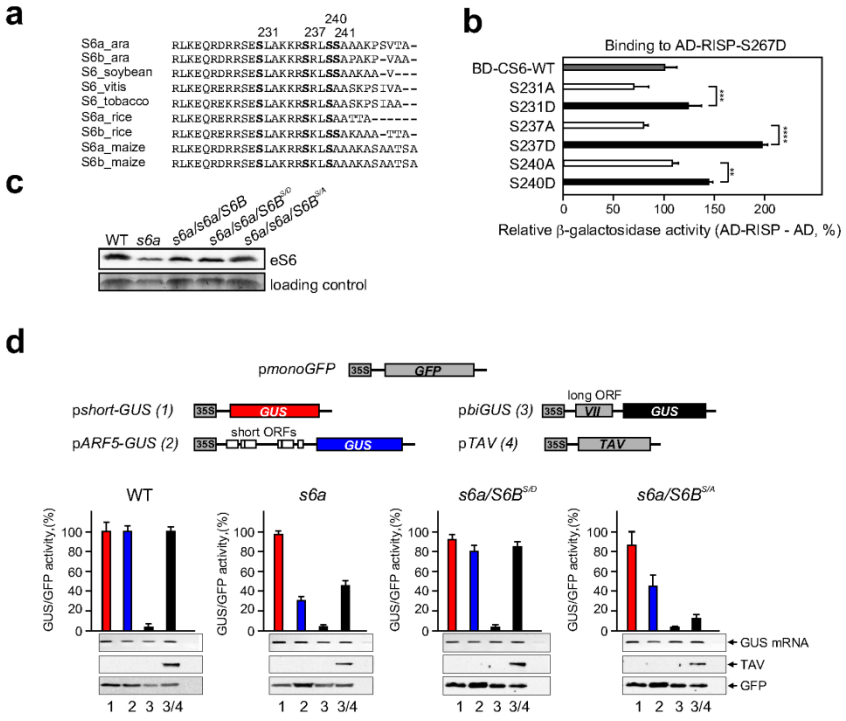

Mancera et al_Fig. 7

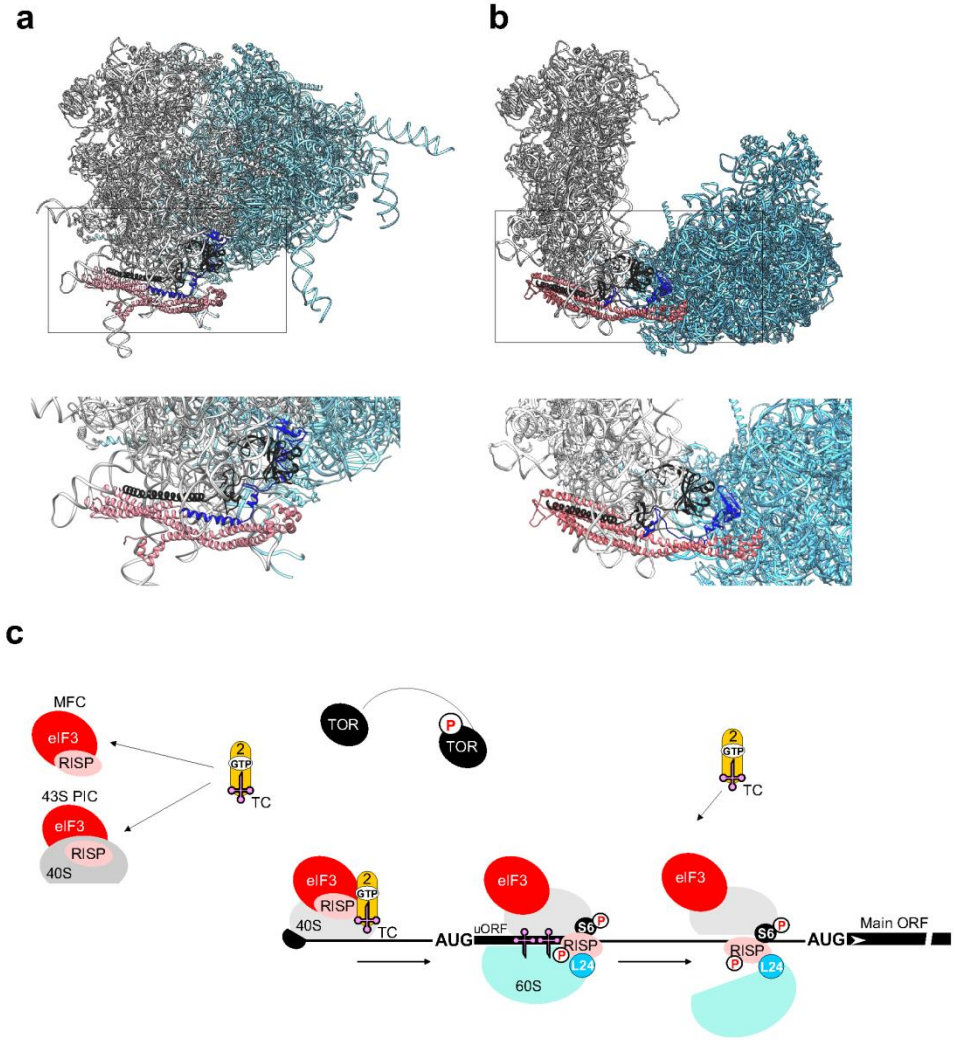

6. Article-3:

GTPase ROP2 promotes translation reinitiation at upstream ORFs via activation of TOR

Mikhail Schepetilnikov[1], Joelle Makarian[1], Ola Srour[1], Angèle Geldreich[1], Zhenbiao Yang[2], Johana Chicher[3], Philippe Hammann[3] and Lyubov A. Ryabova[1]*

[1] Institut de Biologie Moléculaire des Plantes, Centre National de la Recherche Scientifique, UPR 2357, Université de Strasbourg, Strasbourg, France

[2] Center for Plant Cell Biology, Department of Botany and Plant Sciences, University of California, Riverside, CA, USA

[3] Platforme Proteómique Strasbourg-Esplanade, Centre National de la Recherche Scientifique, FRC 1589, Université de Strasbourg, Strasbourg, France

*To whom correspondence should be addressed:
lyuba.ryabova@ibmp-cnrs.unistra.fr
Tel: +33 (0)3 67 15 53 31
Fax: +33 (0)3 67 15 53 00

Running title GTPase ROP2 activates TOR

Keywords: phytohormone auxin/ phosphorylation/ S6K1/ endosomes/ signal transduction

Abstract

Target-of-rapamycin (TOR) promotes reinitiation at upstream ORFs (uORFs), which play an important roles in stem cell regulation and organogenesis in plants. Here, we report that, through TOR, small ROP2 GTPase, if activated by the phytohormone auxin, can control reinitiation of uORF-containing mRNAs. Plants with high levels of active ROP2, including those expressing constitutively active ROP2 (*CA-ROP2*), contain high active TOR levels. Moreover, ROP2 physically interacts with, and, when GTP-bound, activate TOR *in vitro*. TOR activation in response to auxin was abolished in ROP-deficient *rop2rop6ROP4 RNAi* plants. GFP-TOR can associate with endosome-like structures in ROP2-overexpressing plants, indicating that endosomes mediate ROP2 effects on TOR activation. *CA-ROP2* is efficient in loading uORF-containing mRNAs onto polysomes and their translation in protoplasts, with both processes being sensitive to the TOR inhibitor AZD-8055. TOR inactivation abolishes ROP2 effects on translation reinitiation at uORFs, but not its effects on cytoskeleton or intracellular trafficking. These findings imply a mode of translation control whereby, as an upstream effector of TOR, ROP2 coordinates TOR function in translation reinitiation pathways in response to auxin.

Introduction

Target-of-rapamycin (TOR) is a main sensor of cell growth in response to nutrients, energy status and growth factors, and is conserved from humans to yeasts and plants. Mammalian TOR (mTOR) occurs in two structurally and functionally distinct complexes: TOR complex 1 (TORC1) and TOR complex 2 (TORC2) (Zoncu *et al,* 2011; Shimobayashi & Hall, 2014). mTORC1—comprising mTOR, raptor, and mLST8—is sensitive to the immunosuppressant drug rapamycin, and regulates cell growth by activating ribosome biogenesis, transcription, and protein synthesis (Hara *et al,* 2002; Loewith *et al,* 2002). mTORC2 mediates cell metabolism and cytoskeletal organization (Cybulski & Hall, 2009). The mTORC1 pathway promotes 5′-cap-dependent translation via phosphorylation of ribosomal protein S6 kinases (mS6Ks) and eIF4E-binding proteins (m4E-BPs) (Ma & Blenis, 2009; Sonenberg & Hinnebusch, 2009). The key eukaryotic translation initiation factor 3 (eIF3) (Hinnebusch, 2006) serves as a scaffold for mS6K phosphorylation by mTOR (Ma & Blenis, 2009). When activated, TOR binds and phosphorylates eIF3-bound S6K1, triggering its dissociation from eIF3 and further activation (Holz *et al,* 2005). The pathways leading to mTOR activation seem to depend on a group of small GTPases, including Rheb (Ras homologue enriched in brain; Long *et al,* 2005), Rac1 (Saci *et al,* 2011) and Rag (Betz & Hall, 2013), that play a variety of roles within cells (Tee & Blenis, 2005; Sancak *et al,* 2008). The ribosome is an upstream mTORC2 effector in yeast and mammals, and thus can trigger its activation (Zinzalla *et al,* 2011).

Plant TOR has multifaceted roles in plant growth and homeostasis. The *Arabidopsis* genome contains a single essential *TOR* gene, down-regulation of which correlates with decreased plant size, resistance to stress (Deprost *et al,* 2007; Menand *et al,* 2002) and elevated life span (Ren *et al,* 2012). *Arabidopsis* RAPTOR and LST8 are structural and functional components of the TORC1 complex (Dobrenel *et al,* 2011; Mahfouz *et al,* 2006; Moreau *et al,* 2012). The best-characterized substrate of TORC1 in plant translation is S6K1 (Schepetilnikov *et al,* 2011; Xiong & Sheen, 2012); indeed, *Arabidopsis* plants silenced for TOR expression display significantly reduced polysome abundance (Deprost *et al,* 2007), suggesting a role for TOR in plant translational control.

We have previously characterized a novel regulatory TOR function in plant translation (Schepetilnikov *et al,* 2013). TOR is critically required for translation reinitiation of mRNAs that harbor upstream open reading frames within their leader regions (uORF-mRNAs). Such mRNAs

encode many potent proteins such as transcription factors, protein kinases, cytokines and growth factors (Schepetilnikov *et al,* 2013); defects in translation of uORF-mRNAs result in severe developmental anomalies (Zhou *et al,* 2010). Reinitiation is usually less efficient than initiation at the first ORF and occurs mainly after translation of short uORFs (Kozak, 2001), thus the latter can be used to down-modulate the production of critical effector proteins. Mutants of subunit h of the important reinitiation factor eIF3 (eIF3h) compromise translation reinitiation on uORF-mRNAs without affecting initiation events (Kim *et al,* 2004), and eIF3h functions in reinitiation under the control of TOR (Schepetilnikov *et al,* 2013). To promote reinitiation events, active TOR binds preinitiation complexes and polyribosomes to maintain the phosphorylation status of eIF3h (Schepetilnikov *et al,* 2013). Recently, it was demonstrated that translational control at uORFs plays a key role in *Arabidopsis* stem cell regulation and organogenesis (Zhou *et al,* 2014). Plant TOR is activated in response to glucose (Xiong *et al,* 2013), the plant hormone auxin (Schepetilnikov *et al,* 2013), and the pathogenicity factor, Cauliflower mosaic virus (CaMV) protein TAV (Schepetilnikov *et al,* 2011) via as yet uncharacterized signal transduction pathways. Auxin is an important regulator of plant developmental processes that can act via activation of members of a multigenic family of 11 small ROP (Rho-like GTPases from plants) GTPases (Winge *et al,* 1997; Vanneste & Friml, 2009). ROPs function in cellular signaling by regulating, among other things, cell shape and auxin responses (Xu *et al,* 2010). Indeed, ROPs, particularly ROPs 2 and 6 in *Arabidopsis*, are activated by auxin (Xu *et al,* 2010). Given that auxin has been suggested as an upstream signal that can trigger ribosomal protein S6 (rpS6) kinase phosphorylation (Beltrán-Peña *et al,* 2002; Turck *et al,* 2004), and was directly implicated in TOR phosphorylation and activation of the TOR pathway towards translation (Schepetilnikov *et al,* 2013), we focus on the relationships and possible links between small ROP GTPases and TOR.

Here, we report that ROP2 and TOR interact physically *in vitro,* and that ROP2 GTPase, if active, triggers TOR phosphorylation, activating the TOR signaling pathway and translation of a highly controlled class of mRNAs harboring regulatory uORFs. Our results uncover a novel mechanism of translation reinitiation control involving small GTPase ROP2 via TOR.

Results

TOR associates with ROP2 via direct binding

Given that auxin activates both TOR protein kinase (Schepetilnikov *et al*, 2013), and plasma membrane-associated ROPs—particularly ROPs 2 and 6 in *Arabidopsis* (Xu *et al*, 2010; Fig 1A)—we asked whether TOR and ROPs interact. In *Arabidopsis*, RAC/ROPs are encoded by 11 genes that comprise a closely related, multigenic family; ROPs 2, 4 and 6 form a distinct subgroup in a phylogenetic tree based on 11 *Arabidopsis* ROP sequences (Fig 1B). First, using the yeast two-hybrid system, we found specific interactions of TOR with ROPs 2, 4 and 6 (Fig 1C). We selected ROP2—the most abundant of the ROP GTPases according to the Genevestigator database (Fig EV1A)—to further examine its association with TOR. Strikingly, GST-ROP2 binds recombinant TOR physically in a GST pull-down assay, but interacts neither with *Arabidopsis* GTPase Sar1b, which is unrelated to Rho GTPases and functions in ER-Golgi trafficking (Bar-Peled & Raikhel, 1997; Jones *et al*, 2003), nor with GST alone, and only weakly with human GTPase Rheb (Fig 1D), indicating plant-specificity in TOR binding. Although ROPs shuttle between a GTP-bound active form and a GDP-bound inactive form, our GST pull-down approach suggested that *Arabidopsis* TOR can interact with GTP, the non-hydrolyzable analogue guanylyl-imidodiphosphate (GMP-PNP), and GDP-bound GST-ROP2 (Appendix Fig S1A). Third, we determined that TOR and ROP2 coimmunoprecipitate; endogenous ROPs coimmunoprecipitated with green fluorescent protein-tagged TOR (GFP-TOR) in *35S:GFP-TOR* expressing *Arabidopsis*, but not with GFP (*35S:GFP* line; Fig 1E; production of complete TOR in the *35S:GFP-TOR* transgenic line was confirmed by sequence coverage identified from MS/MS data; Appendix Fig S1B). *In planta*, endogenous ROPs coimmunoprecipitated with endogenous TOR using anti-TOR, but not control rabbit serum (NRS, Fig 1F). Thus, ROP2 was identified as a direct TOR interactor *in vitro* that associates with TOR-containing complexes in Arabidopsis.

We next delineated the region of TOR responsible for binding ROP2: the N-terminal half of TOR (NTOR), but not the TOR C-terminus, interacts with ROP2 in the yeast two-hybrid system (Fig 1G). To determine whether GTP charging is critical for ROP2 binding to TOR, we assayed NTOR interactions with both constitutively active GTP-bound ROP2 (CA-ROP2) and the dominant negative nucleotide-free ROP2 (DN-ROP2). CA-ROP2 carries a ROP2-Q64L mutation that abolishes GTP hydrolysis, thus keeping ROP2 in the GTP-bound

active state, while a mutation in the consensus aspartate in the G4 motif (ROP2-D121N) results in lowered nucleotide affinity (Berken & Wittinghofer, 2008; Wu *et al,* 2001) (Fig 1A). Our results indicate that nucleotide-free DN-ROP2 binds to both TOR and NTOR in the yeast two-hybrid system (Fig 1G). Moreover, CA-ROP2 binds TOR and NTOR only weakly or not at all in our conditions. Accordingly, TOR interacts reproducibly more strongly with nucleotide-free ROP2 than with ROP2 or CA-ROP2 GST fusions in GST pull-down assays (Fig 1H). This is similar to the human GTPase Rheb, whose binding affinity to TOR is reduced by GTP charging to enable the TOR complex to adopt a configuration that is catalytically active, when GTP-bound Rheb activates mTOR (Long *et al,* 2005). Rac1, another member of the Rho family of GTPases, which also binds directly to mTOR in GTP-bound state independent manner through the C-terminal RKR stretch of aminoacids (Saci *et al,* 2011), facilitates mTOR localization to cellular membranes. A similar motif involving the four basic lysine residues (motif I) is found at the C-terminus of ROPs 1-6 (Fig EV1B) upstream of a CxxL (x = aliphatic amino acid) geranylgeranylation motif (motif II) required for plasma membrane targeting (Fu *et al,* 2005, 2009; Sorek *et al,* 2011; Xu *et al,* 2014). Deletion of motif II alone did not affect binding of ROP2 to TOR (Fig EV1C), while deleting a longer fragment involving both motifs I and II impaired this interaction, suggesting that ROP2 binds TOR through the C-terminal polylysine stretch of amino acids.

TOR is up-regulated in plants with elevated levels of GTP-bound ROP2

To study whether ROP2 and TOR can functionally interact, we examined the effect of ROP2 on TOR phosphorylation status. To test TOR activation, we measured levels of TOR phosphorylated at S2424 using anti-(mTOR-S2448-P) antibodies [mTOR S2448 epitope can be aligned with the S2424 epitope in *Arabidopsis* TOR (Schepetilnikov *et al,* 2013)]. Anti-(mTOR-S2448-P) antibodies specifically recognize both wild type *Arabidopsis* TOR and its phosphorylation mimic TOR-S2424D transiently expressed in *Arabidopsis* suspension culture protoplasts (Appendix Fig S2A). In contrast, a TOR-specific phosphorylation site knockout (S2424A) diminished TOR recognition to endogenous levels. Accordingly, phosphorylation of S6K1 overexpressed in protoplasts, at the TOR-specific hydrophobic motif residue T449 [anti-(mS6K1-T389-P) antibodies] (Schepetilnikov *et al,* 2011; Xiong & Sheen, 2012), increased strongly upon overexpression of TOR or a TOR phosphorylation mimic. Unlike TOR-S2424D, overexpression of TOR-S2424A did not promote S6K1 phosphorylation at T449, suggesting that phosphorylation of S2424 contributes to *Arabidopsis* TOR activation.

These results demonstrate that mTOR-S2448-P antiserum is specific for TOR phosphorylated at S2424.

We demonstrated earlier that external auxin treatment of *Arabidopsis* seedlings promotes TOR activation (Schepetilnikov *et al,* 2013). As expected, incubation of 7 days after germination (dag) seedlings with auxin analogue 1-naphthylacetic acid (NAA) promoted TOR phosphorylation that was abolished by a second generation TOR inhibitor, AZD-8055, regardless of NAA treatment (Fig EV2A). AZD-8055 binds to the TOR kinase domain within the ATP-binding pocket and inactivates TOR (Chresta *et al,* 2010; Montane & Menand, 2013). Next, we examined *yuc1D* (renamed from yucca; Zhao *et al,* 2001), and *curlyfolia1D* (*cuf1D*; Cui *et al,* 2013) plants characterized by high spatial auxin accumulation, which both exhibited pointed and slightly curled downward leaves (Fig EV2B). Importantly, significantly elevated TOR phosphorylation levels were observed in extracts from *yuc1D* and *cuf1D* as compared with that of WT plants (Fig EV2C). To examine levels of active GTP-bound ROPs in *yuc1D* and *cuf1D* plants, we used a pull-down assay with a ROP-interactive CRIB motif-containing protein 1 (Ric1) that specifically targets activated forms of RAC/ROPs, and compared our results to those obtained with *CA-ROP2* (Wu *et al,* 2000; Miyawaki & Yang, 2014). Indeed, Ric1 fused to GST (GST-Ric1), but not GST alone, interacted preferentially with recombinant ROP2 charged with the non-hydrolyzable GTP analogue GMP-PNP, but not with ROP2 preincubated with GDP (Appendix Fig S2B). As shown in Fig EV2C (right panels), this approach revealed elevated levels of ROPs-GTP in extracts from both *yuc1D* and *cuf1D* as compared with that of WT plants, where a statistically more significant increase of active ROP2 levels was demonstrated in *cuf1D*. Thus, to further establish functional interaction of ROP2 and TOR *in planta*, we employed *Arabidopsis* mutants *cuf1D* and *CA-ROP2*, the latter being transgenic for constitutively active GTP-bound ROP2 (CA-ROP2). Note that the phenotypes of *CA-ROP2* and *cuf1D* are similar (Fig 2A). We correlated endogenous GTP-bound ROP levels pulled down by GST-Ric1 from *cuf1D* and WT, or *CA-ROP2* and WT extracts (Fig 2B). As expected, *CA-ROP2* displayed strongly elevated GTP-bound ROP2 levels due to ROP2 mutant overexpression. GTP-bound ROP2 levels in the *cuf1D* mutant were elevated as compared to WT plants. There were no obvious differences in the levels of mRNA encoding ROP and TORC1 complex components between *cuf1D* and WT plants (Fig 2C), suggesting that GTP-bound ROP levels are elevated through a posttranslational mechanism.

Next, both mutants characterized by high levels of GTP-bound ROPs were used to assess the phosphorylation status of TOR and its downstream target S6K1. We confirmed that

phosphorylation of TOR at S2424 in *CA-ROP2* as well as in *cuf1D* extracts prepared from 7 dag seedlings was greatly elevated as compared with WT extracts (Fig 2D). We also observed a significant increase in S6K1 phosphorylation at the TOR-responsive motif residue T449 in *cuf1D* and *CA-ROP2* as compared with WT plants. This further confirms that TOR signaling is up-regulated in extracts with high GTP-bound ROP2 levels. There was no significant difference in TOR protein levels between mutants and the corresponding WT extracts (Fig 2D). Accordingly, TOR phosphorylation at S2424 was abolished by AZD-8055 in WT and *CA-ROP2* seedlings (Fig 2E). Given that AZD-8055 treatment of WT and *CA-ROP2* plants only slightly altered GTP-bound total ROP levels (Fig 2E, right panel), TOR could be considered dispensable for ROP activation.

To show directly that ROP2 induces TOR signaling activation in response to auxin treatment, we depleted ROPs 2, 4 and 6 (Fig 3A and 3B; Ren *et al*, 2016). First, we found that knockout of only ROP2 substantially reduces the level of ROPs immunoprecipitated by TOR to levels similar to that observed in *rop2 rop6* and *rop2 rop6 ROP4 RNAi* plants, strongly suggesting that ROP2 plays a pivotal role in TOR association (Fig 3C). Time-course analysis revealed that the levels of phosphorylated TOR in WT plants increased 8-fold in response to auxin (Fig 3D). Importantly, induction of TOR by auxin was abolished in *rop2 rop6 ROP4 RNAi*, although the initial level of phosphorylated TOR in ROP-deficient extract was somewhat higher than in WT plants, possibly due to induction of other TOR upstream effectors (Fig 3D). Taken together, these results demonstrate that ROP2 largely mediates the activation of TOR in response to auxin.

We also crossed *CA-ROP2* with the *GFP-TOR* line (Fig 4) to test how GFP-TOR phosphorylation is affected by high CA-ROP2 levels *in planta*. Although the phenotype of *GFP-TOR/CA-ROP2* resembles that of *CA-ROP2* (Fig 4A), there was no obvious difference in TORC1 component mRNA levels other than the expected increase in ROP2 mRNA levels (Fig 4B). Note that we used specific primers to discriminate between GFP-TOR and endogenous TOR mRNAs (Appendix Fig S3). However, the TOR phosphorylation level in *CA-ROP2/GFP-TOR* was elevated by about 9-fold above that in *GFP-TOR* (Fig 4C), again showing that GTP-bound ROP2 boosts TOR-phosphorylation.

To assay kinase activity of TOR immunoprecipitated from either *GFP-TOR/CA-ROP2* or *GFP-TOR* extracts (TOR IP), we compared recombinant S6K1 phosphorylation at TOR-responsive T449 *in vitro* using equal amounts of total TOR IP. Consistently, a higher kinase activity of GFP-TOR was found in *GFP-TOR/CA-ROP2* (Fig 4D). Taken together, these results suggest that GTP-bound ROP2 is a putative candidate to impact TOR signaling

activation.

When active, ROP2, together with its binding partner RIC4, interacts with the actin cytoskeleton and promotes the lobing of epidermal pavement cells in *Arabidopsis* leaves, increasing their circularity (Fu *et al*, 2002; Fig 4E cf *CA-ROP2* vs WT). In *GFP-TOR*, the size of the epidermal pavement cells is reproducibly increased as expected for a TOR overexpressor (Menand *et al*, 2002), while their shape remains unaffected (Fig 4E cf. WT versus *GFP-TOR*). Accordingly, *CA-ROP2/GFP-TOR* cells are reproducibly bigger, but their circularity is similar to that in *CA-ROP2*. Moreover, GFP-TOR overexpression, as well as its activation by CA-ROP2, did not influence further the lobe-promoting ROP2 function in cytoskeleton rearrangements, but rather promoted cell growth.

ROP2 promotes TOR accumulation close to the cell periphery

ROPs associate closely with plasma membrane due to a prenylation motif II at the C-terminus (Sorek *et al*, 2011). Results showing that ROP2 interacts physically and functionally with TOR suggest that ROP2 may function in regulating relocation of TOR to the plasma membrane. Microscopic observation showed that transiently expressed GFP-TOR was distributed diffusely in the cytoplasm in *N. benthamiana* cells, mainly at the cell periphery, but appeared as multiple dots upon co-expression with myc-ROP2, and especially with myc-CA-ROP2 (Fig 5A). Moreover, the number and size of GFP-TOR dots increased upon co-expression of myc-DN-ROP2 (Fig 5A, bottom panels). To locate GFP-TOR dots between the cell periphery and the perinuclear region, we realized a series of confocal cross-sections, 0.95 µM in depth, from the top to the central section of cells overexpressing both GFP-TOR and myc-DN-ROP2 (Appendix Fig S4A). GFP-TOR dots close to the cell periphery/ plasma membrane disappeared from view and reappeared progressively towards the central section, strongly suggesting GFP-TOR localization proximal to the plasma membrane. Note the levels of myc-tagged ROP2, DN-ROP2 and CA-ROP2 production in *N. benthamiana* (Fig 5B).

Next, we investigated the subcellular co-localization of GFP-TOR and red fluorescent protein-tagged ROP2 (RFP-ROP2) expressed transiently in *N. benthamiana* cells. GFP-TOR was distributed diffusely, mainly at the cell periphery (Fig 5C). In contrast, when GFP-TOR was co-expressed together with RFP-ROP2 or RFP-CA-ROP2, GFP-TOR appeared as small dots on the periphery of epidermal cells, close to the plasma membrane (Fig 5D). Although ROP2 overexpression induced GFP-TOR association with subcellular structures, neither RFP-ROP2 nor RFP-CA-ROP2 were found co-localized with GFP-TOR. In contrast, the dominant-

negative ROP2 mutant (RFP-DN-ROP2), while promoting formation of GFP-TOR-containing particles, associated within these subcellular structures (Fig 5D). Moreover, nucleotide-free ROP2, DN-ROP2 exhibits tight TOR binding activity, and it appears that TOR is trapped by DN-ROP2, suggesting that nucleotide charging is required for dissociation of ROP2 from the TOR complex. In control experiments, GFP or RFP fused to different ROP2 variants, either alone or in different combinations, did not reveal similar structures in epidermal cells (Appendix Fig S4B and S4C). In addition, neither Rheb, CA- and DN-Rheb (Appendix Fig S4D), nor Sar1b, CA- and DN-Sar1b derivatives were able to induce GFP-TOR association with subcellular structures (Appendix Fig S4E).

To elucidate the role of C-terminal motifs I and II, we investigated the subcellular co-localization of RFP-ROP2ΔII and RFP-ROP2Δ(I+II) with GFP-TOR. The ROP2 deletion mutant lacking the C-terminal CAFL (motif II) that interacted strongly with TOR *in vitro* (Fig EV1C), failed to promote formation of GFP-TOR-containing particles when co-expressed as an RFP-fusion together with GFP-TOR (Fig 5F). With a ROP2 construct lacking motif I responsible for TOR interaction (Fig EV1C), no GFP-TOR association with subcellular structures was seen. In addition, microscopic observation showed that both the polybasic domain and prenylation motif of ROP2 are responsible for ROP2 attachment to the plasma membrane. Indeed, co-localization with the plasma membrane (PM) was somewhat disturbed upon transient expression of a C-terminal RFP-ROP2 deletion mutant (Fig 5E and EV3A). Thus, ROP2 motif I is involved in TOR binding, while motif II is required for targeting of TOR into subcellular structures.

In planta, punctuate dots have been observed by fluorescence microscopy in the root cells of WT seedlings either treated by external auxin (Fig EV3B) or GTP-bound ROP2 expressing *GFP-TOR/CA-ROP2* seedlings (Fig 5G). Analysis of intracellular distribution of TOR suggested the presence of TOR mainly in supernatant (S100) and partially in microsomal (P100) fractions (Fig EV3C). Although NAA treatment of *Arabidopsis* seedlings had no significant effect on TOR intracellular distribution, active TOR-P levels in microsomes were drastically increased. Likewise, the level of active TOR-P in microsomes isolated from *GFP-TOR/CA-ROP2* was increased significantly as compared with *GFP-TOR* (Fig 5H). Taken together, our results suggest that the appearance of punctuate dots correlates with elevated levels of active TOR in microsomes.

We also tracked whether the dominant negative Sar1b-DN mutant that prevents COPII vesicle formation and blocks protein exit from the ER to the Golgi apparatus (Andreeva *et al,* 2000) can also trigger formation of GFP-TOR punctuate dots. Overexpression of myc-Sar1b-

DN in *N. benthamiana* cells inhibits vesicle trafficking and leads to redistribution of Golgi markers to a polygonal network resembling ER structures (Fig EV3D). However, myc-DN-Sar1b failed to replace myc-DN-ROP2 in GFP-TOR punctuate dot induction, and, vice versa, myc-DN-ROP2 overexpression provokes formation of GFP-TOR aggregates that are not co-localized with RFP-Golgi marker, but failed to affect Golgi transport (Fig EV3D and EV3E). Thus, we concluded that ROP2 is highly specific for TOR association.

GFP-TOR co-localizes to endosomes in response to ROP2 overexpression

To establish the nature of the mobile intercellular particles to which TOR relocates upon ROP2 overexpression, several RFP-fused marker constructs were overexpressed transiently together with GFP-TOR and FLAG-CA-ROP2 in *N. benthamiana* leaves (Fig EV4). Only one out of seven different markers—a transiently expressed RFP-RabC1 that specifically labels endosomes (Rutherford & Moore, 2002)—co-localized with GFP-TOR upon co-expression of either FLAG-ROP2, or FLAG-CA-ROP2, or FLAG-DN-ROP2, indicating that TOR can associate with endosomes (Fig 6A).

To confirm these results in *Arabidopsis*, we used *35S:GFP-TOR* and *35S:RFP-RabC1* lines stably producing GFP-TOR and RFP-RabC1, respectively. Consistent with results in *N. benthamiana*, GFP-TOR co-localized mostly with the endosome-like structures revealed by RFP-RabC1 when GFP-TOR and FLAG-CA-ROP2 were transiently co-expressed in *35S:RFP-RabC1* (Fig 6B), confirming GFP-TOR association with endosomes. The reciprocal combination, e.g. RFP-Rab1C and FLAG-CA-ROP2 expressed transiently in an *Arabidopsis* line transgenic for GFP-TOR, displayed RFP and GFP labeled particles that were mostly co-localized (Fig 6C). We conclude that TOR is targeted by ROP2 to endosome-like structures that quickly dissociate during or after TOR association with endosomes. GFP-TOR can be visualized on endosomes with the DN-ROP2 mutant.

We next determined the effect of brefeldin A (BFA) on the distribution of FM4-64 fluorescent endocytosis marker and GFP-TOR. BFA inhibits the formation of exocytic vesicles but does not block plasma membrane (PM) internalization through endocytosis (Richter *et al*, 2007). If GFP-TOR associates with endocytic compartments, it would be integrated into aggregates of endomembranes together with FM4-64 in the presence of BFA. Here, in BFA-treated cells that retained accumulation of GFP-TOR, selected internalized FM4-64 aggregates were found co-localized with GFP-TOR (Fig 6D). These results further

support our hypothesis that GFP-TOR is relocated to endosomes in response to ROP2 activation.

uORF-mRNA loading on polysomes is under the control of CA-ROP2, which functions through TOR

Translation of a special class of uORF-mRNAs via reinitiation requires TOR activation in response to the phytohormone auxin (Schepetilnikov *et al,* 2013). To establish the role of active ROP2 in the control of translation reinitiation, we performed comparative polysome profile analysis in WT and *CA-ROP2* seedling-derived extracts (Fig 7C). *CA-ROP2* plants are characterized by a slightly increased ratio of polysomes to fraction of monosomes and ribosomal subunits as compared with WT and AZD-8055-treated *CA-ROP2* plants (Fig 7A). To monitor polysomal loading of uORF-mRNAs in different ROP2 activation conditions, we selected several endogenous uORF-mRNAs, such as *ARF3*, *ARF5* and *bZIP11*, translation of which includes one or more reinitiation event depending on the uORF configuration within their leader regions, as well as uORF-less mRNAs encoding actin and glycerol-3-phosphate dehydrogenase C2 (GAPC2, Fig 7B). To avoid translation repression of *bZIP11* by sucrose, seedlings were grown on agar medium containing 30 mM sucrose (Wiese *et al,* 2004).

mRNA distribution within polysomal profiles from extracts of WT seedlings and *CA-ROP2* seedlings grown without or with AZD-8055 was monitored in parallel experiments by quantitative RT–PCR (qRT–PCR) for each indicated endogenous mRNA, and results were normalized to an rRNA and a housekeeping gene, *EXP*, levels of which were stably maintained in all conditions tested. As shown in Fig 7D, efficient GAPC2 mRNA loading on polysomes was barely affected by high active ROP2 levels or by TOR inactivation. In contrast, a somewhat toxic effect of CA-ROP2 on loading of actin mRNA into polysomes was apparent. Polysomal accumulation of *bZIP11*, *ARF3* and *ARF5* mRNAs carrying long leaders with uORFs was reproducibly elevated in *CA-ROP2*-derived extracts as compared with WT extracts. Surprisingly, although, the translation/reinitiation events within *bZIP11*, *ARF3* and *ARF5* 5'-UTRs impede or block ribosomal movement towards the main ORF, causing inefficient translation of uORF-mRNAs in WT conditions (Zhou *et al,* 2010), the high polysome/non-polysome ratio gives a false impression of their efficient translation. Possibly, the increased abundance of initiating/reinitiating 40S, and likely uORF-translating 80S, within their leaders would shift these mRNAs towards 80S or even light polysomal fractions. The abundant appearance of uORF-mRNAs in both polysomal and non-polysomal fractions in

CA-ROP2 reflects main ORF translation at much higher levels due to improved reinitiation at uORFs, while a few 40S can still occupy the leader region *in planta* (Fig 7D). *ARF5* mRNA loading, which is nearly negligible in WT seedlings (6 uORFs inhibits *ARF5* mRNA translation by 16-fold; Zhou *et al*, 2010) was improved drastically upon TOR activation in *CA-ROP2*. As expected, TOR inactivation by AZD-8055 abolished cell reinitiation ability. There was no significant effect of AZD-8055 on total mRNA levels in *CA-ROP2* and WT extracts, except that levels of *bZIP11* mRNA were surprisingly high upon AZD-8055 treatment (Fig EV5D), although this did not improve *bZIP11* mRNA loading. AZD-8055 treatment diminished further loading of *bZIP11* and *ARF3* mRNAs on WT polysomes, while *ARF5* loading remained low under our WT+AZD-8055 conditions (Fig EV5B).

Cell reinitiation efficiency depends on retention of active TOR in polyribosomes after the preceding initiation event (Schepetilnikov *et al,* 2013). Here, the phosphorylation level of TOR found in WT extract 80S and ribosomal subunit fractions was below the limit of detection of our antibodies (Fig EV5C). In contrast, in *CA-ROP2* plants, TOR is phosphorylated and associates not only with 80S and ribosomal subunit fractions but also with light polysomes, which contain two or three translating ribosomes on average on the same mRNA. Application of a TOR inhibitor resulted in TOR inactivation and dissociation from polyribosomal profiles (Fig EV5C). Therefore, uORF-mRNA abundance in polysomes is regulated by GTP-bound ROP2 in a TOR-responsive manner for several ARF-encoded genes, and also for auxin-unrelated *bZIP11*, suggesting that GTP-bound ROP2 up-regulates the translation capacity of reinitiation-dependent mRNAs via TOR.

CA-ROP2 up-regulates translation of uORF-containing mRNAs in *Arabidopsis* protoplasts

Our results suggest that active ROP2 promotes uORF-mRNA accumulation in polysomes in a TOR-responsive manner. We tested whether CA-ROP2 seedlings can drive efficient reinitiation of translation. As expected, TOR phosphorylation status was elevated in *CA-ROP2*–derived mesophyll protoplasts as compared with WT protoplasts, and nearly abolished by AZD-8055 after overnight incubation of protoplasts (Fig 8A).

Next, we compared the transient expression of several reporter genes that harbor a □-glucuronidase (GUS) ORF downstream of short 60-nt-, *ARF3*- or *ARF5*-containing leaders (Fig 8B) in mesophyll protoplasts prepared from WT or *CA-ROP2* seedlings. Mesophyll protoplasts were transformed with one of the above plasmids, and a plasmid containing a

single GFP ORF downstream of the TEV IRES (Zeenko & Gallie, 2005) as a control for transformation efficiency.

Under the conditions used, the *ARF5* and *ARF3* leaders fused to the GUS ORF in their authentic initiation context reduced GUS ORF translation by about 80% and 85%, respectively, compared with that of the short-GUS mRNA (Fig 8C) in WT protoplasts. *ARF3*- and *ARF5*-dependent GUS/GFP levels were dramatically increased by 3- to 4-fold in protoplasts prepared from *CA-ROP2* as compared with WT protoplasts, while GUS/GFP levels did not change significantly upon short leader-dependent expression (Fig 8C). GUS-containing mRNA levels as well as GFP levels in either WT or *CA-ROP2* protoplasts were similar during protoplast incubation. *CA-ROP2*-sensitive induction of *ARF3*- and *ARF5*-dependent GUS ORF expression was blocked by treatment with AZD-8055 (Fig 8C). Thus, the CA-ROP2 effect on uORF-mRNA translation is AZD-8055 sensitive and thus TOR responsive.

We next monitored translation reinitiation efficiencies of short-GUS- and ARF5-GUS-containing reporters in mesophyll protoplasts transfected with either ROP2 (WT-ROP2), or CA-ROP2, or DN-ROP2-expression vectors. As can be seen in Fig 8D, ROP2, and especially CA-ROP2, proteins, but not DN-ROP2, were found active in promoting reinitiation at uORFs of ARF5 mRNA. Indeed, the translation efficiency of the ARF5 leader-containing mRNA was increased up to three-fold in CA-ROP2 expressing protoplasts, while DN-ROP2 GTPase failed to increase translation of either short-GUS, or ARF5-GUS mRNAs.

Discussion

Recent results have revealed a role for auxin in TOR signaling activation in plants (Schepetilnikov *et al,* 2013). Moreover, a recent publication confirmed that TOR plays an important role in auxin signaling transduction in *Arabidopsis* (Deng *et al,* 2016). These results prompted us to address the question of which TOR pathway intermediate compounds can transmit signals from auxin or other TOR upstream effectors (environmental changes, glucose and amino acids) to promote protein synthesis via TOR in plants. Our investigations *in vitro* and *in planta* have demonstrated that the small GTPase ROP2 promotes TOR activation in response to auxin; active TOR can up-regulate translation reinitiation at uORFs. Several lines of evidence support this conclusion: first, ROP2 interacts directly with TOR *in vitro*, and both proteins co-immunoprecipitate in plant extracts (Fig 1 and EV1C). Second, plants characterized by high active ROP or CA-ROP2 contain increased levels of active TOR and S6K1 (Fig 2D). Third, inactivation of TOR by AZD-8055 abolishes ROP2 effects on TOR and its downstream signaling, but TOR is dispensable for the active status of ROP2 and other ROPs, strongly suggesting that ROP2 is upstream of TOR (Fig 2D). Importantly, TOR activation in response to auxin was abolished in *rop2rop6ROP4 RNAi* extracts (Fig 3). Fourth, GTP-bound ROP2 dramatically stimulates translation reinitiation of uORF-mRNAs in a manner sensitive to the TOR inhibitor AZD-8055 (Fig 7 and 8A). Strikingly, CA-ROP2 GTPase, but not the dominant negative DN-ROP2, is active in reinitiation at uORFs (Fig 8D). Another interesting phenomenon revealed by our data is the connection between ROP2-containing TOR complexes and endosome-like structures in the cytoplasm.

ROPs—orthologs of mammalian Rho and Rac (Berken & Wittinghofer, 2008)—are promising candidates for regulating the TOR signaling pathway—the main growth-related pathway in eukaryotes. In addition, a connection between auxin and ROP activation has been established (Miyawaki & Yang, 2014), placing ROPs downstream of auxin. Our data suggest that, in addition to ROP2, TOR is able to interact specifically with ROP4 and ROP6, but additional studies are needed to determine the role of these latter ROPs in TOR regulation. ROP2 is expressed in all vegetative tissues, belongs to the largest ROP subgroup (Li *et al,* 1998; 2001) and, according to our data, when active, contributes to TOR signaling activation in an AZD-8055-sensitive manner. We cannot exclude the possibility that ROP6 and ROP2, which functions in cell expansion on different sides of the membrane (Xu *et al*, 2010), exert differential effects on TOR signaling.

ROP2 associates with TOR or TOR-containing complexes *in vitro* and *in planta* (Fig 1

and EV1C). According to our results, only some TOR-binding characteristics of ROP2 resemble those of human Rho-related GTPase Rheb, although both bind physically and activate TOR in the GTP-bound state. However, the ROP2–TOR interaction is plant specific; ROP2 binds to the heat repeat domain of *Arabidopsis* TOR, while Rheb binds within the kinase domain of mTOR (Long *et al,* 2005). This may explain the weak interaction of Rheb with *Arabidopsis* TOR under our conditions. ROP2 binding to TOR can occur via the C-terminal basic stretch of aminoacids (motif I), and *in vitro* does not require ROP2 charging, but GTP somewhat negatively modulates this interaction (this study and Long *et al,* 2005). Consistently, only WT ROP2 or CA-ROP2 are active in promoting reinitiation at uORFs in protoplasts. These results suggest that TOR/GTP-ROP2 complex formation in *Arabidopsis*, albeit possibly transient, is a necessary prerequisite for the physiological activation of TOR kinase. Strikingly, *Arabidopsis* GFP-TOR, when activated by ROP2, can relocate to endosome-like structures labeled by RabC1. The closest RabC1 GTPase mammalian homologue, Rab18, is also associated with endosomes, especially in epithelial cells, and can function in recycling to the plasma membrane (Rutherford & Moore, 2002). Since the TOR cofactor LST8 was also localized on RabC1-labelled endosomes or endosome-like structures (Moreau *et al,* 2012), we suggest that endosomes are sites of TOR complex localization. Although nucleotide-free ROP2 (DN-ROP2) promotes targeting of TOR to endosomes (Fig 5 and 6), it remains endosome associated, indicating formation of inactive complexes, from which DN-ROP2 is unable to dissociate. Thus, we conclude that ROP2 targeting to endosomes is an intermediate step in ROP2 recycling. In plants, the auxin-related ROP2 pathway plays a role in the promotion of endosomal trafficking from early endosomes during PIN1 internalization (Dhonukshe *et al,* 2007; 2008; Nagawa *et al,* 2012). In turn, disruption of membrane trafficking can influence auxin signaling at the level of translation (Rosado *et al,* 2012). In mammals, Rag GTPases are responsible for lysosomal recruitment of mTOR by targeting its cofactor RAPTOR (Bar-Peled & Sabatini, 2014), while our experiments did not reveal interactions between ROP2 and Arabidopsis RAPTOR (data not shown). Interestingly, although both ROP2 and human Rac1 bind TOR via their polybasic domain, ROP2 activates TOR in a way similar to human Rheb. This can reflect the situation in plants, which contain only a single family of Rho-like GTPases.

Consistent with our findings, a subset of ROP GTPases function in auxin signaling to downstream responsive genes (Tao, 2002), indicating that the active ROP2 status can be translated into specific auxin-dependent responses. Auxin is under the control of various environmental and developmental signals that trigger local auxin biosynthesis or its

intercellular polar distribution. High auxin maxima trigger the cell transcription machinery towards expression of auxin-responsive genes via release of repression of the ARF family (Vanneste & Friml, 2009). In the cytosol, ROP2 can trigger TOR activation in response to auxin, or other as yet uncharacterized signals, to induce translation of a highly regulated class of mRNAs containing regulatory uORFs.

Our results provide a new paradigm for translation regulation of a specific class of messages loaded with short uORFs within their leader regions that are responsive to small GTPase ROP2. When overexpressed in protoplasts, active ROP2 renders protoplasts high-reinitiation-permissive. Our results explain this phenomenon via the model presented in Fig 9. Auxin mediates recycling of ROP2-GDP to ROP2-GTP. ROP2 can bind TOR directly via its polybasic domain. GTP-bound ROP2 forms a transient, but potentially active, complex with TOR, which triggers phosphorylation events and conformational changes that result in TOR activation. Although GTP-bound ROP2 interacts somewhat weakly with TOR, the configuration of GTP-charged ROP2 enables TOR to adopt a form that is both catalytically active and capable of producing signaling *in planta*. TOR activation could occur upon complex formation with ROP2 on endosomes. ROP2 then dissociates from TOR and requires recycling. Several GEFs can recycle ROPs (Oda & Fukuda, 2014). Active TOR is loaded on eIF3-containing preinitiation complexes (Holz *et al*, 2005) and polysomes, where it activates S6K1, and both promote translation reinitiation of uORF-mRNAs (Schepetilnikov *et al*, 2013). In our model, ROP2 is activated in response to auxin signals that are transported via an as yet uncharacterized receptor.

Our findings, together with the observation that TOR is required for virus-controlled polycistronic translation—a process normally strictly prohibited in eukaryotes—in CaMV (Schepetilnikov *et al*, 2011) suggests that TOR up-regulation of reinitiation at uORFs could be as harmful in plants as in mammals, where up-regulation of the protein synthesizing machinery contributes to the development of cancer (Ruggero & Pandolfi, 2003). Notwithstanding that auxin regulates a range of distinct effectors, these findings further corroborate the idea that translation reinitiation is achieved via crosstalk between the TOR kinase and ROP2 signaling pathways. The developmental abnormalities identified in rpl24b and *eif3h-1* mutants due to defects in reinitiation at uORFs are largely similar to auxin-related developmental defects (Zhou *et al*, 2010). Thus, TOR can play an important role in modulating auxin responses during plant development. Further studies are needed to understand the roles of ROP2 in TOR activation as well as to identify other TOR effectors in plants.

Materials and Methods

Cell shape analysis and chemical treatment

Interdigitation analysis of *Arabidopsis* pavement cells was performed as described in the Appendix Supplementary Methods. For microscopic observation of GFP-TOR in endosomes, root cells of *GFP-TOR* transgenic plants were treated with 90 µM brifeldin A (BFA; Sigma) for 30 min and stained with 10 µM FM4-64 dye (Sigma).

Time-course experiments

To study the dynamics of TOR-P accumulation upon auxin treatment *in planta* (Fig 3), 7-dag Col0 WT and rop2rop6ROP4 RNAi transgenic seedlings cultured on MS agar plates were transferred into fresh liquid MS medium and incubated for 2–3 hours at 24°C under constant light conditions to avoid additional stress. Seedlings were then transferred to fresh liquid MS medium with or without 100 nM NAA and samples were harvested at 0, 30, 60, 90 and 120 min after induction. The samples for TOR-P analysis were taken 8 hours after incubation with or without 100 nM NAA, or 1µM AZD. TOR levels and phosphorylation status were determined by western blot with specific antibodies.

In vitro kinase assay

Immunoprecipitated GFP-TOR complexes from *GFP-TOR* and *GFP-TOR/CA-ROP2* 7 dag transgenic seedlings were compared for their phosphotransferase activity towards rec S6K1 as a substrate. Kinase reactions were stopped after 0, 5, 10, 15, and 20 min of incubation at 30°C, and incorporation of phosphate was analyzed by immunoblotting with anti-mS6K1-P-T389 antibodies (Cell Signaling). For TOR immunoprecipitation details, see Appendix Supplementary Methods.

Polyribosome analysis

Polysomes were isolated from 7 dag *Arabidopsis* wild-type Col-0 WT and *CA-ROP2* seedlings grown on MS agar plates supplemented (or not) with 0.5 µM AZD-8055. To

monitor *ARFs, bZIP11, GAPC2* and *ACTIN* mRNA loading into polysomes, total RNA isolated from polysomal fractions as indicated were analyzed by qRT-PCR. mRNAs were monitored in sub/ polysomal fractions, and transcript levels for each mRNA were normalized to maximum mean in monosomal fraction (set as 100%). For gene-specific primer sequences, see Appendix Supplementary Methods.

Protoplast assays

Transient expression was analysed in *Arabidopsis* mesophyll protoplasts from WT and *CA-R0P2* 2-week transgenic seedlings. For plasmid construction, transfection and qRT-PCR protocol details, see Appendix Supplementary Methods.

Yeast two-hybrid assay

Yeast two-hybrid protein interaction assays were performed according to Park *et al,* (2001) Constructs containing NTOR, CTOR and TOR fused to the GAL4 AD-domain and ROP1-6, CA-ROP2 and DN-ROP2 fused to the BD-domain were co-transformed into AH109 cells. Transformants were selected onto SD-Leu-Trp plates. Surviving yeast colonies were picked as primary positives and transferred on SD-Leu-Trp-His selection plates to score protein interaction. The assays and dilutions were performed in triplicate. For plasmid construction details, see Appendix Supplementary Methods.

GST pull-down assay

To analyze activation of ROP2 *in vivo* in total plant extracts treated or not with 1 µM AZD-8055. We utilized a biochemical assay, in which GTP-bound active ROP2 was pulled down by use of GST-Ric1 attached to glutathione-agarose beads.

Binding of TOR to GST-fused Sar1b, or Rheb, or ROP2, or ROP2ΔII, or ROP2Δ(I+II) or GST alone, respectively (Fig 1D, 1H and EV1C) was carried out as described in Appendix Supplementary Methods.

Acknowledgments

We are grateful to Y. Hu for *cuf1D* and Y. Zhao for *yuc1D* lines, A. Komar (*DAPCEL Inc*) for recombinant TOR design, and N. Baumberger for helpful assistance in protein analysis. We thank A. von Arnim for comments on the manuscript and C. Meyer for helpful discussions. This work was supported by French Agence Nationale de la Recherché—BLAN-2011_BSV6 010 03 and ANR-14-CE19-0007—funding to L.R.

Author contributions

MS and LR conceived the project. MS performed the experiments and data analysis. LR and MS wrote the paper. JM, OS and AG participated in experiments. ZY provided *rop* mutants, JC and PH performed MS-MS and data analysis.

Conflict of interest

The authors declare that they have no conflict of interest.

References

Andreeva AV, Zheng H, Saint-Jore CM, Kutuzov MA, Evans DE & Hawes CR (2000) Organization of transport from endoplasmic reticulum to Golgi in higher plants. *Biochem. Soc. Trans* 28: 505–512

Bar-Peled L & Sabatini DM (2014) Regulation of mTORC1 by amino acids. *Trends Cell Biol* 24: 400–406

Bar-Peled M & Raikhel NV (1997) Characterization of AtSEC12 and AtSAR1. Proteins likely involved in endoplasmic reticulum and Golgi transport. *Plant Physiol.* 114: 315–324

Beltrán-Peña E, Aguilar R, Ortíz-López A, Dinkova TD & De Jiménez ES (2002) Auxin stimulates S6 ribosomal protein phosphorylation in maize thereby affecting protein synthesis regulation. *Physiol Plant* 115: 291–297

Berken A & Wittinghofer A (2008) Structure and function of Rho-type molecular switches in plants. *Plant Physiol. Biochem.* 46: 380–393

Betz C & Hall MN (2013) Where is mTOR and what is it doing there? *J. Cell Biol.* 203: 563–574

Chresta CM, Davies BR, Hickson I, Harding T, Cosulich S, Critchlow SE, Vincent JP, Ellston R, Jones D, Sini P, James D, Howard Z, Dudley P, Hughes G, Smith L, Maguire S, Hummersone M, Malagu K, Menear K, Jenkins R, et al (2010) AZD8055 is a potent, selective, and orally bioavailable ATP-competitive mammalian target of rapamycin kinase inhibitor with in vitro and in vivo antitumor activity. *Cancer Res.* 70: 288–298

Cui D, Zhao J, Jing Y, Fan M, Liu J, Wang Z, Xin W & Hu Y (2013) The Arabidopsis IDD14, IDD15, and IDD16 Cooperatively Regulate Lateral Organ Morphogenesis and Gravitropism by Promoting Auxin Biosynthesis and Transport. *PLoS Genet.* 9: e1003759

Cybulski N & Hall MN (2009) TOR complex 2: a signaling pathway of its own. *Trends Biochem. Sci.* 34: 620–627

Deng K, Yu L, Zheng X, Zhang K, Wang W, Dong P, Zhang J & Ren M (2016) Target of Rapamycin Is a Key Player for Auxin Signaling Transduction in Arabidopsis. *Front Plant Sci* 7: 291

Deprost D, Yao L, Sormani R, Moreau M, Leterreux G, Nicolai M, Bedu M, Robaglia C & Meyer C (2007) The Arabidopsis TOR kinase links plant growth, yield, stress resistance and mRNA translation. *EMBO Rep* 8: 864–870

Dhonukshe P, Aniento F, Hwang I, Robinson DG, Mravec J, Stierhof Y-D & Friml J (2007) Clathrin-mediated constitutive endocytosis of PIN auxin efflux carriers in Arabidopsis. *Current Biology* 17: 520–527

Dhonukshe P, Tanaka H, Goh T, Ebine K, Mähönen AP, Prasad K, Blilou I, Geldner N, Xu J, Uemura T, Chory J, Ueda T, Nakano A, Scheres B & Friml J (2008) Generation of cell polarity in plants links endocytosis, auxin distribution and cell fate decisions. *Nature* 456: 962–966

Dobrenel T, Marchive C, Sormani R, Moreau M, Mozzo M, Montané MH, Menand B, Robaglia C &

Meyer C (2011) Regulation of plant growth and metabolism by the TOR kinase. *Biochem. Soc. Trans.* 39: 477–481

Fu Y, Gu Y, Zheng Z, Wasteneys G & Yang Z (2005) Arabidopsis interdigitating cell growth requires two antagonistic pathways with opposing action on cell morphogenesis. *Cell* 120: 687–700

Fu Y, Li H & Yang Z (2002) The ROP2 GTPase controls the formation of cortical fine F-actin and the early phase of directional cell expansion during Arabidopsis organogenesis. *Plant Cell* 14: 777–794

Fu Y, Xu T, Zhu L, Wen M & Yang Z (2009) A ROP GTPase signaling pathway controls cortical microtubule ordering and cell expansion in Arabidopsis. *Curr. Biol.* 19: 1827–1832

Hara K, Maruki Y, Long X, Yoshino K-I, Oshiro N, Hidayat S, Tokunaga C, Avruch J & Yonezawa K (2002) Raptor, a binding partner of target of rapamycin (TOR), mediates TOR action. *Cell* 110: 177–189

Hinnebusch A (2006) eIF3: a versatile scaffold for translation initiation complexes. *Trends Biochem. Sci.* 31: 553–562

Holz MK, Ballif BA, Gygi SP & Blenis J (2005) mTOR and S6K1 mediate assembly of the translation preinitiation complex through dynamic protein interchange and ordered phosphorylation events. *Cell* 123: 569–580

Jones B, Jones EL, Bonney SA, Patel HN, Mensenkamp AR, Eichenbaum-Voline S, Rudling M, Myrdal U, Annesi G, Naik S, Meadows N, Quattrone A, Islam SA, Naoumova RP, Angelin B, Infante R, Levy E, Roy CC, Freemont PS, Scott J, et al (2003) Mutations in a Sar1 GTPase of COPII vesicles are associated with lipid absorption disorders. *Nature Genetics* 34: 29–31

Kim TH, Kim BH, Yahalom A, Chamovitz DA & Arnim von AG (2004) Translational regulation via 5' mRNA leader sequences revealed by mutational analysis of the Arabidopsis translation initiation factor subunit eIF3h. *Plant Cell* 16: 3341–3356

Kozak M (2001) Constraints on reinitiation of translation in mammals. *Nucleic Acids Res* 29: 5226–5232

Li H, Shen JJ, Zheng ZL, Lin Y & Yang Z (2001) The Rop GTPase switch controls multiple developmental processes in Arabidopsis. *Plant Physiol.* 126: 670–684

Li H, Wu G, Ware D, Davis KR & Yang Z (1998) Arabidopsis Rho-related GTPases: differential gene expression in pollen and polar localization in fission yeast. *Plant Physiol.* 118: 407–417

Loewith R, Jacinto E, Wullschleger S, Lorberg A, Crespo JL, Bonenfant D, Oppliger W, Jenoe P & Hall MN (2002) Two TOR complexes, only one of which is rapamycin sensitive, have distinct roles in cell growth control. *Molecular Cell* 10: 457–468

Long X, Lin Y, Ortiz-Vega S, Yonezawa K & Avruch J (2005) Rheb Binds and Regulates the mTOR Kinase. *Current Biology* 15: 702–713

Ma XM & Blenis J (2009) Molecular mechanisms of mTOR-mediated translational control. *Nature Reviews Molecular Cell Biology* 10: 307–318

Mahfouz MM, Kim S, Delauney AJ & Verma DP (2006) Arabidopsis TARGET OF RAPAMYCIN interacts with RAPTOR, which regulates the activity of S6 kinase in response to osmotic stress signals. *Plant Cell* 18: 477–490

Menand B, Desnos T, Nussaume L, Berger F, Bouchez D, Meyer C & Robaglia C (2002) Expression and disruption of the Arabidopsis TOR (target of rapamycin) gene. *Proceedings of the National Academy of Sciences* 99: 6422–6427

Miyawaki KN & Yang Z (2014) Extracellular signals and receptor-like kinases regulating ROP GTPases in plants. *Front Plant Sci* 5: 449

Montane MH & Menand B (2013) ATP-competitive mTOR kinase inhibitors delay plant growth by triggering early differentiation of meristematic cells but no developmental patterning change. *J. Exp. Bot.*

Moreau M, Azzopardi M, Clément G, Dobrenel T, Marchive C, Renne C, Martin-Magniette M-L, Taconnat L, Renou J-P, Robaglia C & Meyer C (2012) Mutations in the Arabidopsis homolog of LST8/GβL, a partner of the target of Rapamycin kinase, impair plant growth, flowering, and metabolic adaptation to long days. *Plant Cell* 24: 463–481

Nagawa S, Xu T, Lin D, Dhonukshe P, Zhang X, Friml J, Scheres B, Fu Y & Yang Z (2012) ROP GTPase-dependent actin microfilaments promote PIN1 polarization by localized inhibition of clathrin-dependent endocytosis. *PLoS Biol.* 10: e1001299

Oda Y & Fukuda H (2014) Emerging roles of small GTPases in secondary... [Front Plant Sci. 2014] - PubMed - NCBI. *Front Plant Sci* 5: 428

Park HS, Himmelbach A, Browning KS, Hohn T & Ryabova LA (2001) A plant viral 'reinitiation' factor interacts with the host translational machinery. *Cell* 106: 723–733

Ren H, Dang X, Yang Y, Huang D, Liu M, Gao X & Lin D (2016) SPIKE1 Activates ROP GTPase to Modulate Petal Growth and Shape. *Plant Physiol.* 172: 358–371

Ren M, Venglat P, Qiu S, Feng L, Cao Y, Wang E, Xiang D, Wang J, Alexander D, Chalivendra S, Logan D, Mattoo A, Selvaraj G & Datla R (2012) Target of rapamycin signaling regulates metabolism, growth, and life span in Arabidopsis. *Plant Cell* 24: 4850–4874

Richter S, Geldner N, Schrader J, Wolters H, Stierhof Y-D, Rios G, Koncz C, Robinson DG & Jürgens G (2007) Functional diversification of closely related ARF-GEFs in protein secretion and recycling. *Nature* 448: 488–492

Rosado A, Li R, van de Ven W, Hsu E & Raikhel NV (2012) Arabidopsis ribosomal proteins control developmental programs through translational regulation of auxin response factors. *Proc. Natl. Acad. Sci. U.S.A.* 109: 19537–19544

Ruggero D & Pandolfi PP (2003) Does the ribosome translate cancer? *Nat Rev Cancer* 3: 179–192

Rutherford S & Moore I (2002) The Arabidopsis Rab GTPase family: another enigma variation. *Curr Opin Plant Biol* 5: 518–528

Saci A, Cantley LC & Carpenter CL (2011) Rac1 Regulates the Activity of mTORC1 and mTORC2

and Controls Cellular Size. *Molecular Cell* 42: 50–61

Sancak Y, Peterson TR, Shaul YD, Lindquist RA, Thoreen CC, Bar-Peled L & Sabatini DM (2008) The Rag GTPases bind raptor and mediate amino acid signaling to mTORC1. *Science* 320: 1496–1501

Schepetilnikov M, Dimitrova M, Mancera-Martínez E, Geldreich A, Keller M & Ryabova LA (2013) TOR and S6K1 promote translation reinitiation of uORF-containing mRNAs via phosphorylation of eIF3h. *EMBO J.* 32: 1087–1102

Schepetilnikov M, Kobayashi K, Geldreich A, Caranta C, Robaglia C, Keller M & Ryabova LA (2011) Viral factor TAV recruits TOR/S6K1 signalling to activate reinitiation after long ORF translation. *EMBO J.* 30: 1343–1356

Shimobayashi M & Hall MN (2014) Making new contacts: the mTOR network in metabolism and signalling crosstalk. *Nature Publishing Group* 15: 155–162

Sonenberg N & Hinnebusch AG (2009) Regulation of translation initiation in eukaryotes: mechanisms and biological targets. *Cell* 136: 731–745

Sorek N, Gutman O, Bar E, Abu-Abied M, Feng X, Running MP, Lewinsohn E, Ori N, Sadot E, Henis YI & Yalovsky S (2011) Differential effects of prenylation and s-acylation on type I and II ROPS membrane interaction and function. *Plant Physiol.* 155: 706–720

Tao LZ (2002) Plant Rac-Like GTPases Are Activated by Auxin and Mediate Auxin-Responsive Gene Expression. *Plant Cell* 14: 2745–2760

Tee AR & Blenis J (2005) mTOR, translational control and human disease. *Semin. Cell Dev. Biol.* 16: 29–37

Turck F, Zilbermann F, Kozma SC, Thomas G & Nagy F (2004) Phytohormones participate in an S6 kinase signal transduction pathway in Arabidopsis. *Plant Physiol.* 134: 1527–1535

Vanneste S & Friml J (2009) Auxin: a trigger for change in plant development. *Cell* 136: 1005–1016

Wiese A, Elzinga N, Wobbes B & Smeekens S (2004) A conserved upstream open reading frame mediates sucrose-induced repression of translation. *Plant Cell* 16: 1717–1729

Winge P, Brembu T & Bones AM (1997) Cloning and characterization of rac-like cDNAs from Arabidopsis thaliana. *Plant Mol. Biol.* 35: 483–495

Wu G, Gu Y, Li S & Yang Z (2001) A genome-wide analysis of Arabidopsis Rop-interactive CRIB motif-containing proteins that act as Rop GTPase targets. *Plant Cell* 13: 2841–2856

Wu G, Li H & Yang Z (2000) Arabidopsis RopGAPs are a novel family of rho GTPase-activating proteins that require the Cdc42/Rac-interactive binding motif for rop-specific GTPase stimulation. *Plant Physiol.* 124: 1625–1636

Xiong Y & Sheen J (2012) Rapamycin and glucose-target of rapamycin (TOR) protein signaling in plants. *J Biol Chem* 287: 2836–2842

Xiong Y, McCormack M, Li L, Hall Q, Xiang C & Sheen J (2013) Glucose-TOR signalling reprograms the transcriptome and activates meristems. *Nature* 496: 181–186

Xu T, Dai N, Chen J, Nagawa S, Cao M, Li H, Zhou Z, Chen X, De Rycke R, Rakusová H, Wang W, Jones AM, Friml J, Patterson SE, Bleecker AB & Yang Z (2014) Cell surface ABP1-TMK auxin-sensing complex activates ROP GTPase signaling. *Science* 343: 1025–1028

Xu T, Wen M, Nagawa S, Fu Y, Chen J-G, Wu M-J, Perrot-Rechenmann C, Friml J, Jones AM & Yang Z (2010) Cell Surface- and Rho GTPase-Based Auxin Signaling Controls Cellular Interdigitation in Arabidopsis. *Cell* 143: 99–110

Zhao Y, Christensen SK, Fankhauser C, Cashman JR, Cohen JD, Weigel D & Chory J (2001) A role for flavin monooxygenase-like enzymes in auxin biosynthesis. *Science* 291: 306–309

Zeenko V & Gallie DR (2005) Cap-independent translation of tobacco etch virus is conferred by an RNA pseudoknot in the 5'-leader. *J. Biol. Chem.* 280: 26813–26824

Zhou F, Roy B & Arnim von AG (2010) Translation reinitiation and development are compromised in similar ways by mutations in translation initiation factor eIF3h and the ribosomal protein RPL24. *BMC Plant Biology* 10: 193

Zhou F, Roy B, Dunlap JR, Enganti R & Arnim von AG (2014) Translational control of Arabidopsis meristem stability and organogenesis by the eukaryotic translation factor eIF3h. *PLoS ONE* 9: e95396

Zinzalla V, Stracka D, Oppliger W & Hall MN (2011) Activation of mTORC2 by association with the ribosome. *Cell* 144: 757–768

Zoncu R, Efeyan A & Sabatini DM (2011) mTOR: from growth signal integration to cancer, diabetes and ageing. *Nature Publishing Group* 12: 21–35

Figure legends

Figure 1. Identification of ROP2 as a binding partner of TOR.

A Schematic representation of *Arabidopsis* TOR (S2424 phosphorylation site indicated) and ROP functional domains (G domains, the positions of Q64 and D121 and C-terminal basic K/R-CaaL motifs are indicated).

B Phylogenetic tree of 11 Rop family member proteins. ROPs 2, 4 and 6 are classified in a subgroup (red).

C ROP2, ROP4 and ROP6 identified as putative TOR interactors by the yeast two-hybrid (Y2H) system. BD-ROPs 1–6 were assayed for interaction with AD-TOR. Equal OD_{600} units and 1/10 and 1/100 dilutions were spotted from left to right.

D GST pull-down assay—ROP2-, Rheb-, Sar1b-tagged GST, and GST alone were assayed for interaction with recombinant TOR as indicated on the left panel. GST-fusion protein bound (B) and unbound (U) fractions were stained by Coomassie blue.

E Immunoprecipitation (IP) experiments with anti-GFP-Trap magnetic beads on crude extracts of *GFP-TOR* and *GFP* transgenic plants; for western blots, 10% of the input and 100% of IP fractions were analyzed with anti-GFP, -TOR and -ROP antibodies (ABs).

F Endogenous TOR was immunoprecipitated from *Arabidopsis* extract with anti-TOR ABs (IP) and assayed for association with ROPs by immunoblotting. 10% of the input, 100% of IP or normal rabbit serum (NRS) were analyzed by anti-ROP antibodies.

G Y2H: TOR and its N-terminal domain (NTOR) interact with ROP2 and dominant negative ROP2 (DN-ROP2). AD-TOR, -NTOR and -CTOR were assayed for interaction with BD-ROP2 or -ROP2 mutants -CA-ROP2 and -DN-ROP2 as indicated.

H *Left panel* GST pull-down assay: ROP2-, DN-ROP2-, CA-ROP2- tagged GST and GST alone were assayed for interaction with recombinant TOR. Fractions were stained by Coomassie blue. *Right panel* Quantification of TOR binding to GST-fusion proteins. The value for TOR binding to GST-ROP2 was set as 100%.

Data information: (H) Statistical analysis is based on one-way ANOVA test. Data are presented as mean +/-SEM. ($P<0.05$, n=3).

Figure 2. TOR signaling is up-regulated in *Arabidopsis* with elevated active ROP2 levels.

A Rosettes representative of WT, *cuf1D*, and *CA-ROP2* plants.

B GST-Ric1 (or GST) pull-down IP assays targeting active GTP-bound ROPs in WT, *cuf1D* and *CA-ROP2* seedlings. Active ROPs and total ROPs were detected with an anti-ROP ABs. GST-Ric1 and a loading control (LC) were stained with Coomassie blue.

C The level of endogenous mRNAs, including *actin* (*ACT*), *glycerol-3-phosphate dehydrogenase C2* (*GAPC2*), expressed protein (*EXP*) and others indicated below the bar graphs in WT and *cuf1D* was examined by qRT-PCR. The RNA value in WT extracts was set as 100%.

D TOR and S6K1 levels and their phosphorylation status in either *cuf1D* and WT, or *CA-ROP2* and WT were analyzed by immunoblot with anti-*At*TOR ABs (anti-TOR), anti-(mTOR-S2448-P) and anti-mS6K1, anti-(mS6K1-T389-P) ABs, respectively. The density of bands on western blots were quantified and WT values were set as 100%.

E *Upper panels* Analysis of active ROPs by GST-Ric1 IP in WT and *CA-ROP2* extracts from 7 dag seedlings grown with or without 1 µM AZD-8055. Total ROPs and GST-Ric1 bound ROPs were detected using anti-ROP antibodies. GST-Ric1 and LC were stained with Coomassie blue. Input: Total ROPs, TOR total and its phosphorylation levels were analyzed by western blot. *Left panel* Quantification of ratio between ROPs-GTP and GST-Ric1. The value for ROPs-GTP in WT and *CA-ROP2* was set as 1.

Data information: (C) Values, expressed in arbitrary units, are averages of two technical replicates, and error bars indicate +/-SD. (E) Statistical analysis is based on unpaired t-test (n=3), ns, non-significant.

Figure 3. ROP2 mediates auxin signaling towards TOR.

A Rosettes representative of WT, *rop2*, *rop2 rop6*, and *rop2 rop6 ROP4 RNAi* plants.

B The level of endogenous *ROP* mRNAs in different ROP-deficient plants were examined by a semiquantitative RT-PCR.

C Endogenous TOR was immunoprecipitated from WT and ROP-deficient *Arabidopsis* extracts by immunoblotting with anti-TOR ABs (IP) and assayed for association with ROPs. 10% of the input and 100% of IP were analyzed by anti-ROP antibodies.

D Time-course of TOR and TOR-P accumulation in extracts from 7-dag seedlings before (0 min) and after transfer to medium with NAA analysed by immunoblot with anti-TOR and anti-(mTOR-S2448-P) ABs. The value of TOR-P/TOR at 0 min (no incubation) for each line was set as 1.

Figure 4. GFP-TOR in *CA-ROP2* background is highly phosphorylated, functionally and developmentally active.

A Rosettes representative of WT, *GFP-TOR*, *CA-ROP2* and *GFP-TOR/CA-ROP2* plants.

B The level of endogenous mRNAs including endogenous TOR (TORend) and both GFP-TOR and TOR end (TOR mix) and others indicated below the bar graphs in *GFP-TOR* and *GFP-TOR/CA-ROP2* was examined by qRT-PCR. The RNA value in *GFP-TOR* extracts was set as 100%.

C Total and active ROP and TOR levels, TOR phosphorylation status in either *GFP-TOR* or *GFP-TOR/CA-ROP2* were analyzed as described in Fig 2B and 2D, respectively.

D *In vitro* phosphorylation kinetics of recombinant S6K1 (S6K1) using GFP-TOR immunoprecipitated from *GFP-TOR* or *GFP-TOR/CA-ROP2*. S6K1 total and phosphorylation levels were followed by western blot using anti-S6K1-T389-P or anti-S6K1 ABs. Total S6K1 was stained by Coomassie blue.

E Representative images of pavement cell (PC) morphology in the second true leaf of 21-day-old WT plants and the *GFP-TOR*, *CA-ROP2* and *GFP-TOR/CA-ROP2* mutant lines. Box and Whiskers plot *bottom panels*.

Data information: (B) Values, expressed in arbitrary units, are averages of three technical replicates, and error bars indicate SD. (E) Scale bars are 30 µm. Box and Whiskers plot (Tukey-style) of quantitative analysis of cell circularity (*left panel)* and cell sizes (*right panel)* is presented using unpaired t-test. *p<*0.05*; **p<*0.001*; ns, non-significant.

Figure 5. ROP2 determines TOR appearance as multiple dots close to the cell periphery in an ROP2 C-terminus-dependent fashion.

A *Nicotiana benthamiana* epidermal cells transiently expressing GFP-TOR (*left panel*) and co-transformed (from left to right) with myc-ROP2, or myc-CA-ROP2, or myc-DN-ROP2. Quantitative analysis of GFP-TOR aggregate number (Box and Whiskers plot *left panel*) and sizes (Scatter plot *right panel*).

B Immunoblot analysis with anti-myc or anti-GFP of transiently co-expressed GFP-TOR without or with myc-ROP2, myc-CA-ROP2, or myc-DN-ROP2 in *N. benthamiana* cells.

C–F Fluorescence micrographs showing *N. benthamiana* cells transiently expressing: (C) GFP-TOR; (D) *Upper panels left* GFP-TOR, *central* RFP-ROP2, *right* merged. *Middle panels Left* GFP-TOR, *central* RFP-CA-ROP2, *right* merged. *Bottom panels left* GFP-TOR, *central*

RFP-DN-ROP2, *right* merged; (E) *left* RFP-ROP2, *central* RFP-ROP2ΔII (CAFL), *right* RFP-ROP2Δ(I+II). (F) *Upper panels left* GFP-TOR, *central* RFP-ROP2, *right* merged. *Middle panels Left* GFP-TOR, *central* RFP-ROP2ΔII, *right* merged. *Bottom panels left* GFP-TOR, *central* RFP- ROP2Δ(I+II), *right* merged

G Imaging fluorescence assays showing root cells of *Arabidopsis* 7 dag *GFP-TOR* and *GFP-TOR/CA-ROP2* cells.

H Intracellular disribution of TOR and active TOR. Western blot analysis of variuos fractions following microsome isolation from *GFP-TOR* and *GFP-TOR/CA-ROP2*. The total homogenate (total), nuclear fraction pellet (P10), pellet (P30), pellet (P100), supernatant (S100) were analyzed by western blot with corresponsing antibodies.

Data information: (A) Statistical analysis is based on one-way ANOVA test *left panel, p<0.05*; *right panel p<0.0001*. Scale bars are 5 μm (C–*right panel*, D-F), 10 μm (G), 20 μm (A, C–*left panel*).

Figure 6. TOR localizes to endosomal structures in an ROP2-sensitive fashion.

A Co-localization analysis of GFP-TOR and RFP-RabC1 in *N. benthamiana* epidermal cells expressing FLAG-ROP2 (*upper* panels), FLAG-DN-ROP2 (*central panels*) and FLAG-CA-ROP2 (*bottom panels*).

B *35S:RFP-RabC1 Arabidopsis* line transiently expressing GFP-TOR and FLAG-CA-ROP2. *Left* GFP-TOR, *central* RFP-Rab1C, *right* merged.

C *35S:GFP-TOR Arabidopsis* line transiently expressing RFP-RabC1 and FLAG-CA-ROP2. *left* GFP-TOR, *central* RFP-RabC1, *right* merged.

D Microscopy images of cells stained with FM4-64 treated with brefeldin A (BFA) in the root elongation zone of *GFP-TOR* 7-dag seedlings. GFP-TOR and FM4-64 were detected in the core of the BFA compartment.

Data information: Scale bars are 5 μm (A–C) and 10 μm (D).

Figure 7. GTP-ROP2 mounts up abundance of uORF-mRNA in polysomes in AZD-8055 sensitive manner.

A Statistical analyses of ratio between polysomal and non-polysomal fractions obtained by sucrose gradient fractionation of extracts isolated from WT seedlings and *CA-ROP2* seedlings grown with or without 2-fold reduced concentration of AZD 8055 (0.5 μM).

B uORF (open rectangles) configuration within selected mRNAs.

C Ribosome sedimentation profiling from extracts prepared from WT (*left panel*) and *CA-ROP2* 7-dag seedlings treated (*right panel*) or not (*central panel*) with 0.5 μM AZD-8055. Positions of ribosomal subunits (60S/40S), monosomes (80S) and polysomes are indicated. 18S and 28S rRNA distribution was monitored by agarose gel electrophoresis.

D mRNA association with polyribosomes, 80S and 60S/40S ribosomes was monitored by quantitative PCR (q-PCR) in sucrose gradient fractions and presented as graph bars. The highest value of each selected polysome-bound mRNA among WT, *CA-ROP2* and *CA-ROP2+AZD* was set as 100%.

Data information: Statistical analysis is based on one-way ANOVA test. Data are presented as scatter plot with means, $p<0.01$; ns, non-significant (A). Error bars indicate +/-SD of three replicates (D).

Figure 8. CA-ROP2 hops on reinitiation after uORF translation in AZD-8055-sensitive manner.

A Phosphorylation of TOR at S2424 is augmented in CA-ROP2-overexpressing versus WT mesophyll protoplasts, and diminished in the presence of 0.5 μM AZD-8055. TOR and its phosphorylation levels were assayed by immunoblotting. The western blot density bands were quantified and WT (*left panel*) or CA-ROP2 (-AZD; *right panel*) values were set as 100%.

B GUS-containing reporters with either short, or uORF-containing (*ARF3* and *ARF5*) 5'-UTRs were used for mesophyll protoplasts transformation.

C WT and *CA-ROP2* seedlings growing without (*CA-ROP2*) or with 1 μM AZD-8055 (*CA-ROP2+AZD*) were used to prepare mesophyll protoplasts. Both GFP fluorescence and β-glucuronidase functional activity were analysed in the same 96-well microtiter plate. Functional levels of GUS expressed from pshort-GUS normalized to corresponding GFP levels were set at 100%. GUS-containing mRNA levels and integrity were analyzed by sqRT–PCR; GFP levels were also analysed by immunoblotting; LC—loading control. Results shown represent the means obtained in three independent experiments. Quantification of initiation (short leader) and reinitiation (ARF3/ARF5 5'-UTRs) efficiencies for *CA-ROP2* vs WT, and

CA-ROP2 vs *CA-ROP2+AZD-8055*.

D WT mesophyll protoplasts were transfected in addition to pmonoGFP/ pshort-GUS or pARF5-GUS by the vector expressing either myc-tagged ROP2, or CA-ROP2, or DN-ROP2 under the 35S promoter. GUS/GFP ratio related to the short or ARF5 5'-UTRs was taken as 100%. GUS mRNA levels and integrity were analyzed by sqRT–PCR; ROP2 variants—by immunoblotting using anti-myc ABs (bottom panels). Results shown represent the means obtained in three independent experiments. Quantification of reinitiation (ARF5 UTR) vs initiation (short leader) efficiencies without or with ROP2, CA-ROP2 or DN-ROP2 are shown on the left.

Data information: Quantification represents the means +/-SD obtained in three independent experiments.

Figure 9. Putative model of ROP2 function in TOR activation that signals translation reinitiation.

TOR was shown to be required for auxin responses, and these can converge through a small GTPase ROP2. Active ROP2 mediates TOR activation and thus controls the abundance of potent proteins in a post-transcriptional manner via selective translation mechanism—reinitiation. ROP2 recycling maintains TOR association with endosome-like structures (see Discussion for details).

Expanded View Figure legends

Figure EV1. Characterization of ROPs 2-6 from *Arabidopsis*.

A ROPs 1–6 transcription profiles were taken from the Genevestigator database (https://www.genevestigator.ethz.ch).

B Alignment of the C-terminal tail patterns from Arabidopsis ROPs 1–6 from Arabidopsis and human RAC1. Two motifs are indicated: basic lysine residues (motif I); a CxxL (x = aliphatic amino acid) geranylgeranylation motif (motif II). Two deletion variants used are indicated by solid lines.

Alignment done in agreement with Blossom 62 and Jonson amino-acid substitution matrixes (similar residues are printed in reverse type).

C GST pull-down assay: ROP2-, ROP2ΔII-, ROP2Δ(I+II)-tagged GST and GST alone were assayed for interaction with recombinant TOR. Fractions were stained by Coomassie blue. *Right panel* Results shown represent the means obtained in three independent experiments. Quantification of TOR binding to GST-fusion proteins (n=3). The value for TOR binding to GST-ROP2 was set as 1.

Figure EV2. TOR phosphorylation at S2424 is elevated in response to auxin and in plants with high endogenous auxin levels.

A WT seedlings were treated with either NAA-, or AZD-8055, or TOR was inactivated by AZD-8055 in seedlings treated with NAA during 8 h. TOR levels and its phosphorylation status were analyzed by immunoblot with anti-*At*TOR ABs (anti-TOR) and anti-(mTOR-S2448-P) ABs, respectively. Loading control was stained with Coomassie blue. *Right* Quantification of ratio between TOR-P and TOR (n=3). The value for TOR-P/TOR in WT was set as 1.

B Rosettes representative of WT, *yuc1D* and *cuf1D* plants.

C **A**nalysis of active TOR and ROPs-GTP levels in WT, yuc1D and *cuf1D* 7 dag seedlings.

Input: Total ROPs, TOR total and its phosphorylation levels were analyzed by western blot. GST-Ric1 and Loading control were stained with Coomassie blue. *Bottom* Quantification of ratio between TOR-P and TOR (n=3). The value for TOR-P/TOR in WT was set as 1. *Right*

panels Analysis of active ROPs by GST-Ric1 IP in seedling extracts. GST-Ric1 bound ROPs were detected using anti-ROP antibodies. Quantification of ratio between ROPs-GTP and GST-Ric1 (n=3). The value for ROPs-GTP/GST-Ric1 in WT was set as 1.
Data information: Results shown represent the means obtained in three independent experiments.

Figure EV3. Appearance of GFP-TOR as punctuate dots in response to NAA treatment correlates with an increase of active TOR in microsomes.

A Fluorescence micrographs showing *N. benthamiana* cells transiently expressing: *Upper panels left* GFP-BD-CVIL—plasma membrane (PM) marker, *central* RFP-ROP2, *right* merged. *Middle panels Left* GFP-BD-CVIL, *central* RFP-ROP2ΔII, *right* merged. *Bottom panels left* GFP-BD-CVIL, *central* RFP-ROP2Δ(I+II), *right* merged. PM marker consists of green fluorescent protein (GFP) fused to C-terminal polybasic domain (BD) and isoprenylation motif (CVIL).
B Imaging fluorescence assays showing root cells of *Arabidopsis* 7 dag *GFP* and GFP-*TOR* seedlings before and after treatment with 100 nM NAA.
C Intracellular disribution of TOR and active TOR in WT seedlings before (*left panel*) and after treatment by 100 nM NAA during 8 h *(right panel*). Western blot analysis of variuos fractions—the total homogenate (total), nuclear fraction pellet (P10), 30,000g pellet (P30), 100,000g pellet (P100), 100,000g supernatant (S100).
D *N. benthamiana* cells transiently coexpressing GFP-TOR, or RFP-Golgi, or both with either myc-DN-Sar1b or myc-DN-ROP2.
E Immunoblot analysis with anti-myc ABs of cells.
Data information: Scale bars are 5 µm (A, D); 10 µm (B).

Figure EV4. GFP-TOR specific co-localization with RFP-RabC1 that labels endosomes.

Imaging fluorescence assays showing *Nicotiana benthamiana* cells transiently co-expressing FLAG-CA-ROP2 with GFP-TOR (*left panels*), and intracellular markers (*central panels*) that specifically label early endosomes (RFP-RabC1), endosomes (RFP-RabE1d), autophagosomes (RFP-ATG8a), peroxisomes (mCherry-peroxi), mitochondria (mCherry mito), late endosomes (ARF-ARA7), Golgi (GmMan1-tdTomato), (*right*) merged.
Data information: Scale bars are 5 µm.

Figure EV5. Ribosome profiling of uORF-containing mRNA in WT *Arabidopsis* without or with TOR inhibitor.

A The level of heavy polysomes is reduced in WT *Arabidopsis* treated by AZD-8055 (AZD). Extracts prepared from 7-dag seedlings growing without (WT) and with 0.5 µM AZD-8055 on agar plates (WT+AZD) were subjected to velocity sedimentation through sucrose density gradients. Gradients were fractionated while scanning at 254 nm, and the resulting absorbance profiles are shown (WT and WT+AZD). Positions of ribosomal subunits (RS), monosomes (80S) and polysomes are indicated. rRNA distribution was monitored by agarose gel electrophoresis.

B AZD-8055 treatment down-regulates, albeit not significantly, the abundance of *bZIP11* and the already low polysomal levels of *ARF5* mRNA in WT *Arabidopsis*. Distribution of mRNAs—*Actin*, *GAPC2*, *bZIP11*, *ARF3* and *ARF5*—in fractions were analyzed by qRT-PCR. The highest value of each polysome-bound mRNA was set as 100%.

C TOR and TOR phosphorylation status was analyzed in polysomes prepared from WT, *CA-ROP2* seedlings and *CA-ROP2* line treated by AZD-8055. Three samples from polysomes and two from 80S and ribosomal subunits were taken to monitor TOR by immunoblotting with anti-TOR (*low panels*) and phospho-TOR with anti-(mTOR-S2448-P) (*central panels*). Data shown are representative of two independent blots.

D qRT-PCR of each mRNA in total extracts. The RNA value in WT extracts *left central panels* and *CA-ROP2 right panel* was set as 100%.

Data information: Error bars indicate +/-SD of three replicates (B, D).

Schepetilnikov et al_Fig. 1

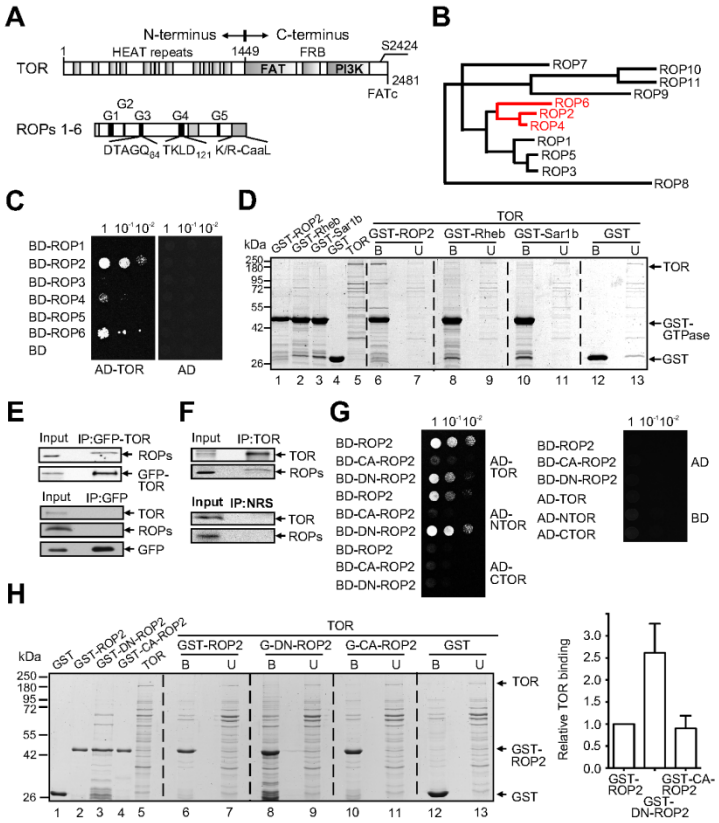

Schepetilnikov et al_Fig. 2

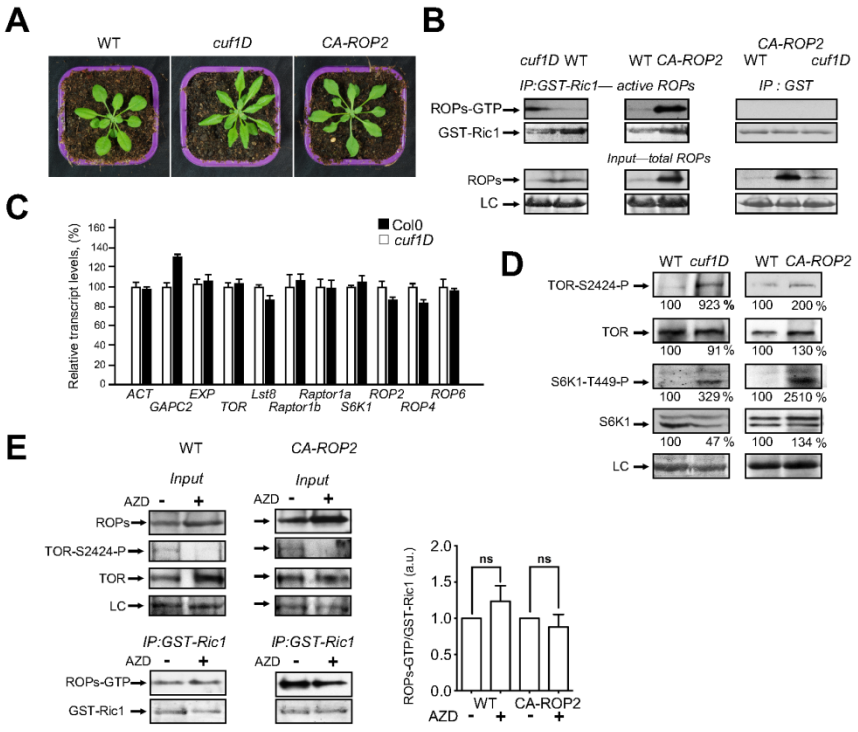

Schepetilnikov et al_Fig. 3

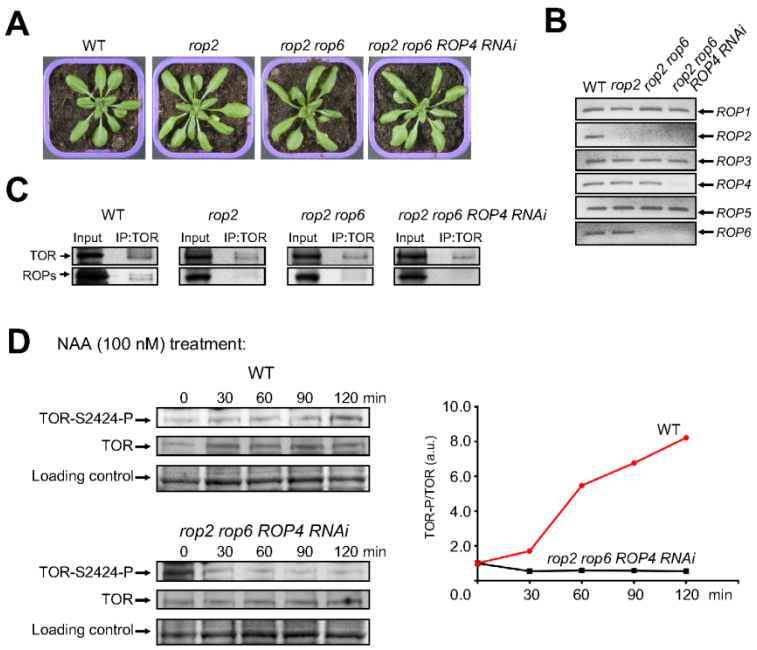

Schepetilnikov et al_Fig. 4

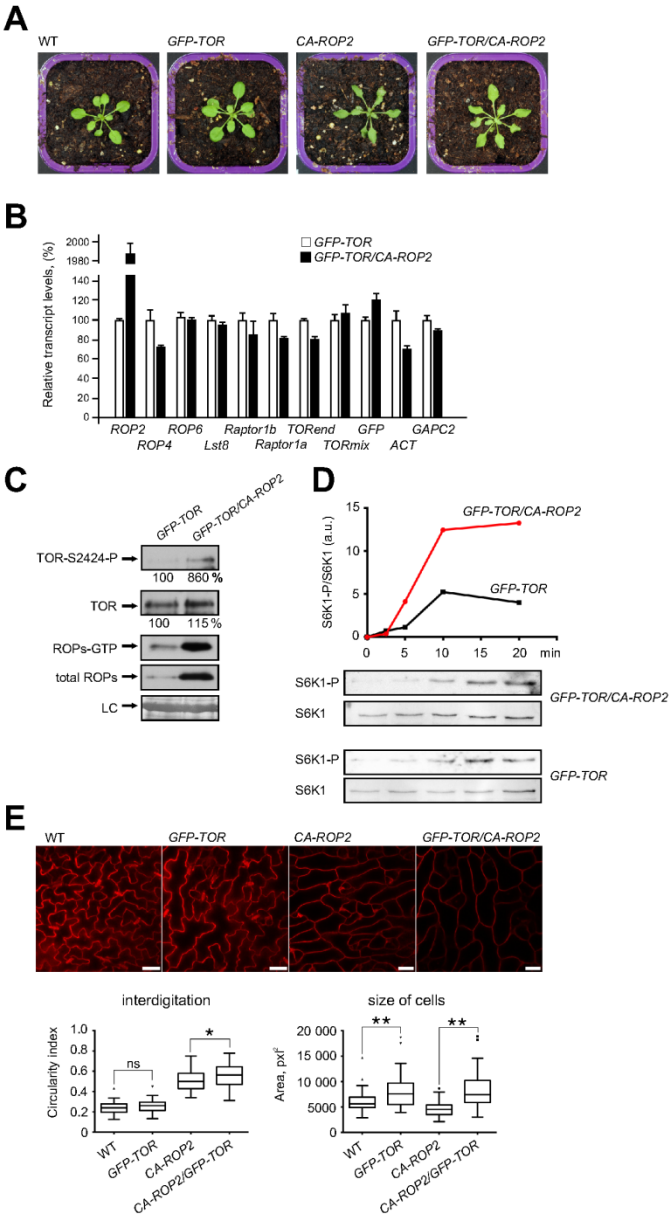

Schepetilnikov et al_Fig. 5

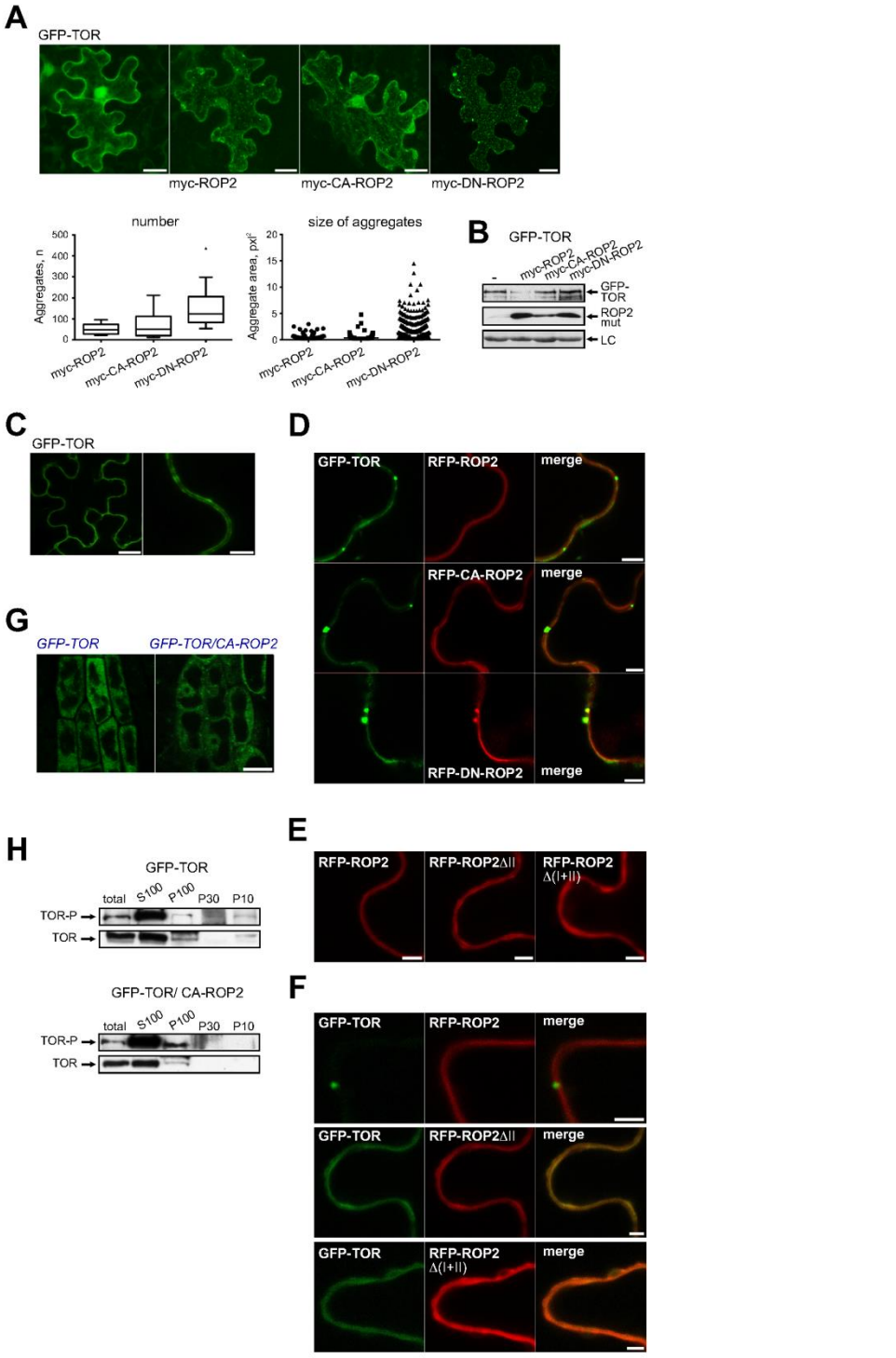

Schepetilnikov et al_Fig. 6

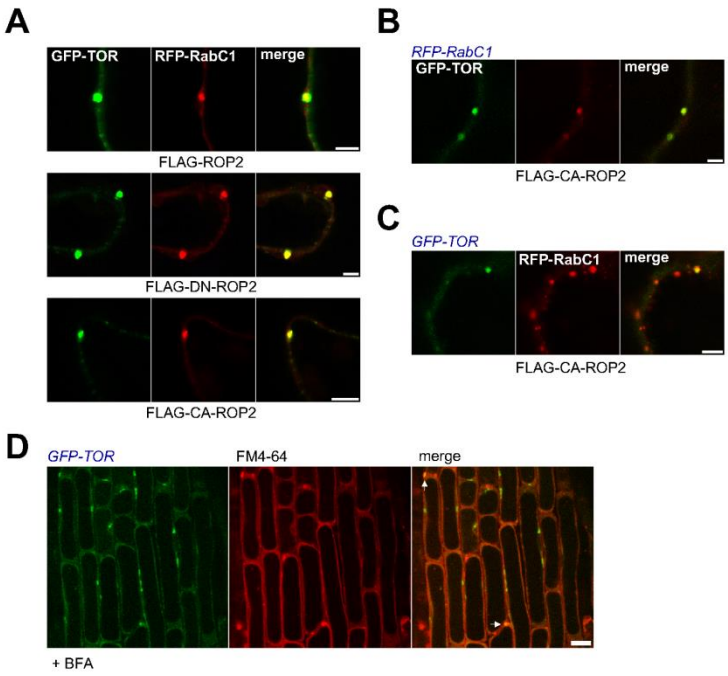

Schepetilnikov et al_Fig. 7

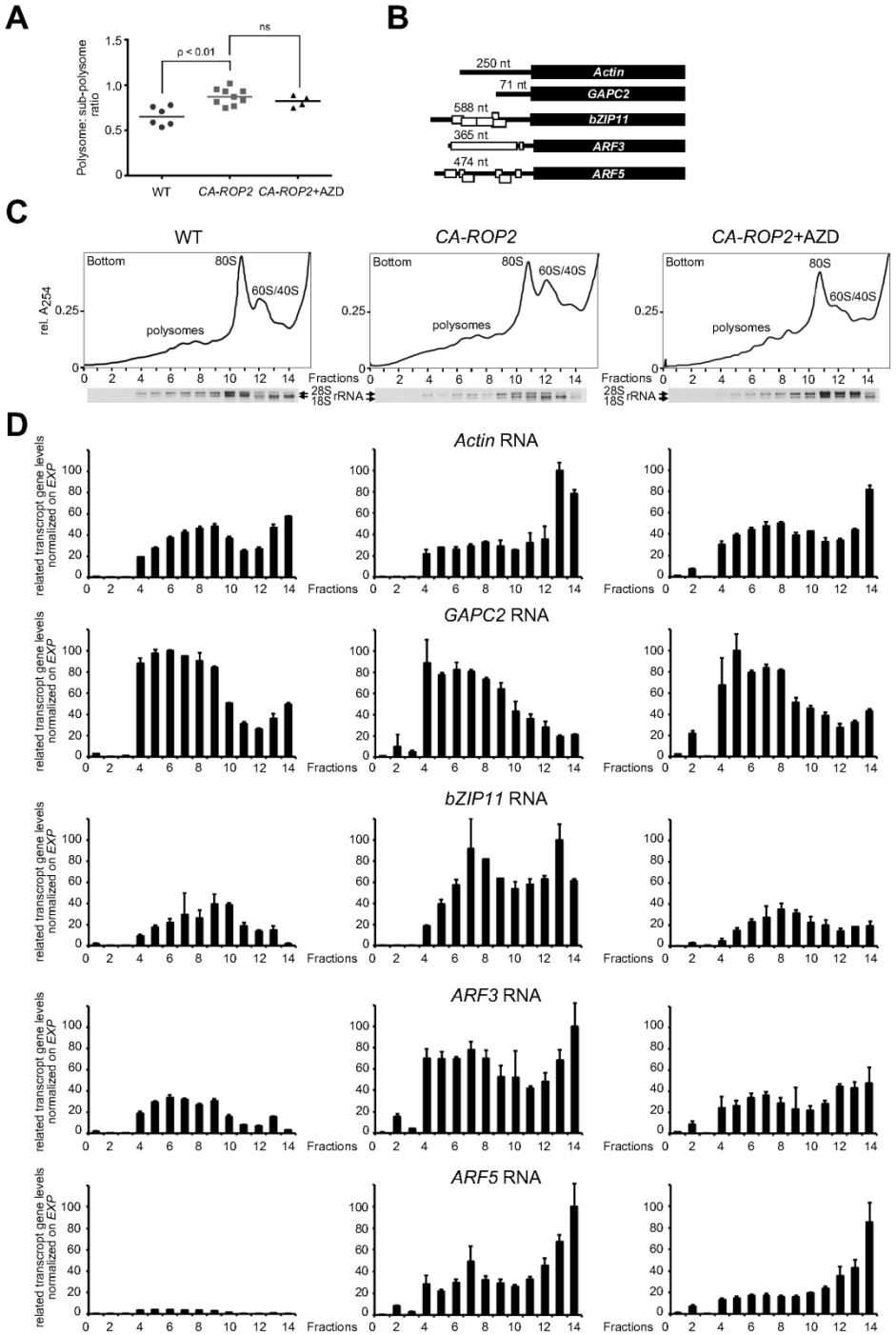

Schepetilnikov et al_Fig. 8

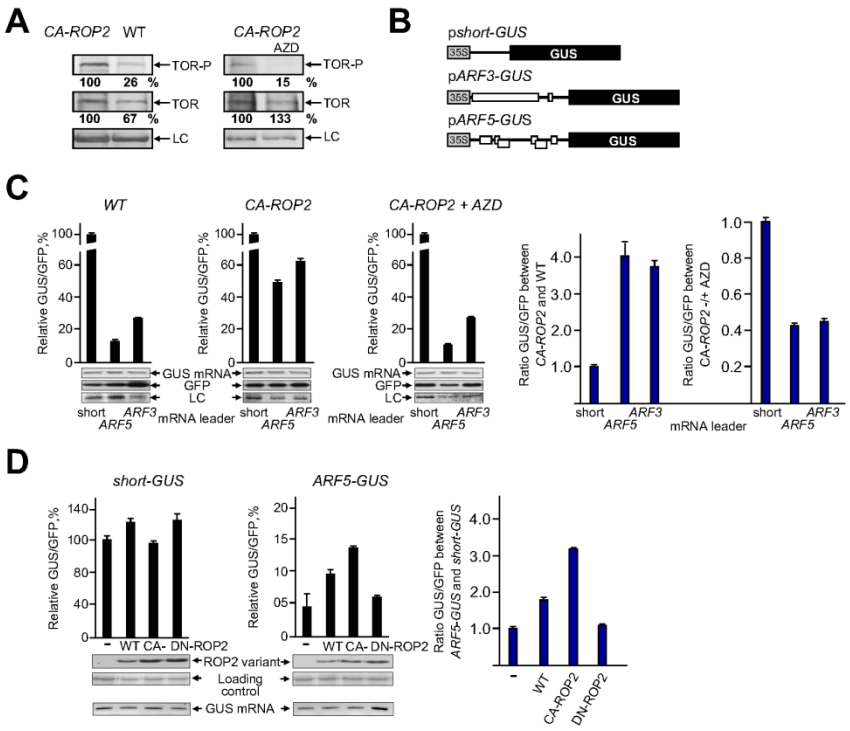

Schepetilnikov et al_Fig. 9

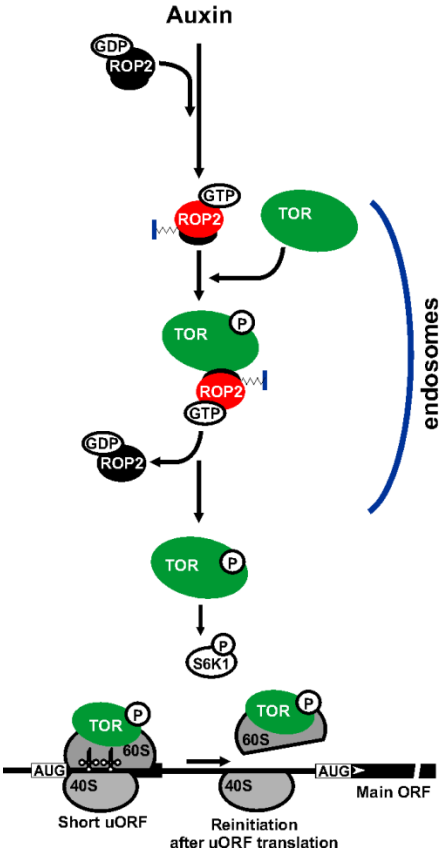

Schepetilnikov et al_Fig. EV1

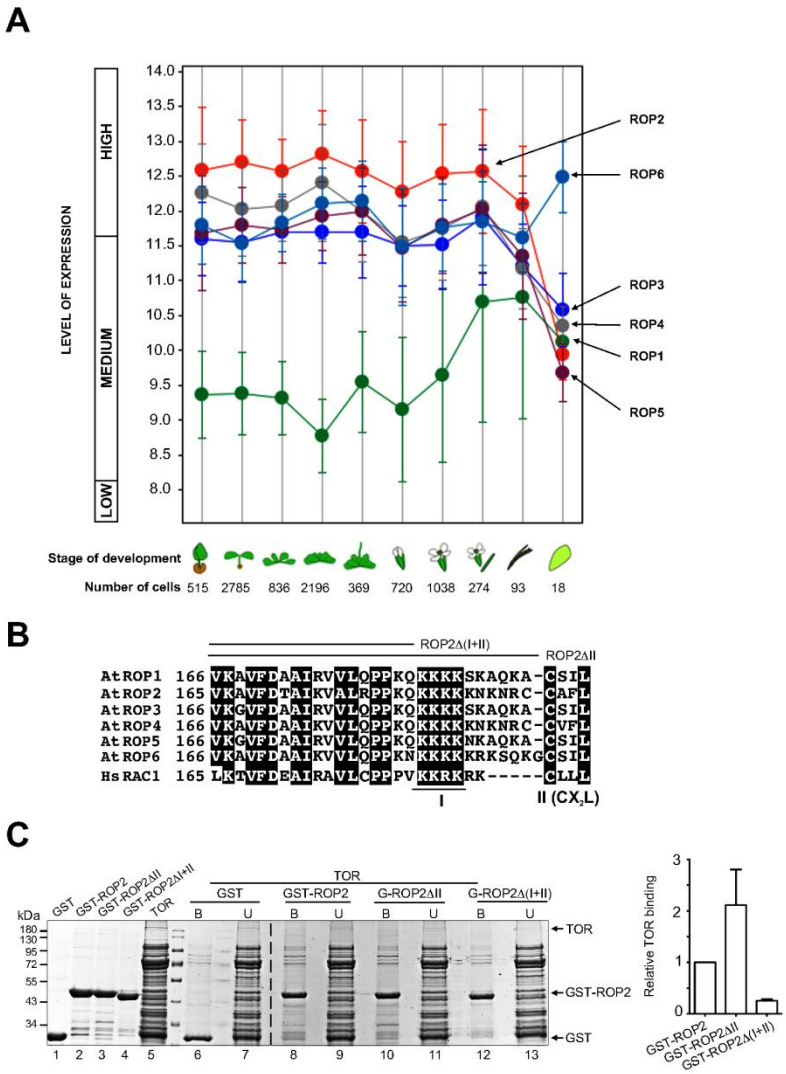

Schepetilnikov et al_Fig. EV2

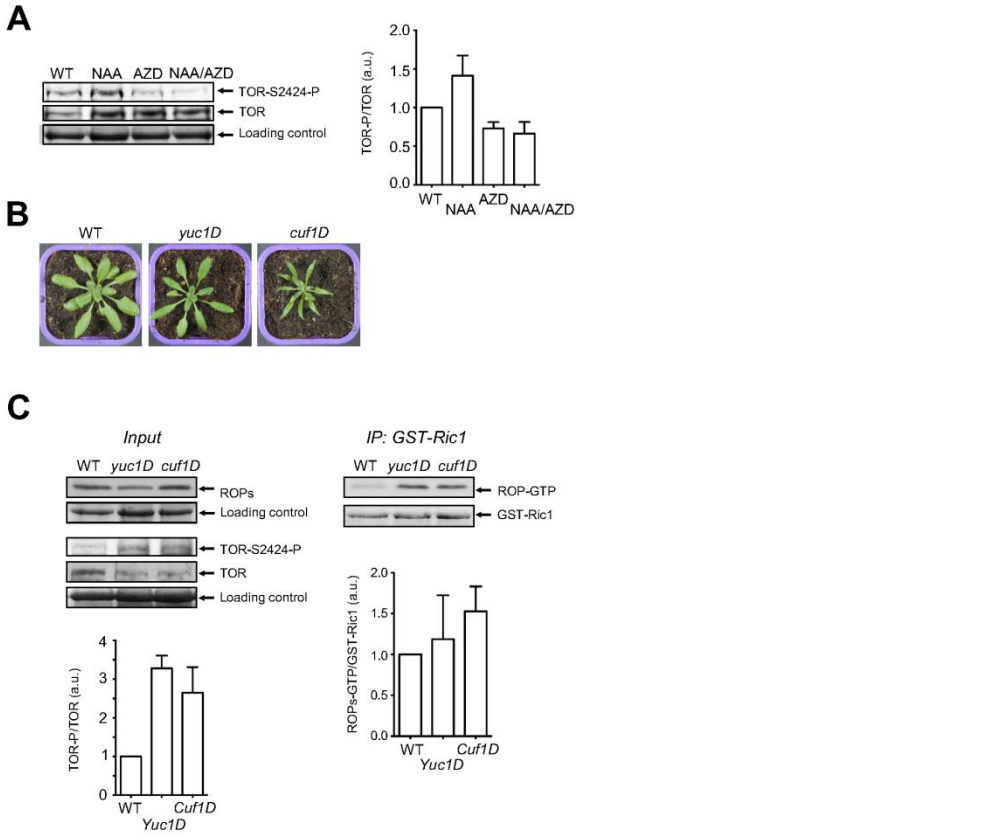

Schepetilnikov et al_Fig. EV3

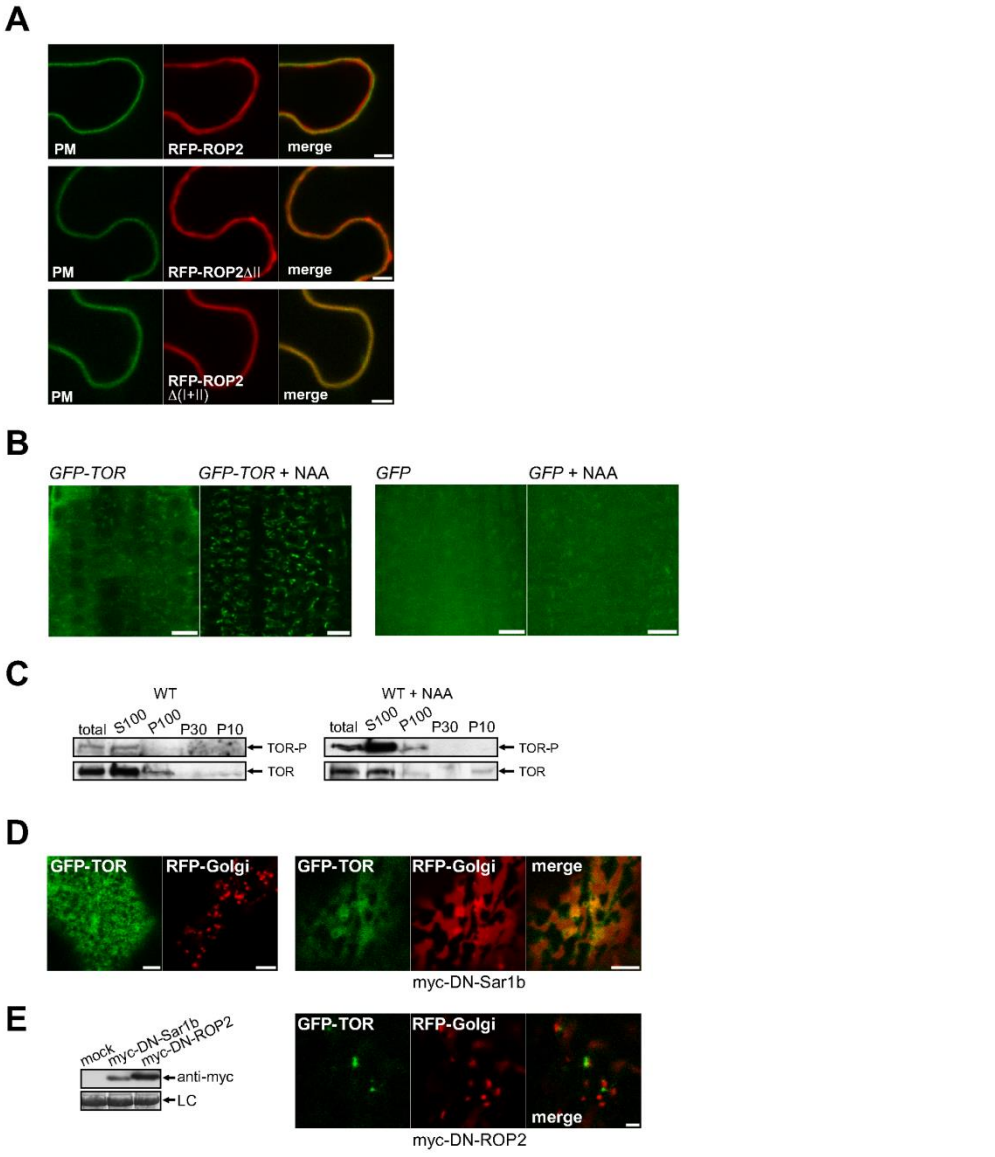

Schepetilnikov et al_Fig. EV4

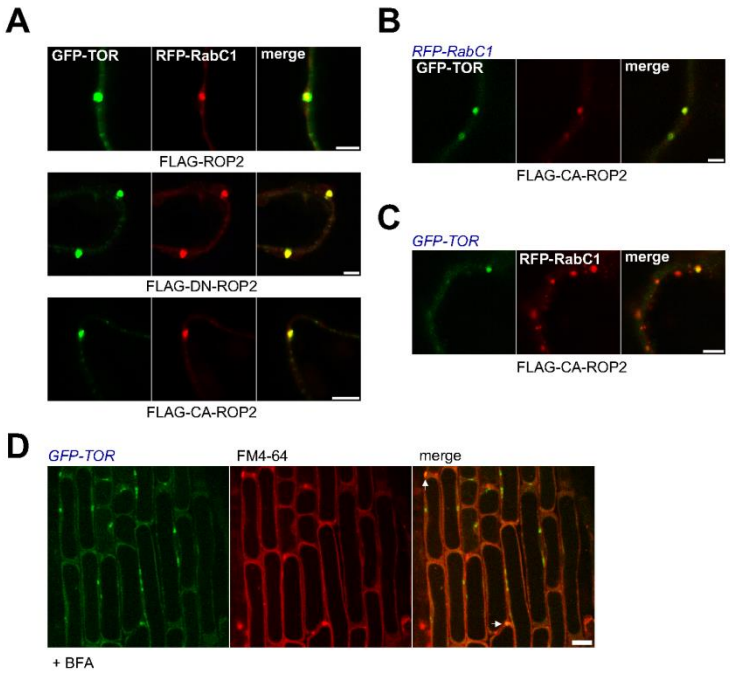

Schepetilnikov et al_Fig. EV5

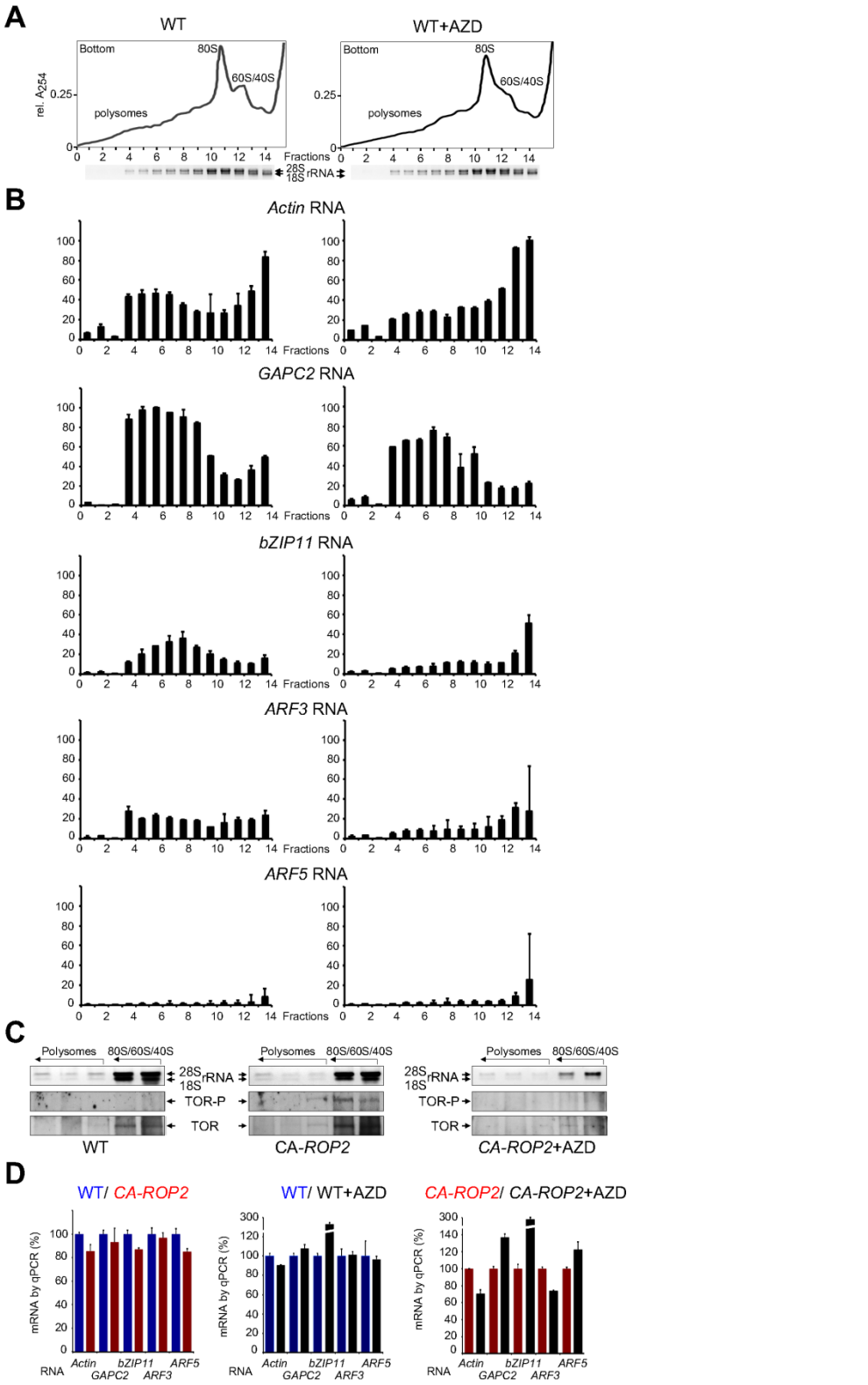

Appendix

GTPase ROP2 promotes translation reinitiation at upstream ORFs via activation of TOR

Mikhail Schepetilnikov[1], Joelle Makarian[1], Ola Srour[1], Angèle Geldreich[1], Zhenbiao Yang[2], Johana Chicher[3], Philippe Hammann[3] and Lyubov A. Ryabova[1]*

[1] Institut de Biologie Moléculaire des Plantes, Centre National de la Recherche Scientifique, UPR 2357, Université de Strasbourg, Strasbourg, France

[2] Center for Plant Cell Biology, Department of Botany and Plant Sciences, University of California, Riverside, CA, USA

[3] Platforme Proteómique Strasbourg-Esplanade, Centre National de la Recherche Scientifique, FRC 1589, Université de Strasbourg, Strasbourg, France

Table of contents

Methods

Plant materials and growth conditions

RFP-RabC1 (N781669) and T-DNA insertion rop2 (SALK_055328C) seeds were obtained from the Nottingham Arabidopsis Stock Centre (NASC). *cuf1D* and *yuc1D* lines, gain-of-function mutants characterized by a high level of auxin biosynthesis, were described in Cui *et al* (2013) and Zhao *et al* (2001) respectively. The double rop2rop6 and triple rop2rop6ROP4 RNAi mutant lines were described in Ren *et al* (2016). The GTP-bound constitutively active ROP2 *CA-ROP2* line was described in Li *et al* (2001). The transgenic line expressing GFP under control of the 35S promoter (35S:GFP) was kindly provided by Patrice Dunoyer (IBMP, Strasbourg, France).

To generate the *GFP-TOR* transgenic line expressing TOR kinase fused to GFP under control of the 35S promoter, stable transformation of flowering *Arabidopsis* plants was performed with *Agrobacterium tumefaciens* strain GV3101 by the floral dip method (Clough & Bent, 1998). The *Arabidopsis* homozygous *GFP-TOR/CA-ROP2* transgenic line was generated by crossing *GFP-TOR* and *CA-ROP2* lines. Transgenic lines were selected for the appropriate resistance, and the presence of the corresponding transgene was verified.

Arabidopsis lines were in Columbia (Col-0) background. Seeds were sterilized in 70% Ethanol and germinated on solid Murashige-Skoog (MS) agar plates for 3 days at +4˚C in the dark. The 7 dag *Arabidopsis* seedlings were grown under long day conditions (16h light/ 8h darkness, 22°C/ 16˚C) with illumination Neon Biolux on MS plates supplied or not with 1 μM (Fig 2, 6, 8 and EV2) or 0.5 μM (Fig 7 and EV5) of AZD-8055 (Chemdea).

Interdigitation analysis

The second true leaves from 21-day-old plants were used for interdigitation analysis of abaxial epidermal cells – pavement cells (PCs) – of the middle part of the leaf blade. Cell outlines were visualized by 30 min staining of cell walls with propidium iodide, and imaged using confocal laser scanning microscopy. Cell area and circularity index were measured by ImageJ. The circularity of a pavement cell is determined by calculating 4π area/perimeter^2. The measurements were conducted consistently on PCs at the same developmental stage. Data were obtained from at least three independent experiments of 30 cells each. Unpaired t-test was performed for all comparisons to determine the *p*-values.

Polyribosome analysis

For polyribosome isolation we used 7 dag *Arabidopsis* wild-type Col-0 WT and *CA-ROP2* seedlings grown on MS agar plates supplemented (or not) with 2-fold reduced (0.5 µM) concentration of AZD 8055. Drug concentration was tested to prevent any overall cytotoxic effect on mRNA polysomal loading during prolonged drug treatment. After harvesting, equal amounts of fresh material were frozen and ground in liquid nitrogen. For cytoplasmic extracts, 500 mg of powder was resuspended in ice-cold extraction buffer [200 mM Tris-HCl, pH 9, 200 mM KCl, 35 mM $MgCl_2$, 25 mM EGTA, 15.4 units/mL heparin, 18 µM cycloheximide, 0.5% NP-40, 1 mM DTT, PHOS-Stop (Roche) and protease inhibitors cocktail (Roche)]. Cell debris was removed by centrifugation. Supernatants were used to control total levels of endogenous mRNA by quantitative RT-PCR (qRT-PCR) and aliquots were loaded onto 13 mL 10% to 50% (w/w) sucrose gradients in 40 mM Tris-HCl pH 8.5, 5 mM EGTA, 20 mM KCl, 10 mM $MgCl_2$ and centrifuged at 39,000 rpm in a Beckman SW41 rotor at 4°C for 2h. Polysomal profiling was done in three independent biological replicates, each including Col-0 WT and *CA-ROP2* seedlings treated (or not) with AZD 8055. To improve translational fidelity and reproducibility, we grow seedlings on the same day under identical conditions. Samples for polysomal profiling were collected immediately the same day. Polyribosomal extract preparation, sucrose gradient sedimentation, RNA isolation and qRT-PCR analysis were performed in parallel for both wild-type Col-0 WT and *CA-ROP2* samples treated (or not) with AZD8055 within each biological replicate.

To monitor mRNA loading into polysomes, qRT-PCR analysis of fractions of all gradients was performed in the same 384-well plate. mRNAs were monitored in sub/ polysomal fractions, and transcript levels for each mRNA were normalized to *EXP* and ribosomal RNA. For each gene, levels of mRNA in each fraction were calculated relative to the fraction with the maximum level of mRNA, which was set as 100. For western blots, polyribosomal fractions were collected, precipitated with 2 volumes of absolute ethanol at 4°C, followed by resuspension of the pellet in hot Laemmli buffer for 5 minutes at 95˚C.

Quantitative real-time PCR analyses

Total RNA was extracted using Trizol (Invitrogen). RNA samples were reverse transcribed into cDNA using SuperScript III reverse transcriptase (Invitrogen) with oligo-$(dT)_{18}$ primer (Fermentas). cDNA was quantified with gene-specific primers using a SYBR Green qPCR kit

(ROCHE) and SYBR Green I Master Light Cycler 480 (Roche). The level of *ROP2* (At1g20090), *ROP4* (At1g75840), *ROP6* (At1g10840), *Lst8* (At3g18140), *Raptor1a* (At5g01770), *Raptor1b* (At3g08850), *S6K1* (At3g08730), *GFP*, *TORend*, *TORmix*, *ARF*3 (At2G33860), *ARF*5 (At1g19850), *bZIP*11 (At4G34590), *ACTIN* (At3g18780) and *GAPC2* (At1g13440) mRNAs was monitored by pairs of gene-specific primers. Transcript levels were normalized to that of *EXP* (At4g26410). For qPCR analysis of *GFP-TOR* and *GFP-TOR/CA-ROP2* transgenic lines, we used specific pair of primers for endogenous TOR (TORend) and GFP-TOR transgene mRNA transcripts (see Appendix Fig S3). The TORmix probe represents set of primers designed so that two oligos hybridize to one exon sequence of *TOR* gene, which permits accumulation of both *TOR* and *GFP-TOR* mRNAs to be detected. The TORend set of oligos hybridizes to the 3`-UTR of endogenous *TOR* mRNA, thus allowing qPCR amplification of only endogenous TOR. Finally, the GFP probe was designed for the *GFP* (green fluorescent protein) gene, and permits detection of the *GFP-TOR* transcript.

The gene-specific primers used were:

ACTIN (At3g18780)	fwd: 5`-gcaccctgttcttcttaccg-3` and rev: 5`-aaccctcgtagattggcaca-3`
GAPC2 (At1g13440)	fwd: 5`-agctgcaacatacgacgaaa-3` and rev: 5`-cccttcattttgccttcaga-3`
EXP (At4g26410)	fwd: 5`-gagctgaagtggcttcaatgac-3` and rev: 5`-ggtccgacatacccatgatcc-3`
*bZIP*11 (At4G34590)	fwd: 5`-ctgcaaggagatcaagaatg-3` and rev: 5`-ggttaggtagtgttgcgttg-3`
*ARF*3 (At2G33860)	fwd: 5`-ccatatcgacccatagcgttttcag-3` and rev: 5`-cccaatgcaaaagggatagtcaaca-3`
*ARF*5 (At1g19850)	fwd: 5`-ggtcagtccatgggatatcgaaaca-3` and rev: 5`-ttcgcggaatcaggaacacgta-3`
ROP2 (At1g20090)	fwd: 5`-gaatgtagttcaaagacacagcaga-3` and rev: 5`-tggctgaagcaccactttta-3`
ROP4 (At1g75840)	fwd: 5`-atcctggtgcagtgcctatt-3` and rev: 5`-tgctttcacattctgctgagtc-3`
ROP6 (At1g10840)	fwd: 5`-ctcgttggaacaaagcttga-3` and rev: 5`-ttcttcaccctgagcggtag-3`
Lst8 (At3g18140)	fwd: 5`-ggatggagaatttcttgtaacagc-3` and rev: 5`-tgatgaccttggtacactttcac-3`
Raptor1a (At5g01770)	fwd: 5`-gatgagaatgaacggattaggg-3` and rev: 5`-agcagagagtcatcaagttcattg-3`
Raptor1b (At3g08850)	fwd: 5`-ttacagcactttctgcttctcaa-3` and rev: 5`-ctttctgatgaggccgagtc-3`
S6K1 (At3g08730)	fwd: 5`-ctcagccatcccctctga-3` and rev: 5`-ttgttgtttcccgattttaagg-3`
TORend	fwd: 5`-gaagatgaagatcccgctga-3` and rev: 5`-gcatctccaagcatatttacagc-3`
TORmix	fwd: 5`-tcacgacattggatttggaat-3` and rev: 5`-aactgctagctccaagtcacg-3`
GFP	fwd: 5`-gaagcgcgatcacatggt-3` and rev: 5`-ccatgccgagagtgatcc-3`

Semi-quantitative real-time PCR analyses

For sqRT-PCR analysis, total RNA from protoplasts was extracted using Trizol. RNA samples were reverse transcribed into cDNA using SuperScript III reverse transcriptase (Invitrogen) with oligo-$(dT)_{18}$ primer (Fermentas). sqRT-PCR was performed with a pair of primers specific for the full-length GUS reporter gene. PCR conditions were as follows: 2 min, 98°C (first cycle); 30 s, 98°C; 30 s, 56°C; 3 min, 72°C (20 cycles).

For characterization of rop2, rop2rop6 and rop2rop6ROP4 RNAi mutant lines, sqRT-PCR was performed with pairs of specific primers to full-length ROP1-6 reporter genes. PCR conditions were as follows: 2 min, 98°C (first cycle); 30 s, 98°C; 30 s, 55°C; 30 s, 72°C (25 cycles). The PCR products were separated on a 1.2% agarose gel and visualized by ethidium bromide staining.

The gene-specific primers used were:

ROP1 (At3g51300)	fwd: 5`-tatacatatgagcgcttcgaggttcgt-3` and rev: 5`-tatagaattctcatagaatggagcatgccttc-3`
ROP2 (At1g20090)	fwd: 5`-tataccatggcgtcaaggtttataaag-3` and rev: 5`-tataggatcctcacaagaacgcgcaacgg-3`
ROP3 (At2g17800)	fwd: 5`-tatacatatgagcgcttcgaggttcat-3` and rev: 5`-tatagaattcttacaaaatggagcaggctttt-3`
ROP4 (At1g75840)	fwd: 5`-tatacatatgagtgcttcgaggtttat-3` and rev: 5`-tatagaattctcacaagaacacgcagcggttc-3`
ROP5 (At4g35950)	fwd: 5`-tatacatatgagcgcatcaaggttcat-3` and rev: 5`-tatagaattcttacaagatggagcaggccttt-3`
ROP6 (At1g10840)	fwd: 5`-tatacatatgagtgcttcaaggtttatc-3` and rev: 5`-tatagaattctcagagtatagaacaacctt-3`

Transient expression and imaging analysis

For transient expression assay in *N. benthamiana*, *Agrobacterium* strain GV3101 with corresponding pBin-based constructs was grown in liquid LB medium with appropriate antibiotics at +28˚C with shaking (220 rpm) for 18h. Bacteria were collected by centrifugation at 3500g for 15 minutes, then resuspended in MES buffer (10 mM $MgCl_2$, 10 mM 2-*N*-morpholino-ethanesulfonic acid (MES) pH 5.6 and 150 µM Acetosyringone). After 2-3h of incubation, OD600 was adjusted to 0.5-1.0 and the suspension was infiltrated into the lower leaf surfaces of young (six- to seven-leaf-stage) *N. benthamiana* plants with a needleless syringe. After 18h of expression, samples were collected for protein extraction and microscopic observation. Fluorescence was detected using a confocal microscope Zeiss

LSM780 (Jena, Germany). Confocal images processing was processed with ImageJ software and the FigureJ plugin.

The plasma membrane marker GFP-BD-CVIL, which consists of green fluorescent protein (GFP) fused to the C-terminal polybasic domain (BD) and isoprenylation motif (CVIL), is described in Gerber *et al* (2009). Intracellular compartment markers that specifically label peroxisomes (mCherry-peroxi), mitochondria (mCherry-mito) and Golgi (GmMan1-tdTomato) are described in Nelson *et al.* (2007). PCR products corresponding to *Arabidopsis ROP2* (At1g20090), *Sar1b* (At1g56330), *RabC1* (At1g20090), *RabE1d* (At5g03520), *Ara7* (At4g19640), *ATG8a* (At4G21980) and human *Rheb* (NM_005614) were amplified from cDNA with pairs of gene-specific primers compatible with GateWay Cloning technology (Invitrogen), cloned into pDONR-Zeo vector (Invitrogen), and then subcloned into pB7WGR2 binary vector (Karimi *et al*, 2002) as in-frame fusion with RFP tag to obtain pB7-WG-RFP-ROP2, -Sar1b, -RabC1, -RabE1d, -Ara7, -ATG8a and –Rheb. The CA- and DN-mutants of ROP2, Rheb and Sar1b were generated using site-directed PCR mutagenesis as follows: by substitution of Gln at position 64 to Asn (CA-Q64N) and Asp at position 121 to Ala (DN-D121A) in ROP2 ORF; by substitution of Gln at position 64 to Asn (CA-Q64N) and Asp at position 60 to Ile (DN-D60I) in Rheb ORF; and by substitution of His at position 74 to Leu (CA-H74L) and Thr at position 51 to Ala (DN-T51A) in Sar1b ORF, respectively. CA-, DN- and ROP2 were subcloned using GateWay Cloning technology (Invitrogen) into pEarleyGate-202 (ABRC stock CD3-688) and pEarleyGate-203 (ABRC stock CD3-689) binary vectors as in-frame fusions with FLAG- and Myc-tags, respectively, to obtain pEG-202-FLAG and pEG-203-Myc-CA, -DN and -ROP2.

PCR products corresponding to ROP2 C-terminal deletions of motif II and (I+II) were amplified from ROP2 cDNA with pairs of gene-specific primers compatible with GateWay Cloning technology (Invitrogen), cloned into pDONR-Zeo vector (Invitrogen), and then subcloned into pB7WGR2 binary vector (Karimi et al, 2002) as in-frame fusions with the RFP tag to obtain pB7-WG-RFP-ROP2ΔII and -ROP2Δ(I+II).

For microscopic observation of GFP-TOR and GFP, intracellular localization in root cells upon NAA treatment (Fig EV3), 7-dag seedlings of *GFP-TOR* and *GFP* transgenic lines were treated in fresh liquid MS medium supplemented or not with 100 nM NAA for 8 hours.

Arabidopsis protoplasts and plasmid constructions

Arabidopsis mesophyll protoplasts from WT and *CA-R0P2* 2-week-old transgenic seedlings were transfected with plasmid DNA by the PEG method described in Yoo *et al,* (2007). After overnight incubation at 26 °C in WI buffer (4 mM MES pH 5.7, 0.5 M Mannitol, 20 mM KCl), with or without 1 µM AZD-5088, transfected protoplasts were harvested by centrifugation, and total protein extracts were prepared in GUS extraction buffer (50 mM NaH_2PO_4 pH 7.0, 10 mM EDTA, 0.1% NP-40). Aliquots were taken immediately for GFP (green fluorescent protein) fluorescent assay, followed by GUS reporter fluorimetric assay as described in Pooggin *et al,* (2000). GUS activity was measured by monitoring conversion of the β-glucuronidase substrate 4-methylumbelliferyl β-D-glucuronide (MUG) into 4-Methylumbelliferone (MU). Fluorescence was measured on a FLUO-star plate reader (BMG Labtechnologies Inc., Durham, NC) at 460nm when excited at 355nm. GUS mRNA levels were monitored by sqRT-PCR.

The constructs pS6K1, pARF3-GUS, pARF5-GUS, pmonoGUS and pmonoGFP were described previously (Schepetilnikov *et al*, 2011; 2013). PCR products corresponding to *TOR* were amplified from TOR cDNA (At1g50030) with pairs of specific primers and cloned into pmonoGUS to replace GUS and obtain construct pTOR. pTOR-S2424A and pTOR-S2424D were generated by substitution of Ser at position 2424 to Ala (S2424A) and to Asp (S2424D), respectively, in TOR ORF by site-directed PCR mutagenesis. CA-, DN- and ROP2 were subcloned using GateWay Cloning technology (Invitrogen) into the pUGW18 (Nakagawa *et al*, 2007) vector, which is suitable for transient expression in protoplasts as an in-frame fusion with 4xMyc-tag to obtain pUGW-4xMyc-CA, -DN and -ROP2 respectively.

Yeast two-hybrid assay and plasmid construction

To generate pGBK-ROP1-6, corresponding PCR products were amplified from ROP1 (At3g51300), ROP2 (At1g20090), ROP3 (At2g17800), ROP4 (At1g75840), ROP5 (At4g35950) and ROP6 (At1g10840) cDNA, respectively, with pairs of specific primers, and cloned into the pGBKT7 (Clontech) as an in-frame fusion with the BD-domain. pGBKT7-CA-ROP2 and pGBKT7-DN-ROP2 were generated by substitution of Gln at positions 64 to Asn (Q64N) and to Asp at positions 121 to Ala (D121A), respectively, in ROP2 ORF by site-directed PCR mutagenesis. PCR products corresponding to NTOR, CTOR, and full-length TOR were amplified from *At*TOR cDNA (At1G50030) with pairs of specific primers, respectively, and cloned into the pGADT7 (Clontech) as in-frame fusions with the AD-domain to obtain pGAD -NTOR, pGAD -CTOR and pGAD-TOR.

Subcellular fractionation

Arabidopsis seedlings were harvested after 7 days growth on MS agar plates, and 3.0 g of tissue was homogenized by gentle grinding on ice with 3 mL of isolation buffer [50 mM HEPES pH 7.5, 50 mM KCl, 5 mM EDTA pH 8.0, 10% Sucrose (w/v), 1 mM DTT, PHOS-Stop (Roche) and protease inhibitor cocktail (Roche)]; 3 mL of homogenates were centrifuged at 10,000 *g* for 30 min at 4 °C to obtain the nuclear P10 fraction. The supernatant was recentrifuged at 30,000 *g* for 60 min at 4 °C to obtain the ER-enriched P30 fraction. The supernatant was further fractionated by centrifugation at 100,000 *g* for 60 min into supernatant (S100) and pellet (microsomal P100) fractions. P10, P30, and P100 pellets were resuspended in 1x Laemmli buffer to volumes that were 10x times those before centrifugation. Fractionated and unfractionated samples of the same volume were analyzed by western blot using GFP, TOR and phospho-TOR specific antibodies.

Immunoprecipitation and kinase assay

For immunoprecipitation, *in vitro* kinase assay, and western blot detection experiments, *Arabidopsis* seedlings were cultured on MS agar for 7 days after germination (7 dag), harvested and ground in liquid nitrogen followed by homogenization in fresh ice-cold extraction buffer [50 mM Tris pH 7.5, 150 mM KCl, 0.1% NP-40, GM-132 (Sigma), Complete protease inhibitors cocktail (Roche)]. For immunoprecipitation of TOR complexes, plant samples were homogenized in extraction buffer and insoluble material was removed by centrifugation (two repetitions of 15 min, 12000g, 4°C). Lysate was pre-cleaned by incubation with protein A-agarose beads (Roche) at 4°C for 10 min. The supernatant was then incubated with either Normal rabbit serum (NRS), or anti-*At*TOR serum prebound to A-agarose beads, or with GFP-Trap magnetic beads (Chromotek) for 1h at 4°C. Immunoprecipitates were washed three times with the extraction buffer supplemented with 300 mM KCl, eluted from the beads with 1x Laemmli buffer for 5 min at 95°C, and analyzed by western blot.

For *in vitro* kinase assay, GFP-TOR immunoprecipitates were washed 3 times with extraction buffer followed by a brief wash with kinase buffer-1 (50 mM HEPES pH 7.5, 50 mM KCl, 5 mM $MgCl_2$), and finally resuspended in kinase buffer-2 (50 mM HEPES pH 7.5, 50 mM KCl, 5 mM $MgCl_2$, 0.5 mM rATP). Kinase reaction was carried out at 30°C in kinase buffer-2, with small aliquots of immunoprecipitated GFP-TOR complexes in the presence of

100 ng rec S6K1 purified as described in **Protein expression, purification and GST pull-down assay.** Kinase reactions were stopped after 0, 5, 10, 15, and 20 minutes of incubation at 30˚C, and incorporation of phosphate was analyzed by SDS-PAGE and immunoblotting with anti-mS6K1-P-T389 antibodies (Cell Signaling). Quantification of phospho-S6K1 bands was performed using ImageJ software. The graph in Fig 3D shows kinetics of S6K1 phosphorylation by TOR kinase: the *y*-axis represents fold changes in phospho-S6K1 band density normalized to the total S6K1 amount (a.u. arbitrary units) and the *x*-axis – time of kinase reaction in min.

Western blot assay

Rabbit anti-*At*TOR polyclonal antibodies were described in Schepetilnikov *et al.* (2011). Rabbit polyclonal anti-mS6K1 antibodies were from Santa-Cruz Biotechnology. Phospho antibodies—anti-mTOR-P-S2448 (#2971) and anti-mS6K1-P-T389 (#9205)—directed against the indicated phosphorylated form of either TOR or S6K1 described in Schepetilnikov *et al.* (2011) were from Cell Signaling. For detection of ROP GTPases in *Arabidopsis* plant total extracts, we used rabbit polyclonal anti-AtRac3 (Sigma), and for detection in *N. benthamiana* of transiently expressed of ROP GTPases fused to myc-tag, we used anti-c-Myc (Roche). Anti-GFP (A11122) antibodies were from Molecular Probes, Life Technologies. For western blot detection we used HRP-conjugated secondary anti-rabbit or anti-goat IgG antibodies (Sigma) and ECL kit (Roche).

Protein expression, purification and GST pull-down assay

PCR products corresponding to *Arabidopsis Ric1* (At2g33460), *ROP2* (At1g20090), *Sar1b* (At1g56330) and human *Rheb* (NM_005614) were amplified from corresponding cDNAs with pairs of gene-specific primers and cloned into pGEX-6P1 (Pharmacia Biotech) as in-frame fusions with the GST-domain to obtain pGEX-Ric1, pGEX-ROP2, pGEX-Sar1b and pGEX-Rheb respectively. PCR products corresponding to ROP2 C-terminal deletions of motif II and (I+II) were amplified from corresponding ROP2 cDNAs with pairs of gene-specific primers, and cloned into pGEX-6P1 (Pharmacia Biotech) as in-frame fusions with the GST-domain to obtain pGEX-ROP2ΔII and pGEX-ROP2Δ(I+II). pGEX-CA-ROP2 and pGEX-DN-ROP2 were generated by substitution of Gln at position 64 to Asn (Q64N) and to Asp at position 121 to Ala (D121A), respectively, in ROP2 ORF by site-directed PCR mutagenesis.

PCR products corresponding to S6K1 (At3g08730) and ROP2 (At1g20090) were amplified from cDNA with pairs of gene-specific primers compatible with GateWay Cloning technology (Invitrogen), cloned into pDONR-Zeo vector (Invitrogen), and then subcloned into pHGWA vector (kindly provided by Dr D. Busso, IGBMC, Strasbourg, France) as an in-frame fusion with 6xHis tag to obtain pHGWA-S6K1 and pHGWA-ROP2 constructs, respectively.

The *E. coli* codon-optimized TOR construct was designed by A. Komar (DAPCEL Inc) and synthesized (GenScript**)**. Codon-optimized TOR construct encoded for the full-length TOR protein with the C-terminal 6xHis tag separated by the Gly-linker sequence was cloned into the pET3a vector (Novagen) to obtain pET3a-TOR. Proteins were expressed in BL21(DE3) pLysS (Stratagene) and purified according to manufacturer's protocol.

The rec S6K1-6xHis protein was expressed in BL21(DE3) pLysS (Stratagene) and affinity purified on a 1mL His-Trap column according to manufacturer's protocol. In order to obtain high purity of rec S6K1 for use as a substrate, and to prevent inhibition of the kinase reaction, the final step of S6K1-6xHis purification included an exchange solution to kinase buffer and imidazole elimination using Zeba 5mL desalting columns.

For the ROP2 activity test *in vitro*, binding of ROP2, charged or not with GDP or GMP-PNP (GTP non-hydrolyzed analog; Sigma), to TOR (Fig S1), or GST-Ric1 (Fig S2), or GST alone, respectively was carried out in buffer A-150 (50 mM Tris and pH 7.5, 150 mM KCl) supplemented with 5 mM $MgCl_2$ in a 200 µl reaction mixture for 1h with rotation at room temperature. Preparation of GDP- or GMP-PNP-charged ROP2 was carried out in two steps. In the first step, nucleotide-free ROP2 was obtained by incubation of recombinant ROP2 in nucleotide exchange buffer (50 mM Tris pH 7.5, 150 mM KCl, 10 mM EDTA and 5 mM $MgCl_2$) for 30 minutes at room temperature. Then, nucleotide-free ROP2 was incubated with 100 µM GDP, or GMP-PNP, or no nucleotides, in nucleotide-binding buffer (50 mM Tris pH 7.5, 150 mM KCl, 10 mM $MgCl_2$) for 1h at room temperature. Free nucleotides were removed by column size exclusion chromatography.

Binding of TOR to GST-fused Sar1b, or Rheb, or ROP2, or ROP2ΔII, or ROP2Δ(I+II) or GST alone, respectively (Fig 1D and EV1C) was carried out in buffer A-150 (50 mM Tris and pH 7.5, 150 mM KCl) in 200 µl reaction mixture for 1h with rotation at room temperature. Binding of TOR to GST-fused CA-ROP2, or DN-ROP2, or ROP2, or GST alone, respectively (Fig 1H), was carried out in buffer A-150 supplemented with 5 mM $MgCl_2$ in a 200 µl reaction mixture for 1h with rotation at room temperature. Glutathione-Sepharose bead-bound complexes were washed three times with buffer A-300 (50 mM Tris and pH 7.5,

300 mM KCl). The presence of TOR and ROP2 in the bound fraction (B) as well as 20 µl of the unbound fraction (U) was analyzed by SDS-PAGE following Coomassie blue staining.

Mass spectrometry analysis

Samples were prepared for mass-spectrometry analyses as described in Chicher *et al.* (2015). Briefly, samples solubilized in Laemmli buffer were precipitated with 0.1M ammonium acetate in 100% methanol. After a reduction-alkylation step (Dithiothreitol 5 mM - Iodoacetamide 10 mM), proteins were digested overnight with 1/25 (w/w) of sequencing-grade porcin trypsin (Promega). Peptide mixtures were resolubilized in water containing 0.1% FA (solvent A) before being injected into nanoLC-MS/MS (NanoLC-2DPlus system with nanoFlex ChiP module; Eksigent, ABSciex, Concord, Ontario, Canada, coupled to a TripleTOF 5600 mass spectrometer ABSciex). Peptides were eluted from the C-18 analytical column (75 µm ID x 15 cm ChromXP; Eksigent) with a 5%–40% gradient of acetonitrile (solvent B) for 90 minutes. Data were searched against a TAIR database containing the GFP-TOR sequence as well as decoy reverse sequences (TAIR10_pep_20101214). Peptides were identified with Mascot algorithm (version 2.2, Matrix Science, London, UK) through the ProteinScape 3.1 package (Bruker). Proteins with a minimum score of 30, and a *P*-value<0.05, were validated respecting a false discovery rate (FDR) <1%.

Data analysis and software

To quantify bands on western blots, we applied ImageJ software based analysis (http://rsb.info.gov/ij). The area under the curve (AUC) of the specific signal was corrected for the AUC of the loading control (corresponding substrate). The highest value of phosphorylation with the wild type extract was set as 100% and other conditions were recalculated. To analyze the phylogenetic relationship between plant ROP family members, we used the web service Phylogeny (Dereeper *et al*, 2008). Microscopy was done on a confocal microscope Zeiss LSM780 (Jena, Germany), and image analysis was performed with ImageJ. Data were analyzed with GraphPad Prism statistical software.

A

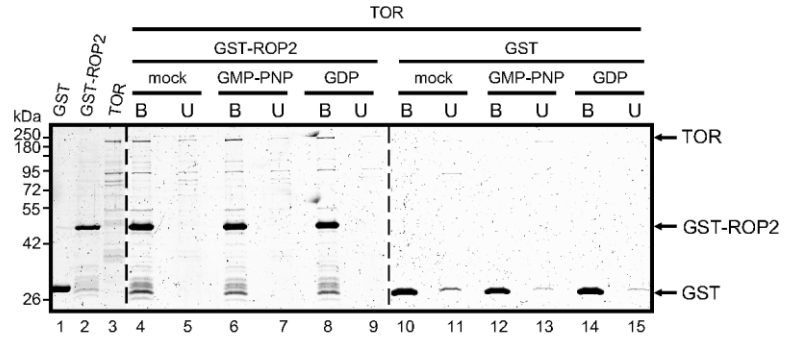

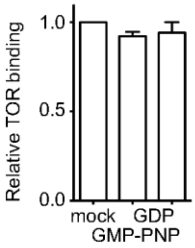

B

MVSKGEELFT	GVVPILVELD	GDVNGHKFSV	SGEGEGDATY	GKLTLKFICT	TGKLPVPWPT	LVTTLTYGVQ	CFSRYPDHMK	80
QHDFFKSAMP	EGYVQERTIF	FKDDGNYKTR	AEVKFEGDTL	VNRIELKGID	FKEDGNILGH	KLEYNYNSHN	VYIMADKQKN	160
GIKVNFKIRH	NIEDGSVQLA	DHYQQNTPIG	DGPVLLPDNH	YLSTQSALSK	DPNEKRDHMV	LLEFVTAAGI	TLGMDELYKD	240
ITSLYKKAGL	MSTSSQSFVA	GRPASMASPS	QSHRFCGPSA	TASGGGSFDT	LNRVIADLCS	RGNPKEGAPL	AFRKHVEEAV	320
RDLSGEASSR	FMEQLYDRIA	NLIESTDVAE	NMGALRAIDE	LTEIGFGENA	TKVSRFAGYM	RTVFELKRDP	EILVLASRVL	400
GHLARAGGAM	TSDEVEFQMK	TAFDWLRVDR	VEYRRFAAVL	ILKEMAENAS	TVFNVHVPEF	VDAIWVALRD	PQLQVRERAV	480
EALRACLRVI	EKRETRWRVQ	WYYRMFEATQ	DGLGRNAPVH	SIHGSLLAVG	ELLRNTGEFM	MSRYREVAEI	VLRYLEHRDR	560
LVRLSITSLL	PRIAHFLRDR	FVTNYLTICM	NHILTVLRIP	AERASGFIAL	GEMAGALDGE	LIHYLPTIMS	HLRDAIAPRK	640
GRPLLEAVAC	VGNIAKAMGS	TVETHVRDLL	DVMFSSSLSS	TLVDALDQIT	ISIPSLLPTV	QDRLLDCISL	VLSKSHYSQA	720
KPPVTIVRGS	TVGMAPQSSD	PSCSAQVQLA	LQTLARFNFK	GHDLLEFARE	SVVVYLDDED	AATRKDAALC	CCRLIANSLS	800
GITQFGSSRS	TRAGGRRRRL	VEEIVEKLLR	TAVADADVTV	RKSIFVALFG	NQCFDDYLAQ	ADSLTAIFAS	LNDEDLDVRE	880
YAISVAGRLS	EKNPAYVLPA	LRRHLIQLLT	YLELSADNKC	REESAKLLGC	LVRNCERLIL	PYVAPVQKAL	VARLSEGTGV	960
NANNNIVTGV	LVTVGDLARV	GGLAMRQYIP	ELMPLIVEAL	MDGAAVAKRE	VAVSTLGQVV	QSTGYVVTPY	KEYPLLLGLL	1040
LKLLKGDLVW	STRREVLKVL	GIMGALDPHV	HKRNQQSLSG	SHGEVPRGTG	DSGQPIPSID	ELPVELRPSF	ATSEDYYSTV	1120
AINSLMRILR	DASLLSYHKR	VVRSLMIIFK	SMGLGCVPYL	PKVLPELFHT	VRTSDENLKD	FITWGLGTLV	SIVRQHIRKY	1200
LPELLSLVSE	LWSSFTLPGP	IRPSRGLPVL	HLLEHLCLAL	NDEFRTYLPV	ILPCFIQVLG	DAERFNDYTY	VPDILHTLEV	1280
FGGTLDEHMH	LLLPALIRLF	KVDAPVAIRR	DAIKTLTRVI	PCVQVTGHIS	ALVHHLKLVL	DGKNDELRKD	AVDALCCLAH	1360
ALGEDFTIFI	ESIHKLLLKH	RLRHKEFEEI	HARWRRREPL	IVATTATQQL	SRRLPVEVIR	DPVIENEIDP	FEEGTDRNHQ	1440
VNDGRLRTAG	EASQRSTKED	WEEWMRHFSI	ELLKESPSPA	LRTCAKLAQL	QPFVGRELFA	AGFVSCWAQL	NESSQKQLVR	1520
SLEMAFSSPN	IPPEILATLL	NLAEFMEHDE	KPLPIDIRLL	GALAEKCRVF	AKALHYKEME	FEGPRSKRMD	ANPVAVVEAL	1600
IHINNQLHQH	EAAVGILTYA	QQHLDVQLKE	SWYEKLQRWD	DALKAYTLKA	SQTTNPHLVL	EATLGQMRCL	AALARWEELN	1680
NLCKEYWSPA	EPSARLEMAP	MAAQAAWNMG	EWDQMAEYVS	RLDDGDETKL	RGLASPVSSG	DGSSNGTFFR	AVLLVRRAKY	1760
DEAREYVERA	RKCLATELAA	LVLESYERAY	SNMVRVQQLS	ELEEVIEYYT	LPVGNTIAEE	RRALIRNMWT	QRIQGSKRNV	1840
EVWQALLAVR	ALVLPPTEDV	ETWLKFASLC	RKSGRISQAK	STLLKLLPFD	PEVSPENMQY	HGPPQVMLGY	LKYQWSLGEE	1920
RKRKEAFTKL	QILTRELSSV	PHSQSDILAS	MVSSKGANVP	LLARVNLKLG	TWQWALSSGL	NDGSIQEIRD	AFDKSTCYAP	2000
KWAKAWHTWA	LFNTAVMSHY	ISRGQIASQY	VVSAVTGYFY	SIACAANAKG	VDDSLQDILR	LLTLWFNHGA	TADVQTALKT	2080
GFSHVNINTW	LVVLPQIIAR	IHSNNRAVRE	LIQSLLIRIG	ENHPQALMYP	LLVACKSISN	LRRAAAQEVV	DKVRQHSGAL	2160
VDQAQLVSHE	LIRVAILWHE	MWHEALEEAS	RLYFGEHNIE	GMLKVLEPLH	DMLDEGVKKD	STTIQERAFI	EAYRHELKEA	2240
HECCCNYKIT	GKDAELTQAW	DLYYHVFKRI	DKQLASLTTL	DLESVSPELL	LCRDLELAVP	GTYRADAPVV	TISSFSRQLV	2320
VITSKQRPRK	LTIHGNDGED	YAFLLKGHED	LRQDERVMQL	FGLVNTLLEN	SRKTAEKDLS	IQRYSVIPLS	PNSGLIGWVP	2400
NCDTLHHLIR	EHRDARKIIL	NQENKHMLSF	APDYDNLPLI	AKVEVFEYAL	ENTEGNDLSR	VLWLKSRSSE	VWLERRTNYT	2480
RSLAVMSMVG	YILGLGDRHP	SNLMLHRYSG	KILHIDFGDC	FEASMNREKF	PEKVPFRLTR	MLVKAMEVSG	IEGNFRSTCE	2560
NVMQVLRTNK	DSVMAMMEAF	VHDPLINWRL	FNFNEVPQLA	LLGNNNPNAP	ADVEPDEEDE	DPADIDLPQP	QRSTREKEIL	2640
QAVNMLGDAN	EVLNERAVVV	MARMSHKLTG	RDFSSSAIPS	NPIADHNNLL	GGDSHEVEHG	LSVKVQVQKL	INQATSHENL	2720
CQNYVGWCPF	W							

Appendix Figure S1.

A **Analysis of TOR binding to ROP2 preincubated with either GMP-PNP or GDP.** ROP2 interacts with both GMP-PNP and GDP in a GST pull-down assay. GST-ROP2 and GST alone bound to glutathione beads were preincubated without (mock) or with GMP-PNP or GDP. The beads were washed and further incubated with recombinant TOR. The TOR unbound (U) and bound (B) fractions were analyzed by Coomassie staining. *Right panel* Quantification of TOR binding to GST-fusion proteins. The value for TOR binding to GST-ROP2 (mock) was set as 1.

Data information: Quantification represents the means +/-SEM obtained in two independent experiments.

B **Characterization of GFP-TOR protein from the *Arabidopsis 35S:GFP-TOR* line.** Sequence coverage (highlighted in grey) for recombinant GFP-TOR obtained with trypsin digestion from 2 independent enrichment experiments (green and pink bars, respectively). Tryptic and semi-tryptic peptides identified by LC-MS/MS were validated by MASCOT's identity scores (p-value < 0.05).

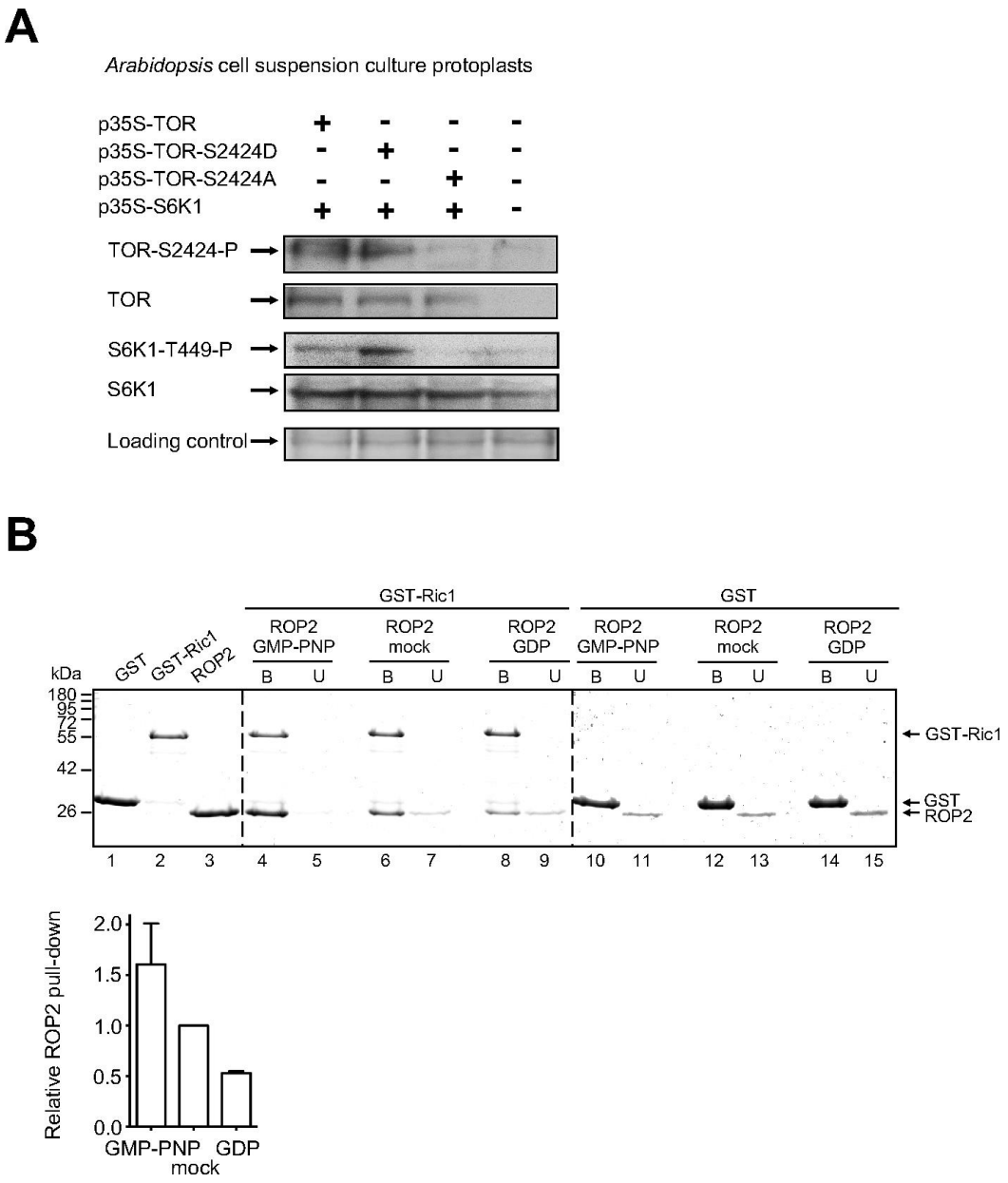
A
Arabidopsis cell suspension culture protoplasts
p35S-TOR + - - -
p35S-TOR-S2424D - + - -
p35S-TOR-S2424A - - + -
p35S-S6K1 + + + -
TOR-S2424-P
TOR
S6K1-T449-P
S6K1
Loading control
B
GST-Ric1
GST
ROP2 GMP-PNP
ROP2 mock
ROP2 GDP
B U
kDa
GST
GST-Ric1
ROP2
180
95
72
55
42
26
GST-Ric1
GST
ROP2
1 2 3 4 5 6 7 8 9 10 11 12 13 14 15
Relative ROP2 pull-down
2.0
1.5
1.0
0.5
0.0
GMP-PNP
GDP
mock

Appendix Figure S2

A Phosphorylated S2424 (S2424-P) in *Arabidopsis* TOR is a specific target of phospho-antibodies against mammalian TOR phosphorylated S2448 (S2448-P).

Anti-(mTOR-S2448-P) antibodies specifically recognize TOR, its phosphorylation mimic TOR-S2424D, but not TOR phosphorylation knockout TOR-S2424A transiently produced together with S6K1 in *Arabidopsis* WT protoplasts. Suspension culture protoplasts were co-transfected with plasmids expressing S6K1 under the 35S promoter (p35S-S6K1), and either p35S-TOR, p35S-TOR-S2424D, or p35S-TOR-S2424A (TOR S2424 phosphorylation site mutants) as indicated. Transiently expressed TOR and its derivatives were assayed by immunoblotting using anti-*At*TOR antibodies (anti-TOR) and anti-(mTOR-S2448-P). S6K1 levels and phosphorylation status were assayed by anti-mS6K1 and anti-(mS6K1-T389-P). Protein loading was assessed by Coomassie blue staining (LC, loading control).

B **Ric1 specifically binds active GTP-bound ROP2 *in vitro*.**

GST-Ric1 pull-down active GTP-bound ROPs. GST-Ric1 as well a GST alone bound to glutathione beads were incubated with recombinant ROP2 preincubated without (mock) or with GMP-PNP or GDP. The beads were washed, and the unbound (U) and bound (B) fractions were analyzed by Coomassie staining. Purified recombinant GST, GST-Ric1 and ROP2 proteins are shown on the left panel. *Bottom panel* Quantification of ROP2 pull-down by GST-Ric1 proteins. The value for ROP2 binding to GST-Ric1 (mock) was set as 1.

Data information: Quantification represents the means +/-SEM obtained in two independent experiments.

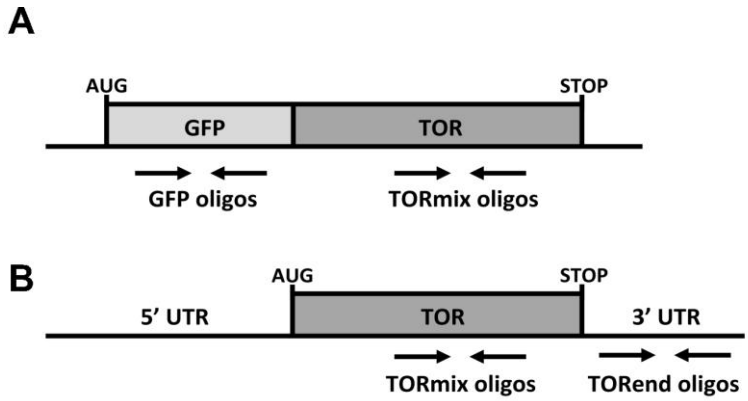

Appendix Figure S3.**Monitoring of endogenous, GFP-tagged and total TOR mRNA levels.**

A, B Primer design for monitoring of *GFP-TOR* (A) and endogenous *TOR* mRNA levels (B) in *GFP-TOR/CA-ROP2* or *GFP-TOR* transgenic plants

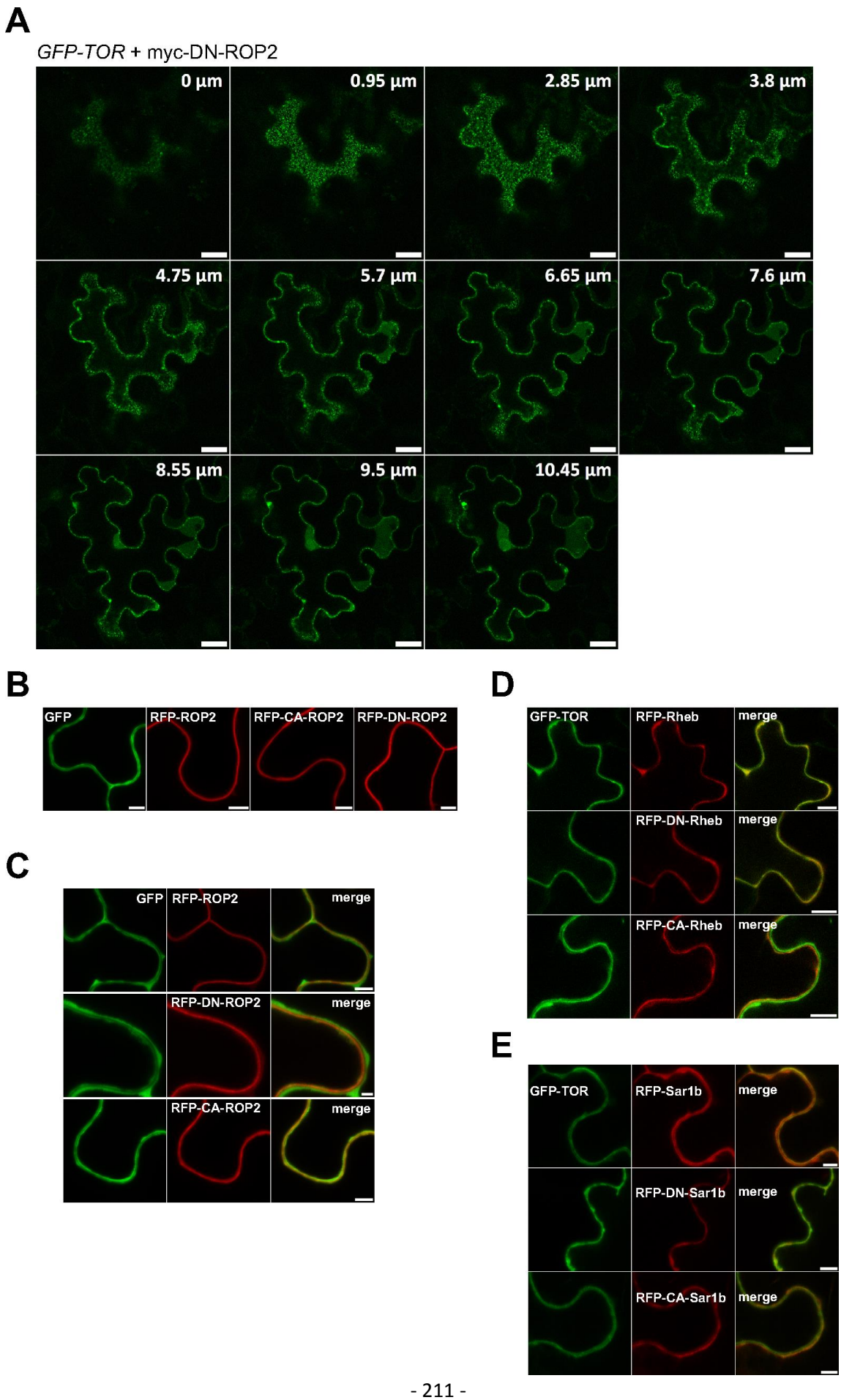
A
GFP-TOR + myc-DN-ROP2
0 µm
0.95 µm
2.85 µm
3.8 µm
4.75 µm
5.7 µm
6.65 µm
7.6 µm
8.55 µm
9.5 µm
10.45 µm
B
GFP
RFP-ROP2
RFP-CA-ROP2
RFP-DN-ROP2
C
GFP
RFP-ROP2
merge
RFP-DN-ROP2
merge
RFP-CA-ROP2
merge
D
GFP-TOR
RFP-Rheb
merge
RFP-DN-Rheb
merge
RFP-CA-Rheb
merge
E
GFP-TOR
RFP-Sar1b
merge
RFP-DN-Sar1b
merge
RFP-CA-Sar1b
merge

Appendix Figure S4.

A **Analyses of GFP-TOR dot distribution between the N. benthamiana cell periphery and the perinuclear region upon DN-ROP2 overexpression.** DN-ROP2 promotes GFP-TOR-containing multiple dot formation close to the cell periphery. Cross-section of an *Nicotiana benthamiana* epidermal cell showing the distribution of GFP-TOR punctuated dots upon overexpression of myc-DN-ROP2 in the cytoplasm. Serial sections were taken from the top at every 0.95 µm of cell depth.

Data information: Scale bars are 20 µm.

B-E **Small GTPases—Rheb and Sar1b—failed to promote GFP-TOR-containing aggregate formation in the cytoplasm of *Nicotiana benthamiana* cells.** B, C ROP2 variants failed to promote GFP-containing aggregate formation in the cytoplasm of *Nicotiana benthamiana* cells. Imaging fluorescence assays showing cells transiently expressing either GFP, or RFP-ROP2, or RFP-CA-ROP2, or RFP-DN-ROP2 (A) as well as their combination (B). *Upper panels Left* GFP (green), *central* RFP-ROP2 (red), *right* merged. *Middle panels Left* GFP (green), *central* RFP-CA-ROP2 (red), *right* merged. *Bottom panels Left* GFP (green), *central* RFP-DN-ROP2 (red), *right* merged.

D, E Sar1b and Rheb variants fail to promote GFP-TOR localization with subcellular structures in *Nicotiana benthamiana* cells. (C) *Upper panels Left* GFP-TOR (green, *1*), *central* RFP-Rheb (red, *2*), *right* merged. *Middle panels Left* GFP-TOR (green, *1*), *central* RFP-DN-Rheb (red, *2*), *right* merged. *Bottom panels Left* GFP-TOR (green, *1*), *central* RFP-CA-Rheb (red, *2*), *right* merged. (D) *Upper panels Left* GFP-TOR (green, *1*), *central* RFP-Sar1b (red, *2*), *right* merged. *Middle panels Left* GFP-TOR (green, *1*), *central* RFP-DN-Sar1b (red, *2*), *right* merged. *Bottom panels Left* GFP-TOR (green, *1*), *central* RFP-CA-Sar1b (red, *2*), *right* merged.

Data information: Scale bars 5 µm.

Appendix references

Chicher J, Simonetti A, Kuhn L, Schaeffer L, Hammann P, Eriani G & Martin F (2015) Purification of mRNA-programmed translation initiation complexes suitable for mass spectrometry analysis. *Proteomics*

Clough SJ & Bent AF (1998) Floral dip: a simplified method for Agrobacterium-mediated transformation of Arabidopsis thaliana. *Plant J.* 16: 735–743

Cui D, Zhao J, Jing Y, Fan M, Liu J, Wang Z, Xin W & Hu Y (2013) The Arabidopsis IDD14, IDD15, and IDD16 Cooperatively Regulate Lateral Organ Morphogenesis and Gravitropism by Promoting Auxin Biosynthesis and Transport. *PLoS Genet.* 9: e1003759

Dereeper A, Guignon V, Blanc G, Audic S, Buffet S, Chevenet F, Dufayard JF, Guindon S, Lefort V, Lescot M, Claverie JM & Gascuel O (2008) Phylogeny.fr: robust phylogenetic analysis for the non-specialist. *Nucleic Acids Res* 36: 465–469

Gerber E, Hemmerlin A, Hartmann M, Heintz D, Hartmann M-A, Mutterer J, Rodríguez-Concepción M, Boronat A, Van Dorsselaer A, Rohmer M, Crowell DN & Bach TJ (2009) The plastidial 2-C-methyl-D-erythritol 4-phosphate pathway provides the isoprenyl moiety for protein geranylgeranylation in tobacco BY-2 cells. *Plant Cell* 21: 285–300

Karimi M, Inzé D & Depicker A (2002) GATEWAY vectors for Agrobacterium-mediated plant transformation. *Trends Plant Sci.* 7: 193–195

Li H, Shen JJ, Zheng ZL, Lin Y & Yang Z (2001) The Rop GTPase switch controls multiple developmental processes in Arabidopsis. *Plant Physiol.* 126: 670–684

Nakagawa T, Kurose T, Hino T, Tanaka K, Kawamukai M, Niwa Y, Toyooka K, Matsuoka K, Jinbo T & Kimura T (2007) Development of series of gateway binary vectors, pGWBs, for realizing efficient construction of fusion genes for plant transformation. *J. Biosci. Bioeng.* 104: 34–41

Nelson BK, Cai X & Nebenführ A (2007) A multicolored set of in vivo organelle markers for co-localization studies in Arabidopsis and other plants. *The Plant Journal* 51: 1126–1136

Pooggin MM, Hohn T & Futterer J (2000) Role of a short open reading frame in ribosome shunt on the cauliflower mosaic virus RNA leader. *J. Biol. Chem.* 275: 17288–17296

Ren H, Dang X, Yang Y, Huang D, Liu M, Gao X & Lin D (2016) SPIKE1 activates ROP GTPase to modulate petal anisotropic growth in Arabidopsis. *Plant Physiol.***:** pp.00788.2016

Schepetilnikov M, Dimitrova M, Mancera-Martínez E, Geldreich A, Keller M & Ryabova LA (2013) TOR and S6K1 promote translation reinitiation of uORF-containing mRNAs via phosphorylation of eIF3h. *EMBO J.* 32: 1087–1102

Schepetilnikov M, Kobayashi K, Geldreich A, Caranta C, Robaglia C, Keller M & Ryabova LA (2011) Viral factor TAV recruits TOR/S6K1 signalling to activate reinitiation after long ORF translation. *EMBO J.* 30: 1343–1356

Yoo SD, Cho YH & Sheen J (2007) Arabidopsis mesophyll protoplasts: a versatile cell system for transient gene expression analysis. *Nat Protoc* 2: 1565–1572

Zhao Y, Christensen SK, Fankhauser C, Cashman JR, Cohen JD, Weigel D & Chory J (2001) A role for flavin monooxygenase-like enzymes in auxin biosynthesis. *Science* 291**:** 306–309

III. Conclusions & Perspectives

A review of recent TOR research in plants highlighted TOR as an important regulator of nutrient sensing, growth and lipid metabolism in plants (Dobrenel et al. 2016). The core components of TORC1 signalling are well conserved between mammals and plants—a single essential TOR gene was identified in mammals and plants in comparison to yeast, which possess two copies of TOR gene, TOR1 and TOR2. However, only two components of the *Arabidopsis* TORC1 complex were identified up to date—Raptor (Dobrenel et al. 2011) and LST8 (Moreau et al. 2012). Moreover, components of the TORC2 complex are either not yet found, or this complex does not exist in dicots. Thanks to recently discovered TOR upstream effectors—auxin (Schepetilnikov et al. 2011; Schepetilnikov et al. 2013; Deng et al. 2016), glucose (Xiong et al. 2013); the pathogenicity factor, Cauliflower mosaic virus (CaMV) protein TAV (Schepetilnikov et al. 2011) and established phosphorylation analysis of known TOR downstream targets—S6K1 (Schepetilnikov et al. 2011; Xiong and Sheen 2012) and the ribosomal protein S6—dissection of the plant TOR signaling pathway and their intermediate factors is in progress. One such factor immediately upstream of TOR was identified as a small GTPase ROP2 (Rho-like GTPases from plants; this thesis). ROP2 physically binds and activates TOR. Auxin mediates ROP2 activation by recycling of ROP2 from GDP- to GTP-bound active form that functions in TOR activation. Strikingly, auxin signaling towards TOR activation is abolished in ROP-deficient *rop2rop6ROP4 RNAi* plants.

The role of TOR in translation was first demonstrated by Deprost et al. (2007), and, later the role of TOR in reinitiation after short ORF translation was suggested by Schepetilnikov et al. (2013) that showed that TOR activation boost translation of uORF-containing mRNAs. Several TOR downstream targets linked to translation reinitiation have been characterized in *Arabidopsis*—Reinitiation supporting protein (RISP) by Mancera et al. (this thesis), eIF3 subunit h (eIF3h) (Thiébeauld et al. 2009; Schepetilnikov et al. 2013), a major TOR downstream target in translation the 40S ribosomal protein S6 (eS6 or RPS6) by

Mancera et al. (this thesis). RPS6 is a downstream target of the TOR-S6K signalling pathway in mammals and plants, but the role of its phosphorylation in translation remains unclear. Here we obtained data that suggest the role of RPS6 in reinitiation after short ORF or TAV-activated reinitiation after long ORF translation in plants.

My data indicate that TOR regulates translation initiation of mRNAs, when initiation is dependent on cap structure. Search for *Arabidopsis* peptides that harbor eIF4E-binding site revealed a family of small proteins (ToRPs; TOR Regulatory Proteins). The most striking feature of these proteins is their phosphorylation in TOR-responsive manner that suggests their control by TOR. Two TOR phosphorylation sites have been identified, while identification of others would require MS-MS and phosphopeptide analysis. For this purpose, myc-ToRP1 or ToRP2 overexpressing *Arabidopsis* plantlets were prepared for phosphoproteomic analysis in conditions of either auxin or AZD-8055 treatment. This work is in progress. My experiments revealed three and five phosphorylation states of ToRP1 and ToRP2, respectively. We demonstrated phosphorylation of ToRPs in response to auxin treatment, but we need to prove that ToRPs are direct targets of TOR in plants. To address this question, I propose to perform the kinase assay with TOR immunoprecipitated from GFP-TOR overexpressing lines (available in our laboratory) to measure ToRPs phosphorylation status with or without TOR inhibitor AZD-8055.

We have identified three conserved motifs within ToRPs that are required for efficient ToRP1 protein binding to eIF4E, suggesting that three motifs cooperate to overcome eIF4G binding to eIF4E. We plan to use the yeast three-hybrid system that permits expression of both ToRP1 and eIF4G proteins to study their competition for eIF4E binding. Normally, TOR substrates are presented for TOR phosphorylation by Raptor via their TOR signaling motif (TOS) essential for Raptor binding. In plants, although S6K1 binds Raptor, TOS-like signals

within S6K1 or ToRPs are not yet identified. Instead, we found that ToRP1 is capable of direct TOR binding. Thus, it remains to be studied how S6K1 and ToRPs are phosphorylated by TOR. At least ToRP2 has an ability to suppress cap-dependent translation, as manifested by mRNA that encodes CYCB1;1 known to be strictly cap-dependent. Further work is required to reveal the effect of ToRPs on global mRNA translation, and, particularly, translation of mRNA containing a 5' TOP motif at their 5' end, that in mammals requires 4E-BP suppression by TOR (Thoreen et al. 2012).

Future studies would clarify the functional significance of ToRP proteins in translation initiation and plant development. An encouraging result is that the resulting *torp1 torp2* knockout plants are somewhat bigger than control WT plants. In contrast, overexpression of myc-tagged ToRP1 seems to be partly toxic for *Arabidopsis*. Thus, our results led to the characterization of eIF4E-binding proteins—ToRP1 and ToRP2—that are phosphorylated by TOR and function in cap-dependent translation initiation in *Arabidopsis*. We believe that our results open a new avenue to study TOR cap-dependent translation control in plants.

IV. Materials & Methods

1. Materials

1.1. Bacterial strains

1.1.1. DH5α Escherichia coli strain

In my study, DH5α was the most frequently used *E. coli* strain for routine cloning applications. In addition to supporting blue/white screening, recA1 and endA1 mutations in DH5α increase insert stability and improve the quality of plasmid DNA prepared from minipreps. Characteristics of DH5α strain were listed in **Table—1**.

Table—1 │DH5α E. coli strain characteristics

Genotype: *F- 80dlacZ M15 (lacZYA-argF) U169 recA1 endA1hsdR17 (rk-, mk+) phoAsupE44 -thi-1 gyrA96 relA1*
Resistance: *None*
Applications: *Cloning*
Origin: *Life Technologies*

1.1.2. BL21 (DE3) pLysS Escherichia coli strain

The characteristic of BL21 (DE3) pLysS *E. coli* strain used in this study were listed in **Table—2**. BL21 (DE3) pLysS *E.coli* was routinely used for the expression and production of recombinant fusion proteins, and have the advantage of being deficient in both *lon* and *ompT* proteases. Strains carry both the DE3 lysogen and the plasmid pLysS. DE3 indicates that the host is a lysogen of λDE3, and therefore carries an IPTG-inducible T7 RNA polymerase gene under control of the *lacUV5* promoter. pLysS constitutively expresses low levels of T7 lysozyme, which reduces basal expression of toxic target proteins by inhibiting basal levels of T7 RNA polymerase.

Table—2 │BL21 (DE3) pLysS E. coli strain characteristics

Genotype: *F^- ompT $hsdS_B(r_B^- m_B^-)$ gal dcm (DE3) pLysS (Cam^R)*
Resistance: *Chloramphenicol (25 µg/mL)*
Applications: *Production of recombinant proteins*
Origin: *Novagen*

1.1.3. GV3101 Agrobacterium tumefaciens strain

GV3101 Agrobacterium strain was used for Agrobacterium-mediated transformation of plants. This strain is a "disarmed strain", which means that the DNA containing the tumors inducing genes has been removed from the Ti-plasmid. Characteristics of this strain were listed in **Table—3**.

Table—3 │ GV3101 Agrobacterium tumefaciens strain characteristics

Characteristics: *It carries a disarmed Ti plasmid containing the vir genes needed for T-DNA transfer, but has no functional t-DNA region of its own*
Resistance: *Rifampycin (50 µg/mL) and Gentamycin (50 µg/mL)*
Applications: *Production of transgenic plants* *Transient and stable transformation of plants*
Origin: *Kindly provided by Jean-Michel Davierre (Institut de biologie moléculaire des plantes, Strasbourg)*

1.2. Yeast strain

AH109 Saccharomyces cerevisiae strain

AH109 is a strain of yeast *(Saccharomyces cerevisiae)* was used in biological research for two-hybrid screening. AH109 is diploid strain, no need to do mating giving the advantage of co-transfection with two plasmids. The strain is sold commercially by Clontech Laboratoires Ltd. The genotype of this yeast strain was listed in **Table—4**.

Table—4 │ AH109 S. cerevisiae strain characteristics

Genotype: *MATa, trp1-901, leu2-3, 112, ura3-52, his3-200, gal4 Δ, gal80Δ, LYS2::GAL1UAS-GAL1TATA-HIS3, GAL2UAS-GAL2TATA-ADE2, URA3::MEL1 UAS-MEL1TATA-lacZ, MEL*
Resistance: *None*
Applications: *Yeast-two hybrid system*
Origin: *Clontech laboratories Ltd.*

1.3. Growth media

Bacterial and yeast growth media components were purchased from Ozyme inc. (St quentin en Yvelines, France) and Sigma-Aldrich Ltd. (Illkirch, France). Bacterial (*DH5α E.coli* and *Agrobacterium tumefaciens*) cells were routinely grown in liquid nutritionally rich **LB medium** (Luria Bertani media) containing the appropriate antibiotic. For expression of recombinant proteins in BL21 (DE3) pLysS cells, LB medium was supplemented by 0.4% (w/v) glucose to increase the production of soluble protein. The addition glucose allows complete suppression of the T7 promoter in the absence of IPTG. Solid media was prepared by the addition of 2% (w/v) agar in order to form gel for bacteria to grown on. For yeast cells growth, we used non-selection and rich **YPD medium** or standard minimal synthetic **media SD** lacking the appropriate amino acids. As before, solid media was prepared by adding of 2% (w/v) agar. All medium used for bacterial and yeast growth were autoclaved and then used under sterile conditions.

LB media: *1% (w/v) tryptone, 0.5% (w/v) yeast extract, 0.5% (w/v) NaCl*

YPD media: *1% (w/v) yeast extract, 2% (w/v) peptone, 2% (w/v) glucose*

SD media: *0.675% (w/v) yeast nitrogen base without amino acids, 2% (w/v) glucose*

1.4. Antibiotics

Antibiotics used in this study were listed in **Table—5**. All antibiotics were purchased from Sigma-Aldrich Ltd. (Illkirch, France) and were prepared as water, 50% ethanol or DMSO stock solutions and stored at -20 °C.

Table—5 │ Antibiotics used in this study

Antibiotic	[Stock]	[Final]
Ampicillin sodium salt	100 mg/mL in 50% EtOH	100 µg/mL
Chloramphenicol	50 mg/mL in 50% EtOH	25 µg/mL
Rifampicin	100 mg/mL in DMSO	50 µg/mL
Hygromycin	35 mg/mL in dH_2O	35 µg/mL
Gentamycin	50 mg/mL in dH_2O	50 µg/mL
Spectinomycin	100 mg/mL in dH_2O	100 µg/mL

1.5. Antibodies

Primary and secondary antibodies used in this study are listed in **Table—6.** In addition to this list, I was used antibodies raised against plant ToRP1 and ToRP2. Polyclonal Rabbit ***anti-ToRP1/2*** antibody was raised against the central conserved motif (CRLLRGKQTMTEFEPL) and prepared by Eurogentec®. The antibody was used at 1:5000 dilutions in 5% (w/v) non-fat dried milk in PBS-T. ToRP phosphoantibodies (***Anti-S49-P*** and ***Anti-S89-P***) were raised against peptide (YSPSPSPYR[pS]PVTLP) and (ERFYYRQ[pS]PPPSGK) that contains S49 and S89 phosphorylated sites respectively, and obtained from ProteoGenix®. Thesis rabbit polyclonal antibodies were used at 1:1000 dilutions in 5% (w/v) non-fat dried milk in PBS-T for detection of phosphorylated ToRP1 and ToRP2 in my 2Dgel experiments.

Table—6 | Antibodies used in this study

Antibody	Description	Dilution	Buffer	Source
Primary				
anti-cMyc	Rabbit polyclonal IgG against residues 408-439 (EQKLISEEDL) of the human p62c-Myc protein	1:2500	PBS-T	Santa Cruz Biotechnology
anti-GFP	Rabbit polyclonal IgG fraction	1:5000	PBS-T	ThermoFisher Scientific (Invitrogen)
anti-GST	Mouse monoclonal IgG against recombinant purified full-length GST	1: 5000	5% (w/v) non-fat dried milk in PBS-T	ThermoFisher Scientific
anti-FLAG	Rabbit polyclonal IgG against (DYKDDDDK) Flag sequence	1:5000	5% (w/v) non-fat dried milk in PBS-T	Sigma-Aldrich
anti-AteIF4E1	Rabbit polyclonal IgG against the 26 kDa Arabidopsis eIF4E1	1:2000	PBS-T	Dr. Jean-Luc Gallois (INRA GAFL, Avignon-France)
anti-AteIFiso4E	Rabbit polyclonal IgG against the 22 kDa Arabidopsis eIFiso4E	1:2000	PBS-T	Dr. Jean-Luc Gallois (INRA GAFL, Avignon-France)
Secondary				
anti-mouse	HRP conjugated whole IgG from goat	1:10000	PBS-T	ThermoFisher Scientific
anti-rabbit	HRP conjugated whole IgG from goat	1:10000	PBS-T	ThermoFisher Scientific

1.6. Plasmids

1.6.1. pGEX-6P1

The Bacterial vector pGEX-6P1 (of 4.9 kb) is used for expressing GST fusion proteins with a PreScission protease site. This vector contains an origin of replication recognized in *E. coli*, and β-lactamase gene which confers on transformed bacteria the resistance to ampicillin for selection. It contains a cloning cassette that allows cloning of a DNA sequence in the same reading frame as that of GST to obtain a fusion protein containing GST tag located on its N-terminal. A cleavage site specifically recognized by the PreScission protease; is located

between GST sequence and cloning cassette to cleave the GST with the recombinant protein. GST expression is under the control of a promoter (Ptac) inducible by IPTG which binds to the repressor $lacI^q$. pGEX-6p1, pGEX-eIF4E1 and pGEX-eIFiso4E3 were used to express GST alone, GST-eIF4E1 and GST-eIFiso4E3 fusion proteins respectively, in which they contains a N-terminal GST tag required for purification.

1.6.2. pET3a

pET3a is a bacterial vector of 4.6 Kb mostly used for the cloning and *in vivo* expression of recombinant proteins in E. coli. pET3a vector carry an N-terminal T7•Tag® sequence and BamH I cloning site. The advantage of the features of the T7 bacteriophage gene 10 is promoting high-level transcription and translation. pET3a contains an IPTG-inducible T7 RNA polymerase gene under control of the *lacUV5* promoter, β-lactamase gene for ampicillin resistance and pBR322 origin of replication.

The genes of ToRP1 and ToRP2 were synthetically designed and optimized for codon usage in *E. coli* by Dapcel, Inc. The protein coding sequence of FLAG-ToRP1-6xHis or FLAG-ToRP2-6xHis was then cloned downstream of the T7 promoter and gene 10 leader sequences, and transformed into BL21 (DE3) pLysS *E. coli* strain for expression. Purification of FLAG-ToRP1-6xHis and FLAG-ToRP2-6xHis will be described in separately chapter.

2. Methods

2.1. Techniques for nucleic acids

2.1.1. Isolation of plasmid DNA from E. coli

DNA plasmids used in my study, as a template for PCR or bacterial and yeast cell transformations was isolated from *E. coli* using the microcentrifugation protocol from NucleoSpin® Plasmid Miniprep kit (Macherey-Nagel). It consists of a bacterial lysis step followed by purification on a silica column. The experimental protocol provided with kit was strictly followed.

2.1.2. Agarose gel electrophoresis

DNA molecules are separated according to their size by electrophoretic migration on agarose gel [0.5% to 2% (w/v)] prepared in 0.5X **TBE buffer**. After heating in a microwave, ethidium bromide was added to a final concentration (0.5 µg/mL). DNA samples were prepared by adding 6X **DNA loading dye** and loaded into the wells contained within the gel. 5 µL of 1 kilobase pair (kb) DNA marker (GeneRuler 1 kb DNA Ladder) was routinely included as a DNA standard. After migration under a constant electric potential, the DNA fragments were visualized by fluorescence under UV.

TBE buffer: *100 mM Tris, 90 mM Boric acid, 2.5 mM EDTA, pH 8.0*

6X DNA loading dye: *0.25% (w/v) bromophenol blue, 0.25% (w/v) xylene cyanol FF, 30% (v/v) glycerol*

2.1.3. Purification of DNA fragments from agarose gel

After separation on agarose gel, the DNA fragments of interest were excised from the gel under UV. DNA was then extracted and purified from the gel using the NucleoSpin® Gel and PCR Clean-up extraction kit (Macherey-Nagel). It consists on excision of a DNA fragment from agarose gel, solubilization of gel by heating at 50 °C for 5-10 min in appropriate buffer followed by purification on a silica column. The experimental protocol provided with kit was strictly followed.

2.1.4. Polymerase Chain Reaction (PCR)

PCR is an exponential amplification of DNA provided by a series of cycles; denaturation-hybridization-elongation; with two oligonucleotide primers specific to the ends of the fragment to be amplified. The reaction mixture was typically made up to a total volume of 50 µL that contains the components listed in **Table—7.** The PCR reaction was realized in automated apparatus (T Gradient thermocycler, Biometra) that comprise 25-30 cycles in standard conditions listed in **Table—8**.

Table—7 │ Standard PCR reaction mix

Component	**Quantity (for 50 µL reaction)**
DNA template	50-100 ng
Forward primer	0.5 µM
Reverse primer	0.5 µM
dNTPs mix	0.2 mM
5X Phusion HF buffer	1X
Phusion DNA polymerase	1 U

Table—8 │ Standard PCR conditions

Step	Temperature	Time	Number of cycles
1-Initiation denaturation	98 °C	30 sec	1
2-Denaturation	98 °C	5-10 sec	Repeat steps 2-4 for 25-30 cycles
3-Anneal	45 °C-72 °C	10-30 sec	
4-Extension	72 °C	15-30 sec/Kb	
5-Final extension	72 °C	5-10 min	
6-Hold	4 °C	Indefinite	

2.1.5. Cloning by Restriction endonuclease digestion of DNA

DNA was digested using two restriction endonucleases that act simultaneously in the same buffer under conditions recommended by the suppliers. In general, about 1 µg of DNA was digested with 5 units of enzyme in a total volume of 100 µL containing the appropriate buffer for maximum activity for both enzymes, for 2-4 hours at 37 °C. After enzymatic digestion, plasmid DNA or PCR product was resolved by agarose gel electrophoresis followed by purification on NucleoSpin® column.

2.1.6. Ligation of DNA

Ligation of the linearized plasmid and insert DNA was performed in 3:1 molar ratio (Insert/vector) for 1-2h hour at room temperature in a total volume of 20 µL. The mixture reaction was outlined in **Table—9.**

Table—9 │ DNA ligation reaction

Component	Quantity (ng) or Volume (µL)
DNA plasmid	150 ng
DNA insert	300 ng
10X T4 DNA ligase buffer	2 µL
T4 DNA ligase	1 U

The ligation product was used for transformation into competent bacterial cells that will be after selected on solid LB media containing the appropriate antibiotic. DNA was subsequently isolated from bacteria, purified and analyzed by restriction endonuclease digestion.

2.1.7. Transformation of competent bacterial cells

Chemically competent bacterial *E. coli* cells were thawed on ice for 20 minutes. Total volume of ligation mix was added to 100 µL of bacteria and the transformation mix was then incubated on ice for 20 minutes. Heat shock was performed for 90 sec at 42 °C to facilities the uptake of DNA into the bacteria, followed by addition of 500 µL of LB media. The transformed cells were incubated for 1 hour at 37 °C for the cells to recover and express the antibiotic resistance. They were subsequently plated out onto solid LB containing the appropriate antibiotic and incubated overnight at 37 °C.

2.1.8. Agrobacterium transformation

The 300 ng of plasmid DNA was added to 40 µL of chemically competent *Agrobacterium GV3101* cells and incubated at 37 °C for 5 min. LB liquid media was added immediately after the heat shock. The bacterial suspension was incubated for 2 hours at 28 °C, and then spread on LB agar plates containing appropriate antibiotics. Plates were incubated at 28 °C for 2-3 days, until colonies appear.

2.2. Techniques for protein

2.2.1. SDS-polyacrylamide gel electrophoresis

Proteins were separate according to their molecular weight by electrophoretic migration in sodium dodecyl sulfate polyacrylamide gel in denaturing conditions (Laemmeli 1970). The

matrix meshes were defined by the ratio acrylamide /N, N' methylene bisacrylamide (37.5/1 in the case of protein gel). The gel comprises two parts: an upper **stacking gel** (3 cm high) and a lower **resolving gel**, which differ by the crosslinking and the buffer. Polymerization of acrylamide/bisacrylamide was catalyzed by the addition of ammonium persulfate (APS) and tetramethylenediamine (TEMED) to a final concentration of 8 mM and 200 nM, respectively.

Stacking gel: *5% (v/v) acrylamide, 150 mM Tris-HCl (pH 6.8), 0.2% (w/v) SDS*

Resolving gel: *7.5%-15% (v/v) acrylamide, 375 mM Tris-HCl (pH 8.8), 0.2% (w/v) SDS*

Proteins were loaded on the gel after addition of 0.2 volume of 4X **Laemmli buffer** and electrophoresis was performed in **Running buffer** under constant electric potential of 100-150 V. Migration is monitored by visualization of the front migration and the colored marker molecular size. Resolved proteins were subjected to either Coomassie™ blue staining or immunoblot analysis.

4X Laemmli buffer: *250 mM Tris-HCl (pH 6.8), 40% (v/v) glycerol, 8% (w/v) SDS, 0.004% (v/v) bromophenol blue, 1% (v/v) β-mercaptoethanol*

Running buffer: *25 mM Tris-base, 190 mM glycine, 0.1% (w/v) SDS*

2.2.2. Protein staining

a. Coomassie™ blue staining

Proteins resolved using SDS-PAGE were visualized by submerging the gel in **Coomassie™ blue staining solution** under slow agitation overnight and then the gel were decolorized by several baths in **Distaining solution**.

Coomassie™ blue staining solution*: 0.25% (w/v) Brilliant Blue R-250, 10% (v/v) acetic acid, 40% (v/v) ethanol*

Distaining solution: *15% (v/v) acetic acid, 15% (v/v) ethanol*

b. Colloïdal blue staining

Colloïdal blue staining was preferably used when the amount of protein is very low. The gel containing proteins was incubated in **Fixation solution** under slow agitation for 3 hours and then the proteins were stained overnight in the presence of **Staining solution**. The gel was washed with several successive water baths to remove excess colloidal blue.

Fixation solution: *1% (v/v) acetic acid, 45% (v/v) ethanol*

Staining solution*: 0.1% (w/v) Brilliant Blue G-250, 17% (w/v) ammonium sulfate, 0.5% (v/v) acetic acid, 34% (v/v) ethanol*

2.2.3. Immunological detection of proteins by Western blot

This technique allows revealing on membrane a particular protein using specific antibody raised against this protein.

a. Transfer of proteins onto a membrane

After separation on SDS-PAGE gel, proteins were transferred and immobilized onto Immobilon®-P PVDF (Polyvinylidene Difluoride) membranes with 0.45 µm pore size (Millipore®, France). The set (protein gel-membrane) were arranged in a "sandwich" between two layers of Whatman 3 mm filter paper pre-soaked in **Transfer buffer** and placed in BioRad Criterion® Blotter electrophoretic transfer cell. Gel and membrane were placed so that proteins bind to the membrane by migration from cathode to anode. Transfer was performed for 1 hour at 4°C under constant voltage of 100 V.

Transfer buffer*: 30 mM Tris base, 230 mM glycine, 20% (v/v) ethanol*

b. Immunological detection of proteins

PVDF membrane was equilibrated in **Washing buffer** and the free sites are saturated by proteins from milk by incubation for 1 hour with constant agitation in blocking buffer. Primary antibody specific was added to the solution, and then the whole was incubated with agitation overnight at 4 °C. The membrane was then washed three times with washing buffer, with each washing interval lasting 10 min. The appropriate secondary antibody conjugated to horseradish peroxydase (HRP) was diluted in **Blocking buffer** and incubate with gently mixing for 1 hour at room temperature. To eliminate excess secondary antibody, membrane was washed three times (10 min each) in washing buffer. Proteins were visualized using Enhanced Chemical Luminescence kit (ECL, Roche). It consists on chemiluminescent reaction catalyzed by peroxidase and producing an emission of photons instead of secondary antibodies binding. Light emission was revealed by autoradiography using Fujifilm general purpose blue medical X-ray film (Fujifilm®, France).

Washing buffer: *PBS-T : 140 mM NaCl, 3 mM KCl, 1.5 mM KH2PO4, 8 mM Na2HPO4, 0.1% (v/v) Tween-20*

Blocking buffer: *5% non-fat dried milk (w/v) in PBS-T*

2.2.4. Protein purification

a. Expression of recombinant fusion proteins in E. coli

The cDNA encoding eIF4E1 or eIFiso4E3 proteins was introduced into the expression vector pGEX-6P1 providing a GST tag fused to the N-terminus of the protein interest. For expression of FLAG-ToRP1-6xHis or FLAG-ToRP2-6xHis, the cDNA encoding the protein of interest was introduced into pET3a vector. The recombinant vector obtained was used to be transformed into BL21 (DE3) pLysS *E. coli* strain. A single colony of cells transformed was used to inoculate 50 mL of LB medium containing 0.2% (w/v) glucose and the appropriate

antibiotics (100 µg/mL ampicillin and 25 µg/mL chloramphenicol), and incubated overnight in a 37 °C shaking incubator. 2 liters of the same LB medium was inoculated with the overnight preculture and incubated at 30 °C until the bacterial culture reached the exponential growth phase (OD_{600} about 0.5). Induction of recombinant protein expression was done by adding Isopropyl β-d-1-thiogalactopyranoside (IPTG) to a final concentration of 0.5 mM and bacteria growth was continued for 1 hour at 30 °C. Cells were harvested by centrifugation for 25 min at 4 °C at 8000 x g, and bacterial pellets were stored at -20 °C or used immediately for purification.

b. Purification of GST fusion proteins

Presence of GST tag at the N-terminus of the fusion protein allows the protein to interact strongly with Glutathione coupled to Sepharose 4B beads. The technique of "batch" in eppendorf tubes was used to purify some hundred micrograms of protein. However, to get big amount of protein (in the milligram range), purification was performed using GST-trap HP column of 1 mL (GE Healthcare®). Protein was eluted by a specific cleavage between GST and the protein using PreScission® protease (Amersham). Separated GST remains attached to sepharose beads while the protein will be eluted since it has no affinity to sepharose beads. All steps of extraction and protein purification are performed at 4 °C.

c. Batch purification

One bacterial pellet obtained from 500 mL culture, was resuspended in 30 mL of **Extraction buffer**. Cells were sonicated by six 30 sec-cycles at 40% of amplification power. Lysate was clarified by centrifugation at 16000 x g for 25 min at 4 °C in order to sediment insoluble proteins. To remove any aggregates, supernatant containing soluble proteins was filtered through a 0.45 µm millipore filter and then incubated with Glutathione Sepharose beads,

prewashed by Extraction buffer, for 2 h or overnight at 4 °C under constant rotation. Glutathione beads and bound GST fusion proteins were pelleted by centrifugation at 500 x g for 1 min. Glutathione beads were washed four times with 1 mL of Extraction buffer and one time with 1 mL of **Exchange buffer**, and then resuspended in 300 µL of Exchange buffer and stored in ice until GST-pull down assays.

Extraction buffer: *50 mM Tris-HCl pH 7.0, 300 mM KCl, 5 % glycerol, cOmplete® protease inhibitor cocktail (Roche®)*

Exchange buffer: *50 mM Tris-HCl pH 7.0, 60 mM KCl*

d. GST-trap 1 mL column

Bacterial pellets prepared from 2 liters of culture were resuspended in 100 mL of **Extraction buffer** and sonicated by eight 30 sec-cycles at 40% of amplification power. Lysate was centrifuged at 16000 x g for 25 min at 4 °C and filtration trough a 0.45 µm filter. Supernatant containing GST fusion protein was loaded on Glutathione Sepharose 4B-column (1 mL) previously equilibrated with 10 mL of Extraction Buffer. The column was washed with 10 mL Extraction buffer, and then with 10 mL **Washing buffer**. The column was then incubated with 1 mL of **Cleavage buffer** containing 20 units of PreScission protease overnight at 4 °C. The protein of interest was eluted by passing of 5 mL of washing buffer on the column. The pure fractions were analyzed by SDS-PAGE, and then each fraction was aliquoted and stored at -80 °C.

Extraction buffer: *50 mM Tris-HCl (pH 7.0), 300 mM KCl, 5 % glycerol, cOmplete® protease inhibitor cocktail (Roche®)*

Washing buffer: *extraction buffer supplemented with 1 mM EDTA (pH 8.0)*

Cleavage buffer: *extraction buffer supplemented with 20 units of PreScission protease*

2.2.5. GST pull-down assays

Equivalent molar ratios of purified proteins (FLAG-ToRP1-6xHis) were incubated with GST-fusion proteins (GST-eIF4E1 and GST-eIFiso4E3) or GST alone at 4 °C for 2 h under constant rotation. Binding of GST or either GST-eIF4E or GST-eIFiso4E3 to FLAG-ToRP1-6xHis was carried out in a 200 µL **Binding buffer**. Incubation was followed by centrifugation at 500 x g for 5 min, and 20 µL of the first supernatant (unbound fraction, U) was collected for analysis. Glutathione beads and associated proteins (bound fraction, B) were washed 3 times with 500 µL of Binding buffer, and then the interacting proteins were eluted from sepharose beads by adding 0.2 volume of 4X Laemmli buffer. Total bound fraction and unbound fraction were separated by electrophoresis on 15% SDS-PAGE followed by Coomassie™ blue staining or immunoblotting.

Binding buffer: *50 mM Tris-HCl (pH 7.5), 150 mM NaCl*

2.2.6. Cap-binding assay

Cap-binding assay was used to study the interaction between FLAG-ToRP1-6xHis or FLAG-ToRP2-6xHis with eIF4E1 and eIFiso4E3 pre-bound to Immobilized γ-Aminophenyl-m^7GTP (C_{10}-spacer) (Jena Bioscience). It consists in two steps, first binding of eIF4E1 and eIFiso4E3 to the m^7GTP agarose, and then loading of FLAG-ToRP1-6xHis or FLAG-ToRP2-6xHis in the cap-binding complex.

eIF4E1 and eIFiso4E3 proteins used in this study were purified using GST-trap HP column and eluted by a specific cleavage of GST by PreScission® protease (as described before). 100 µL of m^7GTP beads were washed and equilibrated in **Binding buffer**. eIF4E1 or eIFiso4E3 was added to the beads in 500 µL reaction mixture for 2 hours at 4 °C under constant rotation. m^7GTP beads and bound eIF4E1 or eIFiso4E3 were pelleted by centrifugation at 500 g for 1 min, and then washed once with 500 µL binding buffer. 20 µL of the first supernatant

(unbound fraction, U) and of resuspended beads (bound fraction, B) were used for analysis in SDS-PAGE, to evaluate the efficiency of cap-binding. Next step was to mix eIF4E1- or eIFiso4E3-bound to the m^7GTP beads with recombinant proteins (FLAG-ToRP1-6xHis or FLAG-ToRP2-6xHis). Binding was carried out in reaction mixture containing 500 µL of Binding buffer for 1 h at 4 °C under constant rotation. Beads and associated proteins (bound fractions, B') were recovered by simple centrifugation as before and washed five times with **Washing buffer**. 20 µL of the first unbound fraction (U') and of bound fractions (B'), as well as (U) and (B) fractions recuperated from the first round, were used for separation on 15% SDS-PAGE gel followed by Coomassie™ blue staining or immunoblotting analysis.

Binding buffer: *50 mM Tris-HCl (pH 7.5), 100 mM KCl*

Washing buffer: *50 mM Tris-HCl (pH 7.5), 200 mM KCl*

2.2.7. Two-dimensional IEF/SDS-PAGE (2D gel)

a. Trizol total protein extraction

For total protein extraction we used 7 days after germination Arabidopsis wild-type Col0 WT, or ToRP1/ToRP2 overexpressing seedlings treated with either TOR inhibitor (AZD-8055) or synthetic auxin (2,4-D —2,4-Dichlorophenoxyacetic acid).

One gram of treated Arabidopsis seedlings was finely ground with liquid nitrogen. Protein extraction was carried out by using Trizol (Tri Reagent®, Molecular Research Center) method. Briefly, the powder was homogenized by adding 1 mL of Trizol. Trizol extracts were incubated for 5 min at room temperature and then 200 µl of chlorophorom were added to samples, vortexed for 15 sec and then incubated for 3 min at room temperature. Extracts were centrifuged for 15 min at 12000 x g at 4 °C; the aqueous phase was discarded completely and the DNA was precipitate with 300 µL of absolute ethanol and sedimented by centrifuging from the organic phase at 4 °C for 5 min at 2000 x g. The phenol ethanol supernatant obtained

is critical for protein. To precipitate proteins, 2 Volume of isopropanol were added to this supernatant, incubated for 10 min at room temperature, and centrifuged for 10 min at 4 °C at 12000 x g. The protein precipitate obtained was washed three times with 0.3 M guanidine hydrochloride in 95 % ethanol and once with absolute ethanol. Further, the protein precipitate was dried for 5-10 min and resuspended in 100 µL of **IEF buffer**.

> ***IEF buffer:*** *7 M urea, 2 M thiourea, 0.2 % triton-100 (v/v), 4 % CHAPS (w/v), and 20 mM Tris-HCl (pH 8)*

After extraction, proteins were treated for further 2D gel analysis. 95 µl of protein samples were reduced by adding 50 mM DTT and incubated for 10 min at room temperature. Proteins were also alkylated by incubation for 15 min at 37 °C with 100 mM iodoacetamide. After reduction of alkylation, samples were proceeded to buffer exchange on G25 resin equilibrated with IEF buffer, and then ready to be loaded in 2D gel.

b. Two-dimensional IEF/SDS-PAGE (2D gel)

Proteins are separated according to two properties in two dimensions on 2D gel electrophoresis. The first dimension consists in separation of proteins according to their isoelectric point (pI) by isoelectric focusing (IEF) using IPG strips (Immobilized pH gradient strips) with ampholytes covalently bound to a gel, or carried ampholytes that migrate through a gel to generate the pH gradient. pI is the pH at which the net charge on the protein is zero. IEF works by applying an electric field to protein within a pH gradient. Charged proteins are separated as they migrated thought the pH gradient until they reached a pH equal to their pI. In this way, each protein becomes focused according to its pI.

In order to obtain a gradient stability and reproducibility over extended focusing runs, we used commercially IPG stripes. In my case, we were used ReadyStrips IPG strips (BioRad) of

7 cm length that allow loading of 10-100 µg of proteins in pH range 7-10. The pH gradients were realized by covalently incorporation of ampholytes into polyacrylamide gels.

The first electrophoresis dimension is performed in 2 steps using Protean IEF apparatus (BioRad): Active rehydration at 50 Volt during 24 hours, allowing proteins entry into the gel, then isoelectric focalizing step.

The first-dimension separation procedure involves IPG strip rehydration followed by isoelectric focusing using Protean IEF apparatus (BioRad). IPG strips were placed horizontally on a flatbed electrophoresis unit and rehydrated in a 125 µL of Rehydration solution containing the sample proteins and the necessary additives. Active rehydration was occurs at 50 Volt for 8-15 hours, and allows protein to be loaded and separated onto the gel. The composition of Rehydration solution is listed in **Table—10**.

Table—10 **| *Rehydration solution composition***

Rehydration solution	Amount	Role
Sample	120.5 µL	/
Carrier ampholytes	0.2 % (v/v)	enhance protein solubility and produce more uniform conductivity across the pH gradient
Bromophenol Blue Dye	0.004 %	allows IEF progress to be monitored
DTT	20 mM (w/v)	cleaves disulfide bonds to allow proteins to unfold completely

IEF was performed by gradually increasing the voltage across the IPG strips to at least 4000 V and maintaining this voltage for at least several thousand Volt-hours. Low amperage was applied (50 µA per strip). The protocol of IEF is listed in **Table—11.**

Table—11│ IEF protocol

Step	Voltage	Phase	Time	Temperature
1	250 V	Rapid	15 min	20 °C
2	4000 V	Progressive	2 h	20 °C
3	4000 V	Rapid	Volts x hours	20 °C
4	500 V	Rapid	5 h	20 °C

After IEF, we proceeded to the second-dimension separation immediately or stored the IPG strips at -80 °C. The second-dimension separation consists to separate proteins according to their molecular weight. The SDS-PAGE was performed on vertical systems (PROTEAN 3 BioRad) , and it consists of four steps: (1) Preparing the second-dimension gel, (2) equilibrating the IPG strip in SDS buffer, (3) placing the equilibrated IPG strip on the SDS gel, and (4) electrophoresis.

The equilibration step saturates the IPG strip with the SDS buffer system required for the second-dimension separation. It was performed with 10 mL of Equilibration solution for 15 min. An additional equilibration step for 20 min, replaces DTT with iodoacetamide to reduce point streaking and other artifacts. The composition of the Equilibration solution is listed in **Table—12.**

After equilibration step, IPG strip were placed on the top of SDS-PAGE (15% to separate 17 and 26 kDa proteins) covered by a thin layer of 0.5% low melting agarose that helps proteins to penetrate the gel. Electrophoresis was performed at 20 Volt during 15-30 min to allow protein penetration on the gel then at 100 Volt for 1-2 hours. Because of the small amount of proteins used on this technique, the second-dimension gels were blotted onto a PVDF membrane for immunochemical detection of specific proteins.

Table—12 *Equilibration solution composition*

Equilibration solution	Amount	Role
Tris-HCl (pH 8.8)	0.375 M	maintains IPG strip pH in a range appropriate for electrophoresis
Urea	6 M	Together with glycerol reduces the effects of electroendosmosis by increasing the viscosity of the buffer
Glycerol	20 %	together with urea reduces electroendosmosis and improves transfer of protein from the first to the second-dimension
SDS	2 %	denatures proteins and forms negatively charged protein-SDS complexes
DTT	100 mg	preserves the fully reduced state of denatured, unalkylated proteins
Iodoacetamide	150 mg	alkylates thiol groups on proteins, preventing their reoxidation during electrophoresis
Bromophenol blue	0.002 %	allows monitoring of electrophoresis

2.2.8. Yeast two-hybrid assay

Yeast two-hybrid system (Y-2H) was used to study *in vivo* the interaction between ToRP1 and eIF4E1 and TOR.

a. Preparation of competent AH109 yeast cells

50 mL of YPD media were inoculate with a single colony 2–3 mm in diameter from a fresh plate (no more than 3 weeks old) and grown overnight at 30 ˚C with shaking at 250 rpm. The overnight culture was diluted to an OD_{600} of 0.2-0.3 in fresh YPD media and continued to grow until the OD_{600} reaches 0.6. The culture was centrifuged at 1000 x g for 10 min, and then the supernatant was discarded. Cell pellet was washed by 50 mL 1X **TE buffer** followed

by centrifugation again. The supernatant was decanted and cell pellet was resuspended in 1.5 mL of freshly prepared, sterile 1X **TE/LiAc buffer** and kept in ice until transformation.

TE buffer: *10 mM Tris-HCl (pH 7.5), 1 mM EDTA*

TE/LiAc buffer: *TE buffer, 100 mM Lithium acetate*

b. Transformation of competent yeast cells

Competent yeast cells transformation was followed by the Lithium acetate/single-stranded carrier DNA/polyethylene glycol method. This method currently gives the highest efficiency and yield of transformants.

In a separate 1.5 mL tube containing 1 µg of the BD-bait encoding DNA, 1 µg of the AD-prey encoding DNA and 100 µg of herring testes carrier DNA, 100 µL of yeast competent cells were added to each tube and mixed well by vortexing. 600 µL per transformation of sterile freshly made **PEG/LiAc solution** were added to tube followed by a gentle vortexing to mix. The mixtures were incubated at 30 °C for 30 min with shaking at 250 rpm. A volume of 70 µl of DMSO was added to each transformation. The contents of the tubes were mixed well by gentle inversion, and then incubated at 42 °C for 15 min heat shock. Cells were chilled on ice for 1-2 minutes and then centrifuged for 30 sec at 16000 x g at room temperature. The supernatant was removed and the cells were resuspended in 200 µL of sterile dH_2O. The entire transformation mix was plated onto solid selective minimal SD media lacking the appropriate amino acids to allow for selection of successfully transformed cells. The plates were incubated at 30 °C for 3-5 days until colonies appear.

PEG/LiAc: *40% (v/v) polyethlylene glycol-3350, 10 mM Tris-HCl (pH 7.5), 1 mM EDTA, 100 mM Lithium acetate*

c. Preparation of yeast whole cell lysates

In order to evaluate the BD-bait and AD-prey expression levels, by immunoblot analysis, yeast whole cell lysates were prepared using the urea/SDS protein extraction method. Five mL of the appropriate selective media was inoculated by five yeast cell colonies, and the culture was incubated overnight at 30 °C with shaking at 250 rpm. The overnight culture was diluted at an OD_{600} of 0.3 in the appropriate volume of fresh YPD media the following day and was further incubated at 30 °C until an OD_{600} of 0.8. 1.5 mL of cells was pelleted by centrifugation at 1000 x g for 5 min at 4 °C in duplicates. Cell pellet was immediately resuspended in 150 µL of **urea/SDS cracking buffer**, and then incubated at 70 °C for 10 min. After incubation, the mixtures were processed on a mini-Precellys24 Homogenize at one 30 sec cycle of 6500 x g, and then heated for 10 min at 95 °C at 1500 rpm in a Thermomixer® (Eppendorf®, France). Five minutes of centrifugation at max speed at 4 °C was necessary to pellet cell debris. An equal volume of the whole cell lysates was loaded onto a SDS-PAGE gel followed by immunoblot analysis, to assess protein expression levels.

> ***Urea/SDS cracking buffer:*** *8 M urea, 5% (w/v) SDS, 40 mM Tris-HCl (pH6.8), 0.1 mM EDTA, 0.4 mg/mL bromophenol blue, cOmplete® protease inhibitor cocktail (Roche®), PhosSTOP Phosphatase Inhibitor cocktail (Roche®), 1 mM sodium molybdate, 1 mM sodium fluoride, 80 mM β-glycerol phosphate*

2.2.9. Molecular modeling

The 3D putative structure of *Arabidopsis* ToRP1 and ToRP2 proteins were obtained from RaptorX: a Web Portal for Protein Structure and Function Prediction (http://raptorx.uchicago.edu).

2.3. Techniques for plant

2.3.1. Seed sterilization

The seeds were sterilized by 20 min incubation in solution containing 5% (v/v) bleach and 70% (v/v) ethanol, followed by washing in absolute ethanol. Seeds were then dried and plated under a sterile hood on appropriate MS-Agar (Murashige and Skoog medium with MSMO-salt mixture; Sigma®) plates. The plates were stored 24 hours at 4 °C in the dark, for germination synchronization. Arabidopsis thaliana plants were grown for seven days under long-day conditions (16h of light at 21 °C and 8h of darkness at 17 °C). To study Phosphorylation of ToRP proteins in TOR responsive manner, Arabidopsis thaliana seedlings were treated with either TOR inhibitor (AZD-8055) or TOR activator (2,4-D). MS-Agar plates were supplemented with either 0.5 µM AZD or 0.1 µg/mL 2-4D.

2.3.2. Transient expression for protoplast GUS-assays

Protoplasts were prepared from *Arabidopsis thaliana* wild-type, ToRP1 overexpressed, ToRP2 overexpressed or *torp1 torp2* knockout mutant seedlings, under sterile conditions following the protocol described in Yoo et al. (2007). Protoplasts were cotransfected with two reporter plasmids—monocistronic reporter—pmonoGFP (a transfection marker) and β-glucuronidase, GUS reporter fused to 5'-UTR of GIP1 or CyclinB1;1—p*GIP1* 5'UTR-GUS or p*CYCB1;1* 5'UTR-GUS (a cap dependent translation initiation marker). 2 and 5 µg of each leader-GUS-containing constructs were used for co-transfection with 5 µg of pmonoGFP.

Digestion buffer was prepared and then heated for 10 min at 55 °C to inactivate DNase and proteases and enhance enzyme solubility, supplemented with 10 mM $CaCl_2$ and 0.1% BSA. Leaves from 7 dag seedlings were collected and placed in Petri dishes, and then they were finely and slightly cut by tapping tissue on the top in presence of 25 mL of Digestion buffer. Digestion mixtures were vacuum infiltrated for 10 min using a desiccator, and incubated 4

hours at 28 °C with gentle mix. Twenty ml of **W5 solution** were added to the mix. Protoplasts were filtrated through a Miracloth membrane previously submerged in W5 solution and centrifuged for 2 min 1000 x g without brake. Protoplasts were washed with 10 mL of mannitol and resuspended in 1-5 mL of **MMG solution**. The final volume was adjusted to obtain 10^6 protoplasts per 1 mL, the optimal concentration for transfection.

100 µL of protoplasts were mixed with 5 µg of pmonoGFP and either 2 µg or 5 µg of pleader-GUS (pGIP1 5'UTR-GUS or pCYCB1;1 5'UTR-GUS) diluted in 20 µL in the presence of 120 µL of **PEG solution** and then incubated for 15 min at room temperature for PEG-mediated transfection. To stop reaction, 1 mL of W5 solution was added, and protoplasts were centrifuged for 2 min at 1000 x g, and resuspended in 1 mL of **WI solution**. Mixtures were transferred into 12-well culture Greiner plates and incubated in dark for 16 h at 26 °C.

After incubation, protoplasts were pelleted by centrifugation for 2 min at 500 x g, resuspended in 180 µL of dH_2O, and then transferred into fresh 1.5 mL tubes containing 20 µL of **10X GUS Extraction buffer**. After 15 sec of vortex, samples were incubated for 10 min at room temperature, centrifuged for 10 min at 16000 x g and then supernatants were carefully transferred into fresh new tubes for GUS-activity quantification.

GUS-activity quantification is based on the cleavage of β-glucuronidase substrate 4-methylumbelliferyl β-D-glucuronide (MUG) (Jefferson et al. 1987). 150 µL of each sample was loaded by duplicate in an opaque 96-wall plate. GFP-generated fluorescence was measured on a FLUO-star plate reader (BMG Lab technologies Inc., France) at 450 nm when excited at 520 nm. The assay was occurred when 150 µL **2X GUS Assay Buffer** was added to each sample in a 96-wall plate placed in a dark microplate incubator (modem Stat-Fax 2200, Awareness technology®) at 37 °C with orbital mixing at 600 rpm. Fifty µL of the reaction was transferred to 50 µL of **2X Stop Buffer** in a 96-well plate. GUS fluorescence was measured at 355 nm when excited at 460 nm. Values were converted to GUS relative units

and then normalized by GFP protein fluorescence to accommodate differences in protoplasts transfection efficiency.

Digestion buffer: *1.5% (w/v) cellulase R10 (Yakult Pharmaceutical®), 0.4% (w/v) macerozyme R10 (Yakult Pharmaceutical®), 0.4 M mannitol, 20 mM KCl, 20 mM MES (pH 5.7)*

W5 solution: *2 mM MES (pH 5.7), 154 mM NaCl, 125 mM CaCl2, 5 mM KCl*

MMG solution: *0.4 M mannitol, 15 mM $MgCl_2$, 4 mM MES (pH 5.7)*

PEG solution: *30% (w/v) PRG 4000 (Fluka®), 200 mM mannitol, 100 mM $CaCl_2$*

WI solution: *0.5 M mannitol, 20 mM KCl, 4 mM MES (pH 5.7)*

10X GUS Extraction buffer: *500 mM Tris-HCl (pH 7.5), 100 mM EDTA (pH 8.0), 1% (v/v) Triton X-100 and 1% (v/v) Igepal 360®*

2X GUS Assay Buffer: *10X GUS extraction buffer, 2 mM 4-methylumbelliferyl β–D-glucuronide (MUG, Sigma®), 0.1% (w/v) BSA, 1 mM DTT*

2X Stop Buffer: *400 mM sodium carbonate*

V. Résumé en Français

Résumé

Chez les mammifères l'initiation de la traduction et, plus particulièrement, la formation du complexe eIF4F, est principalement régulée par la protéine kinase TOR (Target of rapamycin). Cette voie de régulation fait intervenir les protéines 4E-BP (eIF4E-binding proteins) dont l'activité est modulée par la phosphorylation par TOR. Sous leur forme non-phosphorylée, les 4E-BP se lient au facteur d'initiation eIF4E, empêchent son recrutement dans le complexe eIF4F et inhibent ainsi l'initiation de la traduction. Phosphorylées par TOR, les 4E-BP perdent leur affinité pour eIF4E et sont remplacées par eIF4G ce qui active la traduction. La régulation de l'initiation de la traduction par TOR via 4E-BP a été bien décrite dans plusieurs modèles eucaryotes, tels que la levure, les insectes et les mammifères, mais reste encore obscure chez les plantes. Les recherches réalisées au cours de ma thèse ont permis l'identification de deux protéines homologues de 4E-BP chez *Arabidopsis*. Ces protéines, que nous avons appelées ToRP1 et ToRP2 (TOR Regulatory Proteins), sont caractérisées par la présence d'un motif consensus indispensable pour la liaison à eIF4E, et qui existe chez les protéines 4E-BP des mammifères ainsi que chez eIF4G et eIFiso4G d'*Arabidopsis*. La protéine ToRP1 est capable d'interagir spécifiquement avec eIF4E, mais aussi avec TOR via son extrémité N-terminale en système double-hybride de levure. ToRP1 et ToRP2 ont également été caractérisées comme étant des cibles directement phosphorylées par TOR chez *Arabidopsis*. Deux sérines, en position 49 et 89 dans la protéine ToRP1, ont été identifiées comme des sites potentiels de cette phosphorylation. De plus, l'état de phosphorylation de ces sites affecte l'interaction avec eIF4E en système double-hybride de levure. Par ailleurs, des plants d'*Arabidopsis* déficients en ToRP1 et ToRP2 renforcent la traduction strictement coiffe-dépendante de l'ARNm CYCB1;1, alors que la surexpression de ToRP1 ou de ToRP2 réprime sa traduction. Ces résultats suggèrent donc que les protéines

ToRP, identifiées chez *Arabidopsis,* sont de nouvelles cibles directes de TOR, qui, par leur phosphorylation, régule l'initiation de la traduction coiffe-dépendante.

Mots clés : voie de signalisation de TOR, 4E-BP, initiation de la traduction coiffe-dépendante, *Arabidopsis,* ToRP

Introduction

Chez les eucaryotes, la synthèse des protéines est principalement contrôlée en phase d'initiation, mais les mécanismes moléculaires de la régulation de la traduction ne sont pas entièrement élucidés, en particulier chez les plantes. L'initiation de la traduction débute par l'assemblage coopératif du facteur d'initiation 3 (eIF3), eIF1, eIF1A et du complexe ternaire (TC; eIF2-GTP-Met-ARNt_i^{Met}) sur la petite sous-unité ribosomale 40S, entrainant la formation du complexe de pré-initiation 43S (43S PIC) (Jackson et al. 2010 ; Browning and Bailey-Serres 2015). Le complexe 43S est ensuite recruté sur la coiffe en extrémité 5' de l'ARNm, qui est préalablement activé par liaison du complexe eIF4F composé d'une protéine de liaison à la coiffe (eIF4E), d'une protéine chaperonne (eIF4G) et d'une ARN hélicase 4A (eIF4A) (Hinnebusch 2014). eIF4F recrute l'ARNm au complexe 43S via des interactions entre eIF4G, eIF4B et eIF3 associé à 40S, tandis que le TC délivre l'initiateur Met-ARNt_i^{Met} (Pestova et al. 2007). Le complexe 43S PIC balaye l'ARNm jusqu'à atteindre le premier codon AUG dans un contexte d'initiation approprié, où la grande sous-unité ribosomale 60S sera recrutée et l'élongation commence (Kozak 1999). L'activation de la traduction d'ARNm dépend ainsi de l'assemblage rapide du complexe eIF4F à la coiffe de l'ARNm.

Le complexe mTORC1 (Mammalian/ mechanistic target of rapamycin complex 1) (Kim et al. 2002) est la composante clé d'une voie de signalisation dépendante des nutriments et des hormones, contrôle positivement la croissance cellulaire en partie par stimulation de la traduction. TORC1 facilite la traduction par phosphorylation directe ou indirecte des composants de la machinerie de traduction de l'hôte (Ma and Blenis 2009 ; Roux and Topisirovic 2012). Deux classes principales de substrat de mTORC1 ont été identifiées, les protéines de liaison d'eIF4E (4E-BP, eIF4E-binding proteins) et les protéines ribosomiques kinases S6 (S6Ks) (Gingras et al. 1999a).

4E-BP réprime l'initiation de la traduction en se liant à eIF4E, empêchant ainsi la formation du complexe eIF4F. Chez les mammifères et chez la drosophile, mTORC1 contrôle la traduction à l'étape d'initiation, principalement en affectant l'assemblage du complexe eIF4F sur la coiffe en 5' de l'ARNm via la phosphorylation et l'inactivation des 4E-BP (Gingras et al. 1999a ; Hershey and Merrick 2000 ; Raught et al. 2000). Les 4E-BP exercent leur effet inhibiteur sur l'initiation de la traduction par compétition avec eIF4G pour se lier au même motif de résidus hydrophobes conservés de eIF4E, bloquant ainsi l'initiation de la traduction. En conséquence, eIF4G et les 4E-BP partagent un site de liaison canonique à eIF4E de séquence $YX_4L\phi$ (dénommé 4E-BM, où Y représente Tyr, X désigne n'importe quel acide aminé, L désigne Leu, et ϕ désigne un résidu hydrophobe) (Mader et al. 1995 ; Marcotrigiano et al. 1999). La liaison de 4E-BP à eIF4E est inhibée par phosphorylation à des sites multiples de 4E-BP par TOR, et la traduction cap-dépendante est restaurée (Gingras et al. 1999a ; Gingras et al. 2001). L'hyper-phosphorylation des 4E-BP réduit leur affinité pour eIF4E et les libère de eIF4E. Ceci permet à eIF4E de lier eIF4G, avec la formation subséquente du complexe eIF4F, ce qui conduit à l'activation de la traduction. En réprimant l'initiation de la traduction, les 4E-BP inhibent la prolifération cellulaire et agissent comme des suppresseurs de tumeurs (Martineau et al. 2013).

4E-BPs existent sous forme de trois isoformes-4E-BP1 (PHAS, phosphorylated heat- and acid- stable), 4E-BP2 et 4E-BP3 contenant 118, 120 et 100 résidus d'acides aminés (Pause et al. 1994 ; Lin et al. 1994 ; Lawrence Jr and Abraham 1997 ; poulin et al. 1998). Les protéines 4E-BP1 et 4E-BP2 contiennent plusieurs sites de phosphorylation qui sont sensibles à TOR, et leur phosphorylation se déroule dans un ordre hiérarchique (Gingras et al. 1999a ; Gingras et al. 2001). Bien que la phosphorylation de 4E-BP1 et 4E-BP2 soit sensible à la rapamycine, la phosphorylation de 4E-BP3 ne l'est pas (Lin and Lawrence 1996 ; Kleijn et al. 2002). Trois motifs de 4E-BP, comprenant des motifs non canoniques et canoniques de liaison à eIF4E (4E-BM, eIF4E-binding motifs), sont nécessaires pour que les 4E-BP puissent entrer en compétition avec eIF4G pour la liaison à eIF4E, tandis que le motif en C-terminal (TOS) est un site de liaison à RAPTOR (Peter et al. 2015). La phosphorylation de 4E-BP par TOR régule la disponibilité de eIF4E et donc la traduction coiffe-dépendante. Ainsi, mTORC1 régule l'efficacité de la traduction des ARNm contenant des motifs 5’TOP (5’-terminal oligopyrimidine) (Thoreen et al. 2012).

Chez les plantes à fleurs, le complexe eIF4F existe en tant que eIF4E, qui se couple avec eIF4G, et l'isoforme spécifique de la plante eIFiso4E, qui se couple avec eIFiso4G pour former eIFiso4F (Mayberry et al. 2011; Patrick and Browning 2012). Chez *Arabidopsis*, eIF4E est codé par plusieurs gènes (eIF4E1, eIF4E2 et eIF4E3), alors qu’eIFiso4E est codé par un seul gène. AteIFiso4G est codé par deux gènes, et leur double mutant présente des défauts de croissance et de reproduction (Lellis et al. 2010). Comme les mammifères, les plantes possèdent un seul gène TOR, dont l’inhibition est corrélée avec une diminution de la taille de la plante et une résistance au stress (Menand et al. 2002 ; Deprost et al. 2007 ; Ren et al. 2012). RAPTOR et LST8 d’*Arabidopsis* ont été caractérisés comme des composants du complexe TORC1 (mahfouz et al. 2006 ; Dobrenel et al. 2011 ; Moreau et al. 2012), alors qu'aucun composant du complexe TORC2 n'a encore été identifié chez les plantes. Le

substrat le mieux caractérisé de TORC1, impliqué dans la traduction végétale, est S6K1, par lequel TOR peut contrôler la croissance et la prolifération (Schepetilnikov et al. 2011 ; Xiong and Sheen 2012). Les plantes d'*Arabidopsis* n'exprimant pas TOR présentent une réduction de polysomes (Deprost et al. 2007), ce qui suggère un rôle de TOR dans le contrôle de la traduction des plantes. En effet, nous avons caractérisé une nouvelle fonction régulatrice de TOR dans la réinitiation de la traduction des ARNm possédant des uORF (upstream open reading frames) (Schepetilnikov et al. 2013). Cependant, la question de savoir si TOR peut contrôler l'initiation de la traduction coiffe-dépendante reste toujours ouverte.

Ici, nous avons identifié des petites protéines non structurées chez *Arabidopsis,* cibles de la voie de signalisation de TOR et pouvant interagir avec eIF4E. Leur caractérisation et leur effet sur l'initiation de la traduction coiffe-dépendante sont présentés ci-dessous.

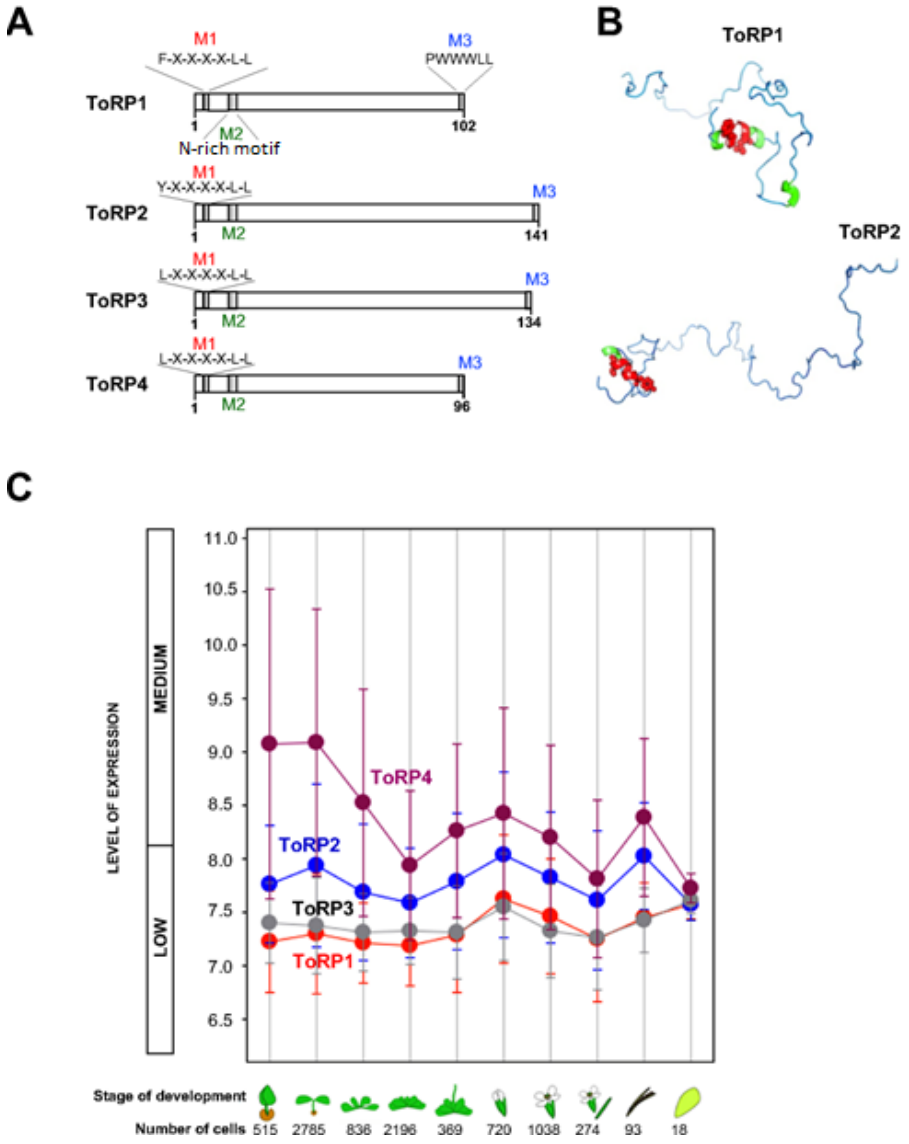

Figure—1 : Identification de petites protéines, chez *Arabidopsis*, ayant un motif de liaison à eIF4E

(A) Représentation schématique des protéines ToRP (TOR regulatory proteins ; ToRP1-4) d'*Arabidopsis*; trois motifs conservés sont représentés: M1-le motif canonique de liaison à eIF4E de séquence YX_4LL (appelé 4E-BM, où Y représente Tyr, X désigne n'importe quel acide aminé et L désigne Leu); M2-le motif riche en asparagine et M3-le motif conservé en C-terminal.

(B) La structure secondaire putative de ToRP1 et ToRP2 générée par le programme RAPTOR qui révèle des hélices-α : *en rouge* et des feuillets-β : *en vert.*

(C) Les profils de transcription des protéines ToRP ont été extraits de la base de données Genevestigator (https://www.genevestigator.ethz.ch).

Résultats

Identification d'une petite famille de protéines ayant des sites canoniques et non-canoniques de liaison à eIF4E

Une analyse approfondie des bases de données d'*Arabidopsis* a permis d'identifier quatre protéines homologues de 102, 141, 134 et 96 acides aminés, que nous avons appelées ToRP (TOR regulatory proteins ; ToRP1, ToRP2, ToRP3 et ToRP4, respectivement) (Figure 1A). Ces protéines contiennent trois domaines conservés, M1-M3, le motif M1 de ToRP2 représente le site canonique de liaison à eIF4E de la séquence $YX_4L\phi$ (dénommé 4E-BM, où Y représente Tyr, X désigne n'importe quel acide aminé, L désigne Leu et ϕ désigne un résidu hydrophobe) trouvé dans tous les 4E-BM de mammifères (Mader et al. 1995 ; Marcotrigiano et al. 1999). ToRP1 contient un motif similaire qui commence par F (Phe), mais l'analyse des 4E-BM dans eIF4G et eIFiso4G révèle à la fois le motif canonique 4E-BM et un motif où Tyr est remplacé par Phe, indiquant que, chez *Arabidopsis*, eIF4E ou eIFiso4E interagissent avec eIF4G ou eIFiso4G via YX_4LL et FX_4LL, respectivement (Figure 1A). De plus, Tyr est remplacé par Leu dans le motif correspondant aux 4E-BM des protéines ToRP3 et ToRP4. Le motif M2 est enrichi en asparagine (Asn), similaire à une séquence présente dans la protéine 4E-BP2 de mammifère (Bidinosti et al. 2010). Le motif M3 est riche en Trp et se trouve à l'extrémité C-terminale des ToRP.

Un modèle 3D d'*Arabidopsis* ToRP1 et ToRP2, généré par RaptorX (Kallberg et al. 2012), prédit, avec une forte probabilité, des protéines intrinsèquement désordonnées qui n'ont pas de structure secondaire (Figure 1B), comme 4E-BP1 (Fletcher et al. 1998 ; Fletcher and Wagner 1998). Malgré sa faible abondance chez *Arabidopsis thaliana*, selon la base de données Genevestigator (Figure 1C), nous avons sélectionné ToRP1 pour examiner plus en détail son association avec eIF4E ou eIFiso4E.

ToRP1 se lie à eIF4E en système double-hybride de levure

En considérant le rôle de 4E-BM dans la liaison à eIF4E, nous avons étudié la liaison de ToRP1 à eIF4E, et nous avons utilisé l'interaction de eIFiso4G à eIF4E comme contrôle positif. Nous avons d'abord déterminé que ToRP1 peut interagir avec eIF4E en système double-hybride de levure, bien qu'avec une intensité légèrement inférieure à celle de eIFiso4G2 (Figure 2A). En outre, la mutation de Phe en Tyr à la première position de 4E-BM de ToRP1 a amélioré substantiellement l'interaction ToRP1-eIF4E, tandis que la substitution de Phe par Val a presque supprimé l'interaction. De façon surprenante, la substitution de Phe par Leu, qui est présente à cette position dans les protéines ToRP3 et ToRP4, n'a pas réduit la liaison ToRP1 à eIF4E, ce qui indique que le motif 4E-BM avec Leu à la place de Tyr peut également induire la liaison à eIF4E comme le type sauvage. Une étude minutieuse des séquences de ToRP n'a pas révélé de motif TOS normalement présent à l'extrémité C-terminale des 4E-BP chez les mammifères, et qui fonctionne en présentant divers substrats à TOR pour leur phosphorylation. Par conséquent, nous nous sommesdemandé si ToRP1 interagit avec TOR directement via sa moitié N- ou C-terminale. De façon surprenante, en système double-hybride de levure, ToRP1 interagit avec le domaine HEAT de TOR (NTOR) (Figure 2), mais pas avec la moitié C-terminale de TOR (données non représentées). Bien que la substitution de Phe pour Val ait aboli la liaison de ToRP1 à eIF4E, la liaison à NTOR n'a pas été affectée, ce qui indique que la liaison à TOR n'est pas dépendante de 4E-BM.

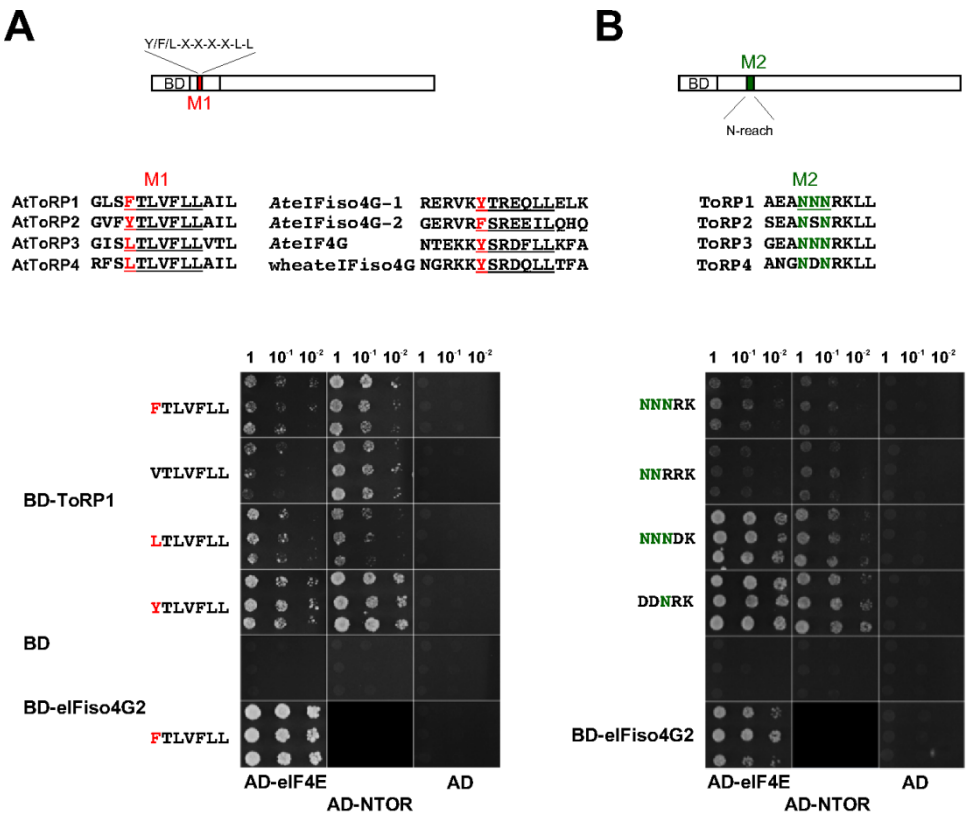
A
Y/F/L-X-X-X-X-L-L
BD
M1
M1
AtoRP1 GLSFTLVFLLAIL
AtoRP2 GVFYTLVFLLAIL
AtoRP3 GISLTLVFLLVTL
AtoRP4 RFSLTLVFLLAIL
AteIFiso4G-1 RERVKYTREQLLELK
AteIFiso4G-2 GERVRFSREEILQHQ
AteIF4G NTEKKYSRDFLLKFA
wheateIFiso4G NGRKKYSRDQLLTFA
1 10-1 10-2 1 10-1 10-2 1 10-1 10-2
FTLVFLL
VTLVFLL
BD-ToRP1
LTLVFLL
YTLVFLL
BD
BD-eIFiso4G2
FTLVFLL
AD-eIF4E
AD
AD-NTOR
B
M2
BD
N-reach
M2
ToRP1 AEANNNRKLL
ToRP2 SEANSNRKLL
ToRP3 GEANNNRKLL
ToRP4 ANGNDNRKLL
1 10-1 10-2 1 10-1 10-2 1 10-1 10-2
NNNRK
NNRRK
NNNDK
DDNRK
BD-eIFiso4G2
AD-eIF4E
AD
AD-NTOR
C
PWWWLL
BD
M3
M3
ToRP1 SGKPWWWLL
ToRP2 SGQPWWWLL
ToRP3 PAKPWWWLL
ToRP4 KSLWSFLNL
1 10-1 10-2 1 10-1 10-2 1 10-1 10-2
PWWWLL
SWWWLL
PWWWWL
PYYYLL
PAAAAA
BD
AD-eIF4E
AD
AD-NTOR

Figure—2 : ToRP1 d'*Arabidopsis* se lie à eIF4E et au domaine HEAT de TOR au niveau de son extrémité N-terminale, alors que les motifs M1-3 atténuent cette liaison en système double-hybride de levure

(A-C) *Bilan des interactions en système de double-hybride de levure* entre eIF4E et eIF4G et ToRP1 ou ses dérivés mutants. *Panneau supérieur* : Présentation schématique de la protéine ToRP1 fusionnée au domaine de liaison de Gal4 (BD; le motif étudié est indiqué). *Panneaux centraux :* (A) Alignement des motifs canoniques de liaison à eIF4E des ToRP1-4 d'*Arabidopsis* et d'eIF4G/eIFiso4G d'*Arabidopsis* et du blé. Alignement des séquences des motifs M2 (B) et des motifs M3 deToRP (C). Les alignements des séquences ont été préparés selon les matrices de substitution d'acides aminés Blossom 62.

Panneau inférieur : Interactions en système double-hybride de levure entre le domaine d'activation Gal4 (AD), AD-NTOR, AD-eIF4E et BD-eIFiso4G2, et ToRP1, WT ou muté, fusionnée à BD. Les interactions en système double-hybride de levure sont présentées en triple exemplaire pour chaque combinaison de protéines de fusion AD et BD. Des unités égales d'OD_{600} et des dilutions 1/10 et 1/100 ont été tachetées de gauche à droite et incubées pendant 2 jours. Les mutations sont mises en évidence en rouge (M1), vert (M2) et bleu (M3).

Le motif M2 de ToRP1 est relié à 4E-BM par l'intermédiaire d'un linker de 9 à 10 acides aminés similaire au motif présent dans 4E-BP2 de l'humain (Peter et al. 2015). Il est intéressant de noter que les mutations de l'asparagine, ou de deux résidus d'asparagine conservés, en aspartate (N26D ou N25D / N26D) dans le motif M2 de ToRP1 augmentent considérablement la liaison à eIF4E et à NTOR (Figure 2B). De plus, la désamination de l''asparagine de 4E-BP2 enrichie au niveau du cerveau a été décrite comme une modification post-traductionnelle spécifique au cerveau (Bidinosti et al. 2010). L'extrémité C-terminale de ToRP1 (M3) est riche en résidus aromatiques et joue un rôle critique dans la liaison de ToRP1 à eIF4E en système double- hybride de levure, puisque les mutations P97S et L100W inhibent les interactions avec eIF4E et la substitution de trois résidus Trp pour Tyr, ou le remplacement des cinq derniers acides aminés par des alanines ont supprimé l'interaction à la fois avec eIF4E et NTOR (Figure 2C).

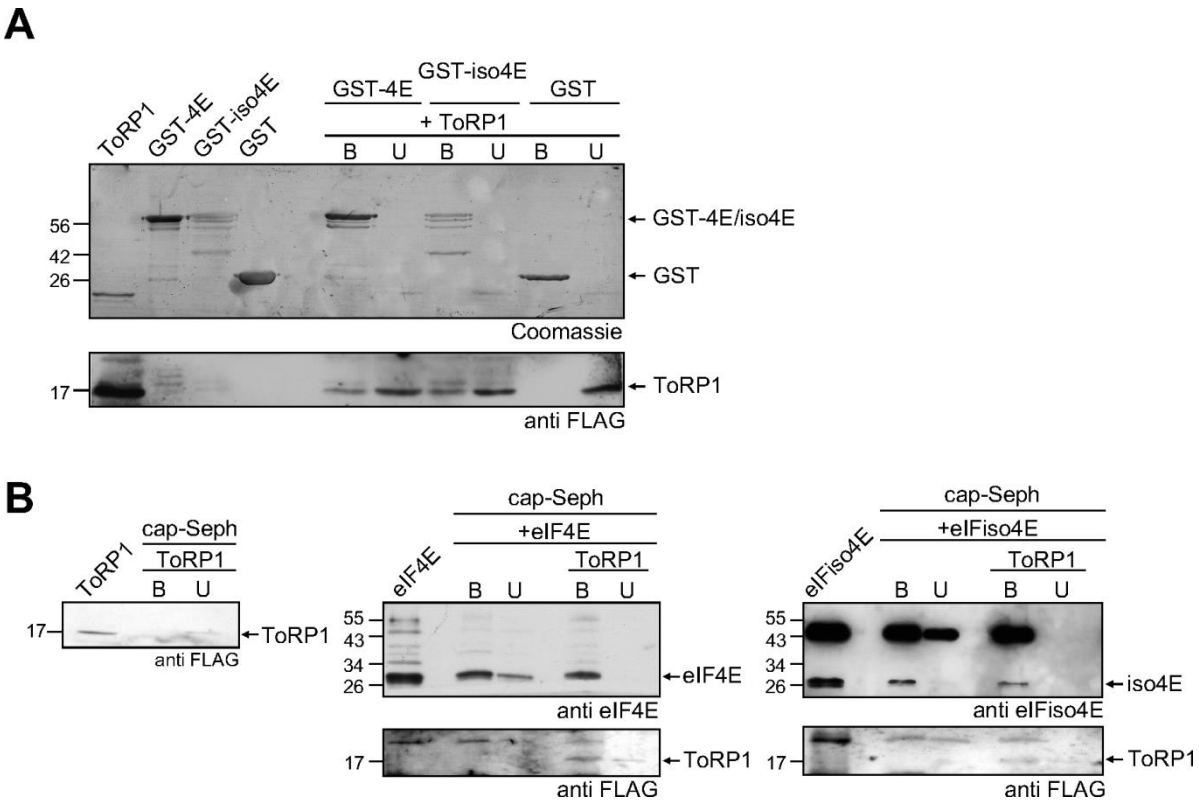

Figure—3: ToRP1 d'*Arabidopsis* interagit spécifiquement avec eIF4E (et eIFiso4E) lorsqu'ils sont liés ou non à la structure de la coiffe

(A) *Expériences de GST pull-down* : les facteurs eIF4E-, eIFiso4E- étiquetés avec la GST et la GST seule ont été testés pour l'interaction avec ToRP1 ayant une étiquette FLAG. *Panneau supérieur* : Les fractions de fusion GST ont été colorées par du bleu de Coomassie. *Panneau inférieur* : ToRP1 a été révélée par Western blot en utilisant des anticorps anti-FLAG. Les résultats montrés représentent les moyennes obtenues dans trois expériences indépendantes.

(B) *Expériences de cap-sepharose pull-down* : ToRP1 n'associe pas à la coiffe seule. *Panneau de gauche :* Des protéines recombinantes eIF4E et eIFiso4E ont été pré-liées au cap-sepharose. Le complexe lavé formé entre eIF4E ou eIFiso4E avec cap-sepharose a été testé pour l'interaction avec ToRP1 étiquetée avec FLAG. eIF4E et eIFiso4E *(panneaux supérieurs)* et ToRP1 *(panneaux inférieurs)* ont été révélées par Western blot avec des anticorps anti-eIF4E et anti-eIFiso4E, et des anticorps anti-FLAG, respectivement.

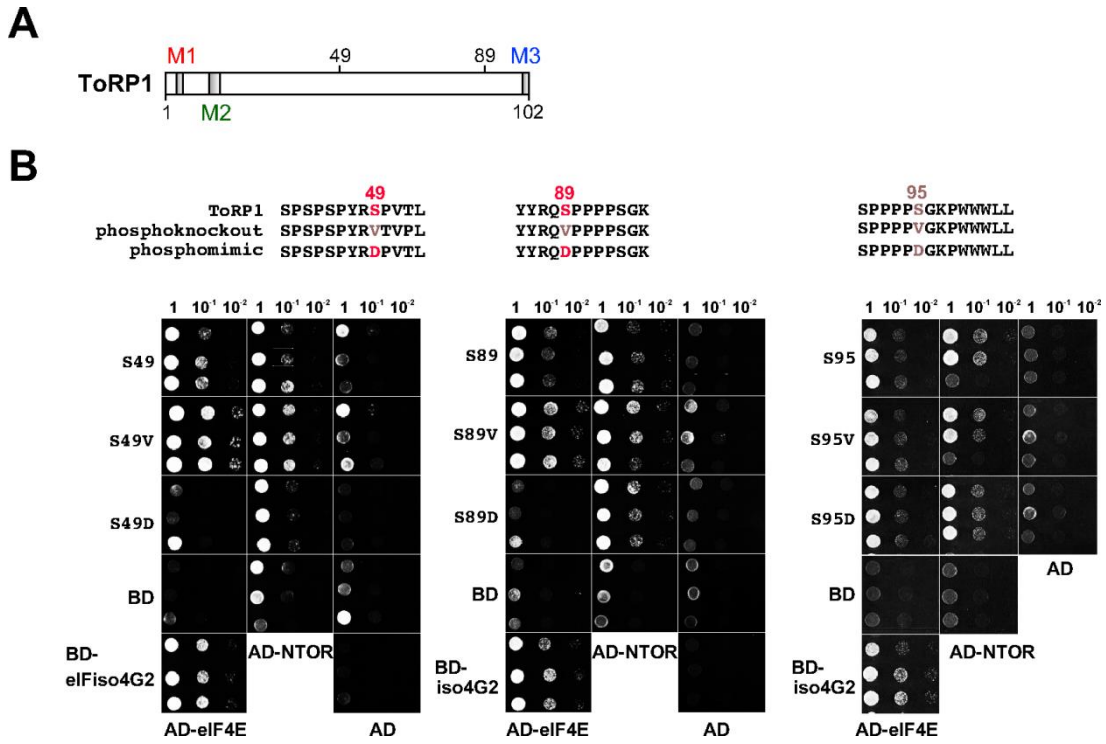

Figure—4 : La liaison de ToRP1 à eIF4E est sensible à la phosphorylation de Ser49 et Ser89

(A) Représentation schématique de ToRP1 (les positions de deux sites putatifs de phosphorylation spécifique de TOR sont indiquées).

(B) *Interactions en système double-hybride de levure*. *Panneaux supérieurs :* la séquence de motif WT comprenant S49, S89 et S95 ainsi les mutations mimétiques et les knockouts de phosphorylation sont indiquées.

Panneaux inférieurs: Interactions en système double-hybride de levure entre AD, AD-eIF4E, AD-NTOR et BD, BD-eIFiso4G2, BD-ToRP1 et ses mutants mimétiques et knockout de phosphorylation. Les interactions en système double-hybride de levure sont présentées en trois exemplaires pour chaque combinaison de protéines de fusion AD et BD. Des unités égales d'OD_{600} et des dilutions 1/10 et 1/100 ont été tachetées de gauche à droite et incubées pendant 2 jours.

L'interaction entre les protéines ToRP et eIF4E a été confirmée par des expériences de pull-down. ToRP1 interagit spécifiquement avec eIF4E-GST et eIFiso4E-GST dans des essais de GST pull-down (Figure 3A). Ensuite, nous avons testé si ToRP1 peut interagir avec eIF4E ou eIFiso4E lorsqu'ils sont liés à la coiffe. Ainsi, nous avons utilisé des billes m^7-GTP-Sepharose 4B préalablement liées à eIF4E ou à eIFiso4E purifiés à partir d'*E. coli*. Tout d'abord, nous avons constaté que ToRP1 ne s'associe pas avec les billes m^7-GTP-Sepharose (Figure 3B-*panneau de gauche*). Ensuite, des billes de m^7-GTP-Sepharose 4B ont été incubées avec un excès de eIF4E ou eIFiso4E (*panneau supérieur*), suivie d'incubation de fractions liées lavées avec ou sans ToRP1. ToRP1 s'associe spécifiquement à eIF4E lié à la coiffe (Figure 3B-*panneau central*) et à eIFiso4E lié à la coiffe (Figure 3B-*panneau de droite*). Ces résultats suggèrent que ToRP1 se lie à eIF4E ou eIFiso4E.

Remplacement de Ser49 ou Ser89 par Val augmente la liaison ToRP1-eIF4E, tandis que mutation de Ser49 ou Ser89 par Asp aboli cette liaison

L'analyse des sites de phosphorylation des substrats connus de TOR—Hs4E-BP1 (motif S65), ULK1 (motif S758), Grp10 (motif S150) et PatL1 (motif S184) (Kang et al. 2013)—a révélé des motifs similaires dans ToRP1 aux positions Ser49 et Ser89 et dans ToRP2 aux positions Ser49 et Ser128, respectivement (Figure 4), indiquant la phosphorylation des ToRP par TOR.

Nous avons envisagé la possibilité que les mutations mimétiques ou knockout des sites de phosphorylation Ser49 ou Ser89 de ToRP1 pourraient affecter ses interactions avec eIF4E. Les ToRP1 mutants S49V ou S89V ont montré une association accrue avec eIF4E, alors que les mutants S49D et S89D n'interagissaient pas avec eIF4E en système double-hybride de levure (Figure 4B-*panneaux gauche et central* respectivement). D'une manière frappante, ToRP1 portant une mutation S49D présentait une liaison fortement réduite à NTOR. En

revanche, des mutations similaires de Ser95, qui n'est pas liée à des sites de phosphorylation connus de TOR, n'ont pas affecté l'interaction ToRP1 ni avec eIF4E ni avec NTOR (Figure 4B-*panneau de droite*). Ainsi, la phosphorylation de ToRP1 affaiblit son association à la fois à eIF4E et NTOR, tandis que ToRP1 déphosphorylée a révélé des interactions plus fortes avec eIF4E. Ces résultats nous ont encouragés à étudier des phosphoisoforms de ToRP1 et ToRP2 *in planta*.

ToRP2 dans *Arabidopsis* présente cinq formes de phosphorylation par électrophorèse bidimensionnelle

Il a été montré précédemment au laboratoire que le traitement de plantules d'*Arabidopsis* par la phytohormone auxine induit la phosphorylation de TOR à S2424 et de S6K1 à T44 (résidu spécifique de TOR), alors que l'utilisation de l'inhibiteur de TOR AZD-8055 conduit à une inactivation de TOR (Schepetilnikov et al. 2013). AZD-8055 se lie au domaine de TOR dans la poche de liaison à l'ATP et inactive cette kinase (Chresta et al. 2010 ; Montané and Menand 2013). En considérant le rôle de l'auxine dans l'activation de TOR, nous avons analysé l'impact de l'activation de TOR sur l'état de phosphorylation des protéines ToRP1 et ToRP2 *in planta*. Pour répondre à cette question, nous avons cultivé des plantules sauvages, ou des plantules qui surexpriment ToRP1 ou ToRP2 7 jours après germination avec soit une concentration de 100 nM d'auxines synthétiques (2,4D) soit une concentration de 0,5 µM d'AZD-8055 (nous avons utilisé une concentration d'AZD-8055 réduite de deux fois pour prévenir tout effet cytotoxique global sur les plantules pendant un traitement médicamenteux prolongé). Pour contrôler l'état de phosphorylation de ToRP1 et ToRP2, nous avons analysé les deux extraits traités par l'auxine et l'AZD-8055 dans des expériences parallèles par électrophorèse en gel bidimensionnelle (2D) et Western blot en utilisant des anticorps

polyclonaux dirigés contre le motif M2, hautement conservé dans ToRP1 et ToRP2; cet anticorps reconnaît ToRP1 et ToRP2.

Pour la première dimension, des bandes de pH 7-10 avec un gradient non linéaire ont été utilisées pour augmenter la résolution dans la région de pH 7-10 qui correspond au pI théorique de 10,4 et 9,9 de ToRP1 et de ToRP2, respectivement. Trois états de phosphorylation différents ont été détectés pour ToRP1 traité avec l'auxine, et aucune phosphorylation n'a été détectée après application d'AZD-8055 (Figure 5A). Cinq états de phosphorylation différents ont été détectés pour ToRP2 en réponse à l'auxine, et des bandes de faible intensité ont été détectées dans des conditions d'inactivation de TOR (Figure 5B). L'isoforme 5 a été détectée dans la position la plus acide (pI = 7) et correspond probablement à la forme hyperphosphorylée de ToRP2. En présence d'auxine, nous avons observé une augmentation des spots 4 et 5 de ToRP2 (Figure 5B-*panneau de gauche*) par rapport à ceux observés avec les échantillons/plantules traitées aux conditions d'AZD-8055 (Figure 5B-*panneau de droite*). La forme hypophosphorylée de ToRP2 a été désignée comme spot 1; ce spot migre en SDS-PAGE avec une mobilité plus lente que celle de ToRP2 quand elle est phosphorylée. Nous avons conclu que ToRP1 et ToRP2 contiennent plusieurs sites de phosphorylation, et que leur phosphorylation est sensible à TOR.

Pour confirmer la phosphorylation de ToRP1 et ToRP2 en réponse à TOR, nous avons généré des plantules *ToRP2ox* qui surexpriment de manière stable ToRP2 avec une étiquette myc sous le contrôle du promoteur 35S. Lorsque des anticorps anti ToRP1/2 ont été utilisés, l'analyse de gel 2D a révélé un profil de phosphorylation pour ToRP2 (Figure 5C-*panneau supérieur*) semblable à celui de la Figure 5B. Dans ce cas, l'auxine a induit une augmentation des taches 4 et 5 de ToRP2 (Figure 5C-*2,4D*) par rapport au modèle correspondant à l'inactivation de TOR, où toutes les isoformes étaient de taille similaire (Figure 5C-*AZD-8055*).

L'identification de Ser49 et de Ser89 comme des sites potentiels de phosphorylation de TOR nous a incité à générer des anticorps phospho-spécifiques qui réagissent contre Ser49-P ou Ser89-P dans ToRP1 et ToRP2. La phosphorylation de Ser49 a été détectée dans les isoformes 4 et 5 de ToRP2 tandis que les anticorps anti-Ser89-P ont reconnu les isoformes 3, 4 et 5 de ToRP2. Ces expériences indiquent que la forme 4 correspond à ToRP2 phosphorylée en Ser49 tandis que la forme 3 correspond à une phosphorylation en Ser89. Donc, ToRP1 et ToRP2 contiennent tous deux des sites de phosphorylation qui sont phosphorylés en réponse à l'auxine de manière sensible à TOR.

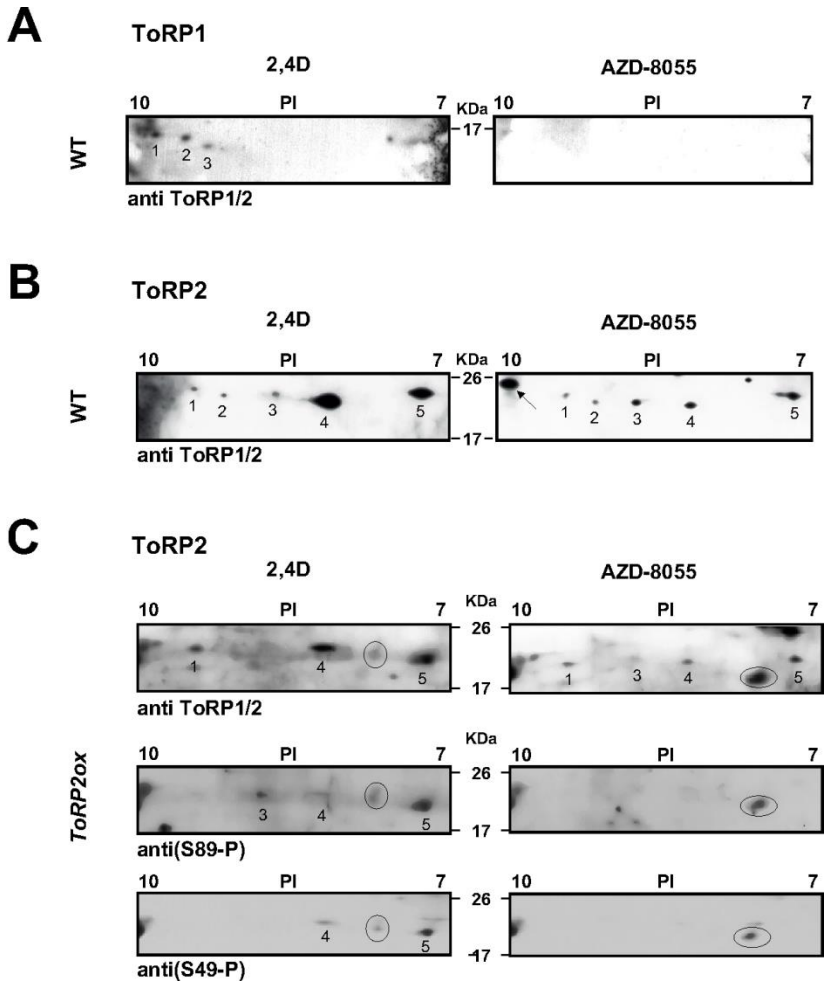

Figure—5 : Sensibilité de la phosphorylation de ToRP1 et ToRP2 à l'auxine et à l'inhibiteur de TOR (AZD-8055) révélée par électrophorèse sur un gel bidimensionnelle

Des échantillons d'extraits préparés à partir des plantules WT (A, B) ou des plantules surexprimant ToRP2 *(ToRP2ox)* (C), cultivés sur un milieu d'agar contenant soit 2,4D soit AZD-8055 ont été séparés en électrophorèse sur un gel bidimensionnelle suivi de Western blot avec des anticorps dirigé contre le motif M2 (anti ToRP1/2 ; *panneau supérieur A, B et C*), et des anticorps phosphospecifiques anti S89-P (*panneau central C*) et anti S49-P (*panneau inférieur C).* Les spots réactifs aux anticorps ont été désignés par 1 à 3 pour ToRP1 et 1 à 5 pour ToRP2. Les résultats sont représentatifs de trois expériences indépendantes.

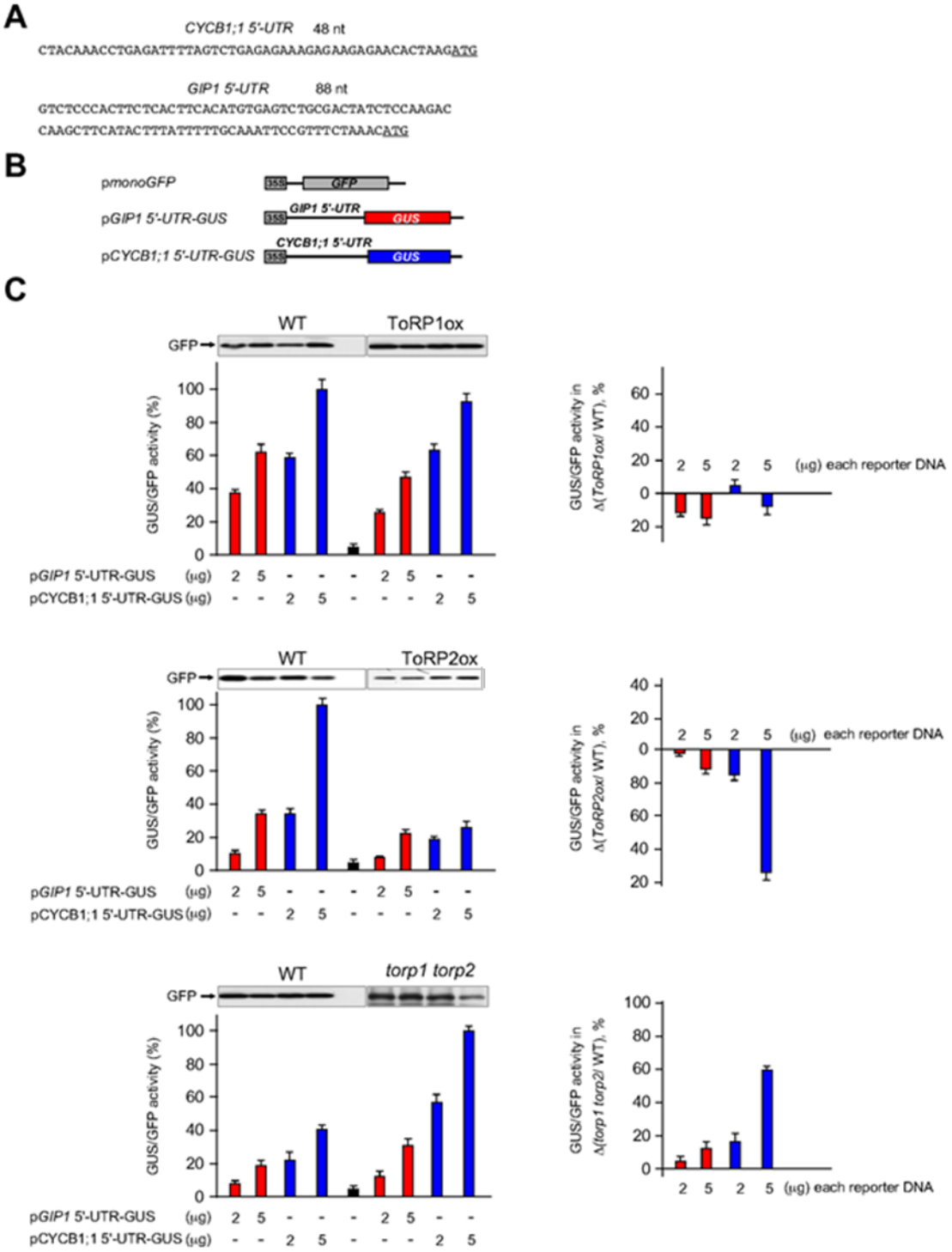
A
CYCB1;1 5'-UTR 48 nt
CTACAAACCTGAGATTTTAGTCTGAGAGAAAGAGAAGAGAACACTAAGATG
GIP1 5'-UTR 88 nt
GTCTCCCACTTCTCACTTCACATGTGAGTCTGCGACTATCTCCAAGAC
CAAGCTTCATACTTTATTTTTGCAAATTCCGTTTCTAAACATG
B
pmonoGFP
pGIP1 5'-UTR-GUS
pCYCB1;1 5'-UTR-GUS
35S
GFP
GIP1 5'-UTR
GUS
CYCB1;1 5'-UTR
C
WT
ToRP1ox
GFP
GUS/GFP activity (%)
pGIP1 5'-UTR-GUS (µg)
pCYCB1;1 5'-UTR-GUS (µg)
GUS/GFP activity in Δ(ToRP1ox/ WT), %
(µg) each reporter DNA
ToRP2ox
Δ(ToRP2ox/ WT), %
torp1 torp2
Δ(torp1 torp2/ WT), %

Figure—6 : Effets de ToRP sur l'initiation de la traduction coiffe-dépendante dans les protoplastes de plantes

(A) Les séquences de deux 5'-UTR des ARNm de CYCB1;1 et de GIP1 utilisés dans les expériences de protoplastes sont présentées.
(B) Structure des plasmides rapporteurs contenant (1) les 5'-UTR des ARNm de CYCB1;1 ou de GIP1 placés en amont de l'ORF de GUS, ou (2) l'IRES de TuMV placé en amont de l'ORF codant pour la GFP.
(C) La traduction coiffe-dépendante est sensible à ToRP1 et ToRP2 dans les protoplastes dérivés de *ToRP1ox*, *ToRP2ox* et *torp1 torp2*. Chaque paire de protoplastes a été transfectée en double exemplaires avec les concentrations indiquées des constructions 5'-UTR-rapporteurs et 5 µg de plasmides rapporteurs contenant de la GFP. 18 heures après la transformation, les protoplastes ont été récoltés et les activités GFP, GUS (β−glucuronidase) ont été mesurées ainsi que le rapport d'activité GUS/GFP a été calculé. La valeur la plus élevée dans chaque paire de protoplastes (WT et *ToRP1ox*, ou WT et *ToRP2ox*, ou WT et *torp1 torp2*) a été fixée à 100%. De plus, l'accumulation de GFP a été vérifiée par Western blot en utilisant des anticorps anti-GFP. Les données sont présentées sous la forme de la moyenne ± barre d'erreur. Le rapport relatif entre le WT et le génotype mutant a été quantifié et présenté dans *le panneau de droite.*
Les niveaux d'ARNm contenant GUS et l'intégrité après 18 h d'incubation ont été analysés par qPCR.

Régulation de la traduction par ToRP1 ou ToRP2 dans des protoplastes de plantes

Vu que ToRP1 et ToRP2 sont phosphorylés de manière sensible à TOR et que la liaison de ToRP1 à eIF4E est régulée par son état de phosphorylation aux S49 et S89 en système double-hybride de levure, nous avons cherché à tester si ToRP1 ou ToRP2 peuvent contribuer à l'initiation de la traduction coiffe-dépendante *in planta*. Nous avons sélectionné deux gènes cellulaires codant pour CYCB1;1 (Li et al. 2005) et GIP1 (Batzenschlager et al. 2013). Dans notre vecteur rapporteur, l'ORF de GUS a été placé en aval de 5'-UTR de CYCB1;1 ou de GIP1 (Figure 6A). Plusieurs génotypes d'*Arabidopsis* ont été utilisés—des plantes surexprimant myc-ToRP1 (*ToRP1ox*) et myc-ToRP2 (*ToRP2ox*) et des plantes d'*Arabidopsis* déficientes *torp1 torp2*, dont les gènes ToRP1 et ToRP2 ont été éliminés en utilisant le

système CRISPR/Cas9 (Fauser et al. 2014)—pour préparer des mésophylles protoplastes. Les protoplastes ont été transformés avec deux plasmides rapporteurs représentés dans la Figure 6B: pmonoGFP, contenant un seul ORF GFP; et pCYCB1;1 5'-UTR-GUS ou pGIP1 5'-UTR-GUS, où GUS sert de marqueur de l'efficacité de l'initiation de la traduction et GFP comme control pour la transformation. Tout d'abord, nous avons comparé l'efficacité de la traduction coiffe-dépendante des génotypes WT et *ToRP1ox* (Figure 6C-*panneaux supérieurs*). Une surexpression transitoire des reporteurs CYCB1;1 5'-UTR-GUS ou GIP1 5'-UTR-GUS conduit à une diminution marginale de la traduction coiffe-dépendante dans *ToRP1ox* par rapport au WT. L'effet négatif de la surexpression de ToRP2 dans *ToRP2ox* a été plus prononcé pour CYCB1;1 5'-UTR-GUS (Figure 6C-*panneau central*). Ici, la surexpression transitoire de CYCB1;1 5'-UTR-GUS a conduit à une diminution de trois fois de l'expression transitoire, alors que la traduction de l'ARNm GIP1 5'-UTR-GUS a été légèrement réduite par rapport au WT. Donc, les plantes transgéniques *ToRP2ox* sont moins efficaces que les plantes WT dans l'initiation de la traduction coiffe-dépendante. Il est à noter que les niveaux et l'intégrité des ARNm contenant GUS pendant 18 h d'incubation de protoplastes se sont révélés similaires pour les deux génotypes étudiés, bien que l'initiation de la traduction de l'ARNm de CYCB1;1 soit fortement dépendante de la structure de la coiffe, sensibles à la suppression par les protéines 4E-BP (Graff and Zimmer 2003).

Pour confirmer que l'initiation de la traduction est sensible, au moins, à ToRP2, nous avons testé si la suppression de ToRP1 et ToRP2 augmenteraient la traduction de nos reporteurs (Figure 6C-*panneaux inférieurs*). En effet, nous avons observé une augmentation significative de la traduction coiffe-dépendante de deux rapporteurs dans *torp1 torp2* par rapport au WT. En accord avec les résultats ci-dessus, le rapporteur CYCB1;1 5'-UTR a été exprimé deux fois plus dans des protoplastes dépourvus de ToRP que dans des protoplastes WT. Nous avons donc conclu que la traduction de l'ARNm de CYCB1;1 est sensible au ToRP2. Globalement,

ces expériences indiquent que les protéines ToRP1 et ToRP2 sont phosphorylées par TOR et peuvent réguler négativement la traduction coiffe-dépendante.

Discussion

Jusqu'à présent on ne savait pas si TOR participait à l'initiation de la traduction coiffe-dépendante chez les plantes. Nous avons identifié un ensemble de protéines—TOR regulatory proteins (ToRP; ToRP 1 à 4)—et nous avons démontré que (1) ToRP1 est capable d'interagir spécifiquement avec eIF4E, mais aussi avec TOR via son extrémité N-terminale *in vitro* (Figures 2 et 3); (2) ToRP1 et ToRP2 sont phosphorylées à plusieurs sites *in planta* qui semblaient être sensible à l'auxine (Figure 5); (3) deux de ces sites de phosphorylation ont été identifiés S49 et S89, et que leur état de phosphorylation module la liaison de ToRP1 à eIF4E en système double-hybride de levure (Figure 4); (4), ces protéines peuvent jouer le rôle de répresseurs de la traduction dans des protoplastes d'*A. thaliana* (Figure 6).

Nos résultats suggèrent que, chez les plantes, TOR peut réguler la traduction coiffe-dépendante via les protéines ToRP d'une manière semblable aux 4E-BP1 et 4E-BP2 chez l'homme, bien qu'elles présentent des caractéristiques propres aux plantes. Parmi les trois motifs conservés dans ToRP, l'un est le site canonique de liaison à eIF4E (4E-BM), le second est un motif riche en N qui ressemble au motif présent dans Hs4E-BP2 (Bidinosti et al., 2010) et le troisième, qui est situé à l'extrémité C-terminale, diffère du motif canonique TOS trouvé dans 4E-BP chez les mammifères. De façon frappante, les substitutions d'acides aminés dans le motif M3 modulent négativement la liaison de ToRP1 à la fois à eIF4E et NTOR, indiquant fortement l'importance de M3 dans la capacité de liaison de ToRP1. Le motif TOS est absent dans ToRP, ce qui suggère que les protéines végétales peuvent interagir directement avec le domaine HEAT de TOR pour leur phosphorylation par TOR.

Des modèles 3D de ToRP1 et ToRP2, générés par RaptorX, prédisent avec une forte probabilité des protéines intrinsèquement désordonnées (Figure 1B), comme cela a été également montré pour les protéines 4E-BP (Fletcher et Wagner, 1998). Chez les mammifères, 4E-BP se lie à eIF4E en coopération par l'intermédiaire de trois motifs: 4E-BM qui adopte une conformation α-hélicoïdale semblable à celle de la protéine eIF4G lorsqu'elle est liée à eIF4E (Marcotrigiano et al., 1999); un second site constitué d'une séquence PGVTS/T à boucle coudée (Peter et al., 2015); et le troisième motif non-canonique à l'extrémité C-terminale (Paku et al, 2012; Gosselin et al., 2011). En effet, un site similaire à la boucle coudée pourrait être trouvé dans ToRP1 et ToRP2; cependant, son implication dans la liaison eIF4E reste à démontrer.

Les protéines ToRP contiennent plusieurs sites de phosphorylation qui ressemblent à ceux présents dans des substrats bien connus de TOR. Deux d'entre eux, lorsqu'ils ne sont pas phosphorylés (Ser49V et Ser89V), permettent une liaison plus forte de ToRP1 à eIF4E, et leurs mutations mimétiques (Ser49D et Ser89D) ont été suffisantes pour dissocier ToRP1 de eIF4E. Donc, l'interaction entre ToRP1 et eIF4E est probablement contrôlée par l'inactivation de TOR par l'AZD-8055 et la déphosphorylation de ToRP (Figure 5).

Il est suggéré que des groupes d'ARNm dépendraient des 4E-BP et, par conséquent, de TOR: «eIF4E-sensentive mRNAs» avec des 5'-UTR larges et structurés (Koromilas et al., 1992), ces ARNm codent des protéines impliquées dans la survie et la prolifération cellulaires comme des cyclines, Myc, VEGF (Vascular endothelial growth factor) ou Bcl-XL (Graff et Zimmer, 2003) et des ARNm ayant des séquences de type TOP à leur extrémité 5' (Thoreen et al., 2012). Ces données sont en accord avec nos résultats qui démontrent une grande sensibilité de la traduction d'ARNm codant pour la cycline à ToRP2. Enfin, nos résultats suggèrent un modèle de la façon dont les protéines ToRP peuvent contribuer au contrôle de l'initiation de la

traduction par TOR (Figure 7). Notre modèle préliminaire indique que, dans des conditions d'inhibition de TOR (AZD-8055), TOR est déphosphorylé, ce qui entraine la déphosphorylation de ToRP 1/2 et leur liaison à eIF4E (eIFiso4E), et à la répression de la traduction des ARNm sensibles à eIF4E. En réponse à l'auxine, TOR devient actif et phosphoryle les ToRP. Les ToRP se dissocient alors d'eIF4E (eIFiso4E), ce qui conduit à la restauration de la formation du complexe eIF4F (eIFiso4F).

Cependant, d'autres recherches sont nécessaires pour révéler le rôle de TOR dans la phosphorylation des ToRP et dans l'initiation de la traduction cap-dépendante *in planta*. Une question restant ouverte est de savoir si les protéines ToRP peuvent surmonter l'affinité de liaison étroite entre les protéines canoniques de liaison à la coiffe de type 1, eIF4E et eIFiso4E, avec leurs sous-unités respectives eIF4G et eIFiso4G, qui est plus élevée que pour les orthologues chez les mammifères et qui est estimée être au niveau sous-nanomolaire (Mayberry et al., 2011). Un modèle alternatif suggère que la liaison à la coiffe d'eIF4E (eIFiso4E) peut être modulée en réponse à l'état redox de la cellule. En effet, il a été démontré que l'état d'oxydation d' eIF4E et eIFiso4E peut être critique pour leur liaison à la coiffe (Monzingo et al., 2007). Enfin, la régulation de l'initiation de la traduction dépendante d'eIF4E chez les plantes pourrait être régulée par diverses voies dépendantes de TOR et/ou des conditions physiologiques de la cellule.

Le contrôle des voies de traduction des ARNm joue un rôle fondamental dans de nombreux aspects de l'expression des gènes, de la croissance cellulaire et de la prolifération. Un nombre croissant d'exemples sont en faveur d'une large influence de la voie de la signalisation de TOR à différentes étapes de la synthèse protéique. Ici, nous avons montré que la voie de signalisation de TOR contribue à l'initiation de la traduction chez les plantes, ouvrant ainsi de larges perspectives sur le contrôle de la synthèse protéiques à plusieurs niveaux.

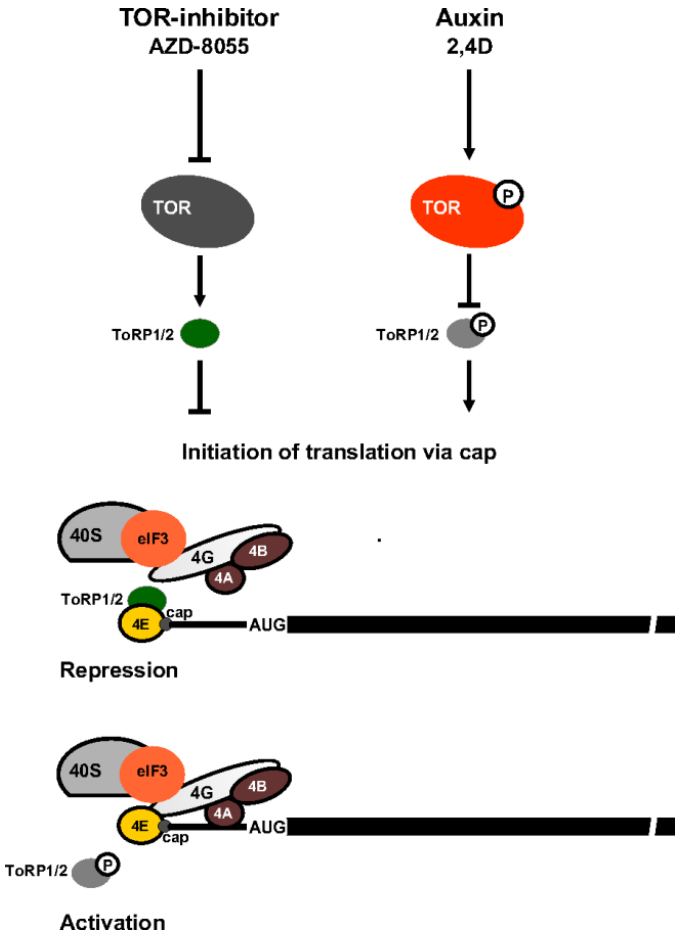

Figure—7 : Modèle provisoire de la fonction de ToRP1 et ToRP2 dans l'initiation de la traduction coiffe-dépendante

La phosphorylation de ToRP1 et ToRP2 est sensible à l'AZD-8055 et en réponse à l'auxine, qui ainsi active TOR peut maintenir les deux protéines dans un état de phosphorylation. Nous avons démontré que les protéines ToRP, lorsqu'elles ne sont pas phosphorylées, se lient à eIF4E, empêchant ainsi la formation de complexe eIF4F. En revanche, TOR déclenche leur phosphorylation, suivie par dissociation d'eIF4E qui permettrait de restaurer le complexe eIF4F (voir Discussion).

VI. Bibliography

Abramson RD, Browning KS, Dever TE, Lawson TG, Thach RE, Ravel JM and Merrick WC (1988) Initiation factors that bind mRNA. A comparison of mammalian factors with wheat germ factors. J Biol Chem 263:5462–5467.

Ahn CS, Han J-A, Lee H-S, Lee S and Pai H-S (2011) The PP2A Regulatory Subunit Tap46, a Component of the TOR Signaling Pathway, Modulates Growth and Metabolism in Plants. Plant Cell 23:185–209. doi: 10.1105/tpc.110.074005

Aitken CE and Lorsch JR (2012) A mechanistic overview of translation initiation in eukaryotes. Nat Struct Mol Biol 19:568–576.

Altmann M, Müller PP, Wittmer B, Ruchti F, Lanker S and Trachsel H (1993) A Saccharomyces cerevisiae homologue of mammalian translation initiation factor 4B contributes to RNA helicase activity. EMBO J 12:3997–4003.

Anderson GH, Veit B and Hanson MR (2005) The Arabidopsis AtRaptor genes are essential for post-embryonic plant growth. BMC Biol 3:1–11. doi: 10.1186/1741-7007-3-12

Armengol G, Rojo F, Castellví J, Iglesias C, Cuatrecasas M, Pons B, Baselga J and Ramón y Cajal S (2007) 4E-Binding Protein 1: A Key Molecular "Funnel Factor" in Human Cancer with Clinical Implications. Cancer Res 67:7551 LP-7555.

Asano K, Clayton J, Shalev A and Hinnebusch AG (2000) A multifactor complex of eukaryotic initiation factors, eIF1, eIF2, eIF3, eIF5, and initiator tRNAMet is an important translation initiation intermediate in vivo. Genes Dev 14:2534–2546. doi: 10.1101/gad.831800

Aylett CHS, Boehringer D, Erzberger JP, Schaefer T and Ban N (2015) Structure of a Yeast 40S–eIF1–eIF1A–eIF3–eIF3j initiation complex. Nat Struct Mol Biol 22:269–271.

Ayuso MI, Hernández-Jiménez M, Martín ME, Salinas M and Alcázar A (2010) New Hierarchical Phosphorylation Pathway of the Translational Repressor eIF4E-binding Protein 1 (4E-BP1) in Ischemia-Reperfusion Stress. J Biol Chem 285:34355–34363. doi: 10.1074/jbc.M110.135103

Bandi HR, Ferrari S, Krieg J, Meyer HE and Thomas G (1993) Identification of 40 S ribosomal protein S6 phosphorylation sites in Swiss mouse 3T3 fibroblasts stimulated with serum. J Biol Chem 268:4530–4533.

Banerjee P, Ahmad MF, Grove JR, Kozlosky C, Price DJ and Avruch J (1990) Molecular structure of a major insulin/mitogen-activated 70-kDa S6 protein kinase. Proc Natl Acad Sci U S A 87:8550–8554.

Bangs JD, Crain PF, Hashizume T, McCloskey JA and Boothroyd JC (1992) Mass spectrometry of mRNA cap 4 from trypanosomatids reveals two novel nucleosides. J Biol Chem 267:9805–9815.

Banko JL, Hou L, Poulin F, Sonenberg N and Klann E (2006) Regulation of Eukaryotic Initiation Factor 4E by Converging Signaling Pathways during Metabotropic Glutamate Receptor-Dependent Long-Term Depression. J Neurosci 26:2167–2173.

Banko JL, Merhav M, Stern E, Sonenberg N, Rosenblum K and Klann E (2007) Behavioral alterations in mice lacking the translation repressor 4E-BP2. Neurobiol Learn Mem 87:248–256. doi: http://dx.doi.org/10.1016/j.nlm.2006.08.012

Banko JL, Poulin F, Hou L, DeMaria CT, Sonenberg N and Klann E (2005) The Translation Repressor 4E-BP2 Is Critical for eIF4F Complex Formation, Synaptic Plasticity, and Memory in the Hippocampus. J Neurosci 25:9581–9590. doi: 10.1523/JNEUROSCI.2423-05.2005

Batzenschlager M, Masoud K, Janski N, Houlné G, Herzog E, Evrard J-L, Baumberger N, Erhardt M, Nominé Y, Kieffer B et al. (2013) The GIP gamma-tubulin complex-associated proteins are involved in nuclear architecture in Arabidopsis thaliana. Front Plant Sci 4:480. doi: 10.3389/fpls.2013.00480

Bellsolell L, Cho-Park PF, Poulin F, Sonenberg N and Burley SK (2006) Two Structurally Atypical HEAT Domains in the C-Terminal Portion of Human eIF4G Support Binding to eIF4A and Mnk1. Structure 14:913–923. doi: http://dx.doi.org/10.1016/j.str.2006.03.012

Belostotsky DA (2003) Unexpected Complexity of Poly(A)-Binding Protein Gene Families in Flowering Plants: Three Conserved Lineages That Are at Least 200 Million Years Old and Possible Auto- and Cross-Regulation. Genetics 163:311 LP-319.

Beretta L, Gingras AC, Svitkin Y V, Hall MN and Sonenberg N (1996) Rapamycin blocks the phosphorylation of 4E-BP1 and inhibits cap-dependent initiation of translation. EMBO J 15:658–664.

Bi X and Goss DJ (2000) Wheat Germ Poly(A)-binding Protein Increases the ATPase and the RNA Helicase Activity of Translation Initiation Factors eIF4A, eIF4B, and eIF-iso4F. J Biol Chem 275:17740–17746. doi: 10.1074/jbc.M909464199

Bidinosti M, Ran I, Sanchez-Carbente MR, Martineau Y, Gingras A-C, Gkogkas C, Raught B, Bramham C, Sossin WS, Costa-Mattioli M et al. (2010) Postnatal deamidation of 4E-BP2 in brain enhances its association with raptor and alters kinetics of excitatory synaptic transmission. Mol Cell 37:797–808. doi: 10.1016/j.molcel.2010.02.022

Brown EJ, Albers MW, Bum Shin T, ichikawa K, Keith CT, Lane WS and Schreiber SL (1994) A mammalian protein targeted by G1-arresting rapamycin-receptor complex. Nature 369:756–758.

Browning KS (1996) The plant translational apparatus. Plant Mol Biol 32:107–144.

Browning KS and Bailey-Serres J (2015) Mechanism of Cytoplasmic mRNA Translation.

Arabidopsis Book 13:e0176. doi: 10.1199/tab.0176

Browning KS, Fletcher L, Lax SR and Ravel JM (1989) Evidence that the 59-kDa protein synthesis initiation factor from wheat germ is functionally similar to the 80-kDa initiation factor 4B from mammalian cells. J Biol Chem 264:8491–8494.

Browning KS, Humphreys J, Hobbs W, Smith GB and Ravel JM (1990) Determination of the amounts of the protein synthesis initiation and elongation factors in wheat germ. J Biol Chem 265:17967–17973.

Browning KS, Webster C, Roberts JK and Ravel JM (1992) Identification of an isozyme form of protein synthesis initiation factor 4F in plants. J Biol Chem 267:10096–10100.

Burd CG, Matunis EL and Dreyfuss G (1991) The multiple RNA-binding domains of the mRNA poly(A)-binding protein have different RNA-binding activities. Mol Cell Biol 11:3419–3424.

Burks EA, Bezerra PP, Le H, Gallie DR and Browning KS (2001) Plant Initiation Factor 3 Subunit Composition Resembles Mammalian Initiation Factor 3 and Has a Novel Subunit. J Biol Chem 276:2122–2131. doi: 10.1074/jbc.M007236200

Checkley JW, Cooley L and Ravel JM (1981) Characterization of initiation factor eIF-3 from wheat germ. J Biol Chem 256:1582–1586.

Cheng S and Gallie DR (2006) Wheat Eukaryotic Initiation Factor 4B Organizes Assembly of RNA and eIFiso4G, eIF4A, and Poly(A)-binding Protein. J Biol Chem 281:24351–24364. doi: 10.1074/jbc.M605404200

Cheng S and Gallie DR (2007) eIF4G, eIFiso4G, and eIF4B Bind the Poly(A)-binding Protein through Overlapping Sites within the RNA Recognition Motif Domains. J Biol Chem 282:25247–25258. doi: 10.1074/jbc.M702193200

Chresta CM, Davies BR, Hickson I, Harding T, Cosulich S, Critchlow SE, Vincent JP, Ellston R, Jones D, Sini P et al. (2010) AZD8055 Is a Potent, Selective, and Orally Bioavailable ATP-Competitive Mammalian Target of Rapamycin Kinase Inhibitor with In vitro and Antitumor Activity. Cancer Res 70:288 LP-298.

Clemens MJ (2004) Targets and mechanisms for the regulation of translation in malignant transformation. Oncogene 23:3180–3188.

Clough SJ and Bent AF (1998) Floral dip: a simplified method forAgrobacterium-mediated transformation ofArabidopsis thaliana. Plant J 16:735–743.

Clouse KN, Ferguson SB and Schüpbach T (2008) Squid, Cup and PABP 55B function together to regulate gurken translation in Drosophila. Dev Biol 313:713–724.

Colina R, Costa-Mattioli M, Dowling RJO, Jaramillo M, Tai L-H, Breitbach CJ, Martineau Y, Larsson O, Rong L, Svitkin Y V et al. (2008) Translational control of the innate immune

response through IRF-7. Nature 452:323–328.

De Benedetti A and Graff JR (2004) eIF-4E expression and its role in malignancies and metastases. Oncogene 23:3189–3199.

Deng K, Yu L, Zheng X, Zhang K, Wang W, Dong P, Zhang J and Ren M (2016) Target of Rapamycin Is a Key Player for Auxin Signaling Transduction in Arabidopsis. Front Plant Sci 7:291. doi: 10.3389/fpls.2016.00291

Dennis MD, Person MD and Browning KS (2009) Phosphorylation of Plant Translation Initiation Factors by CK2 Enhances the in Vitro Interaction of Multifactor Complex Components. J Biol Chem 284:20615–20628. doi: 10.1074/jbc.M109.007658

Dennis PB, Fumagalli S and Thomas G (1999) Target of rapamycin (TOR): balancing the opposing forces of protein synthesis and degradation. Curr Opin Genet Dev 9:49–54. doi: http://dx.doi.org/10.1016/S0959-437X(99)80007-0

Deprost D, Truong H-N, Robaglia C and Meyer C (2005) An Arabidopsis homolog of RAPTOR/KOG1 is essential for early embryo development. Biochem Biophys Res Commun 326:844–850. doi: http://dx.doi.org/10.1016/j.bbrc.2004.11.117

Deprost D, Yao L, Sormani R, Moreau M, Leterreux G, Nicolaï M, Bedu M, Robaglia C and Meyer C (2007) The Arabidopsis TOR kinase links plant growth, yield, stress resistance and mRNA translation. EMBO Rep 8:864 LP-870.

Dever TE and Green R (1999) The Elongation, Termination and Recycling Phases of Translation in Eukaryotes. Cold Spring Harb Perspect Biol 4:a013706–a013706.

Dever TE, Gutierrez E and Shin B-S (2014) The hypusine-containing translation factor eIF5A. Crit Rev Biochem Mol Biol 49:413–425. doi: 10.3109/10409238.2014.939608

Dibble CC and Manning BD (2013) Signal integration by mTORC1 coordinates nutrient input with biosynthetic output. Nat Cell Biol 15:555–564. doi: 10.1038/ncb2763

Dilling MB, Germain GS, Dudkin L, Jayaraman AL, Zhang X, Harwood FC and Houghton PJ (2002) 4E-binding Proteins, the Suppressors of Eukaryotic Initiation Factor 4E, Are Down-regulated in Cells with Acquired or Intrinsic Resistance to Rapamycin. J Biol Chem 277:13907–13917. doi: 10.1074/jbc.M110782200

Dobrenel T, Caldana C, Hanson J, Robaglia C, Vincentz M, Veit B and Meyer C (2016) TOR Signaling and Nutrient Sensing. Annu Rev Plant Biol 67:261–285.

Dobrenel T, Marchive C, Sormani R, Moreau M, Mozzo M, Montané M-H, Menand B, Robaglia C and Meyer C (2011) Regulation of plant growth and metabolism by the TOR kinase. Biochem Soc Trans 39:477 LP-481.

Dorrello NV, Peschiaroli A, Guardavaccaro D, Colburn NH, Sherman NE and Pagano M (2006)

S6K1- and ßTRCP-Mediated Degradation of PDCD4 Promotes Protein Translation and Cell Growth. Science (80-) 314:467 LP-471.

Dufresne PJ, Ubalijoro E, Fortin MG and Laliberté J-F (2008) Arabidopsis thaliana class II poly(A)-binding proteins are required for efficient multiplication of turnip mosaic virus. J Gen Virol 89:2339–48. doi: 10.1099/vir.0.2008/002139-0

Duprat A, Caranta C, Revers F, Menand B, Browning KS and Robaglia C (2002) The Arabidopsis eukaryotic initiation factor (iso)4E is dispensable for plant growth but required for susceptibility to potyviruses. Plant J 32:927–934. doi: 10.1046/j.1365-313X.2002.01481.x

Eguchi S, Tokunaga C, Hidayat S, Oshiro N, Yoshino K, Kikkawa U and Yonezawa K (2006) Different roles for the TOS and RAIP motifs of the translational regulator protein 4E-BP1 in the association with raptor and phosphorylation by mTOR in the regulation of cell size. Genes to Cells 11:757–766. doi: 10.1111/j.1365-2443.2006.00977.x

Fadden P, Haystead TAJ and Jr. JCL (1997) Identification of Phosphorylation Sites in the Translational Regulator, PHAS-I, That Are Controlled by Insulin and Rapamycin in Rat Adipocytes. J Biol Chem 272:10240–10247. doi: 10.1074/jbc.272.15.10240

Fauser F, Schiml S and Puchta H (2014) Both CRISPR/Cas-based nucleases and nickases can be used efficiently for genome engineering in Arabidopsis thaliana. Plant J 79:348–359. doi: 10.1111/tpj.12554

Fletcher CM, McGuire AM, Gingras A-C, Li H, Matsuo H, Sonenberg N and Wagner G (1998) 4E Binding Proteins Inhibit the Translation Factor eIF4E without Folded Structure. Biochemistry 37:9–15. doi: 10.1021/bi972494r

Fletcher CM and Wagner G (1998) The interaction of eIF4E with 4E-BP1 is an induced fit to a completely disordered protein. Protein Sci 7:1639–1642.

Fraser CS, Lee JY, Mayeur GL, Bushell M, Doudna JA and Hershey JWB (2004) The j-Subunit of Human Translation Initiation Factor eIF3 Is Required for the Stable Binding of eIF3 and Its Subcomplexes to 40 S Ribosomal Subunits in Vitro. J Biol Chem 279:8946–8956. doi: 10.1074/jbc.M312745200

Freire MA, Tourneur C, Granier F, Camonis J, El Amrani A, Browning KS and Robaglia C (2000) Plant lipoxygenase 2 is a translation initiation factor-4E-binding protein. Plant Mol Biol 44:129–140. doi: 10.1023/A:1006494628892

Furic L, Rong L, Larsson O, Koumakpayi IH, Yoshida K, Brueschke A, Petroulakis E, Robichaud N, Pollak M, Gaboury LA et al. (2010) eIF4E phosphorylation promotes tumorigenesis and is associated with prostate cancer progression. Proc Natl Acad Sci U S A 107:14134–14139. doi: 10.1073/pnas.1005320107

Gallie DR (2002) Protein-protein interactions required during translation. Plant Mol Biol 50:949–970. doi: 10.1023/A:1021220910664

Gallie DR (1991) The cap and poly(A) tail function synergistically to regulate mRNA translational efficiency. Genes Dev 5:2108–2116. doi: 10.1101/gad.5.11.2108

Gallie DR and Browning KS (2001) eIF4G Functionally Differs from eIFiso4G in Promoting Internal Initiation, Cap-independent Translation, and Translation of Structured mRNAs. J Biol Chem 276:36951–36960. doi: 10.1074/jbc.M103869200

Gasiunas G, Barrangou R, Horvath P and Siksnys V (2012) Cas9–crRNA ribonucleoprotein complex mediates specific DNA cleavage for adaptive immunity in bacteria. Proc Natl Acad Sci U S A 109:E2579–E2586. doi: 10.1073/pnas.1208507109

Gebauer F and Hentze MW (2004) Molecular mechanisms of translational control. Nat Rev Mol Cell Biol 5:827–835.

Gingras A-C, Gygi SP, Raught B, Polakiewicz RD, Abraham RT, Hoekstra MF, Aebersold R and Sonenberg N (1999a) Regulation of 4E-BP1 phosphorylation: a novel two-step mechanism. Genes Dev 13:1422–1437.

Gingras A-C, Raught B, Gygi SP, Niedzwiecka A, Miron M, Burley SK, Polakiewicz RD, Wyslouch-Cieszynska A, Aebersold R and Sonenberg N (2001) Hierarchical phosphorylation of the translation inhibitor 4E-BP1. Genes Dev 15:2852–2864. doi: 10.1101/gad.912401

Gingras A-C, Raught B and Sonenberg N (1999b) eIF4 Initiation Factors: Effectors of mRNA Recruitment to Ribosomes and Regulators of Translation. Annu Rev Biochem 68:913–963. doi: 10.1146/annurev.biochem.68.1.913

Gomez E, Mohammad SS and Pavitt GD (2002) Characterization of the minimal catalytic domain within eIF2B: the guanine-nucleotide exchange factor for translation initiation. EMBO J 21:5292 LP-5301.

Gosselin P, Oulhen N, Jam M, Ronzca J, Cormier P, Czjzek M and Cosson B (2011) The translational repressor 4E-BP called to order by eIF4E: new structural insights by SAXS. Nucleic Acids Res 39:3496–3503. doi: 10.1093/nar/gkq1306

Graff JR and Zimmer SG (2003) Translational control and metastatic progression: Enhanced activity of the mRNA cap-binding protein eIF-4E selectively enhances translation of metastasis-related mRNAs. Clin Exp Metastasis 20:265–273. doi: 10.1023/A:1022943419011

Green and R and Noller HF (1997) RIBOSOMES AND TRANSLATION. Annu Rev Biochem 66:679–716. doi: 10.1146/annurev.biochem.66.1.679

Gromadski KB and Rodnina M V (2004) Kinetic Determinants of High-Fidelity tRNA Discrimination on the Ribosome. Mol Cell 13:191–200. doi: 10.1016/S1097-2765(04)00005-

X

Gwinn DM, Shackelford DB, Egan DF, Mihaylova MM, Mery A, Vasquez DS, Turk BE and Shaw RJ (2008) AMPK phosphorylation of raptor mediates a metabolic checkpoint. Mol Cell 30:214–226. doi: 10.1016/j.molcel.2008.03.003

Haar E Vander, Lee S, Bandhakavi S, Griffin TJ and Kim D-H (2007) Insulin signalling to mTOR mediated by the Akt/PKB substrate PRAS40. Nat Cell Biol 9:316–323.

Hara K, Maruki Y, Long X, Yoshino K, Oshiro N, Hidayat S, Tokunaga C, Avruch J and Yonezawa K (2002) Raptor, a binding partner of target of rapamycin (TOR), mediates TOR action. Cell. doi: 10.1016/S0092-8674(02)00833-4

Hara K, Yonezawa K, Weng Q-P, Kozlowski MT, Belham C and Avruch J (1998) Amino Acid Sufficiency and mTOR Regulate p70 S6 Kinase and eIF-4E BP1 through a Common Effector Mechanism. J Biol Chem 273:14484–14494. doi: 10.1074/jbc.273.23.14484

Hay N and Sonenberg N (2004) Upstream and downstream of mTOR. Genes Dev 18:1926–1945. doi: 10.1101/gad.1212704

Haystead TA, Haystead CM, Hu C, Lin TA and Lawrence JC (1994) Phosphorylation of PHAS-I by mitogen-activated protein (MAP) kinase. Identification of a site phosphorylated by MAP kinase in vitro and in response to insulin in rat adipocytes. J Biol Chem 269:23185–23191.

Heesom KJ, Avison MB, Diggle TA and Denton RM (1998) Insulin-stimulated kinase from rat fat cells that phosphorylates initiation factor 4E-binding protein 1 on the rapamycin-insensitive site (serine-111). Biochem J 336:39–48.

Hernández G, Altmann M, Sierra JM, Urlaub H, Diez del Corral R, Schwartz P and Rivera-Pomar R (2005) Functional analysis of seven genes encoding eight translation initiation factor 4E (eIF4E) isoforms in Drosophila. Mech Dev 122:529–543.

Hernández G, Miron M, Han H, Liu N, Magescas J, Tettweiler G, Frank F, Siddiqui N, Sonenberg N and Lasko P (2013) Mextli Is a Novel Eukaryotic Translation Initiation Factor 4E-Binding Protein That Promotes Translation in Drosophila melanogaster. Mol Cell Biol 33:2854–2864. doi: 10.1128/MCB.01354-12

Hershey JWB (1991) Translational Control in Mammalian Cells. Annu Rev Biochem 60:717–755.

Hershey JWB and Merrick WC (2000) 2 The Pathway and Mechanism of Initiation of Protein Synthesis. Cold Spring Harb. Monogr. Arch. Vol. 39 Transl. Control Gene Expr.

Heufler C, Browning KS and Ravel JM (1988) Properties of the subunits of wheat germ initiation factor 3. Biochim Biophys Acta - Gene Struct Expr 951:182–190.

Hinnebusch AG (2011) Molecular Mechanism of Scanning and Start Codon Selection in Eukaryotes. Microbiol Mol Biol Rev 75:434–467. doi: 10.1128/MMBR.00008-11

Hinnebusch AG (2014) The Scanning Mechanism of Eukaryotic Translation Initiation. Annu Rev Biochem 83:779–812. doi: 10.1146/annurev-biochem-060713-035802

Hinnebusch AG (2016) eIF3: a versatile scaffold for translation initiation complexes. Trends Biochem Sci 31:553–562. doi: 10.1016/j.tibs.2006.08.005

Hinnebusch AG and Lorsch JR (2012) The Mechanism of Eukaryotic Translation Initiation: New Insights and Challenges. Cold Spring Harb Perspect Biol 4:a011544.

Horváth BM, Magyar Z, Zhang Y, Hamburger AW, Bakó L, Visser RGF, Bachem CWB and Bögre L (2006) EBP1 regulates organ size through cell growth and proliferation in plants. EMBO J 25:4909 LP-4920.

Houghton PJ and Huang S (2004) mTOR as a Target for Cancer Therapy. In: Thomas G, Sabatini DM and Hall MN (eds) TOR: Target of Rapamycin. Springer Berlin Heidelberg, Berlin, Heidelberg, pp 339–359

Howell JJ, Ricoult SJH, Ben-Sahra I and Manning BD (2013) A growing role for mTOR in promoting anabolic metabolism. Biochem Soc Trans 41:906 LP-912.

Hsieh AC, Liu Y, Edlind MP, Ingolia NT, Janes MR, Sher A, Shi EY, Stumpf CR, Christensen C, Bonham MJ et al. (2012) The translational landscape of mTOR signalling steers cancer initiation and metastasis. Nature 485:55–61. doi: 10.1038/nature10912

Hsieh AC and Ruggero D (2010) Targeting Eukaryotic Translation Initiation Factor 4E (eIF4E) in Cancer. Clin Cancer Res 16:4914 LP-4920.

Huang H, Yoon H, Hannig EM and Donahue TF (1997) GTP hydrolysis controls stringent selection of the AUG start codon during translation initiation inSaccharomyces cerevisiae . Genes Dev 11:2396–2413. doi: 10.1101/gad.11.18.2396

Igreja C, Peter D, Weiler C and Izaurralde E (2014) 4E-BPs require non-canonical 4E-binding motifs and a lateral surface of eIF4E to repress translation. Nat Commun 5:4790. doi: 10.1038/ncomms5790

Inoki K, Li Y, Xu T and Guan K-L (2003) Rheb GTPase is a direct target of TSC2 GAP activity and regulates mTOR signaling. Genes Dev 17:1829–1834. doi: 10.1101/gad.1110003

Inoki K, Li Y, Zhu T, Wu J and Guan K-L (2002) TSC2 is phosphorylated and inhibited by Akt and suppresses mTOR signalling. Nat Cell Biol 4:648–657.

Iwakawa H, Tajima Y, Taniguchi T, Kaido M, Mise K, Tomari Y, Taniguchi H and Okuno T (2012) Poly(A)-Binding Protein Facilitates Translation of an Uncapped/Nonpolyadenylated Viral RNA by Binding to the 3′ Untranslated Region. J Virol 86:7836–7849. doi: 10.1128/JVI.00538-12

Jackson RJ, Hellen CUT and Pestova T V (2010). The mechanism of eukaryotic translation

initiation and principles of its regulation. Nat Rev Mol Cell Biol 11:113–127.

Jackson RJ, Hellen CUT and Pestova T V (2012) Termination and post-termination events in eukaryotic translation. In: Biology AMBT-A in PC and S (ed) Fidelity and Quality Control in Gene Expression. Academic Press, pp 45–93

Jefferson RA, Kavanagh TA and Bevan MW (1987) GUS fusions: beta-glucuronidase as a sensitive and versatile gene fusion marker in higher plants. EMBO J 6:3901–3907.

Jennings MD and Pavitt GD (2010) eIF5. Small GTPases 1:118–123. doi: 10.4161/sgtp.1.2.13783

Jinek M, Chylinski K, Fonfara I, Hauer M, Doudna JA and Charpentier E (2012) A Programmable Dual-RNA–Guided DNA Endonuclease in Adaptive Bacterial Immunity. Science (80-) 337:816 LP-821.

Källberg M, Wang H, Wang S, Peng J, Wang Z, Lu H and Xu J (2012) Template-based protein structure modeling using the RaptorX web server. Nat Protoc 7:1511–1522. doi: 10.1038/nprot.2012.085

Kang SA, Pacold ME, Cervantes CL, Lim D, Lou HJ, Ottina K, Gray NS, Turk BE, Yaffe MB and Sabatini DM (2013) mTORC1 Phosphorylation Sites Encode Their Sensitivity to Starvation and Rapamycin. Science (80-.). 341:

Kapp LD and Lorsch JR (2004) The Molecular Mechanics of Eukaryotic Translation. Annu Rev Biochem 73:657–704. doi: 10.1146/annurev.biochem.73.030403.080419

Khan MA and Goss DJ (2005) Translation Initiation Factor (eIF) 4B Affects the Rates of Binding of the mRNA m7G Cap Analogue to Wheat Germ eIFiso4F and eIFiso4F·PABP. Biochemistry 44:4510–4516. doi: 10.1021/bi047298g

Khan MA, Yumak H, Gallie DR and Goss DJ (2008) Effects of poly(A)-binding protein on the interactions of translation initiation factor eIF4F and eIF4F·4B with internal ribosome entry site (IRES) of tobacco etch virus RNA. Biochim Biophys Acta - Gene Regul Mech 1779:622–627. doi: http://dx.doi.org/10.1016/j.bbagrm.2008.07.004

Khan MA, Yumak H and Goss DJ (2009) Kinetic Mechanism for the Binding of eIF4F and Tobacco Etch Virus Internal Ribosome Entry Site RNA: EFFECTS OF eIF4B AND POLY(A)-BINDING PROTEIN . J Biol Chem 284:35461–35470.

Kim D-H, Sarbassov DD, Ali SM, King JE, Latek RR, Erdjument-Bromage H, Tempst P and Sabatini DM (2002) mTOR Interacts with Raptor to Form a Nutrient-Sensitive Complex that Signals to the Cell Growth Machinery. Cell 110:163–175.

Kim DH, Sarbassov DD, Ali SM, Latek RR, Guntur K V, Erdjument-Bromage H, Tempst P and Sabatini DM (2003) GbetaL, a positive regulator of the rapamycin-sensitive pathway required for the nutrient-sensitive interaction between raptor and mTOR. Mol Cell.

Kim E, Goraksha-Hicks P, Li L, Neufeld TP and Guan K-L (2008) Regulation of TORC1 by Rag GTPases in nutrient response. Nat Cell Biol 10:935–945. doi: 10.1038/ncb1753

Kim T-H, Kim B-H, Yahalom A, Chamovitz DA and von Arnim AG (2004) Translational Regulation via 5′ mRNA Leader Sequences Revealed by Mutational Analysis of the Arabidopsis Translation Initiation Factor Subunit eIF3h. Plant Cell 16:3341–3356. doi: 10.1105/tpc.104.026880

Kinkelin K, Veith K, Grünwald M and Bono F (2012) Crystal structure of a minimal eIF4E–Cup complex reveals a general mechanism of eIF4E regulation in translational repression. RNA 18:1624–1634. doi: 10.1261/rna.033639.112

Kleijn M, Scheper GC, Wilson ML, Tee AR and Proud CG (2002) Localisation and regulation of the eIF4E-binding protein 4E-BP3. FEBS Lett 532:319–323. doi: 10.1016/S0014-5793(02)03694-3

Konicek BW, Dumstorf CA and Graff JR (2008) Targeting the eIF4F translation initiation complex for cancer therapy. Cell Cycle 7:2466–2471. doi: 10.4161/cc.7.16.6464

Korneeva NL, Lamphear BJ, Hennigan FLC, Merrick WC and Rhoads RE (2001) Characterization of the Two eIF4A-binding Sites on Human eIF4G-1. J Biol Chem 276:2872–2879. doi: 10.1074/jbc.M006345200

Koromilas AE, Lazaris-Karatzas A and Sonenberg N (1992) mRNAs containing extensive secondary structure in their 5’ non-coding region translate efficiently in cells overexpressing initiation factor eIF-4E. EMBO J 11:4153–4158.

Kovacina KS, Park GY, Bae SS, Guzzetta AW, Schaefer E, Birnbaum MJ and Roth RA (2003) Identification of a Proline-rich Akt Substrate as a 14-3-3 Binding Partner. J Biol Chem 278:10189–10194. doi: 10.1074/jbc.M210837200

Kozak M (1999) Initiation of translation in prokaryotes and eukaryotes. Gene 234:187–208. doi: http://dx.doi.org/10.1016/S0378-1119(99)00210-3

Kozma SC, Ferrari S, Bassand P, Siegmann M, Totty N and Thomas G (1990) Cloning of the mitogen-activated S6 kinase from rat liver reveals an enzyme of the second messenger subfamily. Proc Natl Acad Sci U S A 87:7365–7369.

Krishnamoorthy T, Pavitt GD, Zhang F, Dever TE and Hinnebusch AG (2001) Tight Binding of the Phosphorylated α Subunit of Initiation Factor 2 (eIF2α) to the Regulatory Subunits of Guanine Nucleotide Exchange Factor eIF2B Is Required for Inhibition of Translation Initiation. Mol Cell Biol 21:5018–5030. doi: 10.1128/MCB.21.15.5018-5030.2001

Laemmeli U (1970) Cleavage of Structural Proteins during the Assembly of the Head of Bacteriophage T4. Nature 227:680–685.

Laplante M and Sabatini DM (2012a) mTOR Signaling in Growth Control and Disease. Cell 149:274–293. doi: http://dx.doi.org/10.1016/j.cell.2012.03.017

Laplante M and Sabatini DM (2012b) mTOR signaling. Cold Spring Harb Perspect Biol 4:10.1101/cshperspect.a011593 a011593. doi: 10.1101/cshperspect.a011593

Lawrence Jr JC and Abraham RT (1997) PHAS/4E-BPs as regulators of mRNA translation and cell proliferation. Trends Biochem Sci 22:345–349. doi: 10.1016/S0968-0004(97)01101-8

Lax SR, Browning KS, Maia DM and Ravel JM (1986) ATPase activities of wheat germ initiation factors 4A, 4B, and 4F. J Biol Chem 261:15632–15636.

Le H, Browning KS and Gallie DR (2000) The Phosphorylation State of Poly(A)-binding Protein Specifies Its Binding to Poly(A) RNA and Its Interaction with Eukaryotic Initiation Factor (eIF) 4F, eIFiso4F, and eIF4B. J Biol Chem 275:17452–17462. doi:

Le H, Tanguay RL, Balasta ML, Wei C-C, Browning KS, Metz AM, Goss DJ and Gallie DR (1997) Translation Initiation Factors eIF-iso4G and eIF-4B Interact with the Poly(A)-binding Protein and Increase Its RNA Binding Activity. J Biol Chem 272:16247–16255.

Le Bacquer O, Petroulakis E, Paglialunga S, Poulin F, Richard D, Cianflone K and Sonenberg N (2007) Elevated sensitivity to diet-induced obesity and insulin resistance in mice lacking 4E-BP1 and 4E-BP2. J Clin Invest 117:387–396. doi: 10.1172/JCI29528

LeBowitz JH, Smith HQ, Rusche L and Beverley SM (1993) Coupling of poly(A) site selection and trans-splicing in Leishmania. Genes Dev 7:996–1007. doi: 10.1101/gad.7.6.996

Lee VHY, Healy T, Fonseca BD, Hayashi A and Proud CG (2008) Analysis of the regulatory motifs in eukaryotic initiation factor 4E-binding protein 1. FEBS J 275:2185–2199. doi: 10.1111/j.1742-4658.2008.06372.x

Leiber R-M, John F, Verhertbruggen Y, Diet A, Knox JP and Ringli C (2010) The TOR Pathway Modulates the Structure of Cell Walls in Arabidopsis. Plant Cell 22:1898–1908. doi: 10.1105/tpc.109.073007

Lellis AD, Allen ML, Aertker AW, Tran JK, Hillis DM, Harbin CR, Caldwell C, Gallie DR and Browning KS (2010) Deletion of the eIFiso4G subunit of the Arabidopsis eIFiso4F translation initiation complex impairs health and viability. Plant Mol Biol 74:249–263. doi: 10.1007/s11103-010-9670-z

Li C, Potuschak T, Colón-Carmona A, Gutiérrez RA and Doerner P (2005) Arabidopsis TCP20 links regulation of growth and cell division control pathways. Proc Natl Acad Sci U S A 102:12978–12983. doi: 10.1073/pnas.0504039102

Lin TA, Kong X, Haystead TA, Pause A, Belsham G, Sonenberg N and Lawrence JC (1994) PHAS-I as a link between mitogen-activated protein kinase and translation initiation. Science

(80-) 266:653 LP-656.

Lin T-A and Lawrence JC (1996) Control of the Translational Regulators PHAS-I and PHAS-II by Insulin and cAMP in 3T3-L1 Adipocytes. J Biol Chem 271:30199–30204.

Liu Y and Bassham DC (2010) TOR Is a Negative Regulator of Autophagy in Arabidopsis thaliana. PLoS One 5:e11883. doi: 10.1371/journal.pone.0011883

Lomakin IB, Kolupaeva VG, Marintchev A, Wagner G and Pestova T V (2003) Position of eukaryotic initiation factor eIF1 on the 40S ribosomal subunit determined by directed hydroxyl radical probing. Genes Dev 17:2786–2797.

Lorsch JR and Dever TE (2010) Molecular View of 43 S Complex Formation and Start Site Selection in Eukaryotic Translation Initiation. J Biol Chem 285:21203–21207.

Lukhele S, Bah A, Lin H, Sonenberg N and Forman-Kay JD (2013) Interaction of the Eukaryotic Initiation Factor 4E with 4E-BP2 at a Dynamic Bipartite Interface. Structure 21:2186–2196. doi: 10.1016/j.str.2013.08.030

Ma XM and Blenis J (2009) Molecular mechanisms of mTOR-mediated translational control. Nat Rev Mol Cell Biol 10:307–318.

Ma XM, Yoon S-O, Richardson CJ, Jülich K and Blenis J (2008) SKAR Links Pre-mRNA Splicing to mTOR/S6K1-Mediated Enhanced Translation Efficiency of Spliced mRNAs. Cell 133:303–313. doi: 10.1016/j.cell.2008.02.031

Maag D and Lorsch JR (2003) Communication Between Eukaryotic Translation Initiation Factors 1 and 1A on the Yeast Small Ribosomal Subunit. J Mol Biol 330:917–924. doi: http://dx.doi.org/10.1016/S0022-2836(03)00665-X

Mader S, Lee H, Pause A and Sonenberg N (1995) The translation initiation factor eIF-4E binds to a common motif shared by the translation factor eIF-4 gamma and the translational repressors 4E-binding proteins. Mol Cell Biol 15:4990–4997.

Magnuson B, Ekim B and Fingar DC (2011) Regulation and function of ribosomal protein S6 kinase (S6K) within mTOR signalling networks. Biochem J 441:1 LP-21.

Mahfouz MM, Kim S, Delauney AJ and Verma DPS (2006) Arabidopsis TARGET OF RAPAMYCIN Interacts with RAPTOR, Which Regulates the Activity of S6 Kinase in Response to Osmotic Stress Signals. Plant Cell 18:477–490. doi: 10.1105/tpc.105.035931

Majumdar R, Bandyopadhyay A and Maitra U (2003) Mammalian Translation Initiation Factor eIF1 Functions with eIF1A and eIF3 in the Formation of a Stable 40 S Preinitiation Complex. J Biol Chem 278:6580–6587. doi: 10.1074/jbc.M210357200

Mamane Y, Petroulakis E, Rong L, Yoshida K, Ler LW and Sonenberg N (2004) eIF4E - from translation to transformation. Oncogene 23:3172–3179.

Manning J, Beutler K, Knepper MA and Vehaskari VM (2002) Upregulation of renal BSC1 and TSC in prenatally programmed hypertension. Am J Physiol - Ren Physiol 283:F202 LP-F206.

Marcotrigiano J, Gingras A-C, Sonenberg N and Burley SK (1999) Cap-Dependent Translation Initiation in Eukaryotes Is Regulated by a Molecular Mimic of eIF4G. Mol Cell 3:707–716. doi: 10.1016/S1097-2765(01)80003-4

Marcotrigiano J, Lomakin IB, Sonenberg N, Pestova T V, Hellen CUT and Burley SK (2001) A Conserved HEAT Domain within eIF4G Directs Assembly of the Translation Initiation Machinery. Mol Cell 7:193–203. doi: 10.1016/S1097-2765(01)00167-8

Marintchev A (2013) Roles of Helicases in Translation Initiation: A Mechanistic View. Biochim Biophys Acta 1829:799–809. doi: 10.1016/j.bbagrm.2013.01.005

Marintchev A and Wagner G (2004) Translation initiation: structures, mechanisms and evolution. Q Rev Biophys 37:197–284. doi: 10.1017/S0033583505004026

Martineau Y, Azar R, Bousquet C and Pyronnet S (2013) Anti-oncogenic potential of the eIF4E-binding proteins. Oncogene 32:671–677.

Matthews KR, Tschudi C and Ullu E (1994) A common pyrimidine-rich motif governs trans-splicing and polyadenylation of tubulin polycistronic pre-mRNA in trypanosomes. Genes Dev 8:491–501. doi: 10.1101/gad.8.4.491

Mayberry LK, Allen ML, Nitka KR, Campbell L, Murphy PA and Browning KS (2011) Plant Cap-binding Complexes Eukaryotic Initiation Factors eIF4F and eIFISO4F: MOLECULAR SPECIFICITY OF SUBUNIT BINDING. J Biol Chem 286:42566–42574. doi: 10.1074/jbc.M111.280099

Menand B, Desnos T, Nussaume L, Berger F, Bouchez D, Meyer C and Robaglia C (2002) Expression and disruption of the Arabidopsis TOR(target of rapamycin) gene. Proc Natl Acad Sci U S A. doi: 10.1073/pnas.092141899

Metz AM and Browning KS (1997) Assignment of the β-Subunit of Wheat eIF2 by Protein and DNA Sequence Analysis and Immunoanalysis. Arch Biochem Biophys 342:187–189. doi: http://dx.doi.org/10.1006/abbi.1997.0119

Miron M, Lasko P and Sonenberg N (2003) Signaling from Akt to FRAP/TOR Targets both 4E-BP and S6K in Drosophila melanogaster. Mol Cell Biol 23:9117–9126.

Miron M, Verdu J, Lachance PED, Birnbaum MJ, Lasko PF and Sonenberg N (2001) The translational inhibitor 4E-BP is an effector of PI(3)K/Akt signalling and cell growth in Drosophila. Nat Cell Biol 3:596–601.

Mizoguchi T, Hayashida N, Yamaguchi-Shinozaki K, Kamada H and Shinozaki K (1995) Two genes that encode ribosomal-protein S6 kinase homologs are induced by cold or salinity stress

in Arabidopsis thaliana. FEBS Lett 358:199–204. doi: 10.1016/0014-5793(94)01423-X

Montané M-H and Menand B (2013) ATP-competitive mTOR kinase inhibitors delay plant growth by triggering early differentiation of meristematic cells but no developmental patterning change. J Exp Bot 64:4361–4374. doi: 10.1093/jxb/ert242

Monzingo AF, Dhaliwal S, Dutt-Chaudhuri A, Lyon A, Sadow JH, Hoffman DW, Robertus JD and Browning KS (2007) The Structure of Eukaryotic Translation Initiation Factor-4E from Wheat Reveals a Novel Disulfide Bond. Plant Physiol 143:1504–1518. doi: 10.1104/pp.106.093146

Moore PB and Steitz TA (2003) The Structural Basis of Large Ribosomal Subunit Function. Annu Rev Biochem 72:813–850. doi: 10.1146/annurev.biochem.72.110601.135450

Moreau M, Azzopardi M, Clément G, Dobrenel T, Marchive C, Renne C, Martin-Magniette M-L, Taconnat L, Renou J-P, Robaglia C et al. (2012) Mutations in the Arabidopsis Homolog of LST8/GβL, a Partner of the Target of Rapamycin Kinase, Impair Plant Growth, Flowering, and Metabolic Adaptation to Long Days. Plant Cell 24:463–481.

Moreau M, Sormani R, Menand B, Veit B, Robaglia C and Meyer C (2010) Chapter 15 - The TOR Complex and Signaling Pathway in Plants. In: Enzymes BT-T (ed) The Enzymes. Academic Press, pp 285–302

Mothe-Satney I, Yang D, Fadden P, Haystead TAJ and Lawrence JC (2000) Multiple Mechanisms Control Phosphorylation of PHAS-I in Five (S/T)P Sites That Govern Translational Repression. Mol Cell Biol 20:3558–3567.

Murphy JF, Rychlik W, Rhoads RE, Hunt AG and Shaw JG (1991) A tyrosine residue in the small nuclear inclusion protein of tobacco vein mottling virus links the VPg to the viral RNA. J Virol 65:511–513.

Nakamura Y and Ito K (2003) Making sense of mimic in translation termination. Trends Biochem Sci 28:99–105. doi: 10.1016/S0968-0004(03)00006-9

Nanda JS, Saini AK, Muñoz AM, Hinnebusch AG and Lorsch JR (2013) Coordinated Movements of Eukaryotic Translation Initiation Factors eIF1, eIF1A, and eIF5 Trigger Phosphate Release from eIF2 in Response to Start Codon Recognition by the Ribosomal Preinitiation Complex. J Biol Chem 288:5316–5329. doi: 10.1074/jbc.M112.440693

Nelson MR, Leidal AM and Smibert CA (2004) Drosophila Cup is an eIF4E-binding protein that functions in Smaug-mediated translational repression. EMBO J 23:150 LP-159.

Nicaise V, Gallois J-L, Chafiai F, Allen LM, Schurdi-Levraud V, Browning KS, Candresse T, Caranta C, Le Gall O and German-Retana S (2007) Coordinated and selective recruitment of eIF4E and eIF4G factors for potyvirus infection in Arabidopsis thaliana. FEBS Lett

581:1041–1046. doi: 10.1016/j.febslet.2007.02.007

Nicklin P, Bergman P, Zhang B, Triantafellow E, Wang H, Nyfeler B, Yang H, Hild M, Kung C, Wilson C et al. (2009) Bidirectional Transport of Amino Acids Regulates mTOR and Autophagy. Cell 136:521–534. doi: 10.1016/j.cell.2008.11.044

Niedzwiecka A, Marcotrigiano J, Stepinski J, Jankowska-Anyszka M, Wyslouch-Cieszynska A, Dadlez M, Gingras A-C, Mak P, Darzynkiewicz E, Sonenberg N et al. (2002) Biophysical Studies of eIF4E Cap-binding Protein: Recognition of mRNA 5′ Cap Structure and Synthetic Fragments of eIF4G and 4E-BP1 Proteins. J Mol Biol 319:615–635. doi:

O'Brien JP, Mayberry LK, Murphy PA, Browning KS and Brodbelt JS (2013) Evaluating the Conformation and Binding Interface of Cap-Binding Proteins and Complexes via Ultraviolet Photodissociation Mass Spectrometry. J Proteome Res 12:5867–5877. doi:10.1021/pr400869u

Oh WJ and Jacinto E (2011) mTOR complex 2 signaling and functions. Cell Cycle 10:2305–2316. doi: 10.4161/cc.10.14.16586

Okade H, Fujita Y, Miyamoto S, Tomoo K, Muto S, Miyoshi H, Natsuaki T, Rhoads RE and Ishida T (2009) Turnip Mosaic Virus Genome-Linked Protein VPg Binds C-Terminal Region of Cap-Bound Initiation Factor 4E Orthologue Without Exhibiting Host Cellular Specificity. J Biochem 145:299–307. doi: 10.1093/jb/mvn180

Olsen DS, Savner EM, Mathew A, Zhang F, Krishnamoorthy T, Phan L and Hinnebusch AG (2003) <div xmlns="http://www.w3.org/1999/xhtml">Domains of eIF1A that mediate binding to eIF2, eIF3 and eIF5B and promote ternary complex recruitment in vivo</div> EMBO J 22:193 LP-204.

Paku KS, Umenaga Y, Usui T, Fukuyo A, Mizuno A, In Y, Ishida T and Tomoo K (2012) A conserved motif within the flexible C-terminus of the translational regulator 4E-BP is required for tight binding to the mRNA cap-binding protein eIF4E. Biochem J 441:237 LP-245.

Pape T, Wintermeyer W and Rodnina M V (1998) Complete kinetic mechanism of elongation factor Tu-dependent binding of aminoacyl-tRNA to the A site of the E. coli ribosome. EMBO J 17:7490–7497. doi: 10.1093/emboj/17.24.7490

Park H, Browning KS, Hohn T and Ryabova LA (2004) Eucaryotic initiation factor 4B controls eIF3-mediated ribosomal entry of viral reinitiation factor. EMBO J 23:1381 LP-1391.

Park H-S, Himmelbach A, Browning KS, Hohn T and Ryabova LA (2001) A Plant Viral Reinitiation; Factor Interacts with the Host Translational Machinery. Cell 106:723–733. doi: 10.1016/S0092-8674(01)00487-1

Patrick RM and Browning KS (2012) The eIF4F and eIFiso4F Complexes of Plants: An

Evolutionary Perspective. Comp Funct Genomics 2012:287814. doi: 10.1155/2012/287814

Pause A, Belsham GJ, Gingras A-C, Donze O, Lin T-A, Lawrence JC and Sonenberg N (1994) Insulin-dependent stimulation of protein synthesis by phosphorylation of a regulator of 5'-cap function. Nature 371:762–767.

Pestova* VT and Hellen TCU (2000) The structure and function of initiation factors in eukaryotic protein synthesis. Cell Mol Life Sci C 57:651–674. doi: 10.1007/PL00000726

Pestova T V (2000) The joining of ribosomal subunits in eukaryotes requires eIF5B. Nature 403:332–335.

Pestova T V, Borukhov SI and Hellen CU (1998) T. Eukaryotic ribosomes require initiation factors 1 and 1A to locate initiation codons. Nature 394:854–859.

Pestova T V, Lorsch JR and Hellen CUT (2007) 4 The Mechanism of Translation Initiation in Eukaryotes. Cold Spring Harb. Monogr. Arch. Vol. 48 Transl. Control Biol. Med.

Peter D, Igreja C, Weber R, Wohlbold L, Weiler C, Ebertsch L, Weichenrieder O and Izaurralde E (2015) Molecular Architecture of 4E-BP Translational Inhibitors Bound to eIF4E. Mol Cell 57:1074–1087. doi: 10.1016/j.molcel.2015.01.017

Peterson TR, Laplante M, Thoreen CC, Sancak Y, Kang SA, Kuehl WM, Gray NS and Sabatini DM (2009) DEPTOR Is an mTOR Inhibitor Frequently Overexpressed in Multiple Myeloma Cells and Required for Their Survival. Cell 137:873–886. doi: 10.1016/j.cell.2009.03.046

Pisareva VP, Pisarev A V, Hellen CUT, Rodnina M V and Pestova T V (2006) Kinetic Analysis of Interaction of Eukaryotic Release Factor 3 with Guanine Nucleotides. J Biol Chem 281:40224–40235. doi: 10.1074/jbc.M607461200

Pisarev A V, Skabkin MA, Pisareva VP, Skabkina O V, Rakotondrafara AM, Hentze MW, Hellen CUT and Pestova T V (2010) The Role of ABCE1 in Eukaryotic Posttermination Ribosomal Recycling. Mol Cell 37:196–210. doi: http://dx.doi.org/10.1016/j.molcel.2009.12.034

Polunovsky VA, Gingras A-C, Sonenberg N, Peterson M, Tan A, Rubins JB, Manivel JC and Bitterman PB (2000) Translational Control of the Antiapoptotic Function of Ras. J Biol Chem 275:24776–24780. doi: 10.1074/jbc.M001938200

Poulin F, Gingras A-C, Olsen H, Chevalier S and Sonenberg N (1998) 4E-BP3, a New Member of the Eukaryotic Initiation Factor 4E-binding Protein Family. J Biol Chem 273:14002–14007. doi: 10.1074/jbc.273.22.14002

Proud CG (2006) Regulation of protein synthesis by insulin. Biochem Soc Trans 34:213 LP-216.

Proud CG (2004) The multifaceted role of mTOR in cellular stress responses. DNA Repair (Amst) 3:927–934. doi: http://dx.doi.org/10.1016/j.dnarep.2004.03.012

Ramakrishnan V (2002) Ribosome Structure and the Mechanism of Translation. Cell 108:557–572.

doi: 10.1016/S0092-8674(02)00619-0

Raught B, Gingras A-C, Gygi SP, Imataka H, Morino S, Gradi A, Aebersold R and Sonenberg N (2000) Serum-stimulated, rapamycin-sensitive phosphorylation sites in the eukaryotic translation initiation factor 4GI. EMBO J 19:434–444. doi: 10.1093/emboj/19.3.434

Raught B, Peiretti F, Gingras A-C, Livingstone M, Shahbazian D, Mayeur GL, Polakiewicz RD, Sonenberg N and Hershey JWB (2004) Phosphorylation of eucaryotic translation initiation factor 4B Ser422 is modulated by S6 kinases. EMBO J 23:1761–1769. doi: 10.1038/sj.emboj.7600193

Ren M, Qiu S, Venglat P, Xiang D, Feng L, Selvaraj G and Datla R (2011) Target of Rapamycin Regulates Development and Ribosomal RNA Expression through Kinase Domain in Arabidopsis. Plant Physiol 155:1367–1382. doi: 10.1104/pp.110.169045

Ren M, Venglat P, Qiu S, Feng L, Cao Y, Wang E, Xiang D, Wang J, Alexander D, Chalivendra S et al. (2012) Target of Rapamycin Signaling Regulates Metabolism, Growth, and Life Span in Arabidopsis. Plant Cell 24:4850–4874. doi: 10.1105/tpc.112.107144

Revers F, Le Gall O, Candresse T and Maule AJ (1999) New Advances in Understanding the Molecular Biology of Plant/Potyvirus Interactions. Mol Plant-Microbe Interact 12:367–376. doi: 10.1094/MPMI.1999.12.5.367

Richter JD and Sonenberg N (2005) Regulation of cap-dependent translation by eIF4E inhibitory proteins. Nature 433:477–480.

Robaglia C, Thomas M and Meyer C (2012) Sensing nutrient and energy status by SnRK1 and TOR kinases. Curr Opin Plant Biol 15:301–307. doi: http://dx.doi.org/10.1016/j.pbi.2012.01.012

Rodnina M V, Beringer M and Bieling P (2005) Ten remarks on peptide bond formation on the ribosome. Biochem Soc Trans 33:493 LP-498.

Rodnina M V and Wintermeyer W (2009) Recent mechanistic insights into eukaryotic ribosomes. Curr Opin Cell Biol 21:435–443. doi: http://dx.doi.org/10.1016/j.ceb.2009.01.023

Rogers GW, Richter NJ and Merrick WC (1999) Biochemical and Kinetic Characterization of the RNA Helicase Activity of Eukaryotic Initiation Factor 4A. J Biol Chem 274:12236–12244. doi: 10.1074/jbc.274.18.12236

Rojo F, Najera L, Lirola J, Jiménez J, Guzmán M, Sabadell MD, Baselga J and Cajal SR y (2007) 4E-Binding Protein 1, A Cell Signaling Hallmark in Breast Cancer that Correlates with Pathologic Grade and Prognosis. Clin Cancer Res 13:81 LP-89.

Rousseau D, Gingras AC, Pause A and Sonenberg N (1996) The eIF4E-binding proteins 1 and 2 are negative regulators of cell growth. Oncogene 13:2415–2420.

Roux PP and Topisirovic I (2012) Regulation of mRNA Translation by Signaling Pathways. Cold

Spring Harb Perspect Biol . doi: 10.1101/cshperspect.a012252

Rozen F, Edery I, Meerovitch K, Dever TE, Merrick WC and Sonenberg N (1990) Bidirectional RNA helicase activity of eucaryotic translation initiation factors 4A and 4F. Mol Cell Biol 10:1134–1144.

Ruggero D, Montanaro L, Ma L, Xu W, Londei P, Cordon-Cardo C and Pandolfi PP (2004) The translation factor eIF-4E promotes tumor formation and cooperates with c-Myc in lymphomagenesis. Nat Med 10:484–486.

Sabatini DM, Erdjument-Bromage H, Lui M, Tempst P and Snyder SH (1994) RAFT1: A mammalian protein that binds to FKBP12 in a rapamycin-dependent fashion and is homologous to yeast TORs. Cell 78:35–43.

Salas-Marco J and Bedwell DM (2004) GTP Hydrolysis by eRF3 Facilitates Stop Codon Decoding during Eukaryotic Translation Termination. Mol Cell Biol 24:7769–7778.

Sancak Y, Peterson TR, Shaul YD, Lindquist RA, Thoreen CC, Bar-Peled L and Sabatini DM (2008) The Rag GTPases bind raptor and mediate amino acid signaling to mTORC1. Science 320:1496–1501. doi: 10.1126/science.1157535

Sancak Y, Thoreen CC, Peterson TR, Lindquist RA, Kang SA, Spooner E, Carr SA and Sabatini DM (2007) PRAS40 Is an Insulin-Regulated Inhibitor of the mTORC1 Protein Kinase. Mol Cell 25:903–915. doi: 10.1016/j.molcel.2007.03.003

Schaad MC, Anderberg RJ and Carrington JC (2000) Strain-Specific Interaction of the Tobacco Etch Virus NIa Protein with the Translation Initiation Factor eIF4E in the Yeast Two-Hybrid System. Virology 273:300–306. doi: http://dx.doi.org/10.1006/viro.2000.0416

Schalm SS and Blenis J (2002) Identification of a Conserved Motif Required for mTOR Signaling. Curr Biol 12:632–639. doi: http://dx.doi.org/10.1016/S0960-9822(02)00762-5

Schalm SS, Fingar DC, Sabatini DM and Blenis J (2003) TOS Motif-Mediated Raptor Binding Regulates 4E-BP1 Multisite Phosphorylation and Function. Curr Biol 13:797–806. doi: 10.1016/S0960-9822(03)00329-4

Schepetilnikov M, Dimitrova M, Mancera-Martínez E, Geldreich A, Keller M and Ryabova LA (2013) TOR and S6K1 promote translation reinitiation of uORF-containing mRNAs via phosphorylation of eIF3h. EMBO J 32:1087 LP-1102.

Schepetilnikov M, Kobayashi K, Geldreich A, Caranta C, Robaglia C, Keller M and Ryabova LA (2011) Viral factor TAV recruits TOR/S6K1 signalling to activate reinitiation after long ORF translation. EMBO J 30:1343–1356. doi: 10.1038/emboj.2011.39

Schmitt E, Naveau M and Mechulam Y (2010) Eukaryotic and archaeal translation initiation factor 2: a heterotrimeric tRNA carrier. FEBS Lett 584:405–412. doi: 10.1016/j.febslet.2009.11.002

Shahbazian D, Roux PP, Mieulet V, Cohen MS, Raught B, Taunton J, Hershey JWB, Blenis J, Pende M and Sonenberg N (2006) The mTOR/PI3K and MAPK pathways converge on eIF4B to control its phosphorylation and activity. EMBO J 25:2781–2791.

Shimobayashi M and Hall MN (2014) Making new contacts: the mTOR network in metabolism and signalling crosstalk. Nat Rev Mol Cell Biol 15:155–162.

Silvera D, Formenti SC and Schneider RJ (2010) Translational control in cancer. Nat Rev Cancer 10:254–266.

Singh CR, Curtis C, Yamamoto Y, Hall NS, Kruse DS, He H, Hannig EM and Asano K (2005) Eukaryotic Translation Initiation Factor 5 Is Critical for Integrity of the Scanning Preinitiation Complex and Accurate Control of GCN4 Translation. Mol Cell Biol 25:5480–5491. doi: 10.1128/MCB.25.13.5480-5491.2005

Singh CR, He H, Ii M, Yamamoto Y and Asano K (2004) Efficient Incorporation of Eukaryotic Initiation Factor 1 into the Multifactor Complex Is Critical for Formation of Functional Ribosomal Preinitiation Complexes in Vivo. J Biol Chem 279:31910–31920. doi: 10.1074/jbc.M313940200

Sonenberg N (2008) eIF4E, the mRNA cap-binding protein: from basic discovery to translational researchThis paper is one of a selection of papers published in this Special Issue, entitled CSBMCB — Systems and Chemical Biology, and has undergone the Journal's usual peer revie. Biochem Cell Biol 86:178–183. doi: 10.1139/O08-034

Sonenberg N and Hinnebusch AG (2007a) Regulation of Translation Initiation in Eukaryotes: Mechanisms and Biological Targets. Cell 136:731–745. doi: 10.1016/j.cell.2009.01.042

Sonenberg N and Hinnebusch AG (2009) Regulation of Translation Initiation in Eukaryotes: Mechanisms and Biological Targets. Cell 136:731–745. doi: 10.1016/j.cell.2009.01.042

Sonenberg N and Hinnebusch AG (2007b) New Modes of Translational Control in Development, Behavior, and Disease. Mol Cell 28:721–729.

Sonenberg N and Shatkin AJ (1978) Nonspecific effect of m7GMP on protein-RNA interactions. J Biol Chem 253:6630–6632.

Sormani R, Yao L, Menand B, Ennar N, Lecampion C, Meyer C and Robaglia C (2007) Saccharomyces cerevisiae FKBP12 binds Arabidopsis thaliana TOR and its expression in plants leads to rapamycin susceptibility. BMC Plant Biol 7:26. doi: 10.1186/1471-2229-7-26

Spirin AS (2002) Ribosome as a molecular machine. FEBS Lett 514:2–10. doi: 10.1016/S0014-5793(02)02309-8

Sun Y-L and Hong S-K (2013) Sensitivity of Translation Initiation Factor eIF1 as a Molecular Target of Salt Toxicity to Sodic-Alkaline Stress in the Halophytic Grass Leymus chinensis

. Biochem Genet 51:101–118. doi: 10.1007/s10528-012-9546-9

Tarun SZ and Sachs AB (1995) A common function for mRNA 5’ and 3’ ends in translation initiation in yeast. Genes Dev 9:2997–3007. doi: 10.1101/gad.9.23.2997

Tee AR and Proud CG (2002) Caspase Cleavage of Initiation Factor 4E-Binding Protein 1 Yields a Dominant Inhibitor of Cap-Dependent Translation and Reveals a Novel Regulatory Motif. Mol Cell Biol 22:1674–1683. doi: 10.1128/MCB.22.6.1674-1683.2002

Teleman AA, Chen Y-W and Cohen SM (2005) 4E-BP functions as a metabolic brake used under stress conditions but not during normal growth. Genes Dev 19:1844–1848.

Thiébeauld O, Schepetilnikov M, Park H-S, Geldreich A, Kobayashi K, Keller M, Hohn T and Ryabova LA (2009) A new plant protein interacts with eIF3 and 60S to enhance virus-activated translation re-initiation. EMBO J 28:3171–3184. doi: 10.1038/emboj.2009.256

Thoreen CC, Chantranupong L, Keys HR, Wang T, Gray NS and Sabatini DM (2012) A unifying model for mTORC1-mediated regulation of mRNA translation. Nature 485:109–113. doi: 10.1038/nature11083

Turck F, Kozma SC, Thomas G and Nagy F (1998) A Heat-Sensitive Arabidopsis thaliana Kinase Substitutes for Human p70(s6k) Function In Vivo. Mol Cell Biol 18:2038–2044.

Turck F, Zilbermann F, Kozma SC, Thomas G and Nagy F (2004) Phytohormones Participate in an S6 Kinase Signal Transduction Pathway in Arabidopsis. Plant Physiol 134:1527–1535. doi: 10.1104/pp.103.035873

Verrotti AC and Wharton RP (2000) Nanos interacts with cup in the female germline of Drosophila. Development 127:5225 LP-5232.

Wang X, Beugnet A, Murakami M, Yamanaka S and Proud CG (2005) Distinct Signaling Events Downstream of mTOR Cooperate To Mediate the Effects of Amino Acids and Insulin on Initiation Factor 4E-Binding Proteins. Mol Cell Biol 25:2558–2572.

Wang X, Li W, Parra J-L, Beugnet A and Proud CG (2003) The C Terminus of Initiation Factor 4E-Binding Protein 1 Contains Multiple Regulatory Features That Influence Its Function and Phosphorylation. Mol Cell Biol 23:1546–1557. doi: 10.1128/MCB.23.5.1546-1557.2003

Wang X, Li W, Williams M, Terada N, Alessi DR and Proud CG (2001) Regulation of elongation factor 2 kinase by p90(RSK1) and p70 S6 kinase. EMBO J 20:4370–4379. doi: 10.1093/emboj/20.16.4370

Wilhelm JE, Hilton M, Amos Q and Henzel WJ (2003) Cup is an eIF4E binding protein required for both the translational repression of oskar and the recruitment of Barentsz. J Cell Biol 163:1197 LP-1204.

Wittmann S, Chatel H, Fortin MG and Laliberté J-F (1997) Interaction of the Viral Protein Genome

Linked of Turnip Mosaic Potyvirus with the Translational Eukaryotic Initiation Factor (iso) 4E ofArabidopsis thalianaUsing the Yeast Two-Hybrid System. Virology 234:84–92. doi: http://dx.doi.org/10.1006/viro.1997.8634

Wullschleger S, Loewith R and Hall MN (2006) TOR Signaling in Growth and Metabolism. Cell 124:471–484. doi: http://dx.doi.org/10.1016/j.cell.2006.01.016

Xiong Y, McCormack M, Li L, Hall Q, Xiang C and Sheen J (2013) Glc-TOR signalling leads transcriptome reprogramming and meristem activation. Nature 496:181–186. doi: 10.1038/nature12030

Xiong Y and Sheen J (2012) Rapamycin and Glucose-Target of Rapamycin (TOR) Protein Signaling in Plants. J Biol Chem 287:2836–2842. doi: 10.1074/jbc.M111.300749

Xiong Y and Sheen J (2014) The Role of Target of Rapamycin Signaling Networks in Plant Growth and Metabolism. Plant Physiol 164:499–512. doi: 10.1104/pp.113.229948

Yamamoto Y, Singh CR, Marintchev A, Hall NS, Hannig EM, Wagner G and Asano K (2005) The eukaryotic initiation factor (eIF) 5 HEAT domain mediates multifactor assembly and scanning with distinct interfaces to eIF1, eIF2, eIF3, and eIF4G. Proc Natl Acad Sci U S A 102:16164–16169. doi: 10.1073/pnas.0507960102

Yoffe Y, Zuberek J, Lerer A, Lewdorowicz M, Stepinski J, Altmann M, Darzynkiewicz E and Shapira M (2009) Binding Specificities and Potential Roles of Isoforms of Eukaryotic Initiation Factor 4E in Leishmania. Eukaryot Cell 5:1969–1979. doi: 10.1128/EC.00230-06

Yoo S-D, Cho Y-H and Sheen J (2007) Arabidopsis mesophyll protoplasts: a versatile cell system for transient gene expression analysis. Nat Protoc 2:1565–1572.

Yoon H and Donahue TF (1992) MicroReview Control of translation initiation in Saccharomyces cerevisiae. Mol Microbiol 6:1413–1419. doi: 10.1111/j.1365-2958.1992.tb00861.x

Yumak H, Khan MA and Goss DJ (2010) Poly(A) tail affects equilibrium and thermodynamic behavior of tobacco etch virus mRNA with translation initiation factors eIF4F, eIF4B and PABP. Biochim Biophys Acta -Gene Regul Mech 1799:653–658.

Zeenko V and Gallie DR (2005) Cap-independent Translation of Tobacco Etch Virus Is Conferred by an RNA Pseudoknot in the 5′-Leader. J Biol Chem 280:26813–26824. doi: 10.1074/jbc.M503576200

Zhai B, Villén J, Beausoleil SA, Mintseris J and Gygi SP (2008) Phosphoproteome Analysis of Drosophila melanogaster Embryos. J Proteome Res 7:1675–1682. doi: 10.1021/pr700696a

Zhang SH, Lawton MA, Hunter T and Lamb CJ (1994) atpk1, a novel ribosomal protein kinase gene from Arabidopsis. I. Isolation, characterization, and expression. J Biol Chem 269:17586–17592.

Zinoviev A, Léger M, Wagner G and Shapira M (2011) A novel 4E-interacting protein in Leishmania is involved in stage-specific translation pathways. Nucleic Acids Res 39:8404–8415. doi: 10.1093/nar/gkr555

Zoncu R, Sabatini DM and Efeyan A (2011) mTOR: from growth signal integration to cancer, diabetes and ageing. Nat Rev Mol Cell Biol 12:21–35. doi: 10.1038/nrm3025

Ola SROUR

Caractérisation de protéines interagissant avec eIF4E, phosphorylées par TOR et modulant l'initiation de la traduction coiffe-dépendante chez *Arabidopsis*

Résumé

Chez les mammifères l'initiation de la traduction et, plus particulièrement, la formation du complexe eIF4F, est principalement régulée par la protéine kinase TOR (Target of rapamycin). Cette voie de régulation fait intervenir les protéines 4E-BP (eIF4E-binding proteins) dont l'activité est modulée par la phosphorylation par TOR. Sous leur forme non-phosphorylée, les 4E-BP se lient au facteur d'initiation eIF4E, empêchent son recrutement dans le complexe eIF4F et inhibent ainsi l'initiation de la traduction. Phosphorylées par TOR, les 4E-BP perdent leur affinité pour eIF4E et sont remplacées par eIF4G ce qui active la traduction. La régulation de l'initiation de la traduction par TOR via 4E-BP a été bien décrite dans plusieurs modèles eucaryotes, tels que la levure, les insectes et les mammifères, mais reste encore obscure chez les plantes. Les recherches réalisées au cours de ma thèse ont permis l'identification de deux protéines homologues de 4E-BP chez *Arabidopsis*. Ces protéines, que nous avons appelées ToRP1 et ToRP2 (TOR Regulatory Proteins), sont caractérisées par la présence d'un motif consensus indispensable pour la liaison à eIF4E, et qui existe chez les protéines 4E-BP des mammifères ainsi que chez eIF4G et eIFiso4G d'*Arabidopsis*. La protéine ToRP1 est capable d'interagir spécifiquement avec eIF4E, mais aussi avec TOR via son extrémité N-terminale en système double-hybride de levure. ToRP1 et ToRP2 ont également été caractérisées comme étant des cibles directement phosphorylées par TOR chez *Arabidopsis*. Deux sérines, en position 49 et 89 dans la protéine ToRP1, ont été identifiées comme des sites potentiels de cette phosphorylation. De plus, l'état de phosphorylation de ces sites affecte l'interaction avec eIF4E en système double-hybride de levure. Par ailleurs, des plants d'*Arabidopsis* déficients en ToRP1 et ToRP2 renforcent la traduction strictement coiffe-dépendante de l'ARNm CYCB1;1, alors que la surexpression de ToRP1 ou de ToRP2 réprime sa traduction. Ces résultats suggèrent donc que les protéines ToRP, identifiées chez *Arabidopsis*, sont de nouvelles cibles directes de TOR, qui, par leur phosphorylation, régule l'initiation de la traduction coiffe-dépendante.

Mots clés : voie de signalisation de TOR, 4E-BP, initiation de la traduction coiffe-dépendante, *Arabidopsis*, ToRP

Abstract

The target of rapamycin (TOR) is an evolutionarily conserved kinase that is a critical sensor of nutritional and cellular energy and a major regulator of cell growth. TOR controls cap-dependent translation initiation, in particular the assembly of the eIF4F complex, by modulating the activity of eIF4E-binding proteins (4E-BPs). In their unphosphorylated state 4E-BP proteins sequester eIF4E and repress translation. Upon phosphorylation by TOR, 4E-BPs have a low affinity binding to eIF4E and are replaced by eIF4G thus activating translation initiation. 4E-BPs have been discovered in yeast and mammals but remain to be obscure in plants. Here, we identified and characterized two *Arabidopsis* proteins termed TOR Regulatory Proteins (ToRPs 1 and 2) that display some characteristics of mammalian 4E-BPs. ToRP1 and ToRP2 contain a canonical eIF4E-binding motif (4E-BM) found in mammalian 4E-BPs and *Arabidopsis* eIF4G and eIFiso4G. ToRP1 interacts with eIF4E, and, surprisingly, the N-terminal HEAT domain of TOR in the yeast two-hybrid system. ToRP1 and ToRP2 are highly phosphorylated at several phosphorylation sites in TOR-dependent manner *in planta*. Two of these phosphorylation sites have been identified as—S49 and S89—their phosphorylation status modulates ToRP1 binding to eIF4E in the yeast two-hybrid system. In plant protoplasts, ToRP2 can function as translation repressor of mRNAs that are strictly cap-dependent. Our results suggest that ToRPs can specifically bind the *Arabidopsis* cap-binding proteins (eIF4E/eIFiso4E) and regulate translation initiation under the control of TOR.

Keywords: TOR signalling pathway, 4E-binding proteins 4E-BP, *Arabidopsis*, TOR Regulatory Proteins ToRP, translation initiation